La lettre d'informations

Hirlevelek

Bilteni

Novice, zanimivosti

رسالات إخبارية

Revista Periodica

Newsletters

Zpravodaj

Nieuwsbrieven

Spravodaj

Новости

Новини

Bollettino

ALADIN Newsletter 21

ALATNET Newsletter 4

July - December 2001

http://www.cnrm.meteo.fr/aladin/ & **http://www.cnrm.meteo.fr/alatnet/**

ALATNET is supported by the TMR/IHP Programme of the European Commission but the information provided here is the sole responsability of the ALATNET team and does not reflect the Community's opinion. The Community is not responsible for any use that might be made of data appearing here.

If needed, please contact : Dominique GIARD, Météo-France/CNRM/GMAP, 42 av. Coriolis, F-31057 Toulouse Cedex 1
tel: 33 5 61 07 84 60, fax: 33 5 61 07 84 53 (from France, replace 33 by 0), e-mail: dominique.giard@meteo.fr

This joined Newsletters present you the principal work around ALADIN or ALATNET during the first half of 2001. The news about work or events are related with informations that you sent.

An electronic ALADIN Newsletter 21 is available on the ALADIN web site and an electronic ALATNET Newsletter 4 can be consulted on the ALATNET web site.

Due to the increasing delay in the publication of the Newsletters (resulting from the delays in the reception of contributions, their increasing length and the large variety of formats used, the lack of manpower in the Toulouse Support Team, etc ...), the sections concerning events are omitted. The corresponding information is anyway available and regularly updated on the web sites.

Please do bring to my notice anything that you would like to be mentioned in the next Newsletters (ALADIN 22 & ALATNET 5) before the 31th July 2002.

Any contribution concerning announcements, scientific progress, publications, news from the ALADIN versions on workstations or on big computers, verifications results, ... will be welcome.

The operational ALADIN models

1. Introduction

(more details samuel.westrelin@meteo.fr)

Changes in the operational version of ARPEGE along the second half of 2001

From first of August, ATOVS radiances from NOAA16 were assimilated and SST analysis re-activated.

On eleventh of september, cycle 24T1 (new observations files format) of ARPEGE and 15 of ALADIN became operational. At the same time, a mesospheric drag, the suppression of snow falls when cold atmosphere covered warm surfaces and post-processing of CAPE were implemented.

On twelfth of november, CYCORA-ter physics package took place.

2. Operational version in Austria

(more details thomas.haiden@zamg.ac.at)

Nothing new since the last Newsletter.

3. Operational version in Belgium

(more details olivier.latinne@oma.be or luc.gerard@oma.be)

- Since 7 February, "AL12 / CYCORA_bis and 41 levels" has gone operational on SGI Origin 3000 Computer, 16 processors
- AL15 / CYCORA_ter is now running in double suite on the Origin 3000. This implied long work for porting, and various adaptations of post-processing tools.
- We envisage passing to a linear grid.
- AL12 and AL15 have been ported to Linux PCs.
- A new archiving system has arrived, and we also intend to review the selection of data to archive when switching the operational chain to AL15.

4. Operational version in Bulgaria

(more details andrey.bogatchev@meteo.bg)

The work on validation and verification of statistical adaptation scheme continued. Some bugs were fixed and now it runs in pre-operational mode.

The scripts for retrieving the initial and LBC-s were completely rewritten and were implemented operationally in the second half of December. Since that time there were no failures and the requests to the 'pickup' ftp-servers were sensitively decreased.

5. Pre-operational version at Croatian Meteorological Service

(more details bajic@cirus.dhz.hr)

The main change in the ALADIN environment is its installation on a new computer :

Computer type and performance:

- SGI ORIGIN 3400
- 12 CPU MIPS R12000 on IP35 400 MHz

- Main Memory size 3072 Mbytes
- OS IRIX 6.5

Test results for the LACE domain (240x216 points, 31 levels) are shown on the picture.

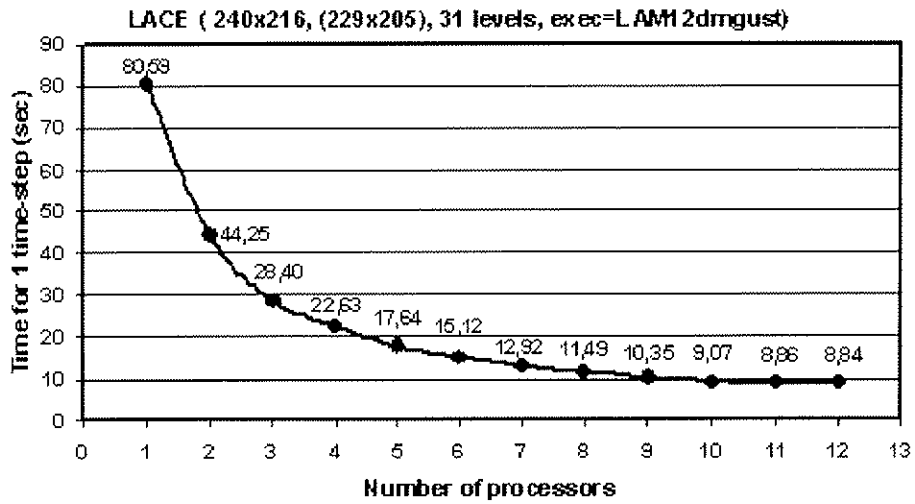

Figure: Integration time for 1 time-step with different numbers of processors.

AL12 version of ALADIN is installed. Scripts are modified to be used on the new computer. ALADIN tools (*aft_time*, *aft_info*, *aft_dele*, *aft_merg*, *edf* and *decdate*) are adapted and installed. Preparation of transfer of the operational suite on the SGI is almost finished. Next step will be to install a new ALADIN version, AL15.

6. Operational version at Météo-France

(more details samuel.westrelin@meteo.fr)

Similar changes as in ARPEGE along these 6 months.

7. Workstation version of ALADIN at Météo-France

(more details jean-marc.audoin@meteo.fr)

On the Sun workstation, using compiler F90 Fujitsu for Sun, the version Al15 has been implemented with the new libraries : *tal*, *tfl*. It runs for configurations e001, ee927. But some compiler problems appeared with the module procedures, as in *MPL_BROADCAST_MOD* with this diagnostic : *" do not ensure that generic procedure MPL_BROADCAST is unambiguous "*.The compiler Fujitsu for Sun doesn't recognize the type of a variable that can be REAL*8, REAL*4 or INTEGER in a generic procedure. To solve this problem, one must split the module procedure for each type of variable, as in the oldest version of module ECSORT in library *xrd* version XR22.

8. Operational version in Hungary

(more details horanyi@met.hu)

As far as the operational ALADIN/HU model suite is concerned there were not any changes. The operational model suite is still based on version AL12.

9. Operational LACE application

(more details vana@chmi.cz)

1. Evolution of the ALADIN/LACE application.

The ALADIN/LACE suite abandoned the data packing in the blending step:

06/08/2001 for 12 UTC network time: the data packing in the work-files is abandoned in the inner part of the blending procedure.

This is a purely technical modification, which purpose is to get the highest possible precision when using any incremental approach (like in the incremental data assimilation algorithm and/or in blending).

Impact on the forecast: The impact, as demonstrated by a short parallel suite, was hardly noticeable on the scores, however this modification is a precaution in order not to accumulate very small errors within the blending cycle.

Technical impact: more volume required in order to store the ALADIN first guess file (unpacked). The increased storage demand only impacts Prague archiving device.

The ALADIN/LACE application switched to the incremental digital filter on:

10/10/2001 for 12 UTC network time: the incremental digital filter is applied

It is a well known fact that any "initialisation" procedure (such as nonlinear normal modes, digital filter, etc.) applied on the initial conditions of the model in order to restore the mass-wind balance is at the same time removing some part of the useful signal owing to various imperfections in the nonlinear calculations. Hence the classical way of initialisation (called mostly as the "external filter" due to its external application with respect to the analysis) is today in advanced NWP models replaced by a fully internal initialisation (applied within the variational data assimilation scheme) and/or by the "incremental" initialisation, which tries to balance only the analysis increments but not the first guess. Back to 1997, the incremental digital filter initialisation (IDFI) was developed in ALADIN as part of the 3d-var R & D action. This IDFI technique, however, was nowhere really applied since it has had no meaning in the dynamical adaptation mode. After completing the blending suite, the Prague Team cleaned-up the IDFI code and scripts and applied it within the blending. Though the blending itself provides already well balanced fields (it was found that no initialisation is needed in the blending cycle), a weak external digital filter was still needed in the production forecasts. This weak external filter was replaced by IDFI, still using only a weak filter.

Impact on the forecast: **i)** Keeping even more the well-developed mesoscale structures in the initial state of the forecast compared to the case when an external DFI was used; **ii)** improved score of the geopotential bias in the altitude (probably due to a better treatment of tidal waves coming in from the LBCs).

Technical impact: relevant changes in the scripts and namelists

Perspectives: the IDFI technique is fully compatible with 3d/4d-var, as proved by 5 years of ARPEGE experience.

2. Parallel Suites & Code Maintenance

The Prague Team launched the following parallel tests to assess the impact of different modifications:

- *Suite ABH :* **"disallowing all packing in the assimilation procedure"**. This suite was quite short (one week only) in order to get sure about the technical change. The purpose of this change is explained above. The suite became operational on 06/08/2001.

- *Suite ABI :* **"incremental DFI & blending"**. The external initialization was completely removed from the ALADIN/LACE suite. The scores were neutral except the improvement of mass field bias in the upper atmosphere. Suite ABI became operational on 10/10/2001.

- *Suite ABJ :* **"IDFI & blending on linear grid"**. After a preliminary tuning of the blending on the linear grid, a parallel test was made. Concerning the scores, these are very similar to the ones of ABI. Further effort will be needed in order to assess potential improvement of the linear grid. Since the usage of linear grid increases the size of data files (for telecommunication and storage), its operational use is not envisaged till some benefices become clear.

- *Suite ABK :* **"CYCORA-ter package"**. New physical parameterization was tested, over the second half of October 2001. The scores were, however, negative nearly for all parameters. That is why the suite was stopped. The negative results were consulted with GMAP. A plausible reason to obtain these bad scores was a particular choice of the testing period (linked to a certain type of weather situation). Since CYCORA-ter was tested in ARPEGE off-line for other seasons with mostly positive impact, it was decided to repeat the test later.

- *Suite ABL :* **"repeat of CYCORA-ter package test"**. Unfortunately, the results were as bad as for Suite ABK, this time the test was run for a full winter situation (end of November to Christmas). This time it was concluded that very probably this behaviour is due to the continental character of LACE domain. The Prague Team decided NOT to apply operationally the CYCORA-ter package in contrary to the decision made for ARPEGE suite unless some further work on the physics would be done. Unfortunately, in general LACE works too little on the physical parameterizations and the team did not have a force to investigate deeper on its own.

The results of parallel tests may be consulted on www.chmi.cz/meteo/ov/lace/aladin_lace/partests/ pages.

10. Operational version in Morocco

(more details radi.ajjaji@cnrm.meteo.fr)

Aladin Morocco: actual situation and perspectives.

After several validation tests comprising all components of Albachir operational suite beginning from observation files creation until the production of charts, it was decided to put AL13 into operations on our new IBM SPII platform.

For the time being, Albachir runs in both assimilation and integration modes (assimilation is based on Canari of course). But this situation is considered as a transitional one: Moroccan Meteorology Direction decided to move to another Albachir configuration massively nested. Aladin will run first on a great area including all North Africa with 25-km resolution coupled with Arpege (320x180x41) and for 72H range. As a beginning assimilation will be based also on Canari as a first step towards BlendVar on this domain. A second finer mesh Aladin model (9 km) will be embedded and coupled with the later but without assimilation. This second model will run to 60H range with 3 hours of coupling frequency. At the end of this second model execution, four local regional models will be launched to 36H range and on a 5-km grid meshes. The schedule of the different tasks is joint to this report.

The 64 kb/s link between Toulouse and Casa is being upgraded to 128 kb/s. This will enable the easy transfer of heavy Aladin North Africa coupling files (about 10 MO per file).

On the side of observations, our BDM is enlarged to receive all observation fluxes on SMT over the world. And another study is beginning to find a solution that will allow the presence of radiances on the BDM. The aim of the huge efforts made on observations is first to be able to move easily to a

variational analysis in Casablanca, and second to be able to verify our projected Albachir configuration. The later is already in an advanced stage for operational Albachir, the first verification results will be send to "*verifala*" very soon.

Intensive studies are being done to validate Albachir new configuration (Asynchronous coupling, Assimilation without observation files coming from Toulouse, Impact of DFI on Canari increments, Investigations on 3D-Var, ...etc).

Since the last December, it is possible to run 3D-Var at Casablanca thanks to Claude Fischer precious help. Lagged NMC statistics had been produced. Now a team comprising three engineers are dedicated to assimilation with the aim to put 3D-Var into operation as soon as possible.

The following table describes some technical aspects of our new projected massively nested configuration.

	Aladin North Africa	Aladin Morocco 9km	4 local regional Aladin
Number of levels	41	41	41
Resolution	25 km	9 km	5 km
Horizontal grid	320 ×180	320 ×360	80 ×80
Maximum range	72 H	60 H	36 H
Cycle to be used	AL13	AL13	AL12
Coupling	Arpege	Aladin North Africa	Aladin Morocco 9km
Assimilation	Canari based	No assimilation	No assimilation
Platform of execution	IBM	IBM	CRAY
Time taken	25 mn	50 mn	15 mn

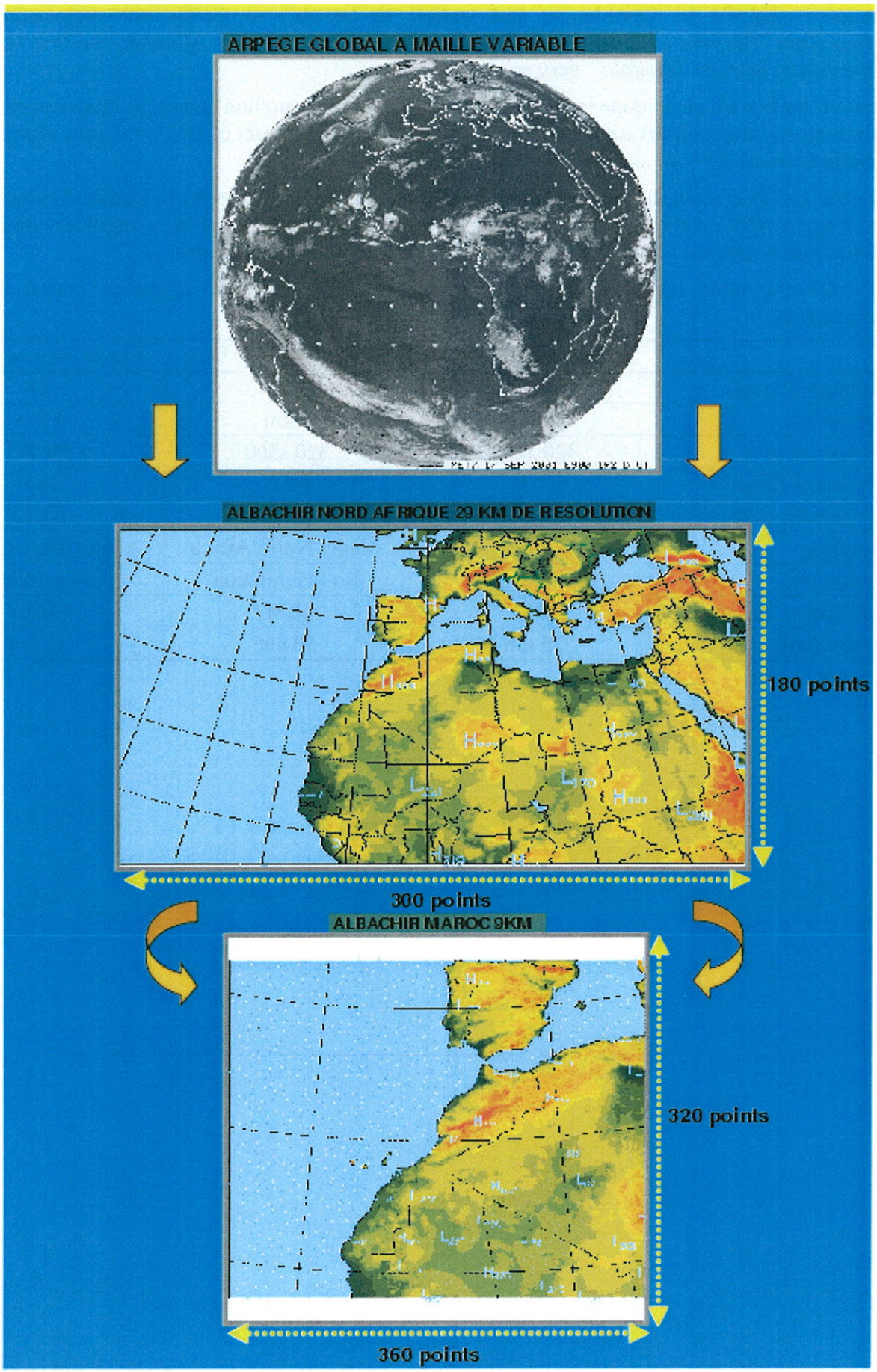
ARPEGE GLOBAL A MAILLE VARIABLE
ALBACHIR NORD AFRIQUE 29 KM DE RESOLUTION
180 points
300 points
ALBACHIR MAROC 9KM
320 points
360 points

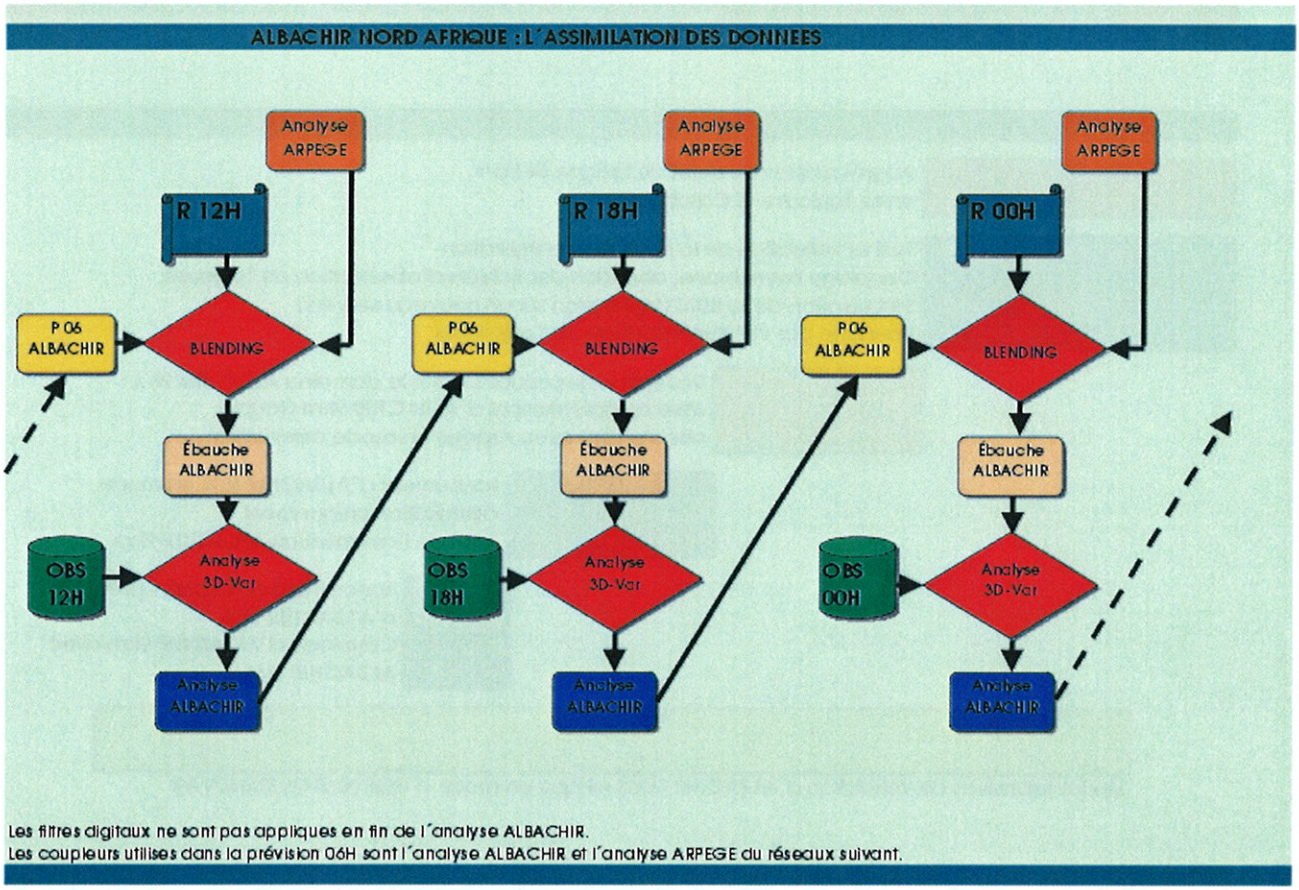

CHAINE OPERATIONNELLE ALBACHIR NORD AFRIQUE IMBRIQUANT ALBACHIR MAROC 9KM

12:00 13:00 14:00 15:00 16:00 17:00 18:00 19:00 20:00 21:00 22:00 23:00 00:00 01:00

1h — Arrivee des analyses long cut-off **ARPEGE** 4D-Var : Coupleurs
Fabrication des fichiers d'observation long cut-off apres extraction de la **BDM**/Casablanca.

1h — Blending (Analyse **ARPEGE** 00H et Ebauche **ALBACHIR** N/A)
Analyse 3D-Var **ALBACHIR** N/A 00H
Prévision **ALBACHIR** P06 issue de 00H
Blending (Analyse **ARPEGE** 06H et Ebauche **ALBACHIR**)
Analyse **ALBACHIR** N/A 3D-Var 06H
Prévision **ALBACHIR** P06 issue de 06H

30 mn — Arrivee de l'analyse **ARPEGE** 4D-Var court cut-off : Coupleur
Fabrication du fichier d'observation court cut-off

30 mn — Blending (Analyse **ARPEGE** avec Ebauche **ALBACHIR** N/A)
Analyse 3D-Var **ALBACHIR** N/A 12H court cut-off.

30 mn — Prévision **ALBACHIR** N/A 72H en mode couplage asynchrone
Production des coupleurs pour **ALBACHIR** MA 9km
Post-processing et graphiques sur le domaine **ALBACHIR** N/A
Diffusion vers les differents usagers.

1h30 — Pévision **ALBACHIR** MA 9km 60H en mode couplage synchrone avec **ALBACHIR** N/A
Post-Processing et Graphiques sur le domaine **ALBACHIR** MA
Diffusion vers les differents usagers.

5h — Arrivée des coupleurs **ARPEGE** qui vont être utilisés dans le réseau suivant

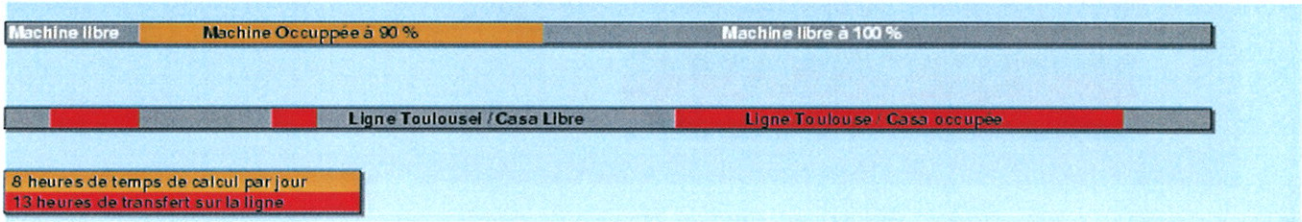

ÉCHÉANCIER DE MISE EN OPÉRATIONNELLE DE LA NOUVELLE CONFIGURATION ALBACHIR

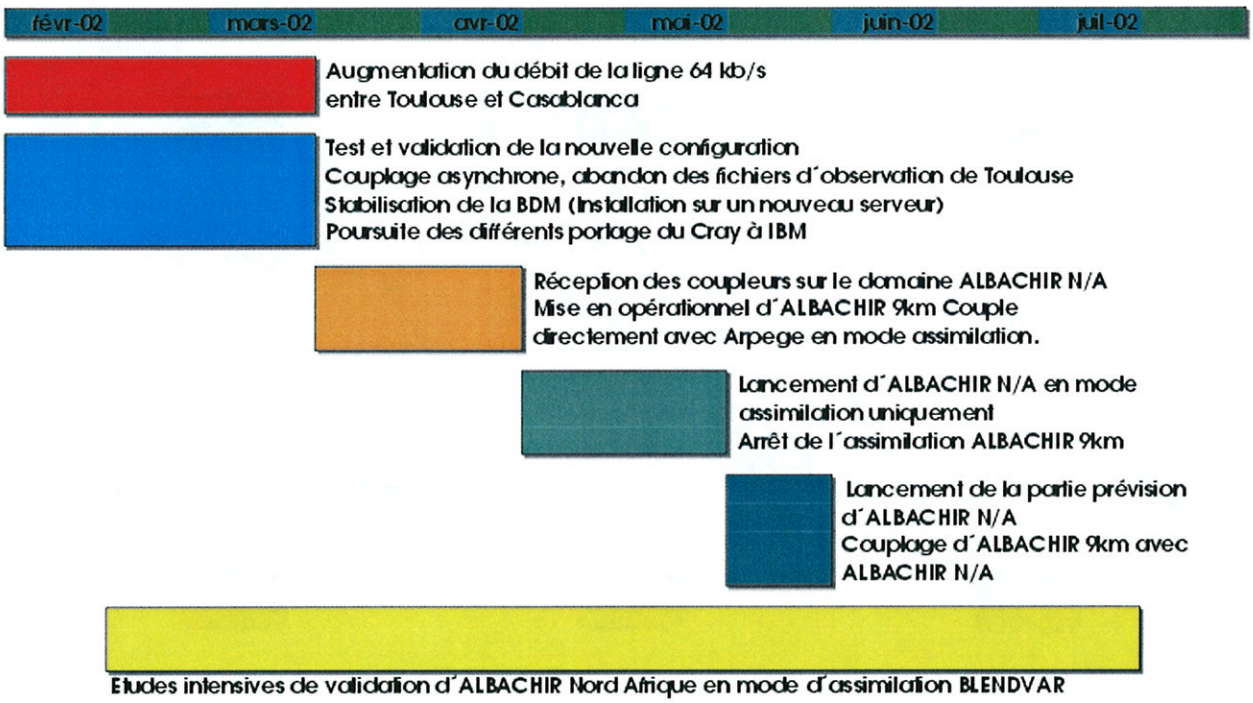

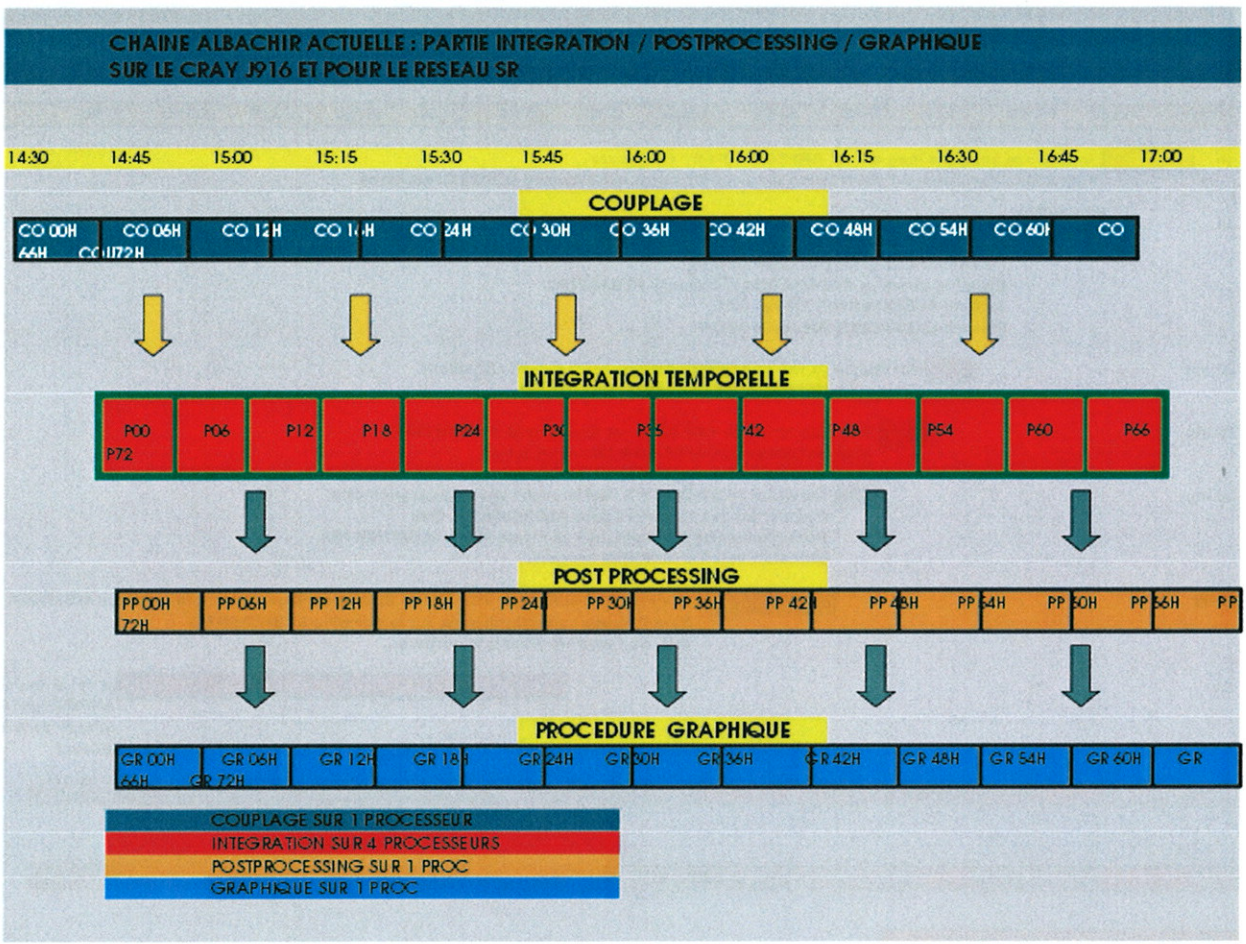

11. Operational version in Poland

(more details zijerczy@cyf-kr.pl)

See the report on deported work.

12. Operational version in Portugal

(more details vanda.costa@meteo.pt)

See the report on deported work.

13. Operational version in Romania

(more details banciu@meteo.inmh.ro)

See the report on deported work.

14. Operational version in Slovakia

(more details Olda.Spaniel@mail.shmu.sk)

Nothing new since the last Newsletter.

15. Operational version in Slovenia

(more details neva.pristov@rzs-hm.si)

A short overview of present state is given in first part since the reports of operational version have not been prepared regularly during last two years.
Characteristics of operational model configuration have not been changed. To recall:

- 11.17 km horizontal and 31 vertical resolution (80*80 points),
- 450 s time-step,
- 48 hours integration twice per day,
- coupling by ALADIN/LACE every 6 hours.

Since 23th November 1999 the operational suite is running on cluster of 5 workstations (description can be found in Newsletter 14) with Linux as operating system. Four processors are used for the integration. The fifth is used for pre-processing (ee927) and visualization. After the completed integration following products are additionally computed:

- dynamical adaptation of surface wind,
- dynamical adaptation of precipitation (since January 2000),
- meteograms,
- time cross-sections (HRID on pseudotemps since August 2000),
- space cross-sections,
- pseudo-satelite movie,
- precipitation for hydrological models.

Correction of the temperature at 2m using Kalman filter is applied in meteograms. Daily verification between direct model output and observations (SYNOP,TEMP) is performed.

The operational model version is still AL11, however AL12 was installed and is used for the research and development work (701, non-hydrostatic version). Different tools are available: programs dealing with FA files (conversion to Vis5d, GrADS format), visualization with GROM and CHAGAL, computing pseudotemps, HRID, Harpe, computing vertical cross-section (ASCS), source code browser, MANDALAY and code for rewriting SYNOP and TEMP observations from local base.

Meteogram on request as web application was ready in the end of year 2001. Users inside met-service can select any point by clicking on image with model domain, inserting geographical coordinates or selecting a station from WMO catalogue. Beside ALADIN/SI model also ALADIN/LACE or ECMWF can be chosen.

Operational performance of the ALADIN/SI model is also important information. For the most of the days the model started and finished in time. The number of unsuccessfully finished model integrations was reduced by factor 2 in year 2001 comparing to year 2000.

	2000		2001	
	00 run	12 run	00 run	12 run
operational not finished	27 (7.4%)	25 (6.8%)	14 (3.8%)	13 (3.6%)
hardware problems	19	15	4	3
missing LBC	7	6	6	4

Still in reasonable time products were available for additional 13 days in year 2000 and 8 days in 2001, when model was re-run by intervention. Two main reasons for missing runs were hardware problems and non-arrival files with lateral and boundary conditions due various causes. The software and hardware environment is stabilized, however few times integration stopped because of floating point exception error, which did not always occur when model was re-run. A view of the execution times for the 00UTC model run in year 2001 is given in Figure 1. Delays occurred mostly because coupling files were delayed.

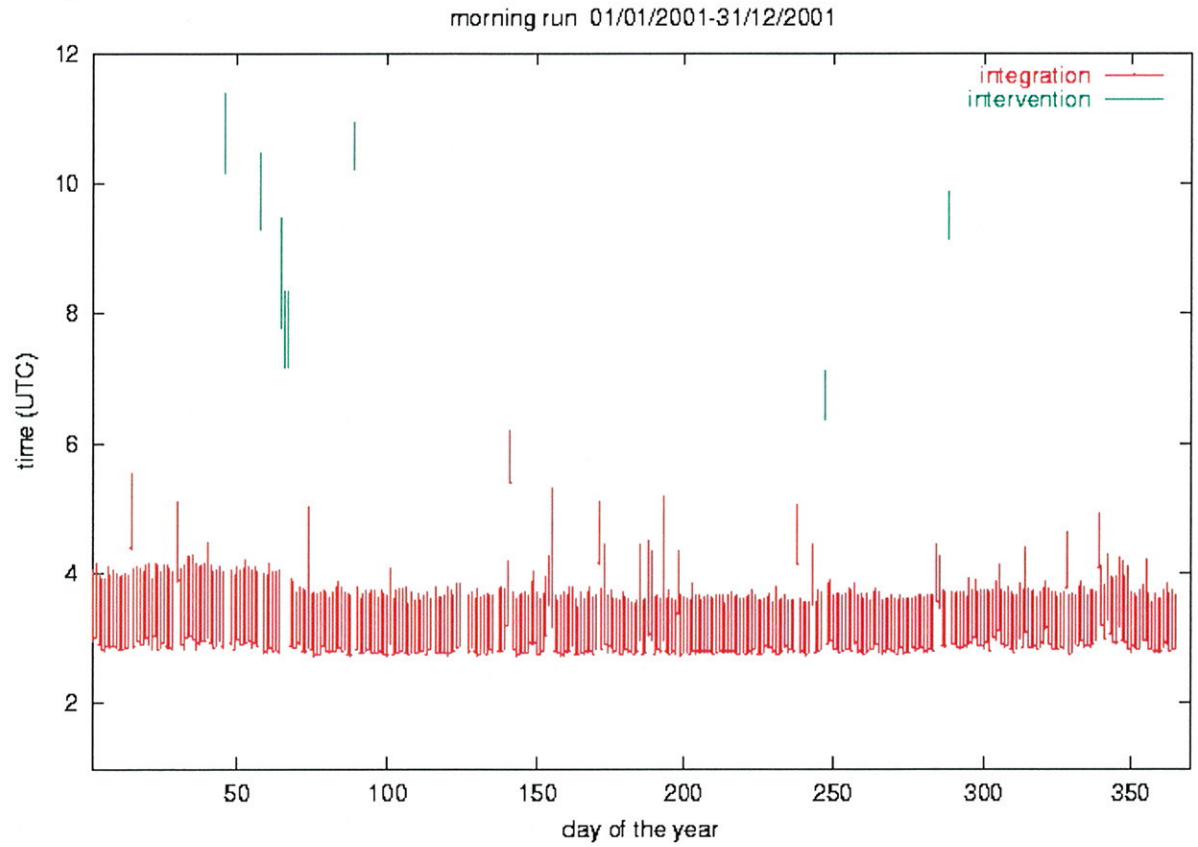

Figure 1: Model integration times for the model ALADIN/SI 00UTC runs in year 2001, operational (red) and re-runs (green).

16. Operational version in Tunisia

(more details nmiri@meteo.nat.tn)

The skill of the youngest ALADIN application is described in a paper.

Deported ALADIN developments during the second half of 2001

1. In Austria

MAP orographic precipitation simulations

Within the framework of the bilateral *Amadeus* project, F. Bouyssel, E. Bazile, and Y. Wang performed additional sensitivity experiments with AL12 on the MAP cases previously studied (see Newsletter 20). Setting horizontal diffusion of water vapour to zero showed little effect, as did switching off digital filter initialization. An academic experiment where a certain supersaturation was allowed to occur (to mimic the cloud water phase and its advection) produced a smoother precipitation field, with smaller amounts, and a downstream shift. It generally brought the simulated field in closer agreement with observations. Unexpected was the large sensitivity of simulated precipitation to the length of the time-step. Changing from 600 to 450 and 300 sec (at $\Delta x=10$ km) gave a significant increase, coming mainly from the resolved (large-scale) part of precipitation. [Further details: *wang@zamg.ac.at*]

Aircraft icing prediction

Experimental daily forecast charts of aircraft icing potential are produced based on ALADIN prognostic fields. The charts can be viewed on-line at :

http://mailbox.univie.ac.at/reinhard.stepanek/icing/icing.html.

The computation of icing potential is based on an empirical formulation developed by the HIRLAM group, with cloud water content, temperature, and vertical velocity as input. It was found that due to the higher resolution of ALADIN-VIENNA compared to the Swedish HIRLAM model, the weight given to vertical velocity in the formulation has to be reduced. Pilot reports from the Austrian civil and armed forces aviation are being collected and studied for verification purposes. [Further details: *reinhard.stepanek@univie.ac.at*]

Prognostic convection scheme

The prognostic convection scheme developed by Gérard (2001) for AL12/CYCORA-bis has been implemented at ZAMG. Experiments on the 10-12 Aug 2000 mountain convection case are being carried out. The goal is to see whether the delayed onset of convection due to prognostic updraft strength and updraft area fraction brings the forecast in closer agreement with radar observations. [Further details: *stefan.greilberger@zamg.ac.at*]

Operational model verification

Starting 2002, a bi-annual operational verification report is being issued by ZAMG. The first report contains a comparison of ALADIN-VIENNA and ECMWF point forecast errors of surface variables for the station Vienna (Hohe Warte) over the last 2.5 years. The figure shows, as an example, results for 10m wind direction and speed. The improvement compared to the ECMWF model is most apparent in wind direction. Note that for wind speed the ALADIN forecast, in spite of a somewhat larger negative bias, manages to have smaller mean absolute error than the global model. [Further details: *klaus.stadlbacher@zamg.ac.at*]

References :

Gérard, L., 2001: Physical parameterizations for a high resolution operational numerical weather prediction model. University of Brussels, Ph.D. Thesis.

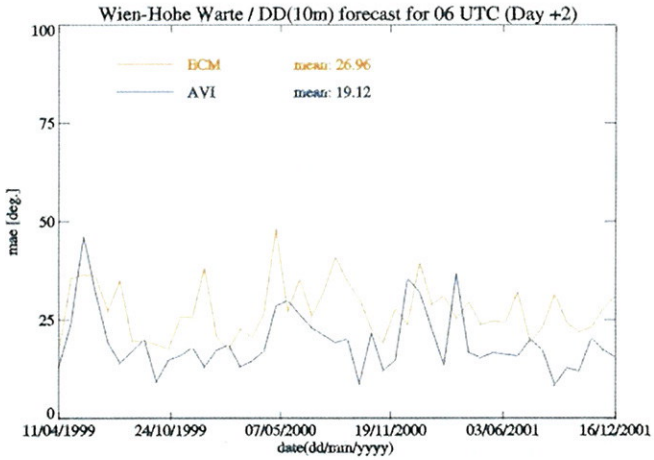

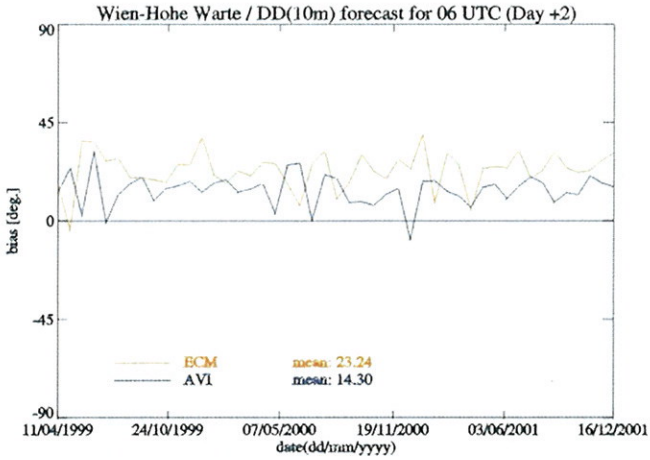

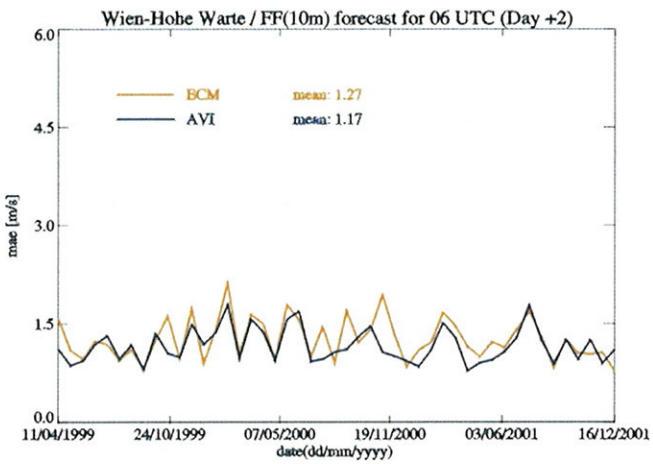

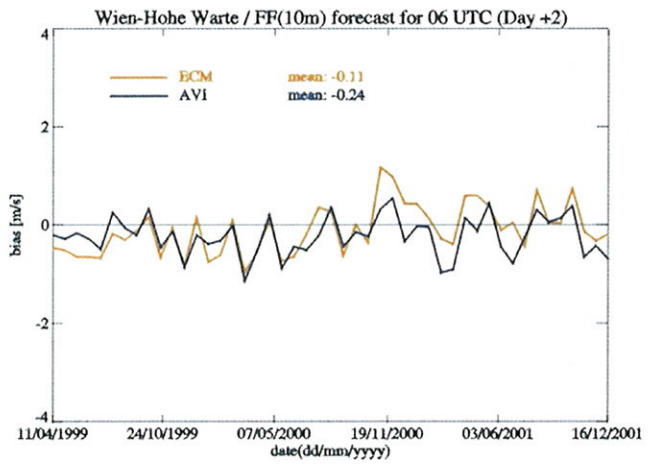

2. In Belgium

Porting to the new computer (Olivier Latinne)

Three months of work were necessary to finalize the migration of the operational ALADIN suite on SGI Origin 3400. Because scripts of the old operational suite were written in standard Kornshell, only some minor modifications were brought, those carried primarily on some parameters of different environment, as well as the suppression of necessity to convert some data files, from "CRAY" to "IEEE 64 bit" formats. The parameters of compilation and execution of ALADIN were optimized, allowing a 48 hour ALADIN run (with 41 levels) to be executed on 16 processors in less than 20 minutes. This number of processors allows a good compromise between the speed of execution of ALADIN and the degradation of performances connected to the increase in the number of processors used. Two comparative tests with the operational chain running on CRAY were successfully realized, for September 19 and 26, 2001. The date of September 19 corresponds of a cyclonic situation, therefore more sensitive to the numerical differences (singularity point corresponding to the cyclonic centre). For the whole of the computed fields only small differences (for instance about 0.1 m/s for the speed of the wind, 1 degree for direction of the wind, 0.1 K for two meters temperature, 1% for humidity) were observed. The purely numerical differences are however probably much smaller, considering that the ALADIN executables on SGI and CRAY used for these tests correspond to two different cycles (and physics). We have however faced many problems during the validation tests, linked to the commercial software of queuing management PBS-PRO. These problems have been corrected by SGI and seem now entirely solved.

Pollution forecasts (Piet Termonia)

This corresponds to the completion of a study demanded by the Brussels Institute for Environmental Management (BIM/IBGE), with the aim to find out whether extreme peaks of pollution in the Brussels region can be predicted using ALADIN. BIM/IBGE provided data of concentrations of the pollutants NO, NO2, PM10, O3. These concentrations where compared to the ALADIN forecasts of a number of meteorological parameters. Two parameters were retained for an operational use: the presence of inversions and a kind of horizontal transport index (wind velocity divided by the Brunt-Vaisala frequency). The results of this research will most probably be applied by the three collaborating institutes RMI, BIM/IBGE, CELINE/IRCEL and the Brussels Ministery of Environment.

3. In Bulgaria

During the stay in Toulouse some experiments were performed over a subdomain of ALADIN-BG with a step of 3 km. The correspondant climatological files were created, and two successful 12 hours runs of the model were realized.

4. In Croatia

See the joint paper.

5. In Czech Republic

See the RC-LACE report.

6. In Hungary

Most of the ALADIN related activities at the Hungarian Meteorological Service were concentrated on ALATNET topics, therefore more details can be found in the ALATNET report of HMS.

At the end of 2001 efforts were done in order to finish the public procurement of the high performance computing facility for the Hungarian Meteorological Service. The IBM company was selected and a 32 processors Regatta server was chosen as future computer of the Service for numerical weather prediction. More details about the machine itself and the migration of the ALADIN code will be given in the next Newsletter.

Roger Randriamampianina started the feasibility study for an implementation of ATOVS data in the ALADIN model. TOVS data were introduced in the ALADIN model (AL11) in summer 1999 (Sadiki and Soci, 1999), but at this stage only the screening was possible. As it was proved (Randriamampianina and Rabier, 2001), the locally received and pre-processed ATOVS radiances have positive impact on subsequent ARPEGE model forecasts and analyses. Moreover, the impact increases by increasing the resolution of the radiances. Based on these results the implementation of the ATOVS radiances in the limited area model ALADIN has special interest. We started this work in autumn 2001. The operational cycle at the Hungarian Meteorological Service is AL12. AL13 is also installed but for research and development only. We apply the one dimensional variational 1d-var assimilation scheme to the pre-processed radiances to obtain quality control flags, vertical profiles of temperature, humidity and surface temperature. We found out, however, that no radiances were injected into the 1d-var. Thus, screening of TOVS/ATOVS radiances is not possible with AL13. The next operational cycle is going to be AL15. Since AL15 with ODB can handle ATOVS radiances (screening) (Kertesz and Fischer, 2001), further implementation of ATOVS radiances should be done with AL15.

References :

Kertesz S. and Fischer C., 2001: Observation management for ALADIN. *Internal report,* available from Météo-France or HMS.

Randriamampianina R. and Rabier F., 2001: Use of locally received ATOVS radiances in regional NWP, *SAF NWP report*, available at Météo-France, HMS or U.K. Met. Office.
Wafaa S. and Soci C., 1999: The observation screening in ALADIN 3D-Var data assimilation system. *Internal report,* available from Météo-France.

Regarding other topics of interest the following activities can be mentioned:
-- A special interface was written in order to provide forecasted radiation components of the model. The forecasted data are compared to the real observations and the throughout analysis also concluded some properties of the radiation parameterisation scheme of the model (article to be found also in this Newsletter).

-- The work on the application of ALADIN precipitation forecasts for hydrological purposes has been continued. The obtained results provide verification of the precipitation fields of the ALADIN model (a separate paper on that topic is planned for the next Newsletter).

7. In Moldova

Nothing new.

8. In Morocco

Most of the effort of the ALADIN team was devoted to the implementation of the operational suite and of a 3d-var assimilation suite on the new computer. See the report on operations for more details.

9. In Poland

Yet another dark side of NWP operational work

In the end of 2001 the Cracow ALADIN Group network was attacked by hackers. Three machines were compromised including our group server. In two cases it was possible to reveal most of elements of the intrusion anatomy. The likely way to hack the machines was exploitation of bugs in versions of *ssh* or *wu-ftpd* installed on our computers - in the end of the year there were exploits widely available in the Internet. After gaining root privileges hackers installed rootkits to hide their presence in the systems and to prepare easy further access to the machines. In one case "*bobkit*" rootkit was used and in another one a clone of "*t0rn v8*". Both rootkits provide hacker with replacements of some commands (among them *ls*, *find*, *du*, *ps*, *pstree*, *top*, *ifconfig*, *netstat*), Trojan versions of other (*ssh*, *login*, ...) also with backdoors, log cleaner, sniffer and some additional libraries.

The presence of the intruders was discovered due to some suspicious behaviour of the systems (e.g. some logs were incomplete). Quick search through catalogues with *mc* showed presence of strange names as "..." or ".. " (of course not seen with replaced *ls*) and proved that somebody installed his malicious stuff. The scanning of tripwire logs and usage of installed *rpms* database revealed more. In latter stage of search we also used *chkrootkit* tool. Analysis of hacker's software made possible to prepare a little trap. Knowing number of port which was being used by hacker backdoor we put it into ports entry configuration file and we waited what would happen. After several days the hacker tried to go back to our server. Firstly he tried to use Trojan *ssh* and he failed, next he tried to use installed backdoor and the trial was automatically blocked. In logs we found out information which made possible to establish that a computer of an institution in Seoul was used to perform the attack.

As a consequence of intrusions two systems had to be installed from scratch and another one was refreshed. We were forced to build a firewall to make protection of our network more reliable and take some additional security measures which increase overall cost of our network administration. Actually we test LIDS package, which is likely to be installed on group server in near future.

10. In Portugal

At 30th of July 2001 (12 UTC run), after a parallel suite during one month and a half and an objective verification for the same period, we introduced AL12_bf02 version (with CYCORA-bis included) in our operational suite.

An objective verification for six months (24th of January - 24th of July), using AL11T2_03 and AL12_bf02, showed that the switching on of CYCORA-bis physical package in ALADIN-Portugal had a nearly neutral impact on the forecasts.

On the analysis/assimilation field the CANARI (AL12) / DIAGPACK is being installed.

The developed diagnostic tools, divergence of Q vector, low-level moisture convergence (1000-850hPa), K-index, Modified K-index, Total-Totals index, Modified Total-Totals index and SWEAT index, were tested on two severe weather events of deep convection, over Portugal. One associated with a cut-off low and the other associated with a strongly precipitating cold frontal system.

A major effort was also devoted to the organization of the 11th ALADIN workshop.

11. In Romania

Simulation of convective systems at different resolutions (Doina Banciu)

The experiments on the simulation of the Cleopatra have been continued by testing the mixed solution (included in CYCORA-ter) for the resolution dependency of the convective scheme: a combination of the explicit dependency method used before CYCORA package and the limitation of the available humidity convergence for the convective scheme by substracting the large scale precipitation, method used in CYCORA packages. The results have shown that the problems encountered in the evolution of the convective and stratiform precipitation when increasing resolution have been cured by using the mixed solution (more details can be found in "Precipitation: resolution and orography" by D. Banciu, S. Alexandru, E. Bazile, L. Gérard and K. Stadlbacher, to appear in the EWGLAM Newsletter, no. 31/2001)

Comparison between CYCORA and CYCORA-bis packages (Simona Stefanescu)

The test carried out before the implementation of CYCORA-bis package in operational have not shown dramatic changes in comparison with the simulation using CYCORA (operationally for the test period in September). The areas covered by precipitation, the speed and the partition between convective and stratiform precipitation are quite similar. However some unrealistic areas of precipitation disappeared by using CYCORA-bis package. Also few differences in the maximum of precipitation amount were noticed.

Implementation of the Aladin model on a SUN platform (Doina Banciu)

The ALADIN Model (version 12) have been implemented on a SUN E4500 server having 8 UltraSparc processor of 400 MHz, with the generous help of Gabor Radnoti. To be able to run the model on this platform it was necessary to re-configure the system for 64 bits environment and to change the compiler Forte 6 HPC update 1 to Forte 6 HPC update 2. Even the SUN platform performance is far from our needs, it is an important improving regarding our old platform DEC and it will allow us to enlarge our operational domain and to integrate the next Aladin versions.

Aladin Meteograms (Steluta Alexandru and Simona Stefanescu)

Meteograms for the main 10 cities over Romania are available on the internal web, for forecaster use, twice per day, till 48 h range. The surface and upper air fields represented are: mean sea level pressure, 2 m temperature, 10 m wind, total precipitation, total and low cloudiness, temperature and wind for 850, 700 and 500 hPa levels.
An example of such meteogram is presented for Oradea.

12 FEB 2002 ora 12

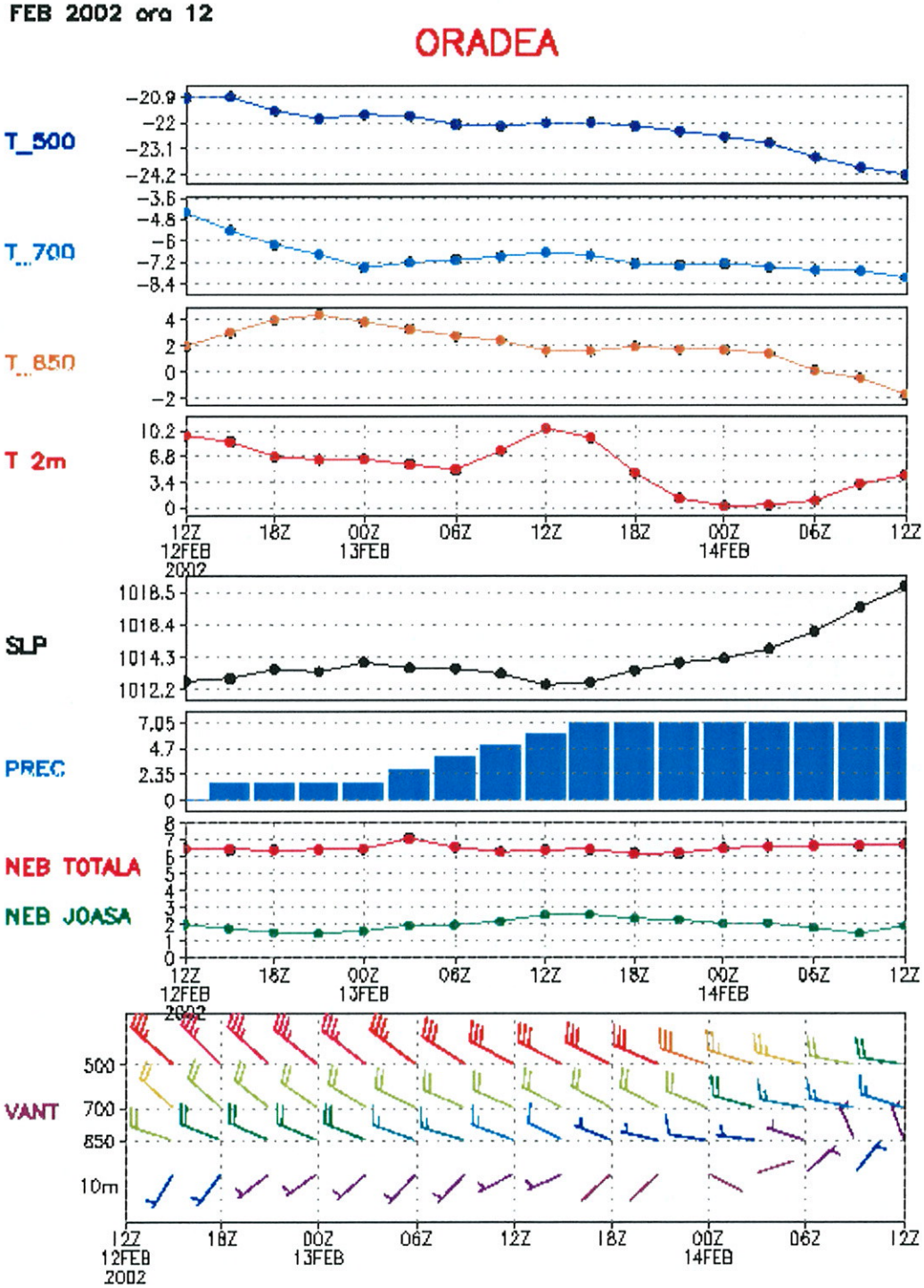

Experiments on the background error statistics for the ALADIN 3d-var data assimilation (Simona Stefanescu under the supervision of Loïk Berre)

The experiments are based on the work of Mohamed Raouindi and Loïk Berre, which have carried out a study on the spectral representation of the latitudinal variability of the bi-dimensional forecast error covariances for temperature at level 18, derived using the NMC method from the ARPEGE coupling files for the ALADIN/Morocco integration domain over a 87 days winter period.
Continuing their experiments, the longitudinal variability of the temperature forecast error covariances was studied. There were realized pseudo-single-observation experiments including calculation and plotting of the latitudinal and longitudinal variation of the correlation function for different locations of the observation point. The latitudinal and longitudinal variation of standard deviation and length scale of the correlation function was investigated. Different evolutions for the latitudinal and longitudinal variability have been observed. The correlation length in "x" direction decreases when increasing the latitude and it can be seen an anisotropy of the correlation function in "y" direction at the northern part of the domain explained by the limits between two regions with very different features (tropics and mid-latitudes). The longitudinal variability study revealed a decrease of the correlation length in "y" direction when decreasing the longitude. In "x" direction, the anisotropy of correlation function is not so obvious like for "y" direction. This will be deepened by the calculation of the spatial variations of the length scales of the covariance functions.

12. In Slovakia

See the papers by Jan Masek and Martin Bellus.

13. In Slovenia

The main developments are described in the section about operations and in a paper by Mateja Irsic and Neva Pristov.

14. In Tunisia

Most of the effort was devoted to the setup of the environment for ALADIN-Tunisia (visualization for forecasters, verification, benchmark and administrative tasks to buy a dedicated computer, ...). See the corresponding paper.

ALADIN developments in Prague during the second half of 2001

Note: all ALATNET related R & D, representing the majority of the effort, is reported in ALATNET Newsletter. Here we sum-up topics which are not referred as ALATNET ones for Prague centre.

Developments in physics

- Convective onset study

A behaviour of the deep-moist convection scheme in ALADIN was studied in the Alpine area. As a first step the summer testing situations were chosen in such a way that the large-scale synoptic forcing was weak, hence the orographic forcing and local heating were dominant. ALADIN was able to simulate the convection in quite a realistic way, except that it was starting systematically too early in the model with respect to the reality. One plausible reason for this early start of convection is that the model PBL is too moist. However it was very difficult to evaluate the realism of humidity profiles: there are too few soundings available around the studied area.

More details can be asked to : Stephan Greilberger and Thomas Haiden.

- *"Adriatic storms" study*

We could observe a few cases of a very strong cyclogenesis simulated by ALADIN over the Adriatic Sea last summer. The model produced quite a deep, small-scale cyclone over the sea, looking unrealistic (too deep). It was figured out that this strong cyclogenesis was present in all ALADIN applications covering the area. There were 3 periods with this strong cyclogenesis : **a)** 17-18th June 2001, **b)** 20th July 2001, **c)** 3-4-5th September 2001. For all these situations the model had a very similar behaviour, regarding the sensitivity to CYCORA-x packages. The weakest cyclogenesis was observed for the pre-CYCORA settings. When getting convinced on the similarity of the model simulations, the case of 20th July was studied more in depth. What was possible to conclude from the available observations (unfortunately absent on the sea surface) was that the forecast was very realistic despite the exaggerated deepening above the sea. There was a cyclogenesis in reality and the diagnosed model fields were corresponding to the cyclogenesis process known in literature for the Adriatic Sea area. A few tests changing the tunings of the physics were made but without having any impact on the forecast. The only found modification to weaken the cyclone was to cut the evaporation from the sea surface. We did not succeed to discover which mechanism(s) were responsible in the model to get so active deepening. Nevertheless these cases are very interesting and shall be used as benchmark for new modifications made in the ALADIN physics.

More details can be asked to : Zoran Vakula, Radmila Brozkova and Jean-François Geleyn.

- *Sensitivity study of the radiation scheme*

The aim of this work was to help in the effort made on development and tuning of the radiation scheme. The radiation scheme is a part of CYCORA-x packages, however, the very last modifications meant to enter the CYCORA-bis package had to be abandoned due to their unstable behaviour when going to 41 levels. Since the problem is quite complex, the work made in Prague aimed at the detection of the most sensitive namelist parameters for the computation of gas absorption coefficients. This was made by comparing to reference results obtained from a more complex but expensive radiation scheme (with 1d column model), all this for 50 vertical profiles chosen randomly around the globe, with special emphasis on one of them. As outcome some better understanding of the scientific problem was reached.

More details can be asked to : Helga Toth, Roger Randriamampianina, Jean-François Geleyn.

Developments in the verification

The verification script based on VERAL was created in order to produce monthly scores for the EWGLAM list of stations. This procedure will take into account all the developments made up to now.

More details can be asked to: Dijana Klaric, Zuzana Huthova, Martin Janousek.

Technical developments

- *TUC: Transparent Use of Clearcase*

When moving the R & D environment to new work-group server *voodoo*, the source-code-utility tool, previously based on MaK software was rebuilt on the shareware software CVS. In order to make the life of developers easy, a set of scripts was prepared in the similar spirit like for ClearCase use at GMAP. Hence, "happy tax payers" may find the familiar commands like "cc_get", "cc_edit", "cc_add", etc..., and also the ". cc_quit" one. There is a documentation available on *voodoo* and the first cycle to be tried is AL15/CY24T1_op1.

More details can be asked to : Filip Vana, Tomas Kalibera.

- *porting the cycle AL15*

Within the fall of 2001 the cycle AL15/CY24T1 was ported to the NEC SX4 platform. In fact, two branches were ported: the branch "op1" for validation, since it is scientifically the same like the current operational version of ALADIN/LACE (CYCORA-bis), and branch "op2", containing the modifications of CYCORA-ter. Within the porting two general bugs were already found and reported: missing interface in one routine in the ALADIN transform package and a bug in computation and write-out of the fluxes. Despite the fact, that these bugs were real ones, they were not detected on the VPP platform. The cycle was validated on 1 processor and gave bit-identical results in the adiabatic mode as the previous cycle. However, another bug manifests itself when the run is switched to more processors: straight after reading the initial conditions and filling the SPA3 & SPA2 arrays the spectral norms of vorticity are affected in a systematic way. The investigation continues.

More details can be asked to: Martin Janousek

- *porting ODB*

The ODB software to create and treat the observation files was ported to the SX4 platform last summer. However, it was not tested yet due to the problems detected in the model cycle.

More details: Metod Kozelj

ALADIN developments in Toulouse during the second half of 2001

The life of permanent staff and visitors in GMAP was strongly perturbed along these months, by 3 successive bursts :

- 11th of September, with its "Vigi-Pirate" counterpart (requiring to present papers whenever entering the site, forbidding to work early or late or during week-ends, ...),
- 21st of September, with some frightening hours and the lost of a few doors and windows in the building,
- the announcement of "ARTT" measures in December, leading to a significant demoralization of the permanent staff and also to a real waste of time.

However we managed :

- to publish the Newsletters;
- to organize a small mini-workshop (10-14/12/2001) to prepare the new medium-term research plan for ALADIN, with contributions from Alica Bajic *(reporter for verification)*, Doina Banciu *(reporter for physics)*, Radmila Brozkova *(reporter for dynamics)*, Ryad El Khatib *(reporter for maintenance)*, Claude Fischer *(reporter for data assimilation)*, Dominique Giard *(reporter for training)*, Jean-François Geleyn *(reporter for operations)*, Thomas Haiden, Jure Jerman *(reporter for applications)*, Jean Nicolau *(reporter for predictability)*, Gabor Radnoti *(reporter for coupling)*, Jozef Roskar, and other ARPEGE / ALADIN scientists in Toulouse at that time;
- to complete the phasing of the assimilation and 923 stuff, building an up-to-date cycle AL15, thanks to Claude Fischer (as usual), Françoise Taillefer, Ryad El Khatib, Jean-Marc Audoin, Dominique Giard, Patrick Saez, and Andrey Bogatchev, Alex Deckmyn, Sandor Kertesz, Valery Spiridonov (+ Neva Pristov from Ljubljana);
- to progress in scientific issues as described below and in the ALATNET report.

Lora Gaytandjieva, Françoise Taillefer and François Bouyssel carried on the work on snow analysis, with some more refinements / simplifications and tests in assimilation mode in ARPEGE. There are still problems, mainly related to vertical interpolations, the lack of quality control and the low density of observations. Sorry, once again it didn't move to operations before winter !

Natalia Camara investigated with François Bouyssel two problems of surface analysis, (i.e. optimal-interpolation analyses of 2 m-temperature, 2 m-relative humidity and 10 m-wind), in the framework of the ALADIN-France version of Diagpack. A reduction (by about one third) of the characteristic lengths for observations allows to use far more data without introducing additional noise, and to get closer to observed fields. An attempt to reduce noise in analysed 2 m fields was performed. The soil moisture of the first guess was arbitrarily fixed to a mean (and sensible : average of field capacity and wilting point, depending only on clay fraction and soil depth) value everywhere. This led to smoother 2 m fields, especially for temperature, and smaller analysis increments, even when changing only superficial moisture. Moreover the analysed relative humidity is closer to observations.

Stjepan Ivatek-Sahdan also aimed at improving the analyses of 2 m fields, but this time in the framework of data assimilation, and addressing the statistical model. He performed a detailed study of forecast-error statistics, based on the computation of "observations - first guess" correlations on a large range on situations (Lönnberg-Hollingsworth method). Results were examined for 4 domains (Europe, USA, Africa, Australia) over 2 months (December 2000 and June 2001), and for twice 3 months (winter, summer) over Europe, to study the geographical and seasonal variability. This demonstrated that the old statistical model, deduced from that of upperair analysis in CANARI, required significant adjustments. The formulation of the coefficient of correlation with distance was changed :

$$\text{from} \qquad \rho_{T/H} = \exp\left(-\frac{r^2}{2a^2_{T/H}}\right) \qquad \text{to} \qquad \rho_{T/H} = \exp\left(-\frac{r}{2a_{T/H}}\right)$$

and those of the standard deviations (σ) and characteristics lengths (a), depending on the mapping factor *m*, retuned :

$$\sigma_{T/H} = \sigma^0_{T/H}\exp\left[-\alpha(m-1/m)\right]^2 \qquad a_{T/H} = a^0_{T/H}\exp\left[-\alpha(m-1/m)\right]$$

with α changed from .02 to .05, (σ^0_T, σ^0_H) from (2.3 K, 17 %) to (1.7 K, 13 %) and (a^0_T, a^0_H) from (350 km, 300 km) to (105 km, 100 km). The experimental and parameterized formulations of the coefficient of correlation are illustrated hereafter. The oscillations observed for Africa (and worse for Australia) are due to the lack of observations over these domains.

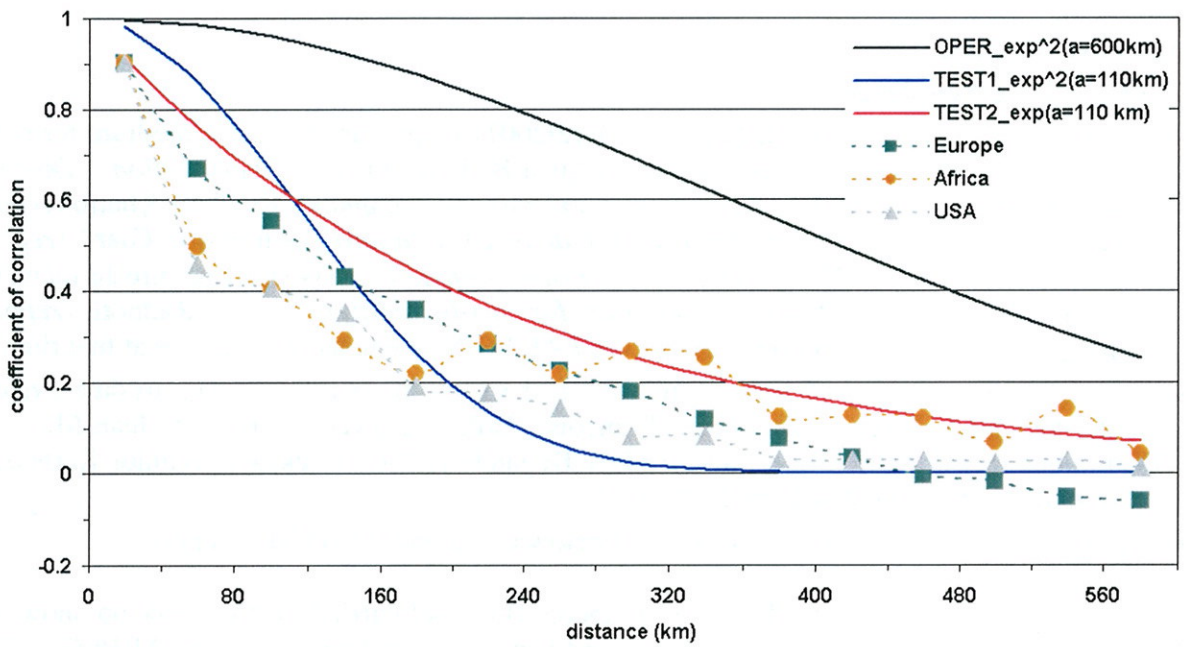

Coefficients of correlation for 2 m temperature: dependency to distance between points for different domains and June 2001 / for different correlation functions

There is a clear seasonal variation of the correlations, slightly weaker over Europe. Tests were performed with ARPEGE with "single-obs" experiments first, then on real situations, to compare the old and new formulations. There is a significant impact, especially in the Southern hemisphere. More experiments are now required to validate or refine the new statistical model.

Françoise Taillefer improved the French pre-operational version of Diagpack (use of more surface observations, new visualization tools).

Rashyd Zaaboul studied ODB, and ported it to the new IBM computer in Casablanca. His report and that of Sandor Kertesz provide a detailed and useful documentation on ODB for ALADIN (in English and in French) : structure, tools, use, compilation, ... Considering the parallel training of Philippe Caille, the ALADIN project can now rely on several experts in ODB.

Martin Janousek and Jean-Daniel Gril analysed together how to interface the new EGGX with the ALADIN & co libraries. We may hope it will be available in the next cycle.

Yong Wang came twice in Toulouse, in the framework of the bilateral AMADEUS project ("Improving the description of precipitations over mountainous areas"). The first stay was devoted to the design of a working plan for the analysis of precipitations, the second one to the possible refinements in the definition of the model orography.

Khoudir Tounsi and Mohamed Hajjej were trained to the use of ALADIN by Jean-Daniel Gril, and performed some case studies with ALADIN-Tunisia for convective events. The vegetation and the orography of the model were carefully controlled, and a new post-processing grid designed.

Besides Jean-Daniel Gril started to make to main ALADIN tools fully portable and to fight with the auxiliary library.

Siham Sbii, with some help from Jean-Marcel Piriou, developed a promising "model to satellite" application. Two additional modules were introduced in the ARPEGE physics to compute simulated cloudy and clear-sky brightness temperatures : first the computation of spectral luminances using the radiation scheme of J.J. Morcrette, second the channel selection and computation of brightness temperatures (to be compared to observed satellite images). As a first step, 4 fields are available (and stored as instantaneous fluxes) : cloudy / clear-sky for infrared / water vapour. The chosen radiation scheme is expensive but covers a wide range of wavelengths, which allows selection for several satellite channels. An alternative is to run as many cheap radiation schemes as required channels. The second necessary step was the management of observations : decoding raw GRIB data to obtain the same output format (latitude, longitude, temperatures), then filtering out stupid values, in order to be able to plot simulated and observed fields with the same colouring.

Martin Bellus, Martina Tudor and François Vinit investigated some odd behaviours of the operational ARPEGE and ALADIN suites. The study of Martin Bellus is described in a separate paper. François Vinit pursued the analysis of the "Trafalgar" case, without finding more indices on the origin of problems. Martina Tudor started on the diagnostic of PBL height. It was computed by searching from the first model level where the Richardson number reaches the critical value 0.5, starting from the surface. But this led to unrealistically low or high values of PBL height in case of a very cold or warm surface. To solve this problem it was decided to start from the lowest model level. This was efficient in removing extreme values but revealed unpleasant wave patterns, associated to very strong horizontal and vertical gradients of temperature. This is clearly due to a fibrillation problem, inducing a computational mode of period twice the time-step. Several remedies were tried. Some partly attenuated the problem, some solved it but cannot be used operationally, some made the situation even worse ...

What proved efficient is a severe reduction of the time-step (divide by 2) or a uniform anti-fibrillation scheme (as applied in IFS). But retuning of the ARPEGE anti-fibrillation scheme, designed to be active locally, only where there should be problems, didn't lead to any improvement (on the contrary !). A first hypothesis to explain this behaviour was that this might be related to the underlying assumption that anti-fibrillation is useless in unstable cases : problems appeared on domains where the atmosphere was unstable in this situation. Later it was found that the anti-fibrillation scheme was in fact responsible, converting temporal oscillations into vertical ones when submitted to strong constraints. A solution is to reduce its spatial variability, limiting variations on the vertical. We may hope to have soon a nice PBL-height diagnostic available in ALADIN and ARPEGE.

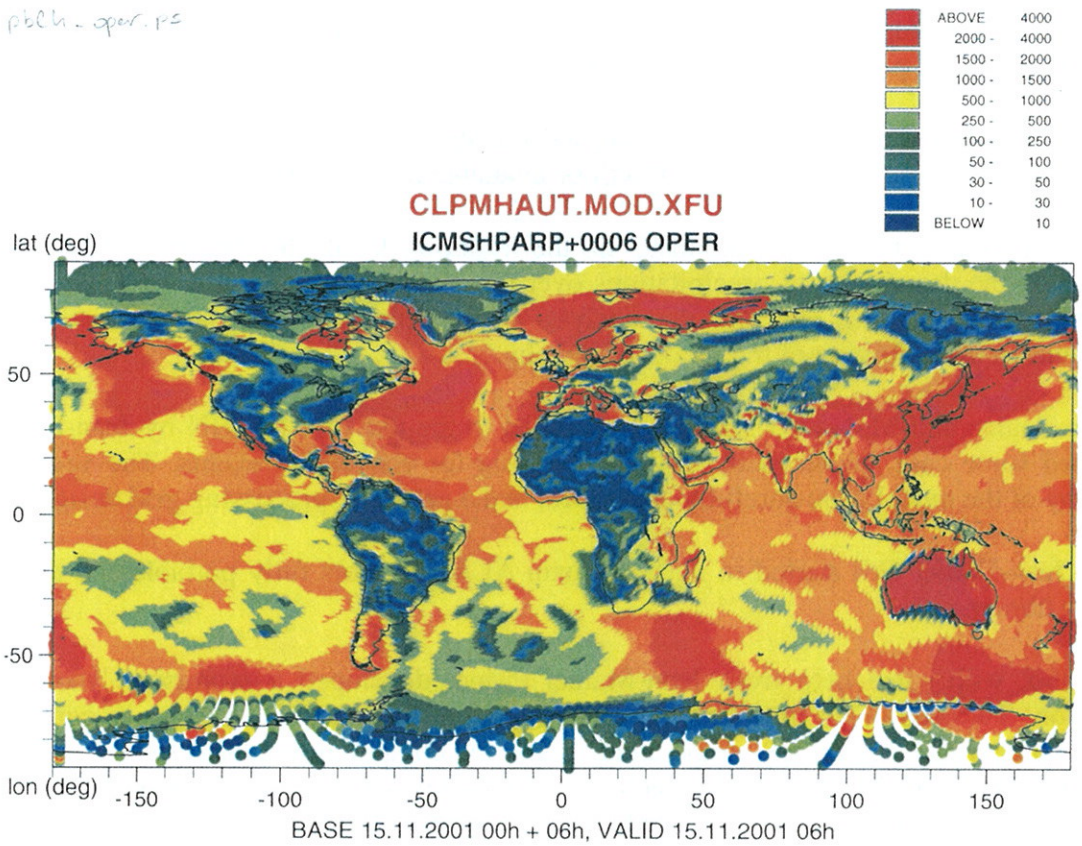

Figure 1. PBL height (old computation)

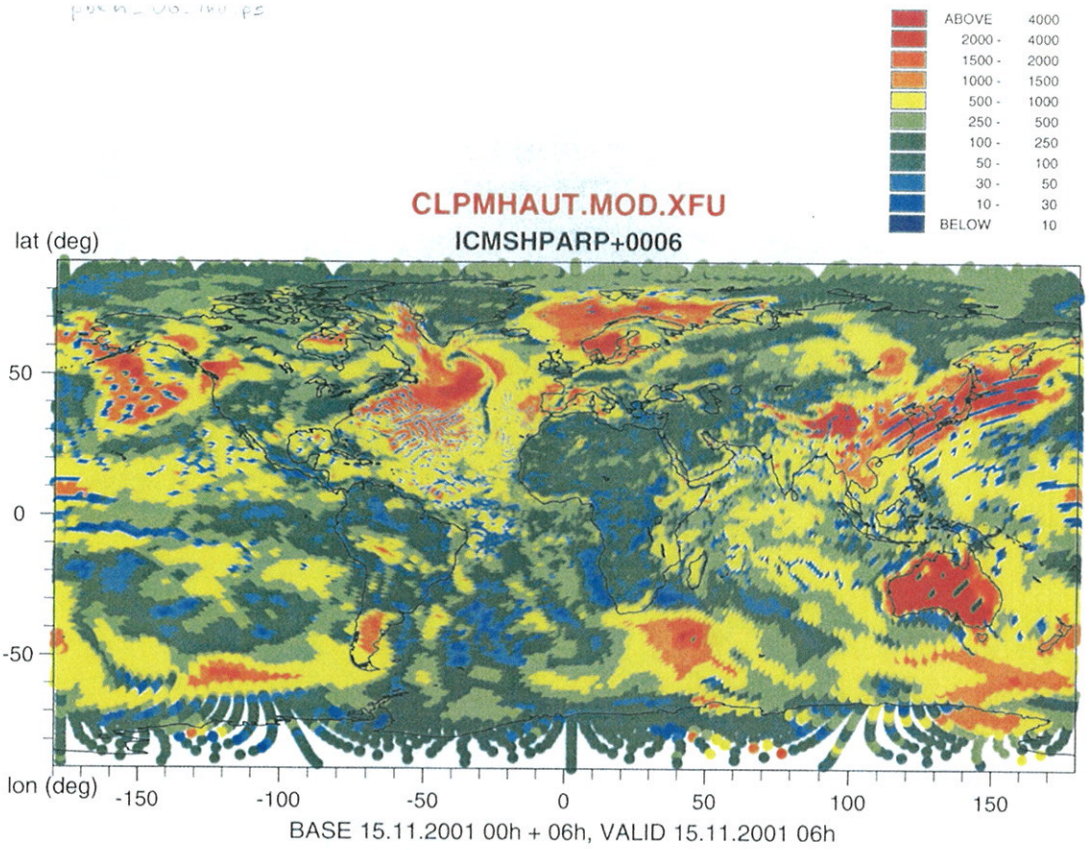

Figure 2. PBL height (new computation)

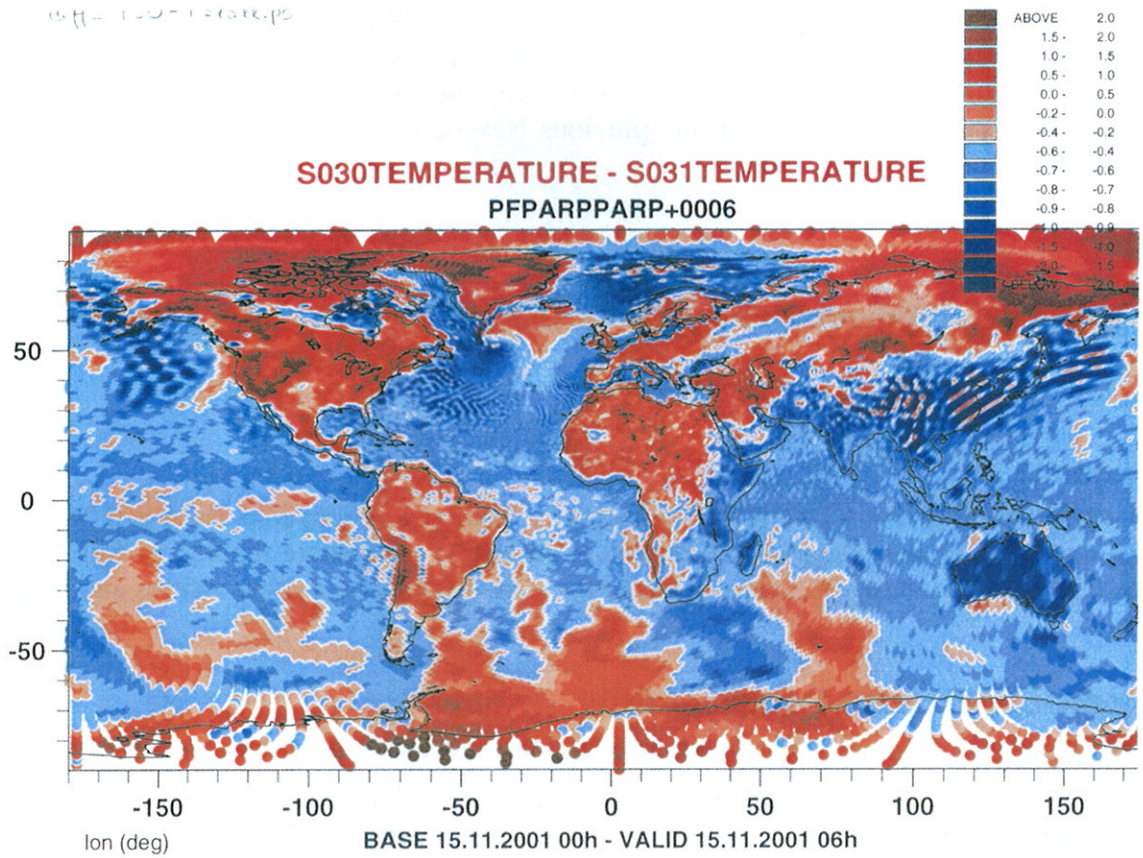

Figure 3. Difference between temperature fields at the two lowest model level (T30-T31)

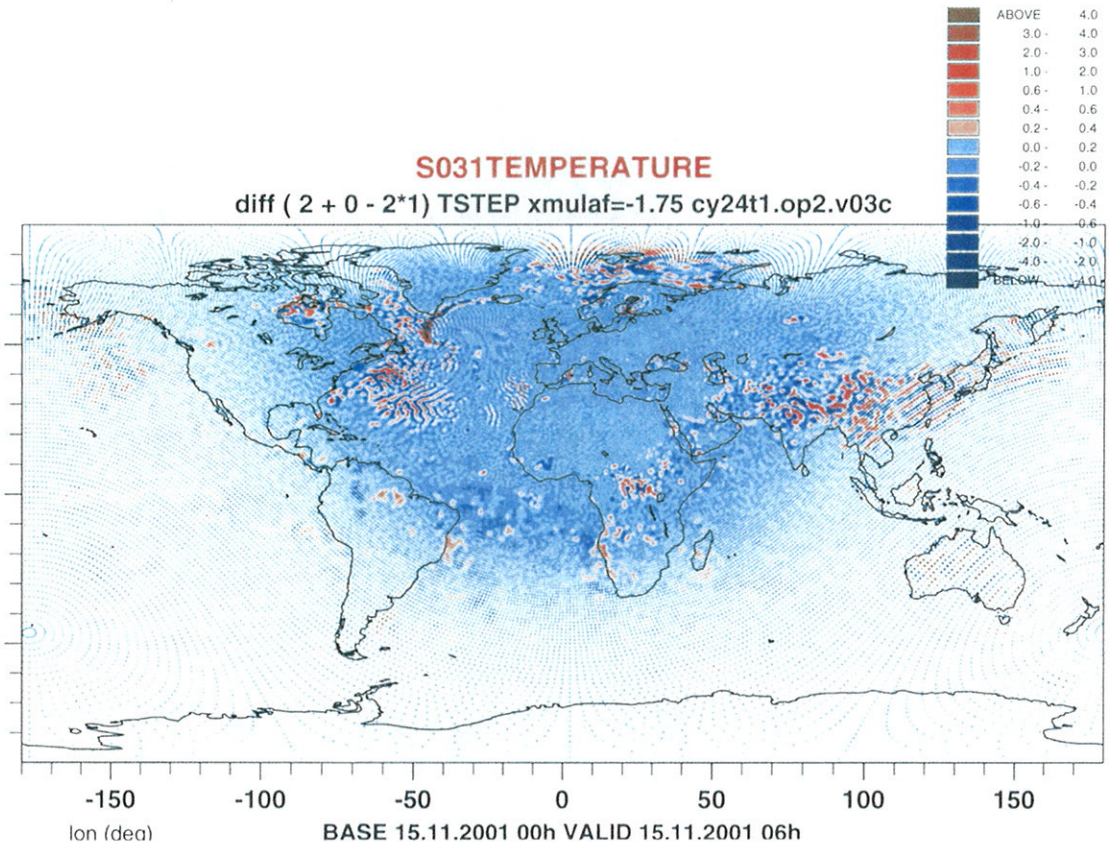

Figure 4. Impact of time discretisation : $T(t+2\Delta t)+T(t)-T(t+\Delta t)$, Δt=900s, at level 31

To end with, a lot of work was devoted to the operational ARPEGE and ALADIN suite : investigating problems within 4d-var (spurious humidity increments, retuning of horizontal diffusion, sensitivity to resolution and time-step, instabilities, ...), debugging the convection scheme, preparing 3 major changes : "New cycles" (described in the previous Newsletter), "CYCORA-ter" and the increase of resolution, correcting mistakes, etc ...

ALATNET developments during the second half of 2001 in the ALATNET centres

1. In Toulouse

The work of the four ALATNET PhD students in Toulouse, Gianpaolo Balsamo, Margarida Belo Pereira, Cornel Soci and Malgorzata Szczech, is described in separate reports, as well as other PhD reports. The summary hereafter corresponds to the joint efforts of the other visitors and the permanent staff.

1. Theoretical aspects of non-hydrostatism (NH)

a) Semi-Lagrangian advection (Pierre Bénard, Jan Masek, Alix Prudhomme)

Previous analyses of the stability of the semi-implicit scheme for 3-time-level semi-Lagrangian advection proved that the initial choice for the pair of additional NH variables (to represent the departure from hydrostatic pressure and the vertical divergence) did not allow stability for realistic

flows. A new pair, named (P - or q=ln(1+P)-, d3) was proposed instead[1]. However further studies showed that stability is no longer ensured in the presence of orography, so that once again the semi-implicit scheme must be iterated for part of the nonlinear terms. This partial iteration must be avoided if these variables are to be combined with the use of a more general predictor-corrector approach and a 2-time-level scheme.

A linear stability analysis considering orography led to the proposal of two new choices for the pseudo-vertical divergence variable, d4 and d5. They are identical analytically, differing only through the time-discretisation of equations. One may expect that d4 would be more precise than d5, but reversely more problematic for the further introduction of diabatism. These two new variables were coded in the 2d (vertical plane) version of ALADIN, and the corresponding stability of NH dynamics systematically studied. Of course the validation, starting from simple academic experiments and examining a wide range of conditions, is only at the beginning. Some noise was observed with d5 near the upper boundary (intrinsic problem or bug ?), and some side problems noticed.

Besides Alix Prudhomme tried to reproduce notorious academical experiments (Héreil and Laprise-1996, Robert-1993) using the vertical plane model, in hydrostatic and non-hydrostatic dynamics. The sensitivity to several parameters was tested for the Héreil-Laprise experiments : background, decentering, filtering of orography, coupling zone, sponge, ... Attempts to simulate Robert's bubble were less successful, since the upper sponge layer introduces distortion.

b) Stability of Eulerian advection

Alena Trojakova investigated in details the stability of Eulerian NH dynamics. She designed a quasi-academic framework, called *ALPIA*, with 5 embedded models of increasing resolutions (from 10 km to 625 m horizontally, from 34 to 128 levels vertically) covering Western Alps and a very simplified initial flow. For each resolution, she tried to determine the maximum time-step ensuring stability, and the corresponding range of CFL numbers reached along the forecast. These CFL values decrease regularly as the resolution increase. At each step, the flows corresponding to the reference and maximum time-steps were also compared. Problems appeared when reached a mesh-size of 2.5 km, requiring a parameterization of the tropopause (to avoid too strong vertical gradients) and a change in NH variables (the initial pair was used for the first experiments).

c) Upper boundary condition

Martin Janousek resumed the work on the radiative upper boundary condition, starting from a recent proposal from Purser and Kar.

4. Removal of the thin layer hypothesis

The case of semi-Lagrangian advection was addressed.

6. Specific coupling problems

Jean-Marc Audoin resumed the work from Tamas Szabo on the coupling of tendencies for surface pressure (so as to limit problems related to differences in orography between the coupling and coupled models). He had first to introduce the modifications in the latest library. He focused afterwards on validation, in the framework of real 3d case studies (while the initial tests were mainly 2d ones). There are still unsolved problems.

8. Adaptation of physics to higher resolution (*Improved representation of boundary layer*)

[1] cf. the review-paper in the proceedings of the 10th ALADIN workshop

Jean-Marcel Piriou designed a new interactive formulation of mixing lengths depending on vertical stability. Tests were performed in the 1d and 3d model. He also analysed the problem of too frequent triggering of shallow convection, in the framework of the EUROCS Stratocumulus Case experiment.

Other refinements were intensively tested and introduced in the operational suite within the "CYCORA-ter" package. They are described in the previous Newsletter (A summary of the latest changes in the parameterization of turbulent fluxes and PBL processes, by Jean-François Geleyn).

9. Design of new physical parameterisations (9d: Improved representation of land surface, including the impact of vegetation and snow)

The new snow description was refined and intensively validated by Eric Bazile, while Adam Dziedzic investigated the skill of a more sophisticated one. Their work will be described in a dedicated paper in the next Newsletter.

Olivier Latinne started a comparative study, in 3d-variational assimilation mode for ARPEGE, to assess the impact on the forecast of the use of a new database, of very high resolution, in the definition of physiographical fields in ALADIN and ARPEGE (vegetation and soil properties).

11. 3D-Var analysis and variational applications

a) Definition of new background error statistics

Loïk Berre computed the spectra of differences between ARPEGE and ALADIN forecasts valid for the same dates and ranges, in order to evaluate the part of small scales and validate the so-called "lagged-NMC" method used to compute background-error statistics for ALADIN.

He resumed the work of Mohammed Raouindi on the geographical variability of such statistics (impact of latitude first) and showed it is possible to introduce it in the formulation of Jb using a simple block-diagonal matrix. This work is now extended to longitudinal variability and a new formulation of Jb, in cooperation with Simona Stefanescu (Ro) and Alex Deckmyn (Be).

b) Cycling : investigation of potential combinations with blending and initialization

Adam Dziedzic, with some help from Claude Fischer, prepared and tested a "Blendvar" assimilation suite for ALADIN-France. Here the DFI-blended initial state is used as the first guess for 3d-var analysis and an additional, external, digital filter initialisation (DFI) is applied afterwards. He ran it over 3 days (28-29-30/12/2000) with a cycling period of 6 h. 48 h forecasts were also run starting from the 00 UTC analyses. This allowed a validation of the latest version of 3d-var and the study of the impact of initialization : with different stop-band edge periods (3 h as in operational dynamical adaptation mode or 1.5 h to reduce damping), and when applied to analysed fields, to the increments of 3d-var analysis or to the combined increments of blending and 3d-var. Investigations (looking at initial and forecasted fields, and at the time-evolution of some variables at 3 gridpoints) showed very small differences between incremental initialization and no initialization. Only full DFI allows to filter noise along the first hours of forecast (with little impact of the stop-band edge). Of course differences decrease with the range of forecast, the maximum ones are obtained at 3 h.

c) Development of variational type applications

Claude Fischer wrote a documentation on the use of variational tools for the a-posteriori validation and the retuning of data assimilation systems. A first diagnostic tool for the a-posteriori validation of 3d- and 4d-var was designed.

d) Management of observations in 3d-var / Screening

Sandor Kertesz updated screening (i.e. the quality control and geographical selection of observations for 3d-var) for ALADIN with Claude Fischer, and built its interface with ODB ("Observation Data

Base", the new tool for observation management just upstream the model). He designed a procedure to build specific "LAM_ODB" databases for ALADIN, containing only observations in the ALADIN domain and wrote the corresponding documentation.

He focused afterwards on the problem of thinning (geographical selection) of AIREP (aircraft) and SATOB (satellite) data, over the ALADIN-France domain. AIREPs provide informations on wind and temperature, with a large dispersion in space (mainly around / between airports) and time (with a peak between 12 h and 18 h UTC) . With the operational thinning distance in ARPEGE, 170 km, most data are rejected. Experiments with decreasing horizontal thinning distances, down to 10 km, were performed. The main improvement is obtained between 25 and 10 km. An impact on 3d-var analysis increments is noticed in the upper troposphere and the stratosphere for wind, in the boundary layer and the stratosphere for temperature. This study enabled to underline a problem induced by the handling of AIREPs in screening, plane by plane independently. This allows to keep observations valid at the same point but not at the same time, so quite different, as input for 3d-var analysis. This fosters the march towards more continuous data assimilation systems (4d-var, or 3d-var at a higher frequency, or any intermediate solution). Problems are different for SATOBs. Thinning must be performed in 2 steps, but observations are far less and used only over sea. So the proposed reduction of the thinning distance is less drastic, from 250 to 150 km.

2. In Bruxelles

The work of the two ALATNET Post-Doc students in Bruxelles, Martin Gera and Ilian Gospodinov, is described in separate reports. The summary hereafter corresponds to the efforts of the permanent staff.

5. Coupling and high resolution modes

Piet Termonia pursued his search for alternatives to improve the interpolation of the temporal interpolation of the coupling data of the ALADIN forecasts. The idea of the introduction of an accelerative correction in the linear interpolation scheme was generalized to a perturbative approach of the interpolation. The upshot of this work is that it turns out to be possible to monitor the quality of the linear interpolation, by comparing higher-order corrections of a perturbative expansion to the lower-order contributions. This could serve as decisive tool to send extra coupling files to the ALADIN partners solely for those forecast intervals where the linear interpolation turns out to be deficient with the operational coupling frequency.

6. Specific coupling problems (6a: "Blending")

Alex Deckmyn performed further tests on DFI blending in the ALADIN-Belgium domain. In this nested model (coupled to ALADIN-France) he compared the results using the ALADIN-France files as initialisation or the ARPEGE long cut-off analysis.
As in other blending results, the change in objective scores is small. The improvements due to blending itself appear slightly larger than those due to the use of the long cut-off analysis.
Because it is difficult to assess the differences with objective scores, we are now looking at wavelet-based methods to study the local scale properties of the blended and non-blended fields. By comparing the information at small scales we are seeing that the fine structure of a blended initialisation is more comparable to that of the 24 h forecast for the same time.

8. Adaptation of physics to higher resolution (8a: Parameterisation of the small-scale features of convection) & 9. Design of new physical parameterisations (Use of liquid water and ice as prognostic variables, implementation of a new microphysics parameterisation)

Luc Gérard worked on the integration of the micro-physics and the convection parameterizations.

3. In Prague

1 Theoretical aspects of non-hydrostatism

1a) Top and bottom boundary conditions *(C. Smith)*

The research work continued in order to understand the reason why the semi-Lagrangian advection treatment creates a spurious standing wave above the top of the mountain. The term responsible for this pattern was found: it comes from the fact to apply the semi-Lagrangian vertical advection on the vertical derivative of a quantity (vertical divergence) instead on the quantity itself (vertical velocity). It is, of course, linked to the formulation of the bottom boundary condition, which is defined for the vertical velocity but the information on the w field is lost when switching to the vertical divergence and there is no easy way to reconstruct (in a unique way) the vertical divergence field (and w field) in the origin point of the trajectory. Several ideas how to cope with this difficulty are being currently explored.

1b) Predictor-Corrector scheme *(J. Vivoda)*

The Predictor-Corrector (PC) scheme was successfully implemented to the library cycle AL12/CY22T1 and scientifically validated: the results correspond well to those of the linear stability analysis. In last Newsletter it was wrongly reported, that the linear stability analysis showed that only one iteration of the PC scheme would have been sufficient to stabilize the 2TL NH scheme. A bug was found in the analysis and now the result says that 3 iterations are necessary to get a safe stability (even in no presence of the orography). The analysis was done for nearly all the options of vertical divergence variables (denoted as *d0*, *d1*, *d2* and *d3*) and it showed a specific outcome for the 2TL scheme compared to 3TL scheme (it was done for the standard vertical temperature profile or for isothermal profile with a flat surface) . For example, after the first iteration the scheme remains highly unstable, no matter which vertical divergence variable is chosen. In 3TL case the benefit of a proper choice of vertical divergence variable is strong already after the first iteration. In 2TL case the benefit of the change of variables becomes noticeable only after the second iteration and gets stronger after the third one. In the model, only the results for the original *d0* and *P0* variables were validated against the linear analysis. The validation for the other combinations will be done after phasing the development in cycle AL15. The PC scheme also contains the possibility to make a decentering of the predictor or corrector step. The test of the impact of the decentering on the stability was inspired by the work of Semazzi. It was indeed confirmed that by heavily increasing the decentering coefficient *XIDT* (up to 0.5) the 2TL scheme becomes more stable. On the other hand such a choice has strong damping effect. An idea to combine the PC scheme with the decentering of the predictor step and gaining the precision by applying the corrector step was tested (this could lead to a stable scheme when doing only one iteration) ; however the non-decentered corrector step brings the instability back.

2. High resolution runs *(D. Cemas)*

The 1 km horizontal resolution domain, including a very sharp orography (the Julian Alps), was prepared. A first trial to run the NH version of ALADIN was made. As expected, the problems with stability were encountered (the test was made with AL12 version, not including new options for prognostic variables). Finally, the stability was reached by lowering the value of reference surface pressure for the semi-implicit background (*SIPR*) to about 800 hPa. With this value it was possible to use a NWP type of time-step. A plausible explication is that in presence of relatively high mountains, which makes the average surface pressure lower, it becomes necessary to adjust the semi-implicit background, too. The tested situation was one of MAP wet cases IOPs, hence the attention was put to simulated precipitations. We could observe a noise in this pattern; the fact which was more or less expected. A trial was made with the linear grid, however, the results were not very sensitive to that. Unfortunately, there was not enough time to make further tuning of the orographic forcing. In addition,

one can reproach a lot of incoherent settings to this type of simulation: inappropriate physics, inadequate ratio between the vertical and horizontal resolutions, etc...; however, as a test bed it is still an interesting experiment.

3. Data assimilation related coupling issues

3.a) The incremental DFI & blending technique operational in ALADIN/LACE *(F. Vana, M. Siroka)*
See the ALADIN Newsletter for details.

3.b) The incremental DFI & blending technique on linear grid *(S. Ivatek-Sahdan, R. Brozkova, F. Vana)*
The linear grid option was tested in ALADIN/LACE together with the blending technique. The aim was to find the optimal value of the "low resolution" truncation used for scales separation between ARPEGE analysis and ALADIN forecast. When going to the linear grid, the nominal "high resolution" of ALADIN gets increased by a factor 1.5. Since the "low resolution" is determined by the empirically found ratio (weighted geometrical average) of the ARPEGE analysis and ALADIN resolution, its application would lead to some increase of the "low resolution", on the other hand the linear grid option may well require other proportion of the weights. Therefore a new tuning was made for the "low resolution" in the interval bounded by two extreme values: the original truncation and its multiplication by 1.5. A new optimal value for the "low resolution" truncation was found; the tuning was performed on the case of a strong cold front passing Germany and Poland. Even a parallel suite has been made. However, there was no signal in the scores, which remained perfectly neutral with respect to the operational suite. This means that details brought in by the increase in spectral resolution are so fine in the scale (like sharpening of the structures, etc.) that the verification against conventional SYNOP and TEMP network (relatively coarse) cannot detect such differences.

3.c) 3d-var strategy in ALADIN *(M. Siroka, G. Boloni)*
The tests of 3d-var algorithms known as "STANDARD","BLENDVAR " and "VARBLEND" continued in two ways: on a case study of a strong cold front and on longer period of May 2001. One of new ingredients was the usage of IDFI technique. The results of the case study confirmed in general way all the previous results of the tests made in 2000, but there was a very interesting novelty: appearance of a gridpoint storm under some conditions.

- *grid point storm story*

The studied situation was characterized by strong convection with many active cells along the frontal limit (the case was from the end of August 2001). In case of STANDARD algorithm the following forecast created a gridpoint storm. It was not a case for the BLENDVAR or VARBLEND algorithms. The question was, whether it was due to the use of lagged background term (in BLENDVAR and VARBLEND) or due to the filtering properties of blending algorithm. Indeed, both these ingredients played a role. When BLENDVAR was combined with the standard background term, the gridpoint storm appeared. On the other hand the VARBLEND & standard background term experiment did not create the gridpoint storm. The conclusion is that the standard background term brings in strong and not well balanced increments of humidity and temperature, responsible for the later development of the gridpoint storm. In case of VARBLEND these increments gets controlled by the blending step following the analysis. Since blending corrects the large scales and keeps untouched the small-scale 3d-var result, we can conclude that the standard background term brings the imbalance rather in the larger part of spectra. This fact means that the STANDARD algorithm in general is not suitable for the coupled mesoscale analysis problem we try to solve in ALADIN. Further, it was figured out that not only the total variance, but also the shape of the background error structure functions play a role in the balance of increments (creation or not of the gridpoint storm). The level of noise was measured by the oscillations of surface pressure in the respective forecasts, but this gives picture rather on the gravity wave noise. The fact, whether the model creates the gridpoint storm or not, depends more on the

temperature-humidity balance. At the moment we know a little on this type of balance, which is in fact a part of ALADIN Jb term (derived by the linear regression from the forecast errors).

- *comparison with pure blending*

It would be very interesting to compare the STANDARD, BLENDVAR and VARBLEND results with those of a simple blending. This is in order to know whether the currently used observations and assimilation method bring some innovation at the small scales or whether we are at the limits of predictability. Such test would be a very useful benchmark, allowing to compare future ingredients of the assimilation and forecast parts of the model (such as more observations, improved Jb and Jo terms, improved model, etc.). Unfortunately, such comparison has not been done yet.

- *lagged statistics for the nested domain*

The lagged statistics were computed for the ALADIN/HU model (Boloni and Horanyi, Proceedings of 10th ALADIN Workshop "on scientific developments", Toulouse 7-8 June 2001, pp 113-119). It was found that the total variances were much smaller than in the coupling model (ALADIN/LACE) and by consequence also the analysis increments are very small. Therefore the parallel verification of both models was done in Prague. It indeed showed that the scores of the two models are nearly identical: the nested model is completely driven by the coupling model in their current configuration.

3.d) Evaluation of the impact of balloon drift in sounding measurements *(M. Benko, M. Siroka, R. Brozkova)*

A set of sounding measurements with recalculated horizontal position of the balloon was monitored in order to evaluate the impact of the balloon drift. The monitoring results are compared to the classically treated sounding data (measurement is considered to keep the same horizontal position within the ascent of the balloon). Only measured parameters were monitored against the ALADIN forecast (at all ranges by 6 hour interval), that means pressure, temperature, wind and humidity. Only the correction of the balloon position was recalculated from the measured wind and not taken directly from the very detailed measurement report (this one is not normally available). The statistics made over one month for sounding stations in LACE verification domain showed a weak worsening of the "scores" in all parameters, increasing with the height (like the drift increases too). Since this result is opposite to what one could expect, it would be interesting to understand this. Either the recalculation of the position is not good, either this is caused by the fact that only the space correction is taken into account while the time correction is neglected. In any case it seems that there is no straightforward benefit from taking the balloon drift into account, contrary to the intuitive feeling, and that the perspective to use this additional information in the data assimilation is almost zero.

3.e) Assimilation of screen level humidity data *(M. Jurasek, M. Siroka)*

The humidity measurements at 2m above the ground are not used in the upperair analysis. This is because these measurements were influencing the surrounding atmosphere in a unrealistic depth, especially in the vertical. The situation has been examined in ALADIN, where the use of screen level measurements were activated in 3d-var. First, the single observation experiments were done both with the standard and lagged background terms. Indeed, the standard Jb caused again large impact of the measurements. For the lagged background structure functions the situation was better. The experiments have shown a strong coupling between humidity and temperature data: there was an impact of several degrees of Kelvin via the Jb coupling (it was again stronger in the standard Jb case). This point should be further investigated.

4. CFL versus Lipschitz criteria *(A. Trojakova, R. Brozkova)*

The study based on the ALPIA type of experiment continues. The tools for the coupling of academic experiments were developed and the work on nested domains started. The model was launched almost without no physics, except the vertical diffusion and exchange of momentum and dry static energy. Also the classical NWP type of setup was used for the horizontal diffusion. Other modifications with respect to the reference library were the following: the improved stabilization of the scheme by introducing a special type of the corrector step; the increased dimensions within DFI algorithm in order

to perform the filtering over a longer window. The integration went very smoothly for the horizontal resolutions of 10 km and 5 km, where relatively long time steps could have been used. First problems with the stability were encountered at the resolution of 2.5 km. Here it was necessary to lower the value of the semi-implicit background pressure. The same problem occur for the horizontal resolution of 1.25 km. It is necessary to mention as well that each time also the vertical resolution was increased. Since the stability problems for 1.25 km domain became quite sever, all the modifications were phased into the cycle AL15, where new options for the NH prognostic variables may be used. However, no alternative choice of the vertical divergence variable was successful even if a tropopause was introduce to mild the temperature profile in the upper part of the domain. Finally, only the variable for the non-hydrostatic pressure departure was changed; together with a low value of the surface semi-implicit pressure it was possible to integrate the 1.25 km domain with a reasonable length of the time step. It was not successful to go further: the trials to integrate the 0.625 km ended always by the instability. Hence, the conclusion, regarding the stability, is that it would become necessary to use the predictor-corrector scheme to get a robust scheme. In any case, the integration becomes very expensive. Another development was made in order to diagnose Lipschitz criteria. This is to detect a possible crossing of the trajectories. For the examined cases the possible length of the semi-Lagrangian time-step determined by Lipschitz criteria remains relatively long. One can also say that there are other problems accompanying the semi-Lagrangian solution which appear already for shorter time steps than those allowed by Lipschitz.

4. In Budapest

Most of the research and development topics were concentrated around the ALATNET scientific plan and described briefly hereafter:

-- In the framework of the ALATNET project Raluca Radu had been started her work on the coupling problem. Raluca received a general training on the coupling problem and she had started to code the spectral coupling into the ALADIN model (more details can be found in the reports of the ALATNET students).

-- Cornel Soci also in ALATNET grants completed a 4 months stay in Budapest dealing with the mesoscale sensitivities of the ALADIN model. Some interesting synoptic cases were studied and the possible improvement of precipitation forecasts were investigated through sensitivity studies taking into account also physical parameterisation aspects. The main achievements of this work is summarised in a scientific paper just to be submitted (more details can be found at reports of the ALATNET students).

-- The Pre-doc student of Steluta Alexandru started her work in Budapest at the beginning of November. Her topic is devoted to the study of the 3d-var scheme of ALADIN in the context of the double-nested technology of the ALADIN/HU model (her report can be also found in this Newsletter).

-- The investigations around the effects of soil texture to the forecasts of the ALADIN model are continued and completed. The results are summarised in a scientific paper under submission.

-- The computation of background error statistics and its sensitivity to the integration lengths and forecast differences of the NMC method had been continued and the main conclusions of this work is summarised in a short report in this Newsletter.

-- The investigations of the possible inclusion of ATOVS radiances into the 3d-var data assimilation system had been started in the autumn (short summary can be found in this Newsletter).

5. In Ljublana

The former Hydrometeorological Institute of Slovenia as the ALATNET centre in Slovenia was merged into The Environmental Agency of Republic of Slovenia (EARS) in the middle of 2001. The EARS as successor of HMIS became the governing institution for ALATNET project in Slovenia. The transition between the two institutions was smooth as far the ALATNET project is concerned, the only problem is that, due to reorganization, the number of persons working in numerical weather prediction and correspondingly in the ALATNET project is now significantly reduced. The work related to ALATNET is now even more connected with the research stays of PhD students in Ljubljana.

The two major topics where research has been performed were "Case studies aspects of NH" and "Spectral coupling".

Case studies aspects of NH

Klaus Stadlbacher finished his first stay in Ljubljana at the end of August 2001. More information about this topic and his stay could be found in his report published in the last Newsletters.

Spectral coupling

The work on this subject was started by the new ALATNET student Raluca Radu. She started her study with stay in ALATNET centre at Hungarian Meteorological Service in Budapest where she got some insight of the spectral coupling problematics. The work continued in Ljubljana. She started with the coding of spectral coupling in the ALADIN model during her stay in Ljubljana in November and December. Due to good preparation of the work in Budapest and good working plan the work started successfully. She is expected to have the basic version of spectral coupling ready at the end of her first stay in Ljubljana (end of May), when also some results will be available. This will be also the time for the first evaluation of the spectral coupling method.

ALADIN PhD studies

1. Radi AJJAJI : "Incrementality deficiency in ARPEGE 4d-var assimilation system"

It has been shown that the bad behaviour of 4d-var system, in some situations, linked to the incremental formulation (the so-called incremental deficiencies) could be encountered not only over desert regions but on Europe as well. The April 24th analysis produced a great negative humidity increment over Pyrenean region at 18 h UTC, and a reasonable one 6 hours after. This situation was a good individual case to try to characterize the context of this abnormal 4d-var property by diagnosing a list of ingredients responsible of such fact.

First, and as usual in all analysis studies, observations used along the 6 hours window were fetched to identify the type which is more likely responsible of underestimating the specific humidity increment. This first study showed that most part of the impact was related to AMDAR and SYNOP data. SATEM, SATOB and all other observation types showed just a little impact.

A geographic zoom over Pyrenean region showed absence of TEMP observation type in all the circle of 300 km radius centred on (43°N, -3°W). This means no humidity information since all other observation types don't inform on humidity. This could have certainly an impact on humidity analysis in sense that humidity analysis will be influenced by 4d-var multi-variate characteristic implied at least by the adjoint of tangent linear integration and observation operators. When forcing *Rv* to *Rd* during the integration of TL/AD models and observation operators, the multi-variate effect especially on humidity field become negligible as it can be seen on these approximate equations.

$$(\frac{\partial}{\partial t}+u_b\frac{\partial}{\partial x}+v_b\frac{\partial}{\partial y})u' = -\frac{\partial u_b}{\partial x}+(f-\frac{\partial u_b}{\partial y})v' - \frac{\partial \phi'}{\partial x}-\frac{R_bT_b}{P_b}\frac{\partial P'}{\partial x}-\frac{\partial \ln(P_b)}{\partial x}R_bT' - \frac{\partial \ln(P_b)}{\partial x}T_b(R_v-R_d)q_v'$$

$$(\frac{\partial}{\partial t}+u_b\frac{\partial}{\partial x}+v_b\frac{\partial}{\partial y})T' = \frac{A_b}{\omega_b}\omega' + \frac{A_b}{T_b}T' - \frac{A_b}{P_b}P' + \frac{A_b}{R_d}(R_v-R_d)q_v' - \frac{A_b}{C_{p_v}}(C_{p_v}-C_{p_d})q_v'$$

$$(\frac{\partial}{\partial t}+u_b\frac{\partial}{\partial x}+v_b\frac{\partial}{\partial y})q_v' = 0.$$

When putting *Rv=Rd* only before executing observation operators with their direct TL and tangent formulations (TL/AD of forecast model being integrated without this forcing), the impact steel unchanged. This means that observation operators are not responsible of the bad analysis increments. But as *Rv=Rd* is applied for all the components of a simulation, some other negative impacts could appear at least caused by assuming *Rv=Rd* into observation operators.

Other experiments performed with slightly modified TESTLI (a procedure testing the tangent linear hypothesis) showed a neutral impact of horizontal diffusion both in Eulerian and semi-lagrangian type integration. TESTLI showed also no difference between finite differences and Tangent Linear model integration when transporting in time a humidity increment.

This indicates that the anomaly resides in the adjoint integration which involves multi-variate effect as all great magnitude terms computed during the direct TL influence humidity during Adjoint reverse integration when there is no other information (observation) to compensate this fact.

An experiment done in the same environment but with an artificial TEMP observation added in the vicinity of the affected Pyrenean region (the TEMP is elaborated from interpolation of guess humidity on a vertical profile) corrected entirely the bad humidity analysis. This enforced the doubts on 4d-var performances over regions with poor observation network.

A diagnostic on the gradient of cost function with respect to specific humidity showed that the bad humidity increments are not produced at the first iteration as it was expected (communication with F. Bouttier) , but they are a result of an accumulation along the iterations : each forward and backward (simulation) execution adds a contribution to the increments that increase them in the same sense.

So, putting *Rv=Rd* as a first (non scientific) solution reduces the multi-variate effect, which is among the strong good characteristics of a 4d-var system, on humidity ; but its non seen effects could be more "dangerous". One can test other solutions as :

- Use more and more observations containing direct or indirect information on humidity.
- Rely more on guess information over poor humidity information regions : Jb handling.
- Use more realistic physics in TL/AD to compensate the multi-variate effect more strongly.
- Force humidity increments to steel realistic at the beginning of the time window by applying analytic or statistic adjustment with respect to other fields increments : a kind of humid balance.
- Use of extra compensating terms in TL/AD to reduce the *(Rv-Rd)* terms magnitude.
- Take into account, in the TL/AD formulation, some second order terms that could become important along the iterations.

As a further step, points 4 and 5 will be tested, and their results will be communicated in the next newsletter.

2. Jean-Marcel PIRIOU : "Correction of compensating errors in physical packages; validation with special emphasis on cloudiness representation"

EUROCS Stratocumulus Case: (i) it has been shown on this case that the top of PBL entrainment is too big if the turbulence scheme uses saturation humidity functions inside the shallow convection functions (option *GCCSV=1.*), this led to an operational change (now *GCCSV=0.*); (ii) The Single Column Model (SCM) interface to this EUROCS case, initially coded by Blazenka Vukelic, has been introduced in the main SCM library.

Turbulence: (i) reading articles ; (ii) introducing an interactive mixing length in the ALADIN turbulence scheme. This reduces the temperatures biases of the mid and high latitudes. The impact on winter cyclogenesis is under study.

Deep convection: the EUROCS idealized humidity case, which compares Single Column Models to Cloud Resolving models with respect to deep convective clouds entrainment, has been run with the ALADIN SCM. The results of the present scheme are pretty good, which tends to show that the job done in *ACCVIMP* about "undilute plumes", following an idea from Steve Derbyshire, has improved the sensitivity of the model with respect to free atmosphere relative humidity.

CLOUDNET project: this European project (CLOUD NETwork) intends to validate operational models versus observed radar and lidar data. The aim is to improve the representation of clouds, cloudiness and microphysics inside operational LAMs and GCMs. The Reading meeting gave an opportunity to discuss "which fields" and "at which time scales" to provide and inter-validate. ALADIN predictions should be sent to an European common data base by the end of 2002.

3. Wafaa SADIKI : "A posteriori verification of analysis and assimilation algorithms and study of the statistical properties of the adjoint solutions"

Nothing new (implementation of the new operational suite and 3d-var in Casablanca).

4. Filip VANA : "The dynamical and physical control of kinetic energy spectra in a NWP spectral semi-lagrangian model"

Nothing new (LACE duties).

ALATNET PhD and Post-Doc studies

1. Steluta ALEXANDRU : "Scientific strategy for the implementation of a 3D-VAR data assimilation scheme for a double nested limited area model"

The purpose of the work is to find the best scientific strategy for the implementation of the 3D-VAR data assimilation scheme for a double nested limited area model. ALADIN/HU is a double nested limited area model, which is coupled with ALADIN/LACE (which is coupled with ARPEGE). The boundary conditions are obtained from ALADIN/LACE integration, at the 12 km resolution. The resolution of the ALADIN/HU model is about 8 km.

To produce a good forecast, a good description of the initial conditions is necessary. The objective of data assimilation is to define the best initial state of the model taking into account all the possible information. 3D-VAR consists in minimizing of a cost function, in order to get the best fit to the available information sources. The cost function is the sum of three terms : J=Jo+Jb+Jc ,where Jo represents the departures from the observations, Jb represents the departures from the first-guess, and Jc controls the amplitude of gravity waves in the analysis. At the moment for ALADIN model only the first two terms are defined.

Most of the time of the first months was devoted to study of the existing informatic environment with special emphasis on the 3D-VAR scripts. In 2000, the 3D-VAR data assimilation scheme was ported to Budapest for the Origin 2000 machine of the Hungarian Meteorological Service. The AL13 version of ALADIN model is used for the 3D-VAR, taking into account classical NMC statistics for the background term and only SYNOP and TEMP observations for the observational term of the cost function. The first-guess is the 6 h forecast from an earlier model run. It contains information on the small scales (the scales of the model), but being a forecast it is not fully precise. The 3D-VAR script is running four times per day (to have the first-guess), but the 48 h integration is made twice per day.

The steps performed in the 3D-VAR script are: first, the transformation of the observational data into ascii file, using Mandalay, then the program OBSORT redistributes the observational data across the available processors, followed by the running of the SCREENING (nconf=002), for calculating the high resolution departures and for screening of observations (i.e. determines which observations to be passed for use in the analysis), then the incremental variational analysis (nconf=131) is performed, using the first-guess (6 h forecast from the previous model run), the observation file prepared by the screening, and the classical background error statistics file. Because the 3D-VAR data assimilation scheme is acting for the upperair meteorological fields, after the variational analysis step, the optimal interpolation (CANARI) analysis is applied for the surface variables, and finally the model integration is realized to obtain the first-guess.

The time-consistency coupling is used for the time being to provide the information about the large scales. Time-consistency means that the lateral boundary data are coming from the same run of the model (LBC0=0 h analysis of the ALADIN/LACE, LBC1=6 h forecast of the ALADIN/LACE). Thus the information is consistent in time. On the other hand, space-consistency means that the zero

coupling file is identical with the initial file (LBC0=INIT file - the ALADIN/HU analysis, LBC1=6 h forecast of the ALADIN/LACE), and this coupling technique will be tested in the future.

Twice per day a verification script is running to evaluate the model performances. The statistical measures (RMSE, bias) are used as indicators of the extent at which model prediction match observations. These objective scores are calculated for the forecast of the model using 3D-VAR scheme, and also for the operational forecast (using the dynamical adaptation). The compared fields are the temperature, the geopotential, the zonal and meridional wind, the relative humidity, the direction and intensity of the wind.

We observed that for example, in the period 17.11.2001-24.12.2001, at the 850 hPa level, the scores are better for the wind and geopotential, for the first 6 h integration, using 3D-VAR scheme. For the geopotential, after the 6 h integration, the scores start to be almost the same. The worst scores are for the relative humidity, where the BIAS is around 5%, in the first 6 h integration of the model with 3D-VAR scheme, and around 1.5% for the operational one, and the RMSE is 17% using 3D-VAR scheme, and 13.5% for the operational. After 42 h integration, we observed that the scores start to be close one each other. Also the model using the 3D-VAR scheme underestimated the temperature, in the first 18 h integration, but less than the operational model. Then the scores are almost the same.

After the understanding of the working environment of the 3D-VAR data assimilation scheme, we decided to focus our attention on the next aspects:

a) Case studies.

For the beginning we chose two cases, from 11.06.2001 and 28.08.2001. First case is from the period that Gergo Boloni made the tests with blendvar and varblend in Prague, and the idea was to see the results for a double nested limited area model. The cases were chosen because we considered them as interesting meteorological situations, with a front passing through the domain. On these two cases we will make the experiments with the different background error statistics (standard, lagged statistics), first guesses (the 6 h forecast of the previous run, blending of the ALADIN forecast with ARPEGE analysis), initialization methods, together with their posteriori evaluation, etc.

b) We want to establish which one of the coupling techniques is better, time-consistency or space-consistency.

c) Then we plan to run 4 times per day the blending procedure for the first-guess. The necessary files, which contains the large scales are provided from Prague. These are the first two historical files from the ARPEGE assimilation cycle, the final blended analysis in the ALADIN/LACE resolution, and the 6h forecast of the ALADIN/LACE model, started from the previous file, with no DFI initialization.

d) Other experiments will be performed using the blendvar and varblend combinations, with the lagged statistics.

Future work

The next months will be devoted to the experiments with the different background error statistics, first guesses, initialization methods and posteriori evaluation. So at the end of this first stay, we would like to get an idea about the best possible version of a 3D-VAR data assimilation scheme for a double nested limited area model.

2. Gianpaolo BALSAMO : "Mesoscale variational assimilation for land surface variables"

Nothing new since the last report, covering part of this semester (work in Italy). Presentation of the results at the joint HIRLAM / SRNWP workshop "on surface processes, turbulence, and mountain effects" (Madrid, 22-24 October 2001).

3. Margarida BELO PEREIRA : "Improving the assimilation of water in a NWP model"

Introduction

The background (6h forecast, also known as first guess) error covariance matrix (known as the B matrix) is one of the most important elements of a data assimilation system, as it determines the filtering and the propagation of the observed information (Daley, 1991). Presently, the B matrix of ARPEGE is determined using the NMC method, which is very easy to implement. This method uses differences between 48 h and 24 h forecasts (fc48-fc24), which start at different times. So, it relies on the differences between the evolution of the 24 h forecast which starts from one analysis (r0) and another one which starts from a 24 h forecast. The analysis r0 is build with the analysis increments from the successive analyses in the assimilation system over the 24 h period between the initial times of the two forecasts. Hence, the forecast differences (fc48-fc24) will appear mostly in data-rich areas, because the analyses will not correct the forecasts in data-sparse areas. This represents a drawback from this method since the largest errors in analyses are likely to be in data sparse areas. A second disadvantage of this method is that it assumes that the structure of the statistics of the forecast error over 24 hours is not dependent on the range of the forecast. However, this assumption is likely to be not true. For these reasons, another method called Analysis Ensemble Method was tried at Environment Canada (Houtekamer et al., 1996) and at ECMWF (Fisher, 1999). In the present work, this new method was "implemented" in the cycle 22T1 of ARPEGE.

Ensemble Method

The idea of this method is to run an ensemble of independent analysis experiments. For each experiment all observations are perturbed adding an independent random number, which has a Gaussian distribution with mean zero and variance equal to the prescribed variance of observation error. The effect of such perturbations is to generate differences in the analysis for each experiment. These differences are a measure of the uncertainties on the analyses, which are propagated to the 6 h forecast and consequently to the next analysis cycle, in the form of uncertainties in the background. After a few days of assimilation, the statistics of the differences between background fields for pairs of members of the ensemble equilibrate and it is assumed that the differences between independent members (experiments) of the ensemble represent the background errors, from which the statistics related to the B matrix can be estimated.

The ensemble consists of 10 31-level 3d-var analysis experiments for the period of 1-30 May 2001. Initial conditions for all experiments were provided by an analysis for 18z of 30 April from a 3d-var unperturbed experiment.

The analysis experiments (members) were arbitrarily numbered from 31 to 40. The differences between the background fields for consecutively-numbered experiments were calculated for each 12z cycle between 4/5/2001 and 30/5/2001. This provided 9x27=243 differences between background fields, from which we estimate the statistics of the background error.

Results : visualization of forecast differences

The differences between the 6 h forecasts were analysed individually during the first days. On the first day of assimilation, the differences were located mainly over the extra-tropics for temperature, and over Land and near the coast for specific humidity, but these differences were spread (as expected) over the whole globe on the second day.

Moreover, the method seems to produce some error structures which seems to be related with the synoptic situations. As an illustration, differences between member 36 and 37 are shown for day 15, for some fields.

It is worthwhile to note that the largest differences (-4.7 hPa) in Geopotential at 850 hPa are located in the area of the low situated in North Atlantic (NA), near Canada (see figures 1 and 2). Moreover, the

differences are also negative in the other depression over NA. This means that for member 37, the two lows are deeper than for member 36. This is an interesting example of the possible link between structures in the background field and structures in the background errors. Moreover, the largest differences in specific humidity (-8.9 and 6.8 g/kg) and in temperature (-5.7 °C) occur in Equatorial Africa on the area of strong gradients associated with the Inter-Tropical Convergence Zone (ITCZ) (see figures 1, 3 and 4).

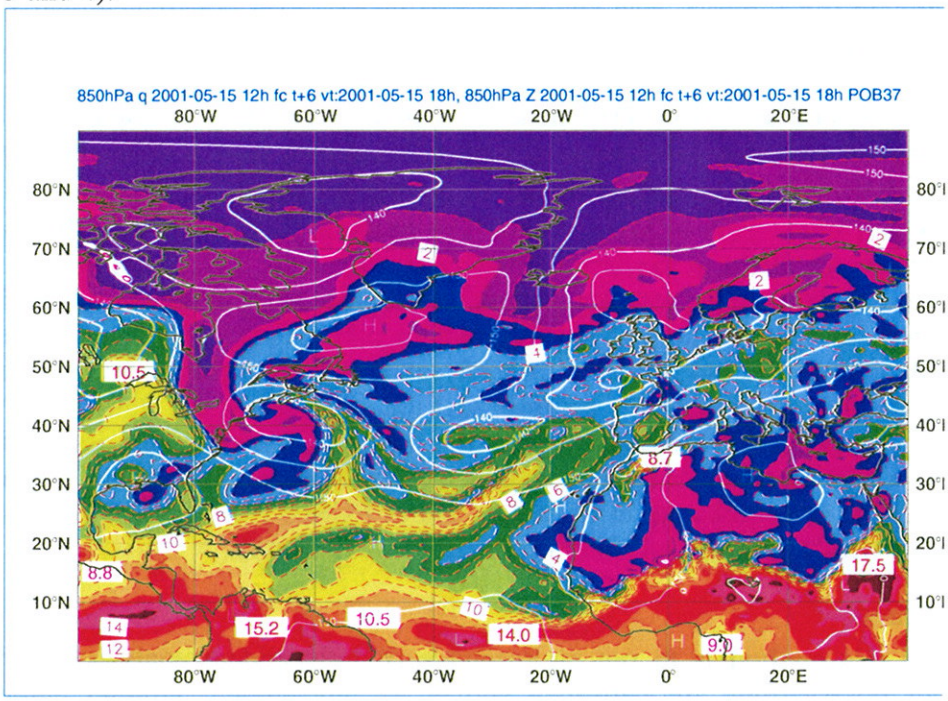

Figure 1 - Geopotential (isolines of 5 hPa) and specific humidity (isolines of 1 g/kg) at 850 hPa for member 37.

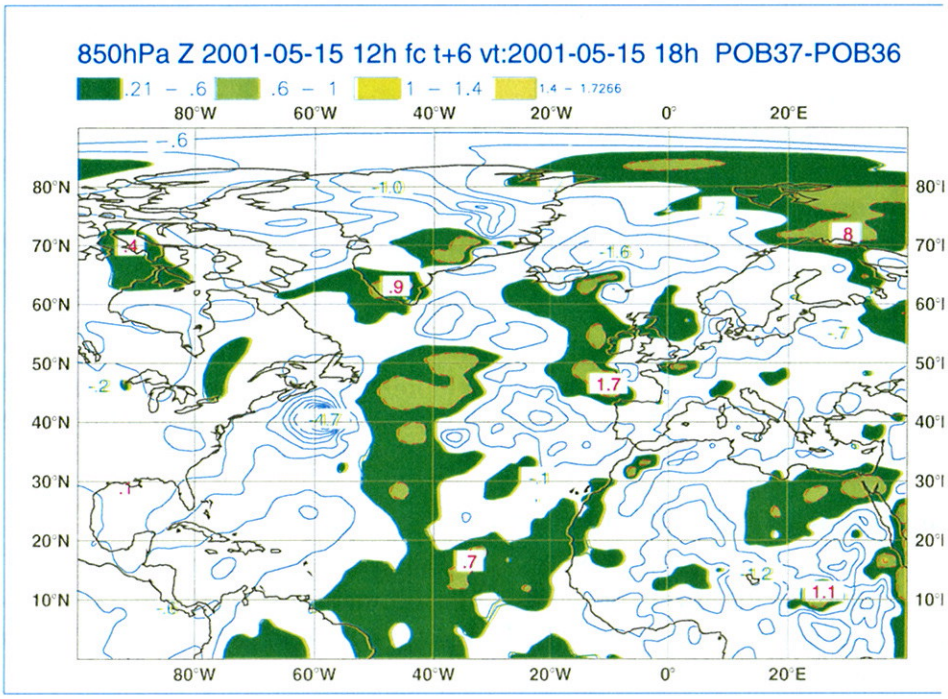

Figure 2 - Differences in geopotential (isolines of 0.4 hPa) at 850 hPa between member 37 and member 36. The areas where the differences are larger than 0.2 hPa are coloured.

The second area of largest uncertainties on q field occurs in the frontal system located in the western part of NA. For member 37, the gradient in q through the cold front is enhanced, due to

positive anomalies (in this text the term anomalies refers to the differences between POB37 and POB36) in the moist sector and to negative anomalies in the dryer part behind the cold front (figures 1 and 3). For temperature, it is worthwhile to mention the positive anomalies in warm sector of the frontal system in NA and the negative anomalies in the cold and cool sectors (see figure 4). As a consequence of these uncertainties there is an intensification of the frontal system in one member (POB37) relatively to the other.

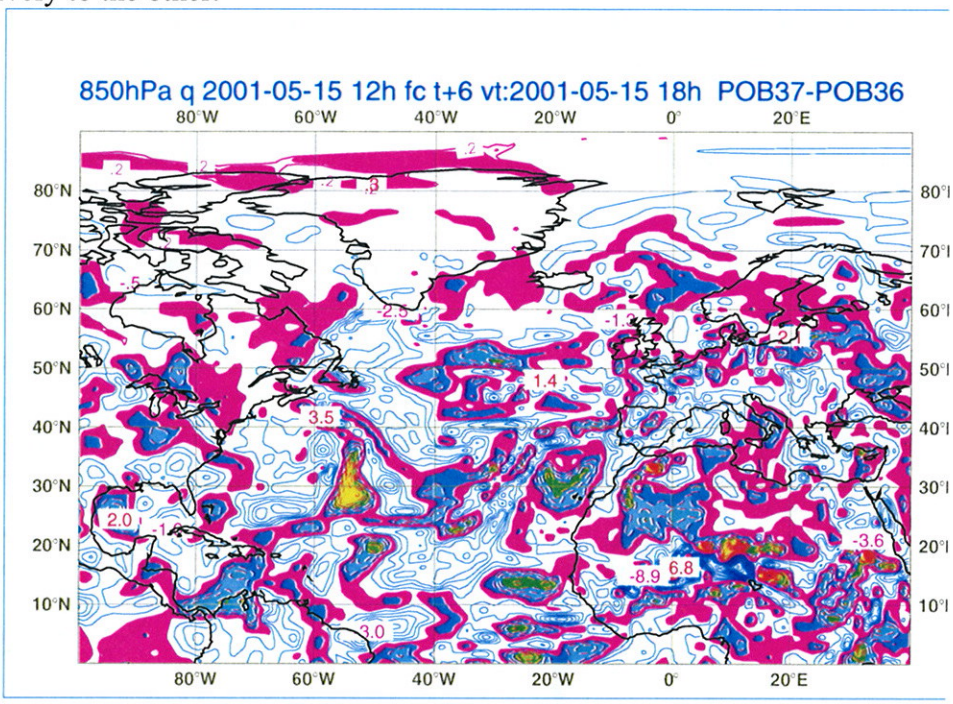

Figure 3 - Differences in specific humidity (isolines of 0.4 g/kg) at 850 hPa between member 37 and member 36. The areas where the differences are larger than 0.2 g/kg are coloured. The maximum positive anomalies are represented in red and burgundy and the minimum are in violet.

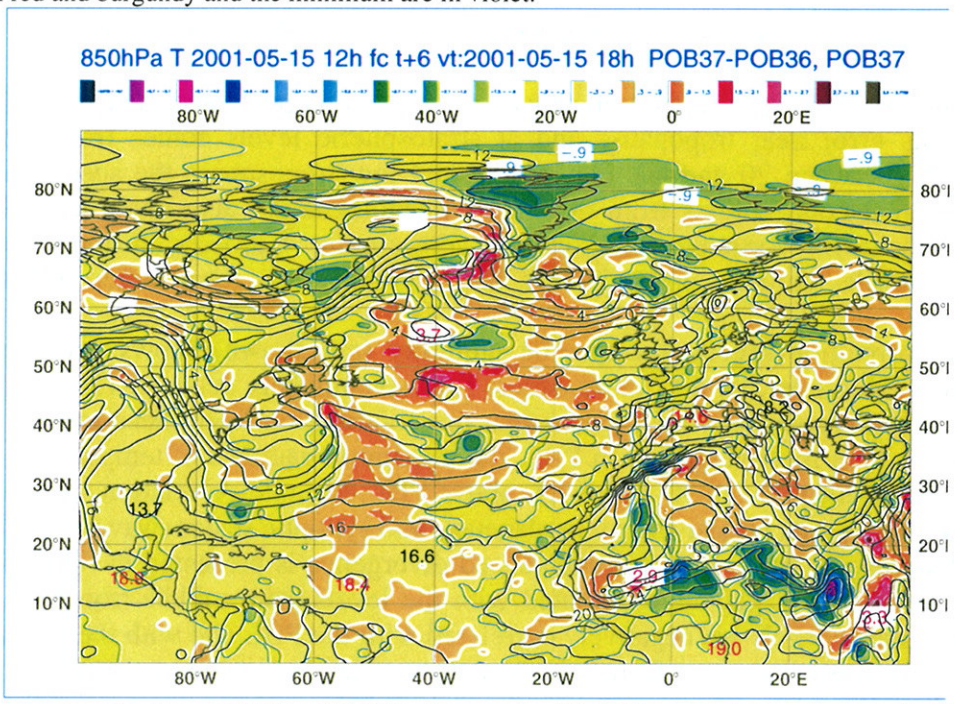

Figure 4 - Temperature (isolines of 2 °C) at 850 hPa for member 37. Differences in temperature (isolines of 0.6 °C) at 850 hPa between member 37 and member 36. The isoline of 0.3 °C is plotted in white. The differences larger than 0.3 °C are plotted in colours from orange to red. The differences smaller than 0.3 °C are plotted in colours from yellow to blues and violets.

Results : preliminary examination of some statistics

The vertical profile of total standard deviations for the first 6 days and for the average over the period 4/5/2001 to 30/5/2001 is plotted in figure 5 for specific humidity and for unbalanced divergence. For both variables it is possible to verify that the global statistics stabilize on the 4th day. The same result is achieved for temperature and vorticity (not shown). This is the reason why the first 3 days are not taken into account to compute the statistics of forecast errors. For both q and divergence the maximum standard deviation occurs in the Planetary Boundary Layer (PBL). Moreover, for q the standard deviation decreases drastically for levels above 700 hPa (level 20).

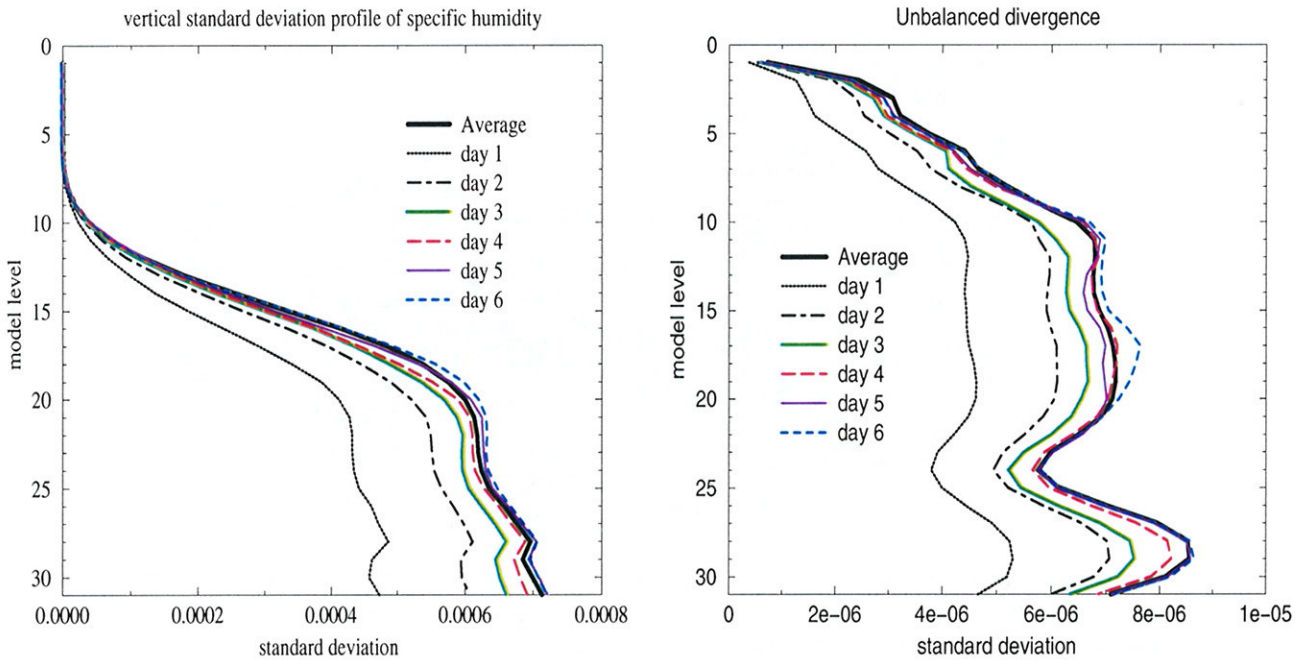

Figure 5 - Vertical profile of standard deviation for specific humidity and unbalanced divergence.

The auto-correlation spectra for unbalanced divergence is presented in figure 6 (left). Most of the variance of its error near tropopause and at stratospheric levels comes from synoptic scales, for wavenumbers[1] between 20 and 40. For middle and low troposphere the spectra are much broader, which means that contributions from mesoscale phenomena are also important. The shape of auto-correlation spectra for vorticity (not shown) is very similar. However, at middle troposphere and at stratospheric levels, vorticity errors have a larger contribution from larger scales than divergence errors.

The auto-correlation spectra for specific humidity (not shown) shows very little variation with vertical levels. Moreover, its maximum occurs for wavenumbers between 15 and 25 and its shape is sharper than for divergence, which means that the contribution from mesoscale to the variance of q error is smaller than for divergence. In PBL, the maximum variance of temperature error comes from wavenumbers between 10 and 30. For levels above PBL, the auto-correlation spectra of temperature is much sharper, having its largest energy in planetary and synoptic scales (wavenumbers less than 10).

The global vertical correlation for unbalanced divergence is presented in figure 6 (right). It shows that bottom levels are negatively correlated with the levels from middle troposphere. Moreover, the middle tropospheric levels are negatively correlated with the PBL and with the upper troposphere. For temperature, the most important feature is the anti-correlation between tropospheric and stratospheric levels (not shown).

[1] the wavenumber 1 corresponds to the earth circumference (40 000 km)

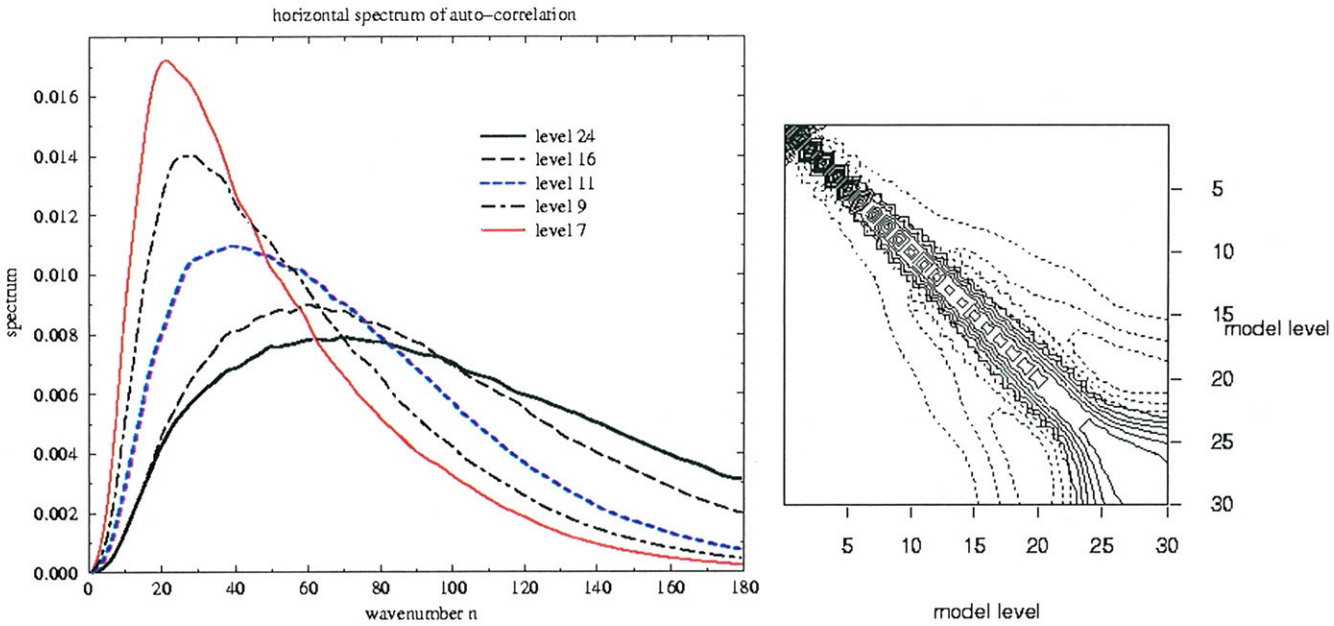

Figure 6 - Auto-correlation spectra for unbalanced divergence and for model levels 24 (near 850 hPa), 16 (near 500 hPa), 11 (near 300 hPa), 9 (near 215 hPa) and 7 (near 140 hPa). Average vertical correlation (on right hand side). Positive values (larger than 0.1) are plotted in solid lines. Negative values (smaller than -0.1) are plotted in dashed lines. The isoline spacing is 0.15.

Perspectives

In the near future we plan to compare the analysis error covariances and forecast error covariances. Moreover, we intend to compare the Analysis Ensemble Method and the NMC method.

References

Daley, R., 1991: Atmospheric Data Analysis. Cambridge University Press, 457 pp.

Fisher, M., 1999: Background Error Statistics derived from an Ensemble of Analyses. ECMWF Research Department Technical Memorandum No 79, September 1999, 12 pp.

Houtekamer et al., 1996: A System Simulation Approach to Ensemble Prediction. Mon. Wea. Rev., 124, 1225-1242.

4. Martin GERA : "Improved representation of boundary layer"

The energy spectrum of turbulence is not homogeneous at reality. Nevertheless, we often except that turbulence is a random process with independence on position, what is a definition of homogeneous turbulent processes. Away from boundaries and from a stable stratified atmosphere this assumptions work correctly. Resolved eddies are isotropic and small energetic eddies can cascade until viscosity dissipation. In other cases anisotropy is assumed. Near the wall, the size of energetic eddies becomes proportional to the distance from this barrier. Increasing the resolution, mainly in the vertical direction, creates a problem with grid anisotropy and does not describe the situation correctly.

The showed difficulties can be partly prevented by choosing the right variables at convenient equations in numerical model. Explicit use of the turbulent kinetic energy (TKE) into equations can touch problems with energy transfer and interrelation between subgrid and resolved scale. This improves the knowledge of developing processes and enables us to put new features and relationships among diagnostic and prognostic variables. TKE directly measures an intensity of turbulence and it can afford new knowledge for parameterization. Adding this equation as prognostic equation can has positive effect for properties of parameterization, although it increases a number of unknowns. Further enhance can be done by non-local view of parameterization. Non-local approach uses not only adjacent

region for parameterization. It can take into account the effects of all various sizes eddy from far-field region.

Understanding the energy transfer s relationships at spectral space can yields new formulation of parameterization schemes. It allows us to examine this equation as a function of wave numbers or eddy size. We do an analysis of TKE terms individually (Borkowski, 1969,Batchelor.1953). It helps us determine a physical process, which generate turbulence and it allows us to find expressions for parameterized variables.

Result of our analyses is spectral function for E (k) and its vertical part. From these analyses is shown that energy equation presents the inertial and the buoyancy subrange well. From this investigation is obvious, that TKE gives a useful information and it is applicable for solved problem.

Full feature of presented equation can be give numerically only. We need expressions for statistical moments. We use 1 and 1/2 closures. After application a Sommeria s hypotheses and tensor decomposition to the isotropic and anisotropic parts, we get formulas for present statistical moments and energy equation. Parameterization of present terms is needed for close the equations. We have information from spectral analyses, that eddy-transfer coefficient has dependence on dissipation term (epsilon).

In spite of new features, the mixing-length (L) is the still arbitrary parameter, which must vary from the LES to the Single column model [epsilon=epsilon (L)]. From computation above is seemed that introducing an equation for dissipation of energy can solve this arbitrary choice. This approach is called k-epsilon closure. Different approach for selection of L can be use, for example formulation of Bougeault and Lacarrere. These all experiences are needed for construction TKE scheme.

5. Ilian GOSPODINOV : "Reformulation of the physics-dynamics interface"

Various studies on the model dynamics

1. Predictor-corrector versus constant acceleration semi-Lagrangian trajectory scheme

Comparison study on the properties of the predictor-corrector method for the hydrostatic adiabatic model and the constant acceleration semi-Lagrangian trajectory scheme has been carried out. The activities were concentrated in implementing the constant acceleration scheme into a more recent version of the model as well as testing the response of this new configuration to extreme weather cases. The aim of this study is to demonstrate the advantages or disadvantages of each method applied to the 3D hydrostatic adiabatic model.

2. Very high resolution with a simplified model

With the help of the simplified 1D shallow water model we studied the response of the model to a very big jump in resolution going from the parent model to the coupled one. The main objective is to study the response of the model to a refined orographic forcing which is available in the very high-resolution 1D limited area model. The result of this study will highlight relevant study with the 3D model.

3. Reformulation of the physics-dynamics interface

A study of the structure of the flow of information in the model concerning the vertical velocity for both hydrostatic and non-hydrostatic model has been carried out. The vertical motion is the most sensitive part of the model dynamics and it could potentially benefit the reformulation of the physics-dynamics interface.

6. Raluca RADU : "Extensive study of the coupling problem for a high resolution limited area model"

Limited area models need information about the state of the atmosphere outside the integration area, so one of the inherent problems is the specification of the lateral boundary conditions. A number of studies have demonstrated that LBCs of LAMs can have a significant impact on the evolution of the predicted fields through the propagation of boundary errors onto the interior of the domain. As each prognostic variable is prescribed at each lateral boundary point, the result is over–determination (ill-posedness) and a consequence is partial reflections that propagate these errors back in the integration area. In order to introduce lateral boundary information coming from large scale model and to damp the reflection produced by limited area model, the Davies–Kallberg relaxation scheme (Davies 1976) is used in ALADIN. This method accepts its ill-posedness and tries to damp reflected spurious waves by using a relaxation zone. Coupling means that every time step the values of the ALADIN model, obtained without any influence of the coupling model, are combined with the values interpolated on the ALADIN grid starting from the coupling model.

During this first ALATNET stay the study has been concentrated on the study of the presently used relaxation scheme and on the improving of a new method for coupling. The investigation of weaknesses of the Davies-Kallberg scheme and possible enhancement of it was the first step. This was tested with 3D numerical experiments on Christmas storm from December 1999. In this case two deep cyclones developed in the middle Atlantic and passed quickly through Western Europe. Some integrations of standard ALADIN model, using hourly ARPEGE global model forecasts as coupling files and applying them as lateral boundary conditions for the LACE domain, were done. The purpose was to study the impact of coupling frequency by comparing the depth of the cyclone in the coupling and coupled model near the time of entering domain using MSLP post-processed fields and observing the entry time in the domain.

25.12.1999 Christmas storm case

Starting from the given data the model arrives to a surprising solution with 6 hours coupling frequency of updating the boundary files. For 18 hours forecast valid for 06UTC in 26.12.99 the cyclone is missing (Fig1a), meanwhile for 3 hours coupling frequency, the pressure field has the value 976 hPa (see Fig1b) and with hourly coupling frequency the same hour, the cyclone has the deepest value 974 hPa (Fig1c) and the closest to the forecasted field by ARPEGE (Fig1d), the reasonably good for that day.

27.12.1999 Christmas storm case

Using 6 hours coupling frequency in integration for 24 hours with coupling files from global model the plotted MSLP field has 984 hPa value for the second cyclone at 21 UTC for 27.12.99, for the same hour a value of 982 hPa using 3 hours coupling files frequency in integration of the model and the deepest value again was obtained using hourly coupling frequency 980 hPa, as in the case of the first storm. For the coupling field obtained directly from global model there is a minimum value 977 hPa from all of them. As we expected the closest value to reality in both cases was that one obtained through hourly frequency of coupling.

Discussion

Because the system was moving very fast it happened that it didn't appear in the coupling zone of the model at the coupling times. ALADIN has no chance to forecast the storm if the cyclone genesis process is outside its domain, as it gets any information through lateral boundary conditions on the existence of such a system. Even if the coupling model forecasts the system, the coupling scheme can fail to pass the information to the LAM, and this was the case. In addition, the forcing field is not the forecasted field of the coupling model for the given time, but the field obtained by temporal interpolation of two forecasts of the global models. If the system had no trace on the coupling zone

(first time is outside the domain, next time is fully entered inside the domain), it cannot be forecasted by LAM. This can happen because the coupling model passes the information to the LAM only by its fields over the coupling zone at discrete times.

Next step is introduction and testing of spectral coupling, considered to be a solution for the problems described above, offered by the fact that ALADIN is a spectral model using Fourier expansions in both horizontal directions. Spectral coupling means blending of large scale spectral state vector with the state vector of the coupled model so that the blended state vector is equal to the large scale one for small wave-numbers and equal to the coupled one for large wave-numbers with a smooth transition in between. A spectral coupling scheme is built on the same analogy as the Davies relaxation scheme. It presents an additional coupling step to the present scheme.

New coupling scheme provides scale selection where large scales are dominated by the spectra of the coupling model and only small scales resolved by the forcing model are dominated by LAM. The potential advantage of spectral coupling is that scales resolved by the coupled model are forced to LAM, even if the location of the system of the given scale is inside the domain. Spectral coupling cannot eliminate spurious inward propagation through the lateral boundaries, without the damping by the standard Davies scheme all waves that exit on one side of the domain would freely enter on the opposite side, but using simultaneous Davies scheme and spectral coupling the advantages of both methods are combined.

This point required code development, which is going at the present moment. It looks reasonable to introduce this step after finishing semi-implicit scheme in spectral space but before applying horizontal diffusion. In principle the idea is to read the spectral coupling fields, introduction of a large scale buffer, make the time interpolation and blend ALADIN spectral fields with interpolated large scale ones by the use of the spectral alpha weight function. In order to avoid too strong external forcing we consider retuning of alpha function of grid-point coupling, and also we keep open the possibility not to apply the spectral coupling at every time step of integration of the model (introduction of step frequency).

References

Davies, 1976:''A lateral boundary formulation for multi-level prediction models'' QJRMS, 102, 405-418

A. Mc Donald, 1997:''Lateral boundary conditions for operational regional forecast models'' a review HIRLAM technical note no.32

R. Lehmann, 1993:''On the choice of relaxation coefficients for Davies lateral boundary scheme for regional weather prediction models'', Meteorology and Atmospheric Physics, 52, 1-14

Gabor Radnoti, 2001:''An improved method to incorporate lateral boundary conditions in a spectral limited area model''

M. Janiskova, 1994:'' Study of the coupling problem''. ALADIN note

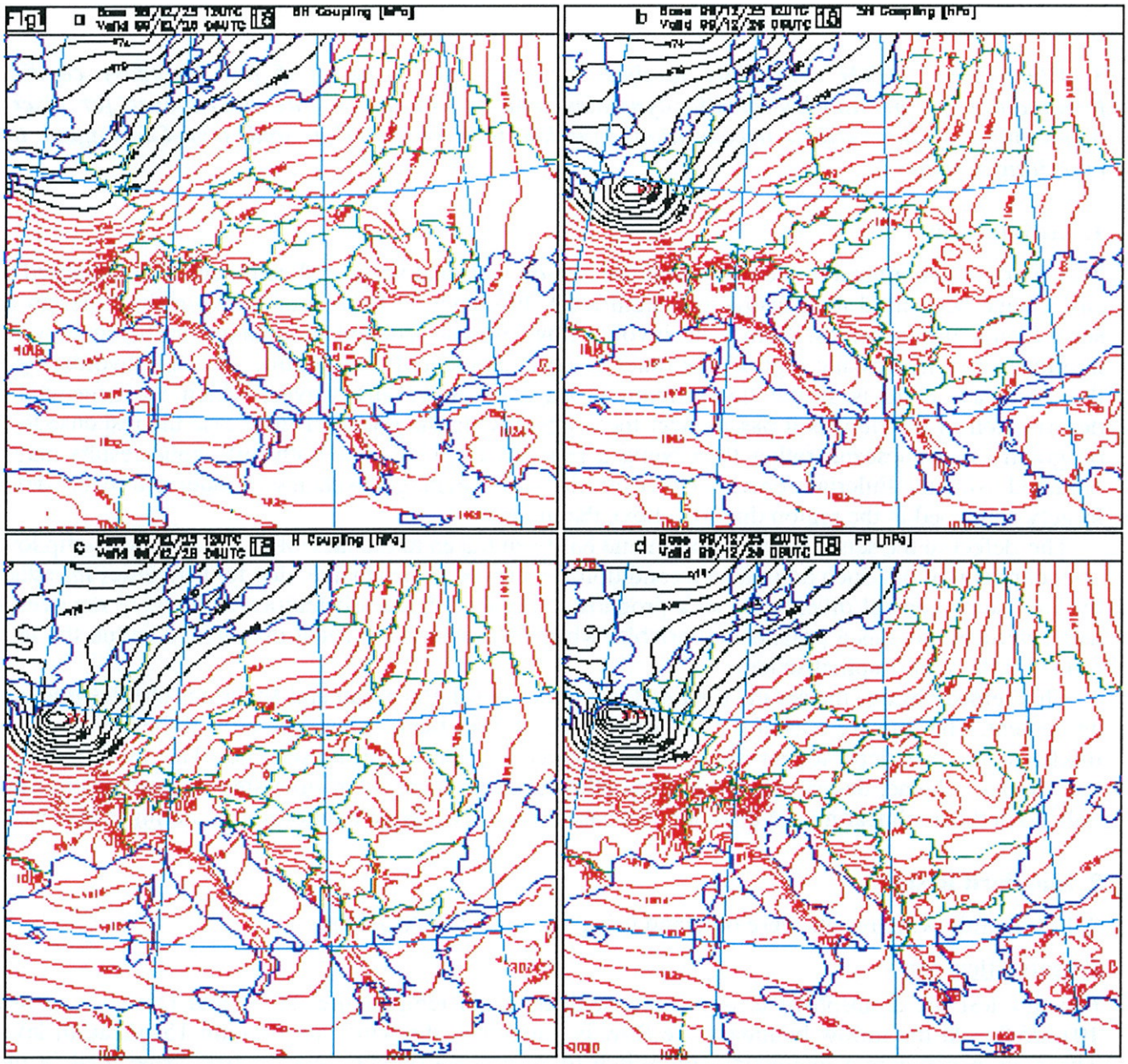

Figure1:
Impact of coupling frequency on MSLP field, forecasted for 18 hours, valid for 26.12.99 06 UTC:
a) for ALADIN using 6 hours coupling files,
b) for ALADIN using 3 hours coupling files,
c) for ALADIN using 1 hour coupling files,
d) for ARPEGE forecast.

7. André SIMON : "Study of the relationship between turbulent fluxes in deeply stable PBL situations and cyclogenetic activity"

The work is just starting. The very first and important progress is the discovery of the big bug in CYCORA_ter. Congratulations ! More news in the next Newsletter.

8. Chistopher SMITH :"Stability analysis and precision aspects of the boundary condition formulation in the non-hydrostatic dynamics and exploration of the alternatives for discrete formulation of the vertical acceleration equation both in Eulerian and semi-Lagrangian time marching schemes"

1. Introduction

This work has continued in the context of the two-dimensional vertical slice model. Two idealised test cases have been used to investigate a significant difference in behaviour between the Eulerian and semi-Lagrangian schemes. Both tests involve flow over an isolated mountain, one being flow in a nonlinear, non-hydrostatic regime; the other being in a potential flow regime, also non-hydrostatic. In the first case there is strong downstream propagation of gravity waves, which are generated by deformation of the flow as it passes over the orography. In the potential flow case the response to the orography is evanescent, rather than being a propagating wave. For both tests good results may be obtained using the Eulerian scheme. However, the semi-Lagrangian scheme introduces a severe defect, largely contained in the region directly above the mountain.

The defect in the semi-Lagrangian scheme has been traced to the lack of an effective free-slip lower boundary condition. Such a boundary condition has proved to be elusive, due to difficulties introduced by the use of vertical divergence as a prognostic variable. These difficulties are largely removed by using vertical wind as a prognostic variable, while still retaining vertical divergence within the linear model of the semi-implicit scheme.

This remedy brings the results obtained using the semi-Lagrangian and Eulerian schemes into close agreement. The primary reason for choosing to use a semi-Lagrangian scheme is to be able to run the model with time-steps longer than those allowed by the Eulerian scheme. The modified semi-Lagrangian scheme, described above, does allow such an increase in time-step. Unfortunately this is only so in the nonlinear non-hydrostatic test case if somewhat large temporal decentering is also used.

2. Standard Results

All of the following results were obtained using version 12 of ALADIN.

Potential flow test

For this test the atmosphere is isentropic, with potential temperature 280 K and reference pressure 101325 Pa. At the inflow boundary the flow is horizontal, the wind speed being 15 m/s at all levels. The flow encounters a mountain with Witch of Agnesi profile (the classic bell-shape used in most studies of this kind). The peak mountain height is 50 m and the half-width parameter is 100 m. Figure 1 shows the vertical wind field after model integrations using the Eulerian and three time-level semi-Lagrangian schemes. The horizontal mesh length is 20 m and the vertical mesh length is approximately also 20 m. There are 39 grid levels. The Eulerian scheme produces a result which is in excellent agreement with an analytical linearized solution. However, the semi-Lagrangian scheme has completely spurious behaviour located over the mountain and extending throughout the depth of the modelled atmosphere.

Nonlinear non-hydrostatic flow test

The inflow boundary condition for this test has a vertical temperature profile for which the Brunt-Väisälä frequency is constant, with value 0.01 Hz. The temperature at zero height is 285 K and the horizontal inflow wind speed is 4 m/s. Again the mountain has the Witch of Agnesi profile but this time with peak height and half-width both 400 m. Figure 2 shows the vertical wind field obtained using, on the left, the Eulerian scheme and, on the right, the three time-level semi-Lagrangian scheme. The mesh length is 80 m in the horizontal and approximately 365 m in the vertical, with 41 levels.

Once more we see that the Eulerian scheme provides a good solution, while the semi-Lagrangian scheme suffers spurious behaviour linked to the orography.

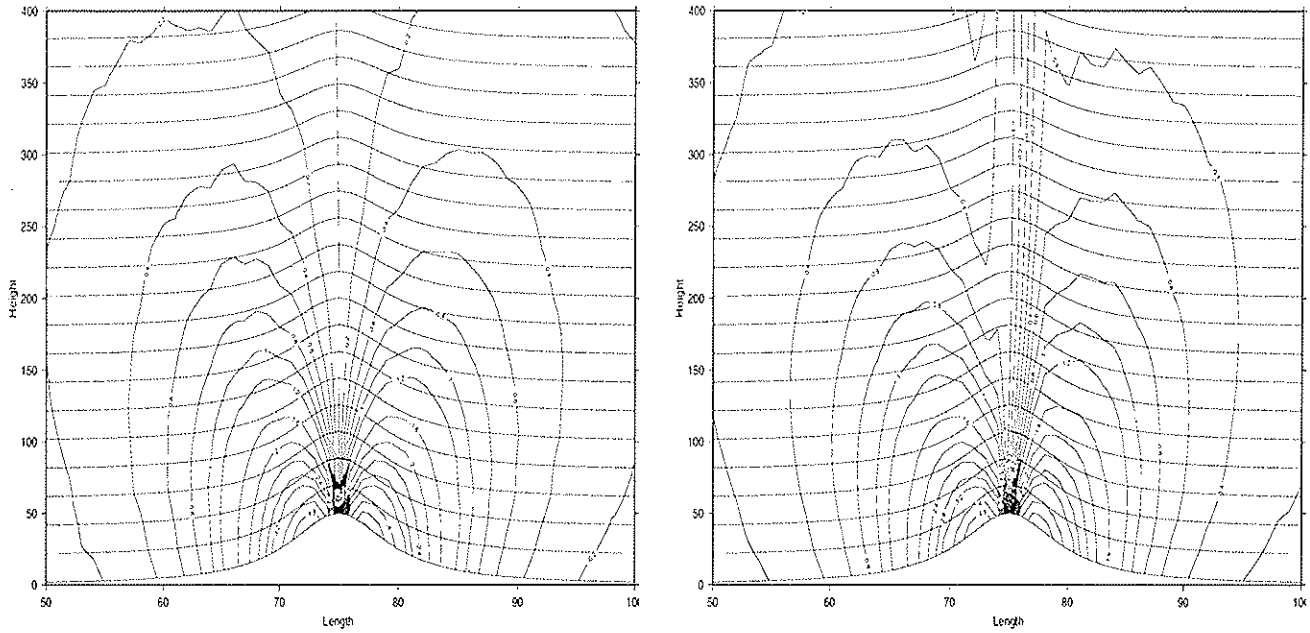

Figure 1 : Steady state solutions of potential flow problem using ALADIN. Left: Eulerian scheme. Right: three time-level semi-Lagrangian scheme. Only part of domain is shown, to highlight the solution close to the mountain. Horizontal lines are geopotential height of grid levels. Time-step 0.1s, 800 steps. The flow is from left to right.

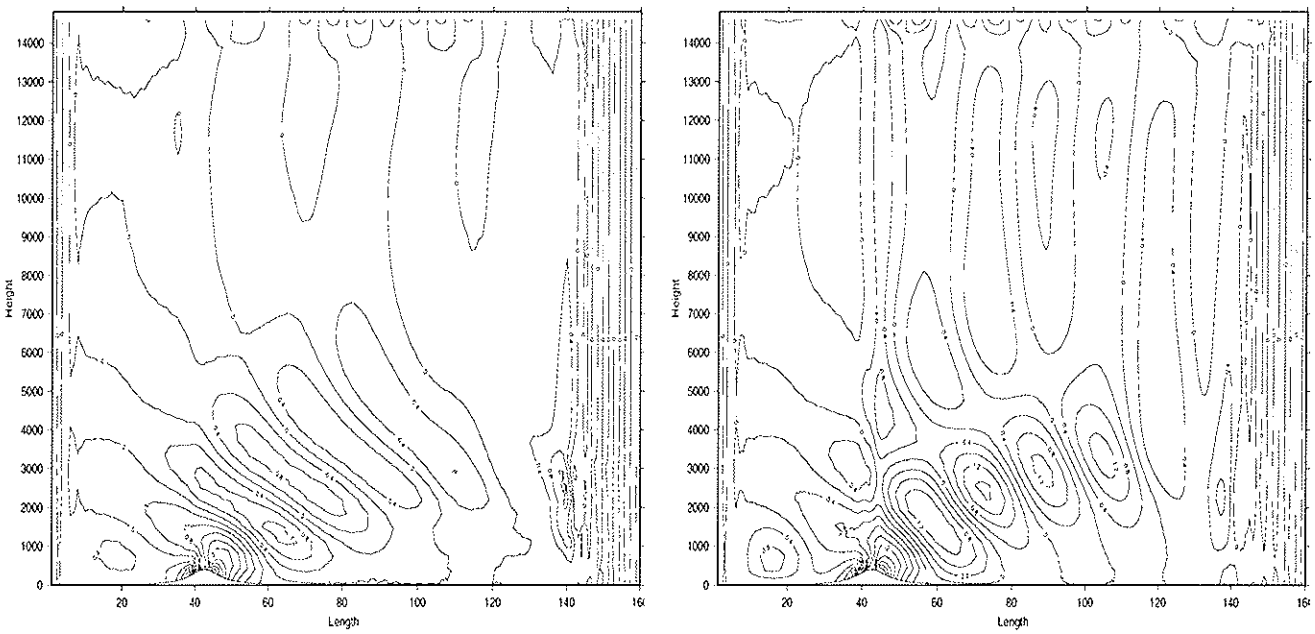

Figure 2 : Steady state solutions for nonlinear non-hydrostatic test, obtained using Eulerian scheme (left) and three time-level semi-Lagrangian scheme (right). Entire domain is shown. Integration in each case is for 1000 steps with time-step 2s.

3. Results using vertical wind as prognostic variable

In this modified scheme vertical wind is used as the prognostic variable. This allows the free-slip lower boundary condition to be imposed simply by over-writing the values of vertical wind on the lower

boundary. This is done at the end of the gridpoint calculations, before the semi-implicit solver is called. If $\mathbf{V}^{+(0)}$ and $w^{+(0)}$ are the horizontal and vertical wind approximations formed at the end of the gridpoint calculations, then we simply set :

$$g w_{L^*}^{+(0)} = \mathbf{V}_L^{+(0)} \cdot \nabla \phi_s$$

where index L^* indicates the lower boundary, index L is the first full model-level above the boundary and ϕ_s is the geopotential height of the orography. The results obtained, using the semi-Lagrangian scheme modified in this way, are shown in Figure 3. It should be noted that further improvement, especially in the potential flow test, is obtained by using so-called linear truncation in the spectral representation. Using additional Fourier modes removes the ''cauliflower'' effect seen in some of the low wind-speed contours.

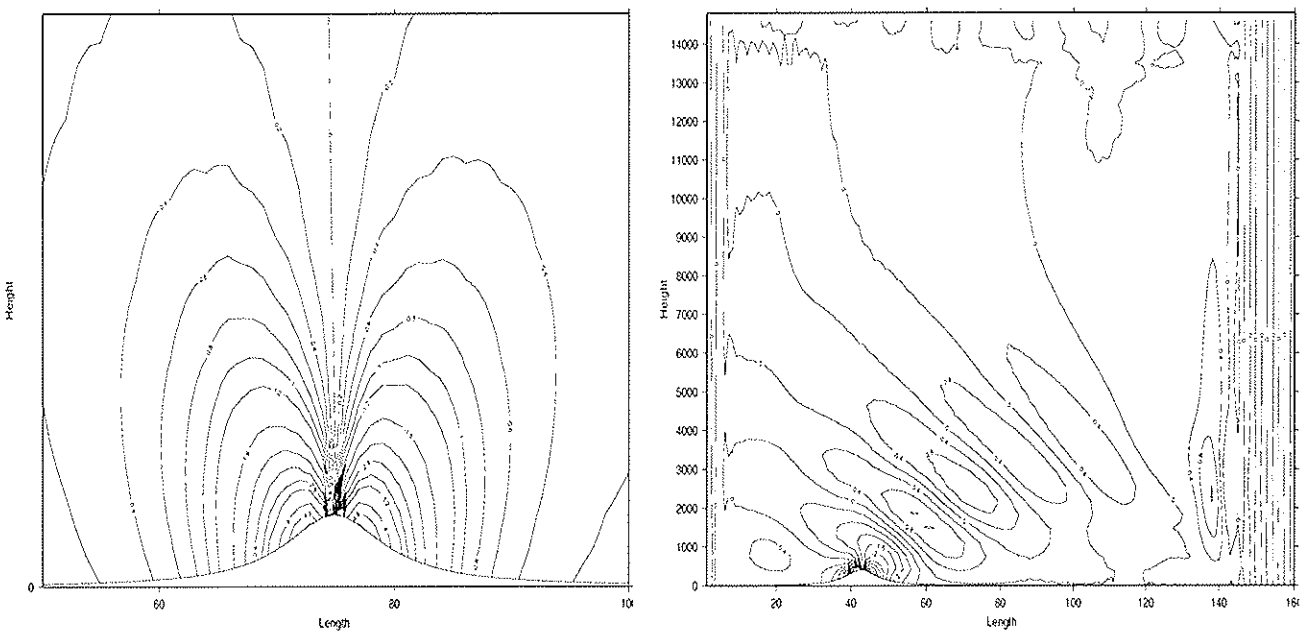

Figure 3 : Results for potential flow test (left) and nonlinear non-hydrostatic flow test (right). These were obtained using the three time-level semi-Lagrangian scheme, with vertical wind as prognostic variable.

4. Discussion

For inviscid flow the free-slip lower boundary condition is a necessary condition connecting the horizontal and vertical winds. Ideally this constraint should be satisfied exactly at all time-levels. However, this is not always the case in weather forecasting models. In practice such a deficiency may not be too detrimental to the model, where physical parameterizations play an important role near the surface. In view of this we may describe the proposed implementation of the free-slip condition as being pragmatic: it is a solution which offers some potential improvement in forecast skill, while still falling short of being the most desirable mathematically correct solution. Instead of the free-slip constraint being built in to the structure of the model, the proposed solution is to reinforce the free-slip condition at every time-step by simple over-writing of data.

In the case where vertical divergence is the prognostic variable, not only do we not have the free-slip constraint built in to the model, it is also not clear how a pragmatic solution may be imposed. Since vertical divergence involves differences in vertical wind across model layers, it would perhaps be necessary to alter data at all model levels, not just near the lower boundary, in order to impose the free-slip condition. The way in which this might be done appears to be entirely *ad hoc*.

Finally, it should be noted that the results obtained using the Eulerian scheme, shown above, were all obtained using integrations at very low Courant numbers. At low Courant numbers the Eulerian

scheme inherits a good approximation to the free-slip condition from the data at previous time-levels. This is not so in the semi-Lagrangian case, where interpolation of data to laterally displaced points is involved.

5. Future work

Future work will investigate the impact of the choice of non-hydrostatic pressure variable on the modified semi-Lagrangian scheme. Also these developments will be carried over into the predictor-corrector framework, which is also currently under development. The goal for bringing these two development lines together is to obtain a robust and stable semi-Lagrangian scheme, with minimal orography-related defects.

9. Cornel SOCI : "Sensitivity study at high resolution using a limited-area model"

A paper entitled : "High resolution sensitivity studies using the adjoint of the ALADIN mesoscale numerical weather prediction model" was submitted to *Idojaras*. Results were also presented at the joint EWGLAM / SRNWP meeting (Cracow, 8-12 October 2001). Now it is time to write the thesis manuscript. More details in the next Newsletter.

10. Klaus STADLBACHER : "Systematic qualitative evaluation of high-resolution non-hydrostatic model"

Nothing new since the last Newsletter (work at ZAMG).

11. Malgorzata SZCZECH-GAJEWSKA : "Use of IASI / AIRS observations over land"

I. Introduction

This is the study of use of observations over land from advanced infrared sounders (with spectral resolution < 0.5 cm^{-1}) such as IASI or AIRS. Previous work focused mainly to the data over sea. Over land the problem is the simultaneous retrieval of atmospheric profiles and of surface characteristics (land surface temperature LST and surface spectral emissivity SSE). Two basic ways of retrieval can be distinguished: joint (simultaneous) of atmospheric and surface parameters and the physical multi-spectral method. The main component of both methods consist of the usage of ancillary information which specifies SSE behaviour or constitutes some a-priori constrains. A first estimate of surface temperature can be taken from model forecast, but emissivity can be provided just by climatological values depending on the land cover type. First part of work comprised inclusion of emissivity fields for chosen spectral ranges into ARPEGE climatological files. The further study will use one-dimensional

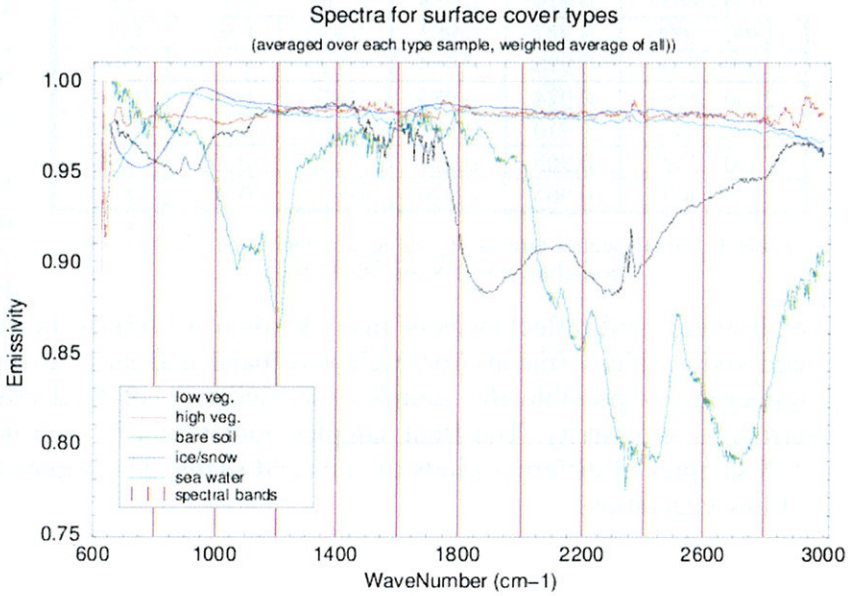

framework to test the retrieval of both profiles and surface values. Then, it will be extended to three-dimensional analysis scheme.

IASI, an Infrared Advanced Sounding Interferometer is jointly developed by EUMETSAT and CNES an will be operational instrument on the EPS-Metop series of satellites (first launch about 2005). The IASI instrument supplies the spectra of the atmosphere in the IR band, with 8461 channels in each spectrum. This gives us great advantage of treating emissivity spectra as separated into 200 cm^{-1} wavebands.

II. Climatology

Fields in climatological files of ARPEGE and ALADIN created by configuration 923 of models are interpolated just one time in case of defined land-sea mask and type of surface. Until this time as a surface characteristics were concerned just two fields - the albedo of bare soil and emissivity, but without annual changes. The emissivity (mean value over entire spectrum) was interpolated or calculated over the final grid as a function of surface type and the maximum fraction of vegetation. The mean values of emissivity were derived from old Navy data.

Work on the creation of new climatological fields of SSE had started with appropriate code changes and creations of new subroutines. As illustrated in Fig.1 we divided almost IASI IR range into 12 equal wavebands: from 600 cm^{-1} to 3000 cm^{-1} with step 200 cm^{-1}. According to them climatological fields of surface spectral emissivity were created. Thus, two approaches of creating climatological files of SSE were used, namely with and without interpolation of emissivity. First one was based on the global emissivity maps from Jean-Louis Roujean (further called as JLR). They had the resolution of 0.5° over the whole world, and were created on base of MODIS spectral library and also 0.5° resolution vegetation maps. Then, those SE maps were taken as an input for configuration 923 (modified one) in which emissivity was interpolated to final ARPEGE grid. The second way was to assign spectral emissivity values, calculated from MODIS and ASTER, to each ARPEGE gridpoint with respect to surface type, percentage of land and maximum fraction of vegetation.

Band [cm^{-1}]	sea	ice	soil	high v.	low v.
600 - 800	0.989	0.994	0.946	0.980	0.970
800 - 1000	0.980	0.989	0.880	0.981	0.982
1000 - 1200	0.979	0.988	0.976	0.982	0.986
1200 - 1400	0.981	0.986	0.984	0.981	0.973
1400 - 1600	0.982	0.988	0.978	0.976	0.923
1600 - 1800	0.979	0.988	0.964	0.973	0.896
1800 - 2000	0.977	0.983	0.882	0.972	0.897
2000 - 2200	0.976	0.984	0.829	0.971	0.899
2200 - 2400	0.974	0.985	0.853	0.972	0.934
2400 - 2600	0.970	0.981	0.843	0.973	0.949
2600 - 2800	0.965	0.971	0.920	0.975	0.962
2800 - 3000	0.965	0.970	0.907	0.980	0.960

Table 1. Mean spectral emissivity values for each type of land cover, based on MODIS and ASTER data

The differences between climatological emissivity fields created in both ways were found joust over land covered by vegetation. They were caused by different vegetation maps usage. To be consistent with the model vegetation cover and because of the emissivity data JLR provided us were without estimation errors we have decided to use the second way of climatological files creation. As an input data for climatology were used the laboratory measured samples of emissivity for different kinds of materials. Main source if it were MODIS and ASTER spectral libraries, which contains respectively emissivities and reflectances of many kinds of materials. In Table 1 are shown the calculated spectral emissivity values (mean) for each waveband and surface type. It was very important to obtain as numerous as possible the samples for each type of land cover, because of calculating background errors for emissivity. The final samples numeration is : sea water - 5 samples, ice/snow - 9 samples, 128 samples of different kinds of soils and sands, 24 samples of high vegetation (trees) and 5 samples of low vegetation.

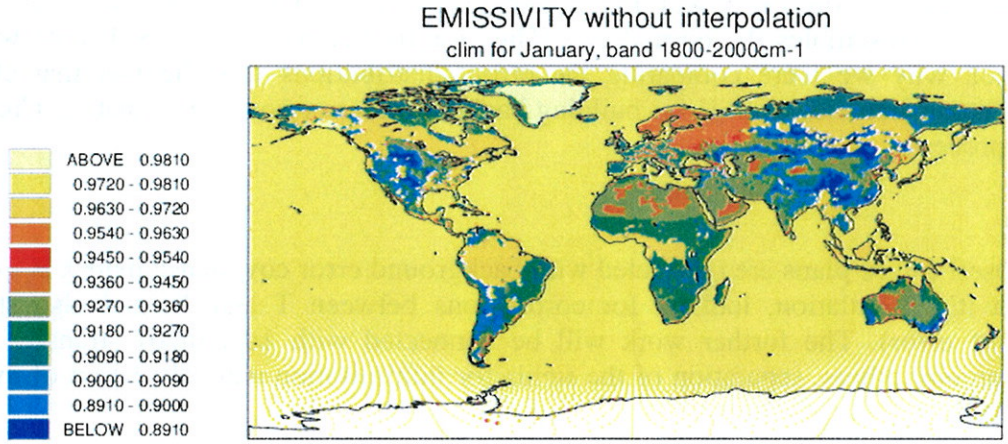

Fig.2 ARPEGE climatological field of surface spectral emissivity for the waveband 1800 - 2000 cm^{-1}. The emissivity values were assigned to surface and vegetation types.

The result of this work are 12 new climatological emissivity fields, with the names: SURFEMI0700.IASI, SURFEMI0900.IASI and so on, respectively to the middle values of the wavebands. Fig.2 shows the climatological map of spectral emissivity for January and waveband 1800-2000 cm^{-1} .

III. Background errors covariance matrix – starting point

During the creation of climatological files one more problem arose, to use directly SSE or convert it to *-log(1-*SSE*)* ? The idea came from Goulven Monnier (personal communication). He found out that for the emissivities he was using (some samples from ASTER spec. lib.) distribution of *-log(1-*SSE*)* around mean value is more Gaussian than for SSE. The emissivity values in general are very close to 1, actually they are lower than 1, so such change would help for the further studies with LSE and SSE inversions. Our sample of the spectral emissivities is much bigger and it's coming from the different sources, so we couldn't assume the same behaviour of SSE - we had to check this. Appropriate tests were done, but instead of making distribution of the emissivity around it's mean values was checked the distribution of the errors

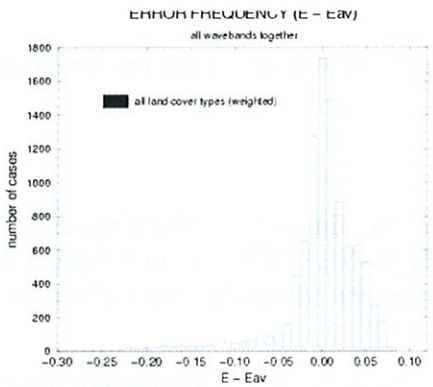

Fig. 3 Errors distribution for direct SSE

(SSE-*av(*SSE*)*) around 0. First it was done for all wavebands together, but separately for each surface cover type. Results showed that the distribution of the errors almost for all surface types (except snow/ice samples) was more Gaussian for the direct SSE than for *-log(1-*SSE*)* values. Afterwards for verifying if it is in general true for all data together was prepared common sample for all types of the surface cover. The compilation of those emissivities was based on weights - importance of each surface type in global aspect. Base for it was taken from ARPEGE model. In it, each surface type covers following percentage of the globe: sea water - 53.4%, ice/snow - 1.4%, high vegetation - 13.5%, low vegetation - 29.2% and bare soil - 2.5%. The

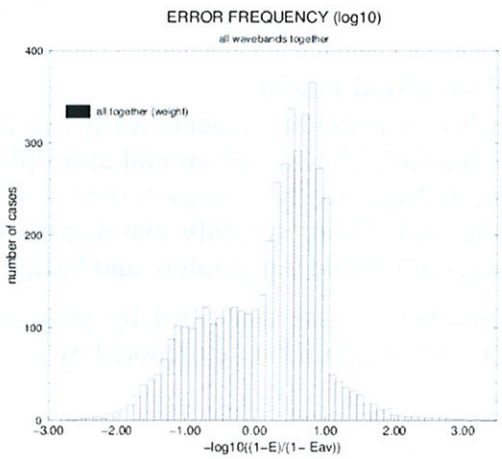

Fig. 4 Errors distribution for *-log(1-*SSE*)*

results you can see on Fig.3 and Fig.4, apparently the distribution of not transformed surface emissivity more resembles the normal one. Thus for further work direct SSE data were taken. The other reason why we were comparing the errors distributions was the fact that already we had calculated some statistics of SSE for building background error covariance matrix. Currently creation of B is in process.

IV. Plans

The closest future plans are connected with background error covariance matrix B - continuation of work with it's calculation, looking for correlations between T and Ts and also statistics for Ts (variance of error). The further work will be connected with 1d radiative-transfer model. It will comprise among others, separation of the fields for minimisation and calculation of the gradients for LST and SSE.

Appendix

Abbreviations used in the document :

IASI	Infrared Advanced Sounding Interferometer
AIRS	Atmospheric Infrared Sounder
SSE	Surface Spectral Emissivity
LST	Land Surface Temperature
ASTER	Advance Spaceborn Thermal Emission and Reflection Radiometer
MODIS	Moderate Resolution Imaging Spectrometer

Laboratory emissivity data were taken (autumn 2001) from :
http://speclib.jpl.nasa.gov/, http://www.icess.ucsb.edu/modis/EMIS/html/em.html

12. Jozef VIVODA :"Analysis of stability of 2TL SI non-extrapolating predictor/corrector scheme in the limit of infinite time step"

1. Introduction

Linearized version of Euler Equations system (EE) is analysed in the limit of infinite time step. Two time level semi-implicit non-extrapolating predictor/corrector (2TLSI-NES PC) time marching scheme is applied on linearized space continuous EE. Results are independent of model space discretisation and their validity can be generalized for other models as well.

EE system is formulated using σ hydrostatic pressure based coordinate ($\sigma=\pi/\pi_s$). Prognostic variables are divergence (D), temperature (T), logarithm of surface pressure ($q=ln(\pi_s)$), vertical divergence d_3 and rescaled pressure departure :

$$d_3 = -\frac{p}{\pi}\cdot\frac{\sigma}{RT}\cdot\frac{\partial w}{\partial\sigma} \qquad \hat{q} = \ln(\frac{\pi}{p})$$

2. Linearized model

Analyses of stability is analytically tractable, if analysed system is linear only. Therefore, the nonlinear EE has to be linearized around atmospheric background state. Background state was chosen to be in rest, hydrostatically balanced, over flat terrain (it could be understood as horizontally independent), isothermal. There are only two degrees of freedom remaining in such a choice of background state , background-state temperature and background-state surface pressure.

Atmospheric state described by prognostic variables can be expressed as infinitesimal perturbation around background state (denoted by a bar) :

$$
\begin{aligned}
D &= D' \\
T &= \overline{T} + T' \\
\pi_s &= \overline{\pi_s} + \pi_s' \\
q &= \overline{q} + q' \\
d_3 &= d_3' \\
\hat{q} &= \hat{q}'
\end{aligned}
\qquad (1)
$$

Before the analysis, the integral operators that appear in the system are replaced by derivative operator $(\partial / \partial \ln\sigma + 1)$. The logarithm of surface pressure will disappear from the equations. Classical linearization yields then to the following linear system ($\mathcal{M}$) :

$$
\begin{aligned}
\frac{\partial D}{\partial t} &= -R\Delta T - \overline{RT}\left(\frac{\partial}{\partial \ln\sigma} + 1\right)\hat{q} \\
\frac{\partial d_3}{\partial t} &= -\frac{g^2}{\overline{RT}}\frac{1}{\alpha}\frac{\partial}{\partial \ln\sigma}\left(\frac{\partial}{\partial \ln\sigma} + 1\right)\hat{q} \\
\frac{\partial T}{\partial t} &= -\frac{R}{C_v}\overline{T}(D + \alpha d_3) \\
\left(\frac{\partial}{\partial \ln\sigma} + 1\right)\frac{\partial \hat{q}}{\partial t} &= -\frac{C_p}{C_v}\left(\frac{\partial}{\partial \ln\sigma} + 1\right)(D + \alpha d_3) - D
\end{aligned}
\qquad (2)
$$

The parameter α is equal to 1 for the purpose of following analyses. If model was formulated using $d = -\pi^* / \pi \, . \, 1 / RT^* \, . \, \partial w / \partial \ln\sigma$, then α would be the ratio of T^* to the background-state temperature. This possibility will be discussed in the summary.

3. Two time level semi-implicit non-extrapolating predictor/corrector scheme (2TLSI-NES)

The scheme is called non-extrapolating since unknown state at time $t + \Delta t / 2$, appearing in two time level scheme formulation, is approximated using relation

$$
X^{t+\frac{\Delta t}{2}} = X^t \qquad (3)
$$

In the following, time instant $t + \Delta t / 2$ is excluded from equations and relation (3) is used implicitly everywhere.

If linearized equations system (2) is referred as $\mathcal{M}$, semi-implicit linear model as $\mathcal{L}$, the nonlinear residual as $\mathcal{R}$ and model state vector X, then the predictor of 2TLSI-NES yields :

$$
\frac{X^{t+\Delta t(0)} - X^t}{\Delta t} = \mathcal{R}X^t + \frac{1}{2}\mathcal{L}\left((1+\varepsilon)X^{t+\Delta t(0)} + (1-\varepsilon)X^t\right) \qquad (4)
$$

Semi-implicit linear model can be obtained from $\mathcal{M}$ just by setting the background-state values of T and π_s to T^* and π_s^* respectively. Here T^* is the reference temperature of semi-implicit linear model and π_s^* is analogically the reference surface pressure.

Non-extrapolating predictor allows to compute first guess at time $t + \Delta t$, using just state at time instant t. This approach is only first order accurate. This is not an obstacle when predictor/corrector scheme is used since second order accuracy is restored during corrector steps. The k-th corrector step is formulated :

$$\frac{X^{t+\Delta t(k)}-X^{t}}{\Delta t}=\frac{1}{2}\mathcal{M}\left((1+\varepsilon)X^{t+\Delta t(k-1)}+(1-\varepsilon)X^{t}\right)+\frac{1}{2}(1+\varepsilon)\mathcal{L}\left(X^{t+\Delta t(k)}-X^{t+\Delta t(k-1)}\right) \quad (5)$$

Parameter ε is first order decentering factor.

4. Analyses of stability

We examine the stability of the normal modes of the time-continuous system. Following Bénard et al. (2002) the geometric structure of the normal modes is :

$$X(x,\sigma,t)=X_0(t)\ \exp(ikx-nH\ln\sigma) \quad (6)$$

Notation H represents the height of the isothermal atmosphere with temperature T^*. Notation n corresponds to $n=i\theta+1/(2H)$ with θ being the vertical wavenumber. Notation k is used for horizontal wavenumber.

Classical Von Neumann stability analysis is used with amplification rate of the scheme λ defined as :

$$\lambda^{(0)}=\frac{X^{(0)}(t+\Delta t)}{X(t)} \quad (7)$$

for predictor and

$$\lambda^{(k)}=\frac{X^{(k)}(t+\Delta t)}{X(t)} \quad (8)$$

for k-th corrector step.

Centred non-extrapolating scheme and also non-extrapolating scheme with first order decentering are truly two time level schemes. Their contains only physical modes and no computational. Therefore four solutions of λ exist in EE system, two represent gravity modes and two represent acoustic modes. The fact that reference and background-state temperatures are chosen to be isothermal leads to possibility to use linear relation between them :

$$\bar{T}=(1+a)T^* \quad (9)$$

Analyses with first order decentering : Predictor

First analyses of predictor is carried out. Relations (6), (7) and (9) are substituted into (4). Structure equation is found as a determinant of model state transition matrix. Solving structure equation for λ four solutions are found.

$$\lambda_1^{(0)}=\lambda_2^{(0)}=\frac{\varepsilon-1}{\varepsilon+1}$$
$$\lambda_3^{(0)}=\frac{-1-2a+\varepsilon}{\varepsilon+1} \quad (10)$$
$$\lambda_4^{(0)}=\frac{-1+a+\varepsilon(1+a)}{(1+a)(\varepsilon+1)}$$

All solutions are real. First two modes $\lambda_1^{(0)}$ and $\lambda_2^{(0)}$ are stable for $\varepsilon \geq 0$. Analysing other two modes the condition for predictor to be stable is found :

$$-\frac{\varepsilon}{1+\varepsilon} \leq a \leq \varepsilon \quad (11)$$

If the predictor is not decentered ($\varepsilon = 0$) then it is unconditionally unstable. Condition could be written as a condition for the range of actual temperature dependent on current value of T^*.

$$T^*\left(1-\frac{\varepsilon}{1+\varepsilon}\right) \leq \bar{T} \leq T^*(1+\varepsilon) \quad (12)$$

Analyses with first order decentering : Corrector

Substituting (6), (7), (9) and (10) into (5), we obtain forth order polynomial equation of every mode of predictor (CAUTION, this approach has been found to be methodologically wrong. Results for predictor are correct but results for corrector presented here are wrong. More details about the methodology can be found in the appendix). Subsequently the solutions of amplification rate are found for k-th corrector :

$$\lambda_1^{(k)} = \lambda_2^{(k)} = \frac{\varepsilon - 1}{\varepsilon + 1}$$

$$\lambda_3^{(k)} = (-a)\lambda_n^{(k-1)} + \frac{(1+a)(\varepsilon - 1)}{\varepsilon + 1} \qquad (13)$$

$$\lambda_4^{(k)} = \frac{a}{1+a}\lambda_n^{(k-1)} + \frac{\varepsilon - 1}{(\varepsilon + 1)(1+a)}$$

There are recurrence relations for the third and the forth mode. Notation $\lambda_n^{(k-1)}$ means any of the mode from previous corrector (or predictor in the case of the first corrector). If any of first two stable modes ($\lambda_1^{(k-1)}$ or $\lambda_2^{(k-1)}$) enter recurrence relations then the following modes are stable.

Before analyses of mixed modes the analyses of "clean" modes is done. If we consider that :

$$\lambda_3^{(k)} = (-a)\,\lambda_3^{(k-1)} + \frac{(1+a)(\varepsilon - 1)}{\varepsilon + 1}$$

we could then write for the amplification factor of the third "clean" mode of k-th corrector :

$$\lambda_3^{(k)} = \frac{2(a+\varepsilon)}{\varepsilon + 1}(-1)^{k-1}a^k + \frac{\varepsilon - 1}{\varepsilon + 1} \qquad (14)$$

This mode is stable in the limit of infinity iterations, if the condition $-1 \le a \le 1$ is satisfied.

If :

$$\lambda_4^{(k)} = \frac{a}{1+a}\lambda_4^{(k-1)} + \frac{\varepsilon - 1}{(\varepsilon + 1)(1+a)}$$

is considered, then amplification rate of the forth "clean" mode of k-th corrector is :

$$\lambda_4^{(k)} = \frac{2}{\varepsilon + 1}\left(\frac{a}{1+a}\right)^{k+1} + \frac{\varepsilon - 1}{\varepsilon + 1} \qquad (15)$$

This mode is stable in the limit of infinity iterations, if the condition $-1/2 \le a \le \infty$ is satisfied.

There are other mixed modes. Their analytical analyses is practically impossible due to oscillating character of the third mode. Their behaviour was studied experimentally and it was found that for the first corrector those modes are the most unstable one. The behaviour of these mode is still in the phase of experimental research.

There is plotted absolute value of the most unstable mode on figure 1 for predictor and first five correctors for the first order decentering factor $\varepsilon = 0.1$.

It is interesting to point that the effect of first order decentering is simply the shift of the curves down along the y-axis by the factor $2\,\varepsilon / (\varepsilon+1)$.

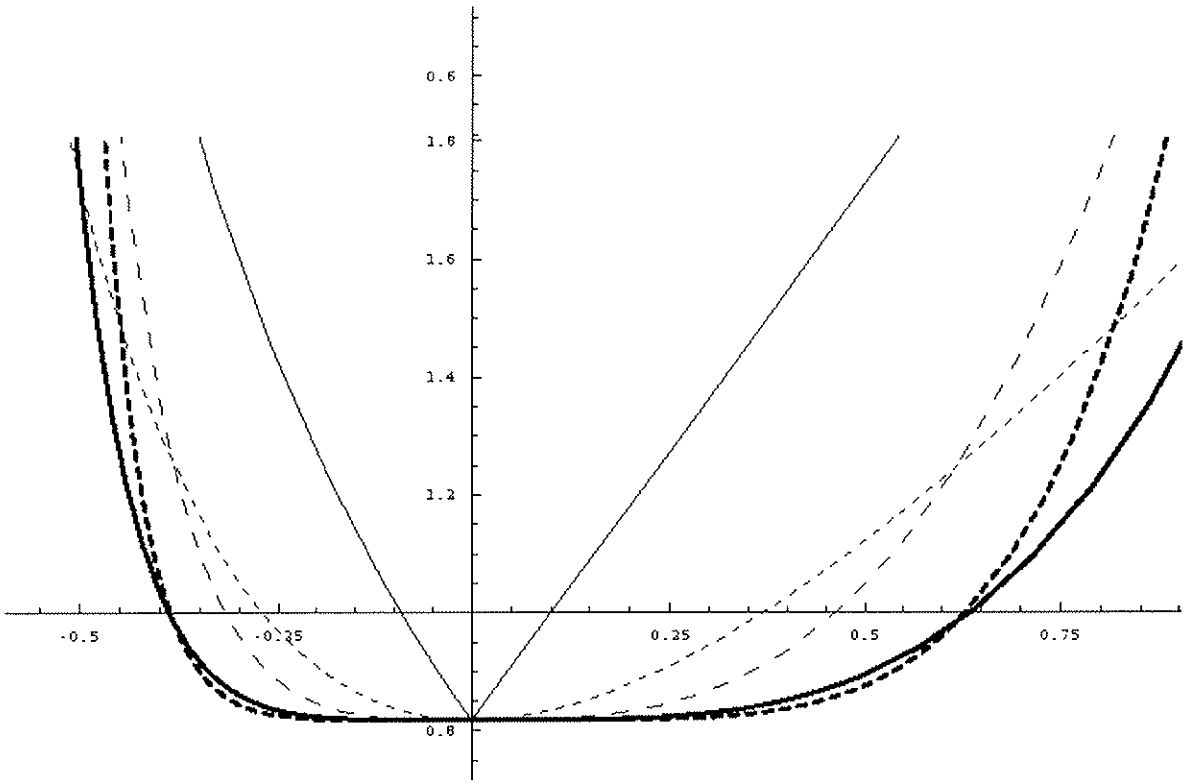

Figure 1: The absolute value of the growth rate of the most unstable mode of the non-extrapolating two-time-level semi-implicit predictor/corrector scheme. The σ vertical coordinate is used and the first order decentering factor is $\varepsilon = 0.1$. Predictor, corrector first, second, third and forth are plotted using thin solid line, thin short dashed line, thin long dashed line, thick solid line and thick short dashed line.

5. Summary

We analysed the two time level semi-implicit non-extrapolating predictor/corrector scheme applied to the space continuous Euler equations. We found that to achieve stability of the first or second corrector it is necessary to apply decentering. We studied first order decentering. It was found that if the stability shall be achieved for large range of temperatures the value of first order decentering factor has to be very large and the accuracy of the scheme is decreased. To get over this problem the second order decentering shall be applied.
We found that for the "clean" modes scheme converge for the range of temperatures :

$$\tfrac{1}{2}T^* \le \overline{T} \le 2T^* \qquad (16)$$

This results anyway can not be generalized yet since there exist mixed modes we could not analytically analysed. This research is still in progress.
It is important to noticed that we analysed also system formulated with pseudo-vertical divergence. It was found that the system is extremely unstable and it diverge.

6. Last minute : Methodology of stability analyses of predictor/corrector schemes

The analyses of stability of predictor/corrector scheme seems to be at a first glance methodologically the same as the analyses of SI scheme. This is true only partially and it is very easy to obtained wrong results doing wrong assumption.

We assume, for the purpose of this appendix, that the 2TL-NES scheme with one corrector can be written for linearized system as :

$$M_{SI}X^* = M_P X^t \qquad M_{SI}X^{t+\Delta t} = M_{CI}X^* + M_{CI}X^t \qquad (17)$$

Here M_{SI} is the matrix appearing from the fact that semi-implicit approach is used. And M_P, M_{CI} and M_{C2} are matrices which represent RHS of predictor resp. corrector step.
There exists two methodological approaches how to compute the growth rate :

1. "matrix" method. Using this method one has to invert M_{SI} and to calculate the total amplification matrix of the PC scheme. This yields :

$$M_{PC} = M_{SI}^{-1} M_{C1} M_{SI}^{-1} M_P + M_{SI}^{-1} M_{C2}$$

   Then the growth rate of particular mode is found as the eigenvalue of the matrix M_{PC}.

2. "polynomial" method. We assume that amplification rates for predictor and corrector are :

$$\lambda^* = \frac{X^*}{X(t)} \qquad \lambda^{(t+\Delta t)} = \frac{X(t+\Delta t)}{X(t)}$$

   and we substitute those assumptions into (17). Eliminating variables the set of two polynomial equations for two variables λ^* and $\lambda^{(t-\Delta t)}$ is obtained. The roots of those set then represent the growth rate of the scheme.

When SI scheme is considered those two approaches are equivalent.

When analysing PC scheme the "polynomial" method is wrong, because we assumed $\lambda^* = X^* / X(t)$, which is not valid any more. It would be valid only in the case when $X(t)$, was an eigenvector of M_P and also M_{CI}. This assumption is not satisfied in our system and therefore the results by using "polynomial" approach are wrong.

The matrix method is only correct one for the predictor/corrector analyses of stability.

Study of some odd behaviour in ARPEGE physics

M. Bellus (SHMI) - J.-F. Geleyn (Météo-France)

1. Introduction

After several changes in the operational code of ARPEGE (change from CYCORA to CYCORA-bis package and afterwards CYCORA-ter parallel suite, decreasing of the horizontal diffusion in the assimilation cycle since September 2001 etc.), there were some model crashes in a rather short time period. It was important to investigate, whether those instabilities in the model were caused by the new modifications in the code or whether they were present (but hidden) in the past too and have been just woken up for instance by decreased horizontal diffusion. On the other hand we wanted to understand the mechanism, which creates such instabilities and to find some solutions in order to avoid them.

2. Investigation

One of the biggest crashes in the operational suite happened on the 10th of October 2001, while running ARPEGE T95 with Eulerian advection scheme (4d-var ARPEGE forecast). That crash was caused by the development of very big temperature gradients in horizontal as well as in vertical directions (see Fig. 2 - top, REF). From the geographical point of view, this temperature anomaly took place over Pacific ocean 40° N and 180° E. In principle, one can avoid this blowing by shortening of the time step or using semi-Lagrangian advection scheme instead of the Eulerian one. With the increased horizontal diffusion, which will smooth the temperature oscillations, we can also succeed.

Coming from CYCORA to CYCORA-bis package, we allow more moisture to be transported to the top of the cloud. This moisture is probably not consumed enough by downdraft and feeds the large scale precipitation (LSP). Afterwards, that water coming from the LSP is evaporating in a thin dry air layer where strong cooling takes part. The instability itself seems to have a numerical source. There is indeed a tendency of very quick cold air mass descent, which creates of course unrealistically strong vertical wind. Furthermore, the vertical CFL (Courant Friedrich Levy) condition is broken and numerical instability can creates such big vertical temperature oscillations (see Fig. 1 - bottom, REF). (This can even create, in some strange way, the better conditions for convection and some positive feedback may causes the further instability amplification.)

Inside CYCORA modifications there was the possibility to smooth the humidity turbulent diffusion tendency (*LCVLIS=.TRUE.*), but subtraction of a constant tendency everywhere would have a relative big impact in the upper atmosphere where the humidity is small, and small one in the lower troposphere. Therefore a scaling of humidity tendency by specific humidity at saturation was introduced with a coefficient (*GCVPSI*) allowing the continuous transition between the non-averaging state (local use of turbulent fluxes when *GCVPSI=1.*) to a complete smoothing (integral computation of turbulent fluxes when *GCVPSI=0.*).

Several tests aimed on moisture distribution in the cloud showed even negative impact to the Pacific case while there was no smoothing of turbulent fluxes in the turbulent diffusion tendency computation for both specific humidity and enthalpy (see Fig. 1 - bottom, T01). The other extreme, when turbulent fluxes of specific humidity and enthalpy were completely smoothed, was also worse than the reference (see Fig. 1 - bottom, T03). On the other hand, the return to the CYCORA situation (*LCVLIS=.FALSE.*, *GCVPSI=0.*) with the local treatment for q and complete smoothing for T, reduced dangerous temperature gradients significantly (see Fig. 1 - top, T06).

The experiments based on the differences between CYCORA and CYCORA-bis setups (we tested the impact of the parameter groups with the similar functionality) were most sensitive for the above mentioned smoothing of turbulent fluxes and to the group of parameters *GCVNU*, *GCVALFA* and *ECMNP*. Though, it did not cure the instability problem completely and quite big vertical oscillations

of temperature tendency were still present. The combination of *GCVNU*, *GCVALFA*, *ECMNP* (CYCORA values) with the smoothing of temperature turbulent fluxes and local computation of specific humidity turbulent fluxes (*LCVLIS=.FALSE.*, *GCVPSI=0.*) did not bring any further improvement (see Fig. 1 - top, T11). But we have shown, that this group of parameters has bigger positive impact (concerning the instability curing) together with *LCVLIS=.FALSE.* rather then with *LCVLIS=.TRUE.* .

Changing the scaling parameter in the specific humidity tendency computation, where instead of specific humidity at saturation we used specific humidity, afterwards specific humidity of wet bulb temperature and finally specific humidity of the cloudy ascent, did not helped at all. But we found out that this Pacific case is very sensitive to the large scale evaporation and melting processes. Suppressing evaporation and melting (separately or together) helped to remove the instability, and vertical oscillations of temperature tendency were smoothed very well (see Fig. 1 - bottom and Fig. 2 - bottom, T04). (The same effect we found later also for the another similar problematic case from 28th December 1999, well known as Xmas storm - although it has nothing to do geographically with the Christmas storm now.)

If there is no evaporation, there is no possibility for enormous cooling by evaporating large scale precipitation. If we force downdraft in convection scheme to get rid of more moisture (just not to feed the LSP with it), one can suspect some improvement concerning the smaller cooling due to the LSP evaporation. But our experiences with the enhanced downdraft were quite different. Furthermore, on the other hand the experiments with suppressed downdraft had positive impact and helped to decrease big temperature oscillations along the vertical.

The problem is not only inside the convection scheme (instability in the model was still present even without convection scheme), but probably in the interaction between it and LSP. There was coded (but not used) a modification of enthalpy and specific humidity turbulent fluxes coming from vertical diffusion by additional fluxes coming from LSP to be used only inside convection scheme. This approach was not used, because of the inconsistency between specific humidity and enthalpy fluxes computations. But now, when the smoothing of specific humidity turbulent fluxes is implemented in the convection scheme, it seems to be logical to use it.

Above mentioned modification of the fluxes used inside convection scheme had positive impact to the Pacific case as well as to the other case from 28th December 1999. We have shown, that this modification can reduce the vertical oscillations of temperature tendency (although not so markedly than the test without evaporation can, see Fig. 1 - bottom and Fig. 2 - second line, 6REF) while it is not significantly touching the global scores (see Fig. 3 - top).

There was suspicion that this modification is responsible for amplification of convective activity oscillations in the tropics (visible on pseudo-satellite images), but we have shown that the problem with such oscillations between the time steps is present even in the operational model and with the same order of magnitude. To find the source of those oscillations we did several tests and found out the source of it inside the shallow convection scheme.

Afterwards, following the idea of Eric Bazile, we coded the smoothing of *ZAUX* parameter, which is a correction of Richardson number due to the shallow convection (computed inside the shallow convection scheme). Smoothed *ZAUX* parameter (using its values from the previous and actual time step, see Fig. 3 - bottom) applied in further stability computations, brought significant improvement concerning the convective activity oscillations. And what is more, this kind of smoothing had a positive impact also to the other fields, mainly to the temperature at the lowest model levels.

3. Conclusion

Modifications in the code of *aplpar.F90* (enthalpy and specific humidity turbulent fluxes coming from vertical diffusion are expanded by fluxes coming from LSP and are used in the convection scheme)

and in the code of *accoefk.F90* (smoothing of the Richardson number correction due to the shallow convection) are worth to be implemented to the operational cycle.

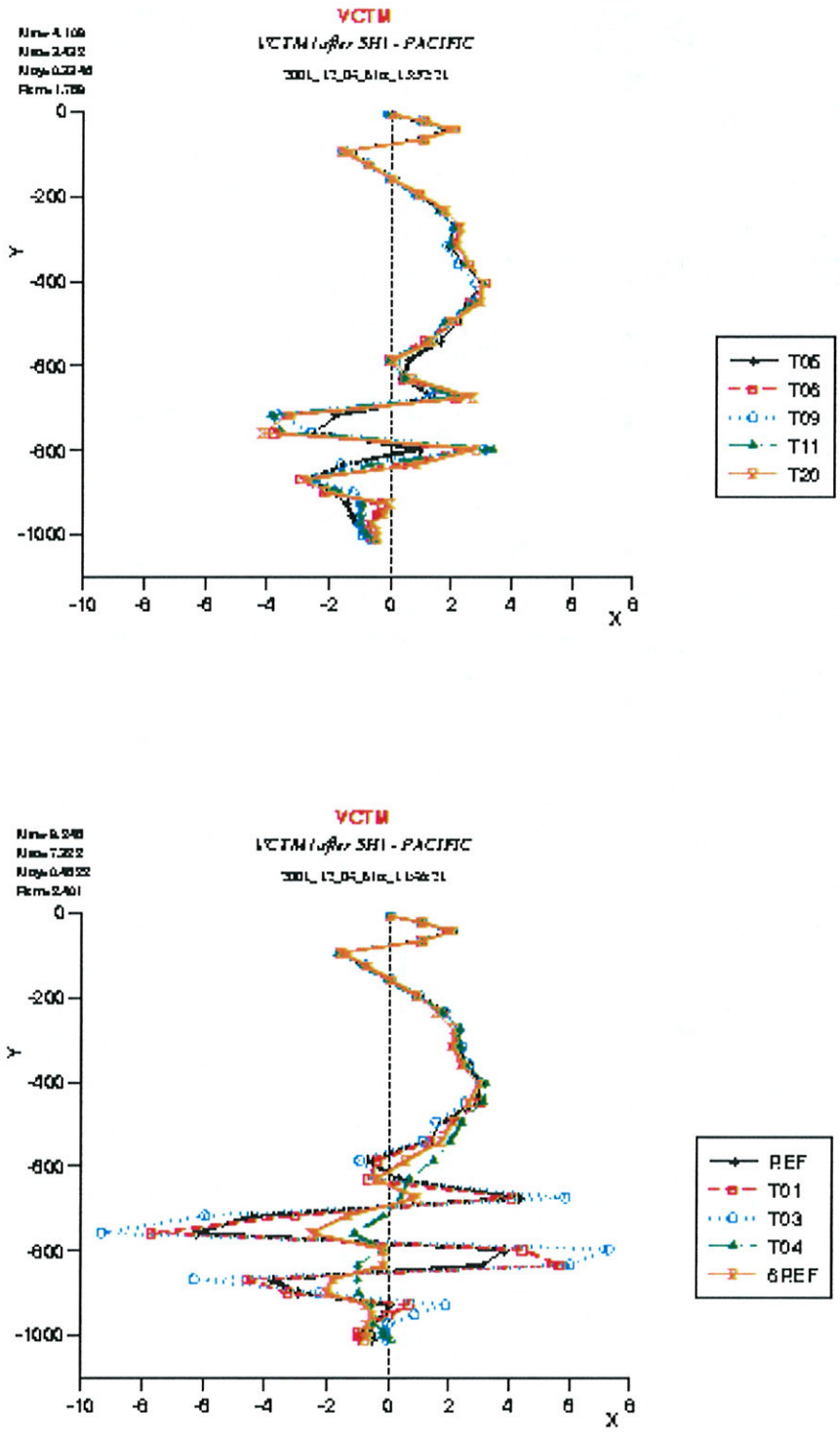

Fig.1

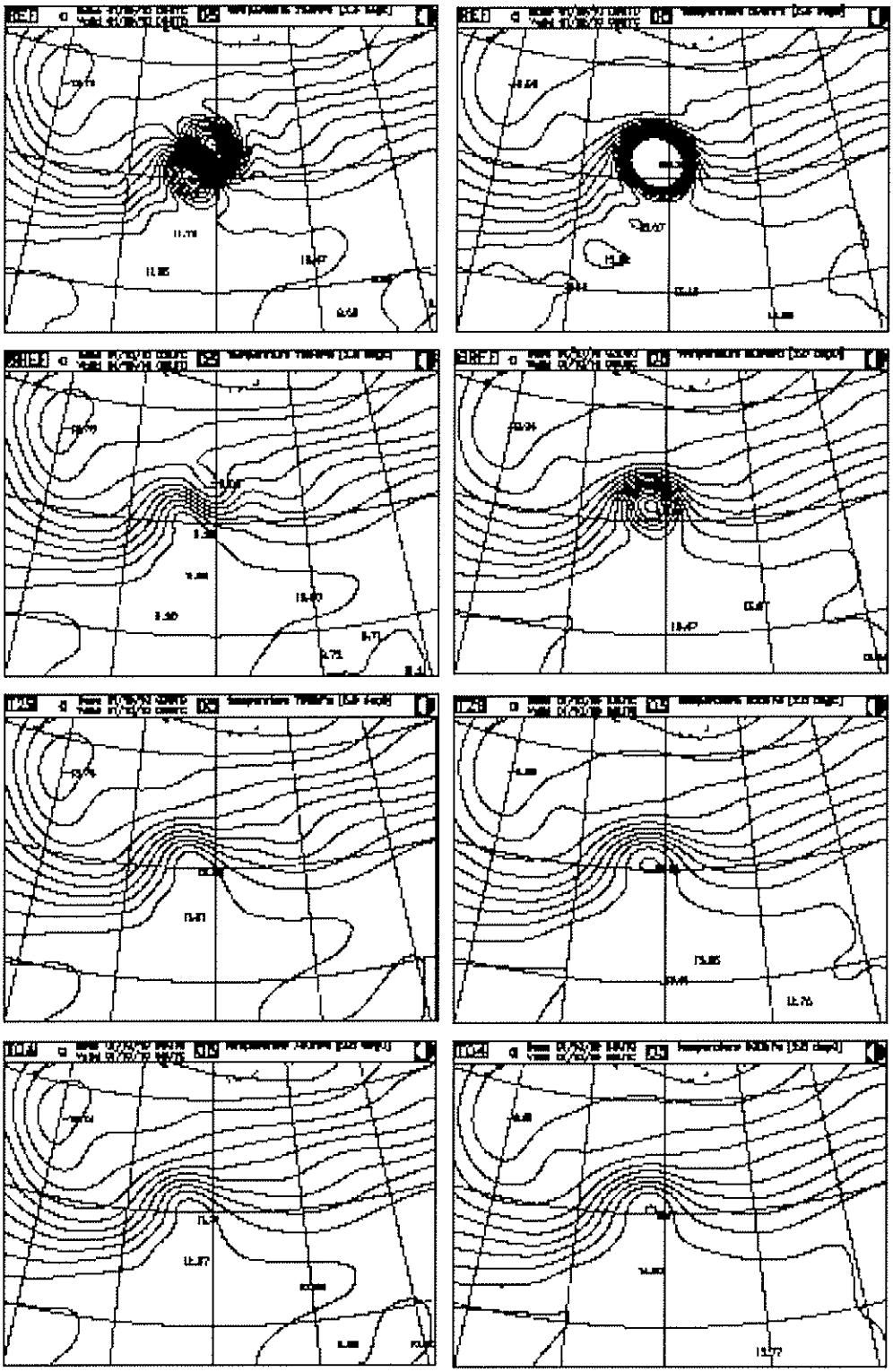

Fig.2

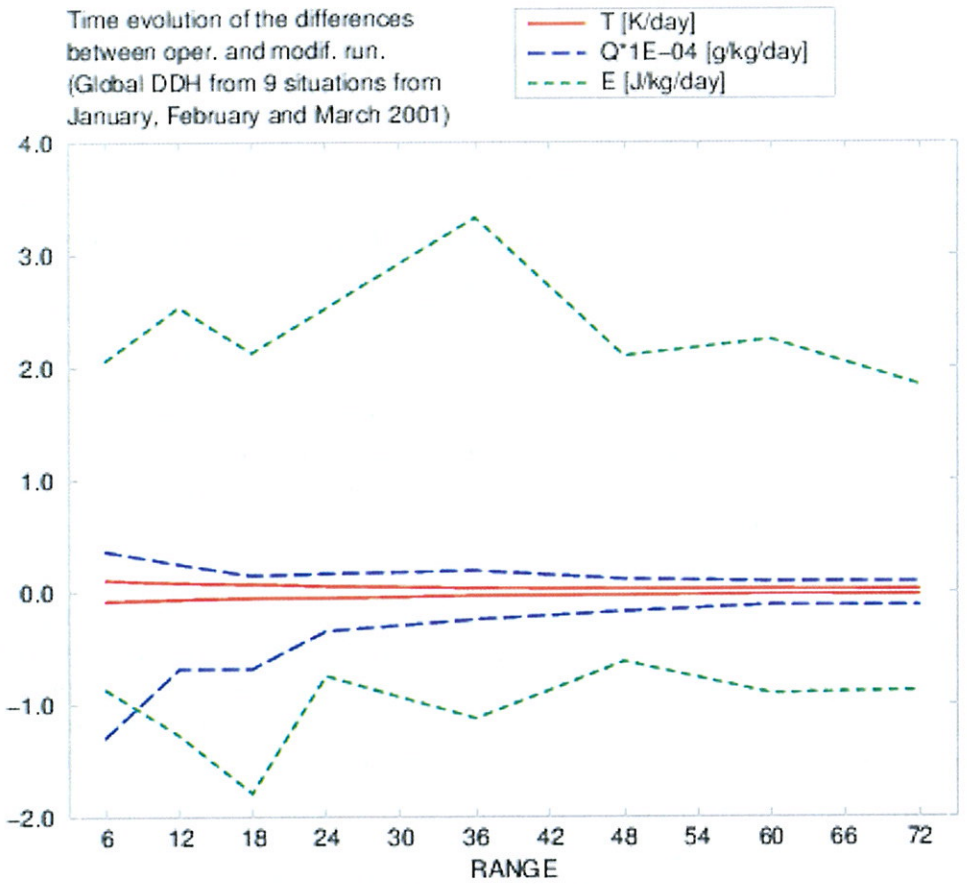
Time evolution of the differences
between oper. and modif. run.
(Global DDH from 9 situations from
January, February and March 2001)
T [K/day]
Q*1E-04 [g/kg/day]
E [J/kg/day]
4.0
3.0
2.0
1.0
0.0
-1.0
-2.0
6
12
18
24
30
36
42
48
54
60
66
72
RANGE

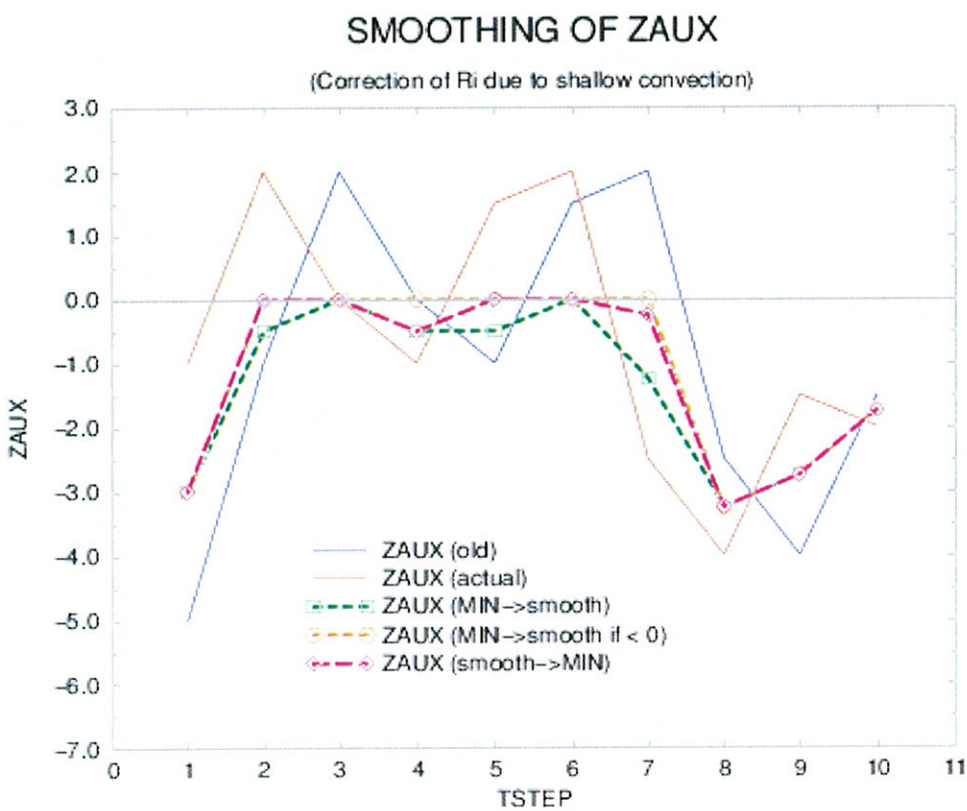
SMOOTHING OF ZAUX
(Correction of Ri due to shallow convection)
3.0
2.0
1.0
0.0
-1.0
-2.0
-3.0
-4.0
-5.0
-6.0
-7.0
ZAUX
0
1
2
3
4
5
6
7
8
9
10
11
TSTEP
ZAUX (old)
ZAUX (actual)
ZAUX (MIN->smooth)
ZAUX (MIN->smooth if < 0)
ZAUX (smooth->MIN)

Fig. 3

Diagnosis of ALADIN precipitation forecast over mountains

Yong Wang (*wang@zamg.ac.at*)

To investigate the problems of NWP precipitation forecast over mountainous areas, two ALADIN model simulations with different model resolution and dynamics were carried out, a) at 9.6 km horizontal resolution, hydrostatic; b) at 4 km horizontal resolution, non-hydrostatic. The area of investigation is the "Ticino-Verzasca-Maggie", which has been well investigated and observed within MAP (Mesoscale Alpine Programme) and the EU-Project RAPHAEL. This area is a complex mountainous area with elevation differences up to 3000 m and typical slopes of about 30 degrees. It is characterized as a region with exceptional rainfall amounts and intensities. The cases we studied are MAP IOP2 (Sep. 19, 00 UTC - Sep. 22, 00 UTC, 1999) and IOP3 (Sep. 25, 00 UTC - Sep. 28, 00 UTC 1999). The methods we used are prognostic (the forecast used is a long model integration, e.g. 24 hours) and semi-prognostic (only one time-step forecast). For validation of the forecasts the precipitation analysis from ETH, Zürich, and radar data are used.

Weather situation for MAP case IOP2 :

In the pre-frontal air over the western Alps ahead of a low pressure system there was a strong convergence zone in the western Po Valley. With warm and moist air advected towards the Alps from the Mediterranean and an easterly low level jet in the lower layers of the troposphere this produced heavy precipitation in the Lago Maggiore area. The event can be described as orographic precipitation, caused by large-scale ascent of moist flow over a high mountain barrier with embedded convection.

Summary of results :

Both ALADIN forecasts (9.6 km hydrostatic and 4 km non-hydrostatic) overestimate the precipitation, the 4 km simulation even more. This is especially true for the south (upslope) side of the mountain. On the north (downslope) side and in the central areas the forecasts look too dry. The precipitation patterns of the 4 km have more spatial variability than the observations. The large-scale part of the total precipitation is larger in the 4 km than in the 9.6 km simulation, as expected. In the South-North direction, the forecasted precipitation pattern is strongly tied to the gradient of the model orography. It is found quite often that the strongest precipitation coincides with the steepest upslope. This correlation is not as strong in the real atmosphere (Figure 1). Use of the 4 km (vs. 9.6 km) resolution gives no significant improvement. In connection with this problem, some work on *E923* will be done, for example using a linear grid. The semi-prognostic method is used to validate the precipitation parameterization. Since NWP models have a high degree of complexity, it is difficult to isolate errors caused by the parameterization from errors caused by other components of the model (e.g. numerical methods, other parameterizations). The semi-prognostic method can to some degree alleviate this problem. It is free of errors other than those caused by the parameterizations and observations. In the semi-prognostic mode the convection scheme gives weaker activity than in reality, and the large-scale precipitation is absent due to the lack of saturated layers in the model analysis (spin-up problem).

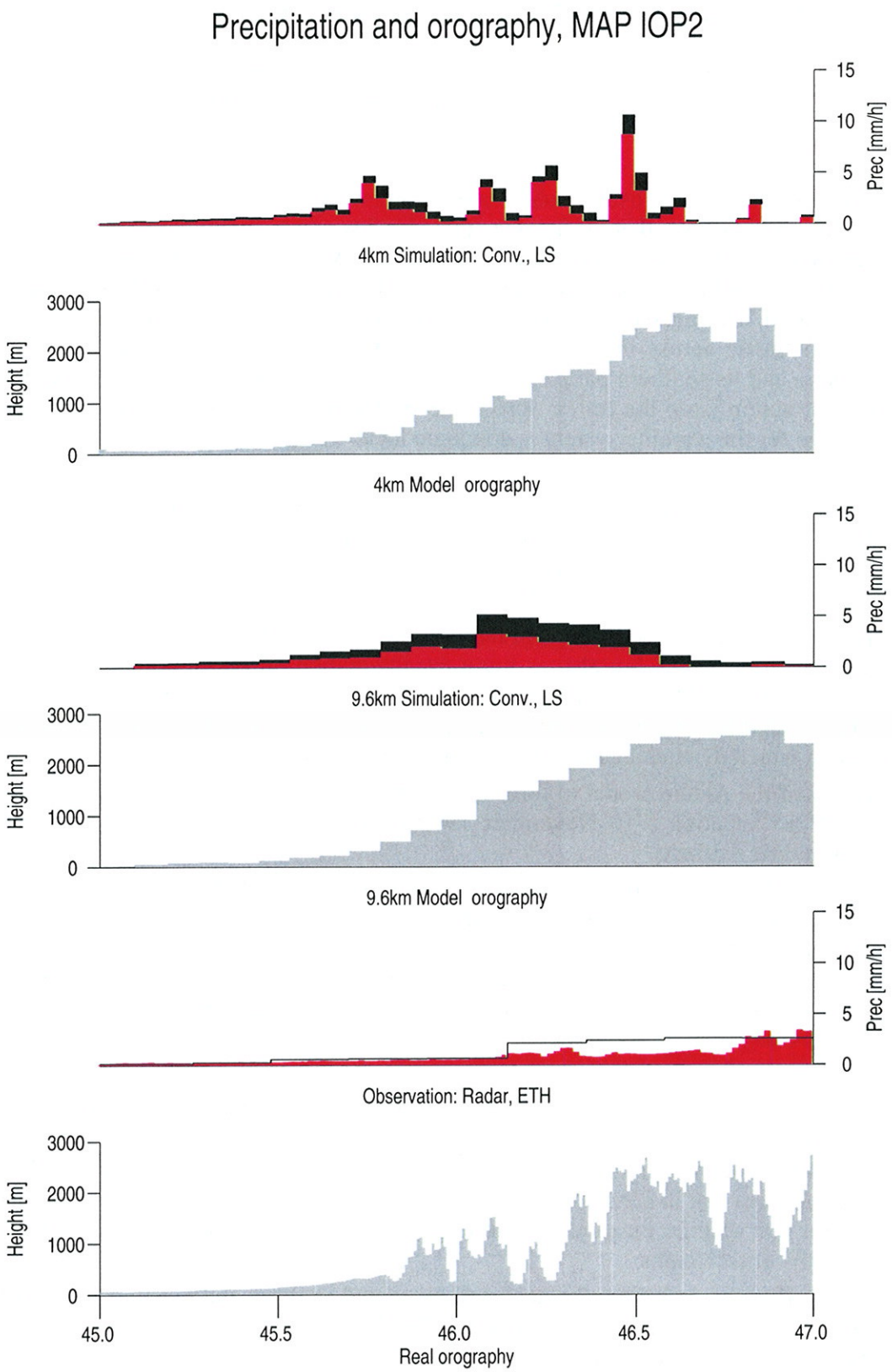

Figure 1: North-South profiles of topography and precipitation rate at 9° E longitude for 20-09-1999. Grey: topography, red: large-scale precipitation, black: convective precipitation. Shown are results from a 4 km run (2 uppermost panels), a 9.6 km run (middle panels), and radar as well as surface observations (thin black line).

MAP IOP 15 case study strong Bura wind on 7th November 1999

Stjepan Ivatek-Sahdan, Martina Tudor and Alica Bajic
Meteorological and Hydrological Service of Croatia

Planning, constructing and using roads and bridges assume insight into behaviour of those meteorological parameters that influence their safety and functionality. The most important meteorological parameter that affects traffic along the Adriatic coast is wind. Each winter several damaging Bura storms hit the coastal region and the islands of Croatia strongly affecting road transport and life in general. During the past years frequent severe winds produced serious difficulties (cars overturning) in traffic across the Dalmatian bridge Maslenica that lies on the main route between northern Croatia and its southern parts. So there is a strong necessity of having proper warning service that enable fast action (stop the traffic across the bridge in order to prevent the accidents and traffic jams). The basis for the warning system is adequate local weather forecast.

Croatian coast is lined with mountains that are relatively small in area, but rather steep with tops above 1500 m that are very close to the coastline. Orographically induced weather patterns in that part are poorly resolved or not resolved at all in large-scale models. Thus, forecast using high resolution models like the ALADIN become crucial.

In NWP practice in Croatia products from integration on the LACE domain with 12 km resolution are used for weather forecasting, but also as input for integration on HRv8 domain with 8 km resolution (SW corner 41.79° N, 8.93° E; NE corner 49.53° N, 21.98° E). Output surface wind fields are dynamically adapted to orography with 2 km resolution. Area around the Maslenica bridge is one of the domains on which dynamical adaptation of surface wind a field is done (figure 1).

The possibility of the Aladin model to forecast the strength and onset time of Bura wind is analysed in the MAP IOP 15 situation 5-10 November 1999 characterized by the strong Bura wind along the northern and middle Adriatic.

Forecast of the 10 m wind field obtain using ALADIN/HRVATSKA (figure 2) without and with dynamically adapted wind field show great influence of orography and consequently great variability in wind velocity. Vertical cross-section indicates the downstream low level jet characteristic for every Bura layer. The Bura layer (NE wind) extends to 1500-2000 m. The SE wind aloft decouples the upper and lower regions and prevents disturbances aloft. The obtained presence of stable layer descent from upstream to downstream region is consistent with upstream acceleration.

Spatial changes in wind speed observed in the dynamically adapted wind field confirm to give realistic pattern of wind speed in that region. This could be seen from the comparison of the ALADIN model output data with wind measurements on Maslenica location (indicated on figure 2) that are given on figure 3. It is obvious that in considered case the ALADIN/HR forecast (8 km resolution) produces too weak winds for that specific location. Dynamical adaptation gives wind speeds that significantly better correspond to the observations.

Although more Bura cases have to be analysed presented analysis and existing forecast practice show that the applicability of dynamically adapted wind fields is big and especially important in issuing the strong wind warnings for a number of special users.

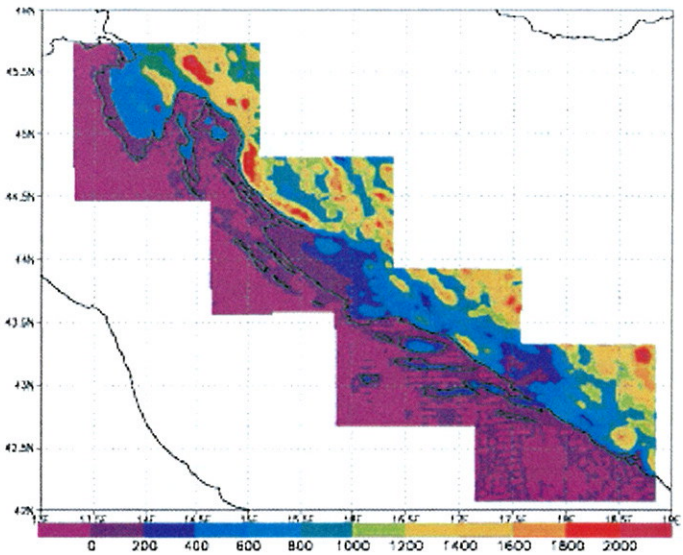

Figure 1. Domains on which ALADIN output surface wind fields are dynamically adapted.

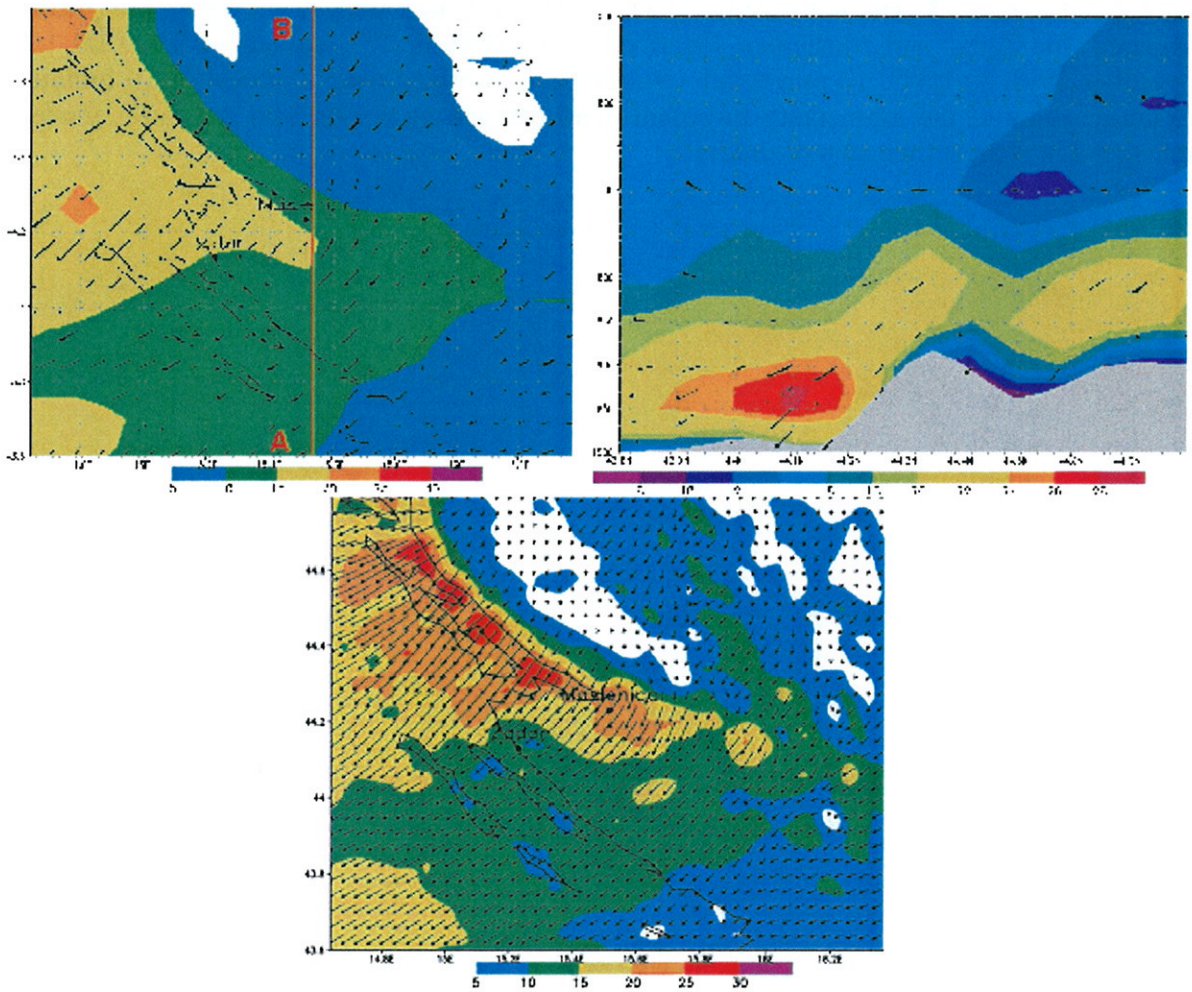

Figure 2. ALADIN/HR :12h forecast of 10 m agl wind field for 7th November 1999 00 UTC run
Top left : vectors and speed in m/s as shaded areas, resol. 8 km
Top right : vertical cross section along A-B line, resol. 8 km
Bottom : ALADIN/HR + dynamical adaptation vectors and speed in m/s as shaded areas resol. 2 km

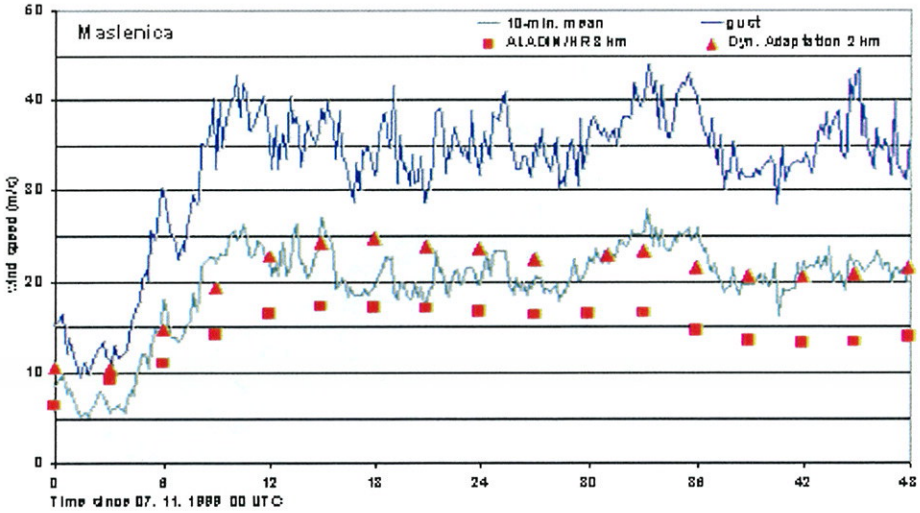

Figure 3.

Wind speed measured data and results of ALADIN simulation with 8 km and 2 km grid models are compared for Zadar and Maslenica locations : period from 7th November 1999 00 UTC to 9th November 1999 00 UTC. 10 min wind - wind speed averaged over a period of 10 minutes ; gust - maximum value of the momentary turbulent wind (measuring period of 1 second) ; model output is wind speed in nearest time step of model

Verification of ALADIN surface variables

30.10.2001
Stefan Greilberger
Stefan.Greilberger@zamg.ac.at
Department of Synoptic Meteorology - ZAMG Vienna/AUSTRIA

ALADIN-VIENNA temperature and precipitation forecasts (for point Vienna) are verified for the synoptic station Vienna/Hohe Warte (WMO Station nr. 11035). Comparisons of forecasts for day 1 and 2 of ECMWF (ECM), ALADIN VIENNA (AVI) and MOS (Model Output Statistics, based on ECM data) have been made for the period 01/2001 - 09/2001. ECM minimum and maximum temperature is calculated out of the model values from 00, 06, 12 and 18 UTC each day, so it is no real model minimum/maximum.

To make precipitation statistics comparable to the meteorologists forecasts, the daily period of detection was chosen between 06 and 18 UTC. In this case the period for the model forecasts is from 06 - 18 UTC, too.

1. Temperature

In Table 1 the forecasts are shown in chronological order (Tmin and Tmax for 2 days). Generally, AVI forecasts for minimum/maximum temperature are better than ECM forecasts and worse than MOS forecasts. Except for maximum day 2, AVI forecast has the lowest RMSE.

Comparing models (AVI and ECM) only, AVI forecasts for minimum temperature are only worse than ECM for day 2 by 2.0 K RMSE. Maximum forecasts in AVI are always better with RMSE of 2.0 K on day 1 and 2.1 K on day 2.

So it is obvious that BIAS (systematic error) also generates some RMSE. For ECM forecasts the minimum temperature BIAS is about +0.5K, for maximum temperature -0.5K. By eliminating BIAS in AVI RMSE will also be reduced.

RMSE Temperature	Station Vienna	ECM	MOS	AVI
	Minimum Day1	1.5	---	1.4
	Maximum Day1	2.2	1.9	1.8
	Minimum Day2	1.7	1.5	1.8
	Maximum Day2	2.4	2.3	2.0

Table 1: RMSE values (in K) for minimum/maximum temperature forecasts for day 1 and day 2.

BIAS Temperature	Station Vienna	ECM	MOS	AVI
	Minimum Day1	0.5		-0.5
	Maximum Day1	-0.7	0.4	-0.3
	Minimum Day2	0.6	0.4	-0.6
	Maximum Day2	-0.6	0.6	-0.1

Table 2: Same as Table 1, but for BIAS

Precipitation Detection	Station Vienna	ECM %	MOS %	AVI %
	POD Day1	74.6	96.4	79.3
	POD Day2	69.1	100.0	78.7
	FAR Day1	51.8	64.7	30.1
	FAR Day2	55.8	66.3	37.0
	TSS Day1	52,3	47,4	42,5
	TSS Day2	44,8	45,5	44,8

Table 3: Statistics for detection of precipitation (counting ''yes''/''no'' predicted / observed). For predicted / observed precipitation more than 0.5 mm (between 06 and 18 UTC) is detected with precipitation ''yes'', otherwise with ''no''. The table shows POD (Probability Of Detection), FAR (False Alarm Rate) and TSS (True Skill Score) for ECM, MOS and AVI.

2. Precipitation

Table 3 compares the precipitation forecast of ECM, MOS and AVI in terms of POD (Probability Of Detection), FAR (False Alarm Rate) and TSS (True Skill Score) also for the period 2001/01 - 2001/09. Detection ''yes'' for both observation and forecast mean more than 0.5 mm cumulated precipitation in the period of 06 to 18 UTC.

POD for AVI is with about 79 % a little bit better than ECM (~72 %), but worse than MOS. MOS has the best POD with 96,4 % to 100 % (=optimum), but on the other hand the highest FAR with about 65 % (optimum = 0 %). AVI has far away the best FAR with only 30 % for day 1 and 37 % for day 2.

In TSS, ECM is best with 52 % and AVI worst with 43 % on day 1. On day 2 no significant differences can be found, only MOS is with 46% a little bit better than ECM and AVI (both 45 %).

3. Summary

Comparing model forecasts like AVI and ECM (*MOS is not a model*), minimum and maximum temperature forecasts of AVI have better RMSE values than ECM forecasts. Precipitation detection (''yes''/''no'') of AVI is also better than ECM, if looking at POD and FAR at the same time.

MOS based on ECM has the best forecast generally, but at the same time it reduces FAR quality. Precipitation - in other words - is predicted too often, when it is not observed.

On the other hand TSS picks ECM as best model for day 1. MOS based on ECM has a lower TTS than ECM. On day 2 there are no significant differences.

So far only temperature minimum/maximum and precipitation detection have been verified. In the future, verification of ECM, AVI and MOS will be extended to additional parameters (precipitation amount, humidity, wind, cloud cover, etc...).

An application of the French MOS to the territory of the Czech republic

Zuzana Huthova, Czech Hydrometeorological Institute

Introduction:

The need for point deterministic weather predictions has been increasing gradually among users of the predictions from the ALADIN numerical model. For construction of point predictions from a numerical model, methods of statistical adaptation are used. Two years ago the work has begun at the Czech Hydrometeorological Institute on statistical adaptations of outputs from the ALADIN numerical model (with high resolution) for point predictions at the sites where synoptic stations are located. Based on the experience of experts from Météo France, the linear regression Model Output Statistics (MOS) method was chosen to adapt the point predictions of two meter temperature, maximum and minimum temperature, wind speed and cloudiness. The application of the French statistical model was developed for the ALADIN-LACE forecasts for 6 hour temperature, cloudiness and wind speed for the Czech synoptic stations. The study is based on a one year period from February 1, 1999 to January 31, 2000. The improved products of the model prediction are compared with the direct model outputs and observations at an independent sample for the period February 1, 2000 to September 30, 2001.

Method:

The aim of the use of statistical adaptation in the Czech Republic is to improve the forecast of the numerical weather model for our stations. Results were obtained for all Czech synoptic stations for temperature, cloudiness and wind speed for the forecast ranges of 24,30,36,42,48 hours, for minimum temperature with forecast range of 30 hours, for maximum temperature with forecast range of 42 hours. The method of multiple linear regression with canonical regression was applied to the output fields of the model ALADIN-LACE. Regression equations were calculated for each station, for each parameter and for each time range separately. The canonical predictors are made up from the 4 grid points surrounding the site considered. The forward stepwise selection is used to determine the optimum number of predictors, and after that the best predictors are selected. The best number of predictors appears in most cases to be equal 3. For each predictand, the best predictors were found. The coefficients in the equations were computed for all predictands and all forecast ranges. To check the performance of the equations (before the start of their operational use), some examples on the independent sample were calculated for May 2000. An example is shown for the prediction of wind speed at the station of Temelin for the forecast range of 36 hours. The lines in the figure indicate: point 1 to point 4 is the direct model prediction from the nearest four gridpoints surrounding the station, "MOS" is prediction improved by statistical adaptation and "observ." is the observation at the station :

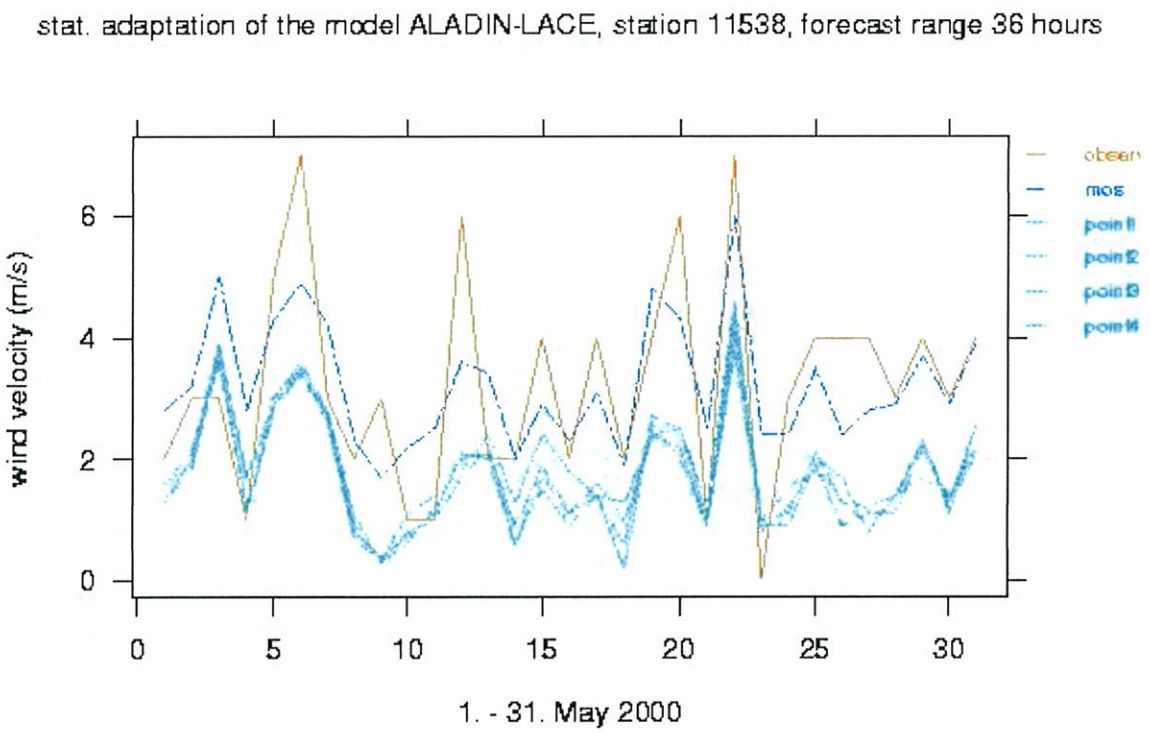

The application of the MOS method to the wind speed prediction for 36 hours at the Temelín station (11538) for May 2000 reduces the root mean square error from 2.0 to 1.2 m/s.

Operational use and results:

The results are satisfactory for the majority of stations, and models are stable enough. The models are used operationally in the Czech Republic since June 2000. The improved products of the model prediction are compared with direct model outputs and observations for independent sample for the period 1.4.2000-30.9.2001. On some examples of averaged Root mean square error it is possible to see how much the MOS equation improves the model outputs: MOS gives smaller root mean square error than direct model outputs for all predictands everywhere. One example is shown for minimum temperature with forecast range of 30 hours. The RMSE of prediction by MOS is much more homogeneous over Czech Republic than the direct model output. The RMSE of direct model outputs ranges from 1.8 to 3.3 at the stations, which is improved by MOS to the range from 1.6 to 2.4.

Multiple Linear Regression model used canonical regression

MINIMAL TEMPERATURE RMS DIRECT MODEL OUTPUTS

period 1.4.2000 – 30.09.2001 forecast range 030 hours

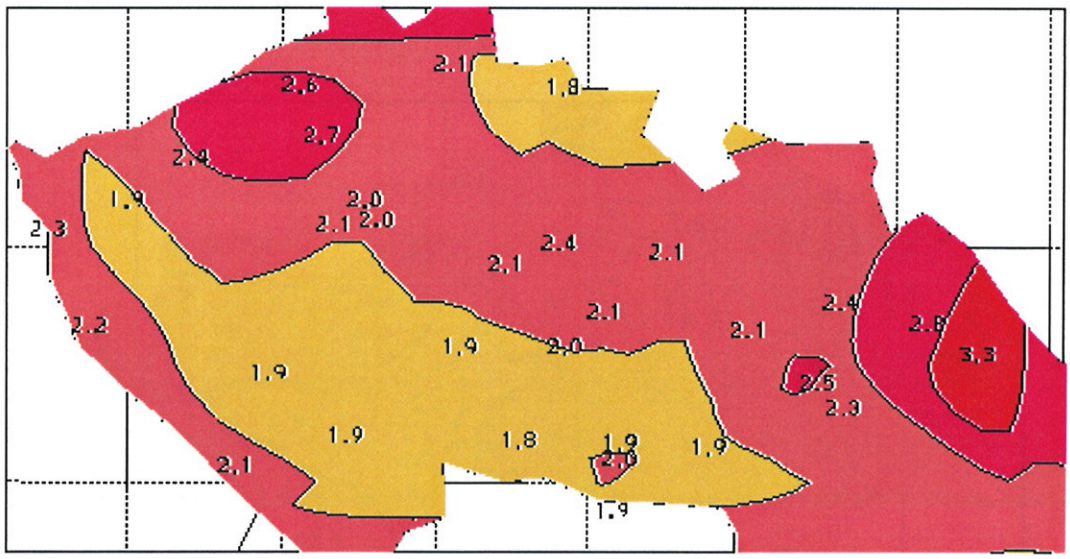

Multiple Linear Regression model used canonical regression

MINIMAL TEMPERATURE RMS IMPROVED MODEL OUTPUTS

period 1.4.2000 – 30.09.2001 forecast range 030 hours

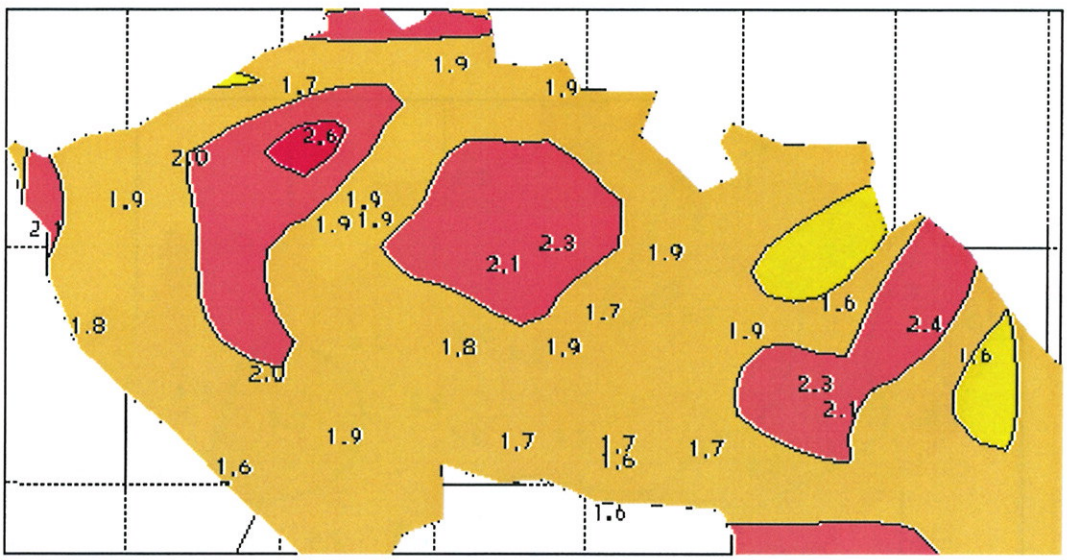

The second example is shown for maximum temperature with forecast range around 42 hours. It has features similar to minimum temperature, however, both direct model output and MOS have large

errors. Maximum temperature remains a problematic element even if MOS applied. The best improvement of RMSE appears at mountain stations and the stations close to mountains.

Multiple Linear Regression model used canonical regression
MAXIMAL TEMPERATURE RMS DIRECT MODEL OUTPUTS
period 1.4.2000 – 30.09.2001 forecast range 042 hours

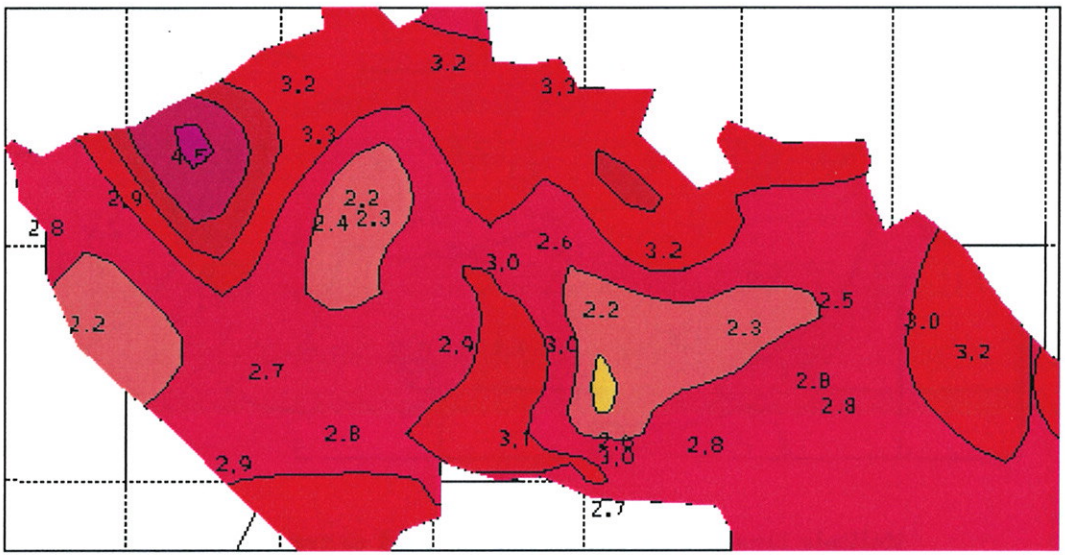

Multiple Linear Regression model used canonical regression
MAXIMAL TEMPERATURE RMS IMPROVED MODEL OUTPUTS
period 1.4.2000 – 30.09.2001 forecast range 042 hours

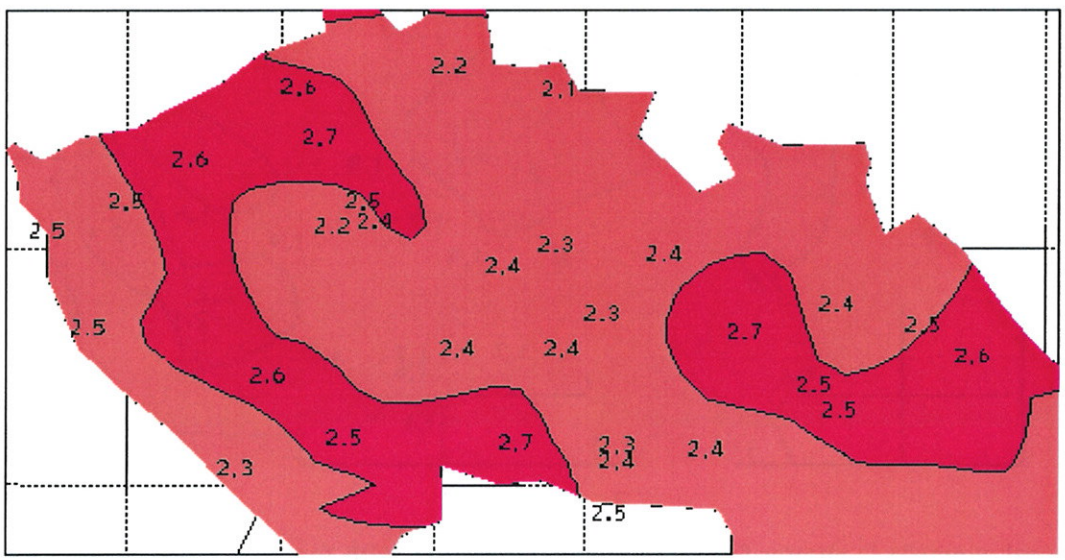

Conclusion and prospects:

The results are satisfactory for the majority of stations, and models are stable enough. The models are used operationally in the Czech Republic. The best number of predictors appears in most cases to be equal 3, for which the equation is acceptably stable and the improvement is sufficient. To obtain larger numbers of useful predictors, better stability and more improvement, probably the sample longer than one year is needed. In October 2001, a two-year sample of model outputs starting at October 1999 was completed. Fields of derived predictors were also calculated. We installed French software *Statw* for the selection of predictors. The first tests on the two-year sample give promising results. We hope that the new MOS, built on the complete two year sample with the independent sample half a year long, will start operating at the Czech Hydrometeorological Institute soon. The outputs of the new MOS will include the same elements as that of the present system in operation, that is, two meter temperature, maximum and minimum temperature, wind speed and cloudiness. The adapted forecast will be issued for the whole forecast range of ALADIN, that is up to 48 hours with a 3 hour step. The output will be issued also in a graphical form (at present, the MOS outputs are operationally available only in the form of tables).

The use of Kalman filter for improving the short range forecast of 2m temperature

Beatrix Izsák (*izsak.b@met.hu*)
Hungarian Meteorological Service

Introduction

Numerical model forecasts are often biased mostly for boundary layer parameters. Its main reason is that model orography differs from the real geographical one. Inaccuracy of the parameterisation of subgrid scale phenomena may be a source of systematic errors as well. To have more realistic forecasts post-processing procedures are used that may be based on either dynamical or statistical considerations. Statistical approach is used to adjust model outputs to reality. Our purpose is to make the 2m temperature model forecast of ALADIN/HU model more accurate. To this end we use the Kalman filter technique because in this method error statistics are intrinsically refreshed. Thus the algorithm rapidly adjusts to weather changes. Forecasts corrected by Kalman filter are performed recursively by combining them with observations. Our Kalman filter model is the adaptation of the program developed by Jozef Vivoda.

Theory of Kalman filter

Here we introduce a simplified version Kalman filter procedure (Homleid, 1996). Let x_t be the state of the unknown discrete stochastic process at time t. The state at time t is associated with that of $t-1$ through the system equation :

$$x_t = F_t \cdot x_{t-1} + w_t \cdot \qquad (1.1)$$

where F_t is the transition matrix of the system and w_t represents the random change between time $t-1$ and t, i.e. w_t is the error of forecast by F_t. F_t is linear. x_t is associated with the observation y_t through the observation equation :

$$y_t = H_t \cdot x_t + v_t \cdot \qquad (1.2)$$

where H_t is the observation matrix and vector v_t stands for the random component of observation error.

Observation matrix H_t and transition matrix F_t change in time but they are supposed to be known. The terms v_t and w_t represent white noise processes with a Gaussian distribution of expected value 0 all along time t and they are assumed to be independent in time. Thus for every time $t \neq s$, $E(w_s\, w_t^T) = 0$ and $E(v_s\, v_t^T) = 0$, where E denotes the expected value. Additionally v_t and w_t are independent noises : $E(v_s\, w_t^T) = 0$ for every s and t. Let W_t denote the covariance matrix of a w_t, i.e. $W_t = E(w_t\, w_t^T)$ and similarly for the covariance matrix of v_t, $V_t = E(v_t\, v_t^T)$.

The Kalman filter provides the recursive estimation of states x_t by taking into account every observation until time t. They are denoted by $y_1, y_2, \ldots, y_t$. To compute the state the estimation of error covariances is used and it is denoted by P_t. To make the estimation from $t-1$ to t two steps are performed. They are summarised below :

$x_{t,t-1}$ is the estimation of x_t at time t by taking into account observations until time $t-1$
$P_{t,t-1}$ is the estimation of the error covariance matrix of $x_{t,t-1}$
$x_{t,t}$ is the estimation of x_t at time t by taking into account observations until time t,
$P_{t,t}$ is the estimation of the error covariance matrix of $x_{t,t}$

Let us suppose that the observations until time $t-1$ are known and we have computed the optimal estimation $x_{t-1,\,t-1}$ as well. If we take into account only the observations until time $t-1$ then the optimum estimation for time t is :

$$x_{t,t-1} = F_t \cdot x_{t-1,t-1} \quad (1.3)$$

The error covariance matrix of state estimation $x_{t,t-1}$ can be computed from :

$$P_{t,t-1} = F_t \cdot P_{t-1,t-1} \cdot F_t^T + W_t \quad (1.4)$$

When the y_t observation for time t is known, the estimation of x_t can be updated from the linear combination of $x_{t,t-1}$ and from the forecast error $(y_t - H_t \cdot x_{t,t-1})$:

$$x_{t,t} = x_{t,t-1} + K_t \cdot (y_t - H_t \cdot x_{t,t-1}) \quad (1.5)$$

In (1.5) K_t denotes the Kalman gain matrix :

$$K_t = P_{t,t-1} \cdot H_t^T \cdot (H_t \cdot P_{t,t-1} \cdot H_t^T + V_t)^{-1} \quad (1.6)$$

The estimation of error covariance matrix can be performed by :

$$P_{t,t} = (1 - K_t \cdot H_t) \cdot P_{t,t-1} \quad (1.7)$$

The system of equations described above is sufficient for performing the Kalman filter algorithm.

To be able to apply this model for improving temperature forecasts one has to estimate the statistical parameters and the matrices characterising the system. Thus one has to determine the state transition matrix F_t and the observation matrix H_t and to estimate the covariance matrices of the noises of the system and the observations W_t and V_t. Additionally one has to estimate the initial states, i.e. $x_{0,0}$ and $P_{0,0}$.

The Kalman filter (KF) in practice

On the basis of Homleid's description Jozef Vivoda developed the model of Kalman filter in Slovakia to improve ALADIN products by surface observation (Vivoda, 1998). Our KF model is its adaptation. We perform the corrected forecasts for the time range 00 to 24 hours with a 1 hour time-steps. The covariance matrix of system noises has been computed from temporal and spatial correlations. Following the way proposed by Homleid to compute the ratio W/V we obtained the value 0.06. The system matrix was the identity. For each city at the n-th time-step H_t is n-dimensional, its k-th component being 1 if at time-step k there was an observation and 0 if not. An advantage of Kalman filter is that the state is rapidly converging to its theoretical value independently from its initial value.

Correction of 2m temperature forecasts of ALADIN/HU

To evaluate a numerical model one computes forecast errors. We have computed mean errors (ME) mean square errors (MSE). ME gives information on the bias or systematic errors of the model and MSE characterizes the magnitude of errors.

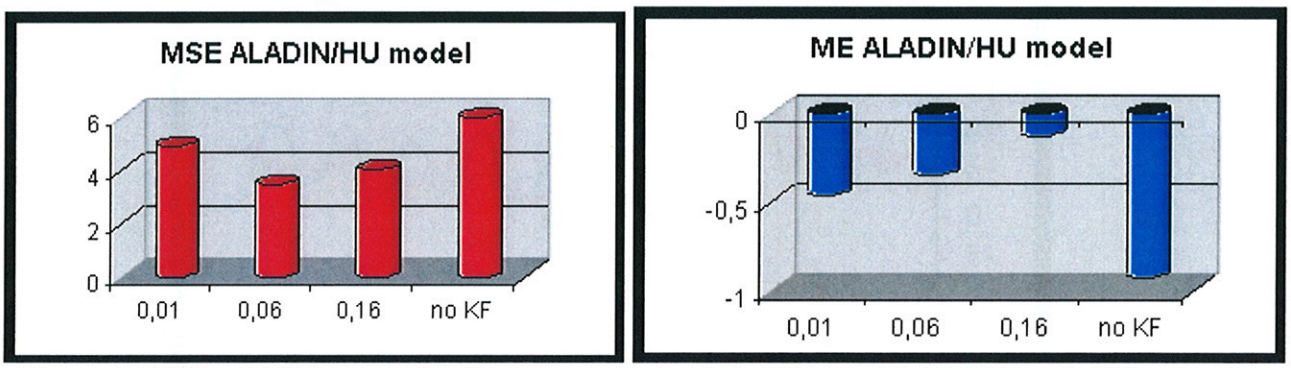

Figure 1. ME and MSE errors for Hungary in the period 2001. 01. 01-04. 20 for 3 different noise ratios of KF and for no KF

In case of ALADIN/HU model there are two stations giving extremely incorrect forecasts. One of them is Kékestetõ (situated in the North-Eastern part of the country being the highest point of Hungary) that is seen by ALADIN/HU model on a height of 357 m while its actual altitude is 1015 m. This difference of 658 m appears as a very significant error in the forecast of temperature, we can speak about a systematic overestimation of 3-4 K. Beside Kékestetõ the meteorological station in Budapest, Kitaibel street (Headquarter of the Hungarian Meteorological Service, situated in the downtown of Budapest) is remarkable with the mean error of 2 K. In case of this meteorological station the error may be caused by the positive temperature anomaly of the urban heat island. In other locations (Poroszló, Jósvafõ and Miskolc for instance) the problem is in the temperature of the surrounding grid points, as in case of these towns the nearest grid points have different geographical characteristics. In case of towns in the Great Hungarian Plain and the Little Plain (Northwestern Hungary) the forecast of ALADIN/HU model is relatively correct as the relief is here the same as the orography used in the model; the difference of altitude does not exceed 10 m in case of these towns, e.g. it is 6 m in case of Gyõr, while the mean error is less than 0,5 centigrade.

Based on the above facts we can say that in Hungary the systematic error originates mainly from the differences between the relief used in the numerical model and the actual orography.

If mean error is W/V=0,01 in towns where the error of the numerical model was moderate or smaller than the average, the Kalman filter improved the forecast. So in case of towns of the Great Hungarian Plain and on West Hungarian areas an improvement of 0,5 centigrade is characteristic on the average. In case of this noise ratio the temperature forecasts of meteorological stations Kékestetõ and Budapest, Kitaibel street are improved very slightly. It is no wonder as according to tests based on constant data series the small noise ratio means that the filter takes into account rather the products of the numerical model than the observed data. Concerning squared errors improvement cannot be really experienced. In some towns this value decreased very slightly but considering all the 32 stations we can state that significant improvement has not followed. (At the same time it is true that we have not even made the situation worse.) If the Kalman filter is run with greater value - W/V=0,16 than the empirical noise ratio, we can see significant change in every respect. The degree of improvement is the highest in case of the two stations with extremely high mean error. The mean errors improved from 3 K to 0,8 K in case of Kékestetõ station while from −3 K to -1,6 K in Budapest, Kitaibel street. Applying this noise ratio we can see that instead of the systematic underestimation of temperature in numerical models the Kalman filter overestimates temperature in nearly one third of towns. Its reason is that in case of such noise ratios the filter relies rather on measurements but with much larger amplitudes as we could see in the test with constant data series. Thus in case of Pécs where the model gave one of the most correct forecasts, the overestimation was nearly 0,3 K what can be attributed to the large amplitudes of the model. Certainly it can be seen as well that both the mean and the squared error decreased significantly.

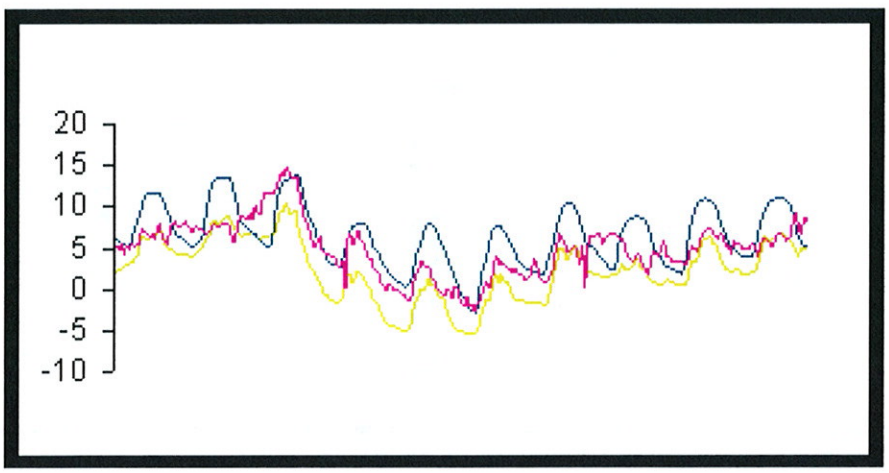

Figure 2. Kékestetõ, values of 2 m temperature (° Celsius) between 11-20.04.2001, synoptic data, ALADIN model, forecast corrected by Kalman filter in case of noise ratio of 0,06

The Kalman filter model has to be run on long period with a noise ratio that relies rather on synoptic values but takes also the results of numerical models properly into account. With the noise ratios applied till now we achieved a conservative, slowly changing, inactive model (value of *W/V*=0,01) and a more rapid filter with great amplitudes (value of *W/V*=0,16). The intermediate value is a stable model that follows the changes slower than that of a *W/V*=0,16 noise ratio but with smaller standard deviation and relies rather on measurements at estimations compared with the filter with *W/V*=0,01 noise ratio. This intermediate solution is the value of *W/V*=0,06 (see Figure 2). Comparing the products of the numerical models with the results of Kalman filter model of three different noise ratios it is obvious that the squared errors are the smallest as a result of this procedure. The squared error of only one station is greater than in case of the most correct filter (*W/V*=0,16) that is of the meteorological station of Budapest, Kitaibel street. This extremely great error is not only the result of positive temperature anomalies of large cities - as filter models improved forecasts in every other case - but the lack of data has also significant role in it. If we examine where we got correct forecasts we can see that the mean errors of temperature forecasts in the areas of Great Hungarian Plain, Little Plain and South-Transdanubia remain below 0,1 centigrade. In these areas also the values of squared errors are 2 K or even less. Besides the mentioned problematic station the squared errors remain below 5 K.

Conclusions

Our objective was to improve the temperature products of numerical models by implementing Kalman filter statistical adaptation procedure. The comparison of our results with the products of numerical models can be seen on Figure 1. We can say that the results of ALADIN/HU model could be improved significantly compared with its 2 m temperature forecast. We have tested the filter with data series of nearly four months for forecasts valid until 24 hours. We examined in which cases the filter makes the numerical model predictions worse. This occurred only in 7 percents of forecasts. The weak point of Kalman filter model is that in case of rapid weather changes the state vector has to change sign rapidly, as the numerical atmospheric model is run daily and thus the estimations are filtered daily. In case of rapid weather change the forecast of the filter has to be disregarded on the first day. The other problem is that the data quality control used by us is very indigenous. A more effective method has to be developed as the incorrect measurements may damage the statistics. If we improve the situation in the above mentioned two respects we can achieve the automatic production of temperature forecasts. The Kalman filter model prepared by us is suitable also for correction of 10 m wind, daily maximum and minimum temperature values if we define statistical parameters for each of these meteorological variables. As we could see in the scientific literature and in the present description very good results can be achieved with Kalman filter. The filter would be really perfect if the numerical weather prediction model was run at the same intervals as the time step of the filter. The statistics in the tests are not final because of the short period, it would be worth to prepare again the verification of our Kalman filter model in one year. If we manage to control the synoptic data more effectively, the statistics will certainly show that the Kalman filter eliminates fully the systematic errors of forecasts.

References:

Bucy, R.S., and Kálmán R., 1961: New results in linear filtering and prediction theory. *Transaction ASME Journal of Basic Engineering*. 83: 95-108.

Homleid, M., 1996: Diurnal Correction of Short-Term Surface Temperature Forecast Using the Kalman Filter. *Weather & Forecasting*, 689-707.

Vivoda, J., 1998: Correction of surface temperature forecast using the discrete Kalman filter. *Meteorologický casopis*, 1.2. 1998, 31-37.

Verification of surface solar radiation fluxes predicted by ALADIN

Zoltán Tóth

Division for Measurement Techniques and Quality Assurance,
WMO Regional Centre for Solar Radiation, Region VI
Department for Environmental Observations
Hungarian Meteorological Service

H-1675 Budapest, P.O. Box 39, Hungary
E-mail: toth.z@met.hu

Abstract - Solar radiation output fluxes predicted by ALADIN were verified using observed data from three station of Hungarian Meteorological Service. Period of June - August 2001 was selected for the study. Differences between observed and forecasted values were analysed separately for all cases and cloudless cases. It was found that ALADIN estimates daily totals essentially correctly but standard deviations of model data series are considerably lower than those of true data series and the model cannot produce sufficiently low daily totals like those occurring in reality. For cloudless cases, using aerosol optical depth to represent radiation transmission condition of the atmosphere, it was found that ALADIN overestimates atmospheric radiation transmission for cases of high turbidity and underestimates it for very clear conditions. It means that radiation transmission scale of the atmosphere produced by the model is more narrow than that of true atmosphere.

1. Introduction

For any user who intends to use solar radiation outputs from ALADIN it is important to know their reliability. It seems that in Hungary the interest for global radiation forecasts of ALADIN increases so it was high time carrying out verification of them. The aim of the study that is shown in this paper was to determine deviations between predicted and observed values as well as to analyse them: to try to understand reasons of them more deeply that means finding of possible insufficiencies in background physics produced by ALADIN. Based on the results to make suitable improvements in the model would be possible if interest would arise. Observed data and forecasted parameters used for the study, the method for verification and its results separately for all cases and cloudless cases with conclusions are shown in the paper.

2. Solar radiation parameters and data used for the study, as well as radiometers from which data come

Parameters that are used for the study were global, direct and diffuse radiation. The observed data came from the solar radiation observatory of Hungarian Meteorological Service which is a WMO Regional Centre for Solar Radiation for Region VI, as well as it is a station of BSRN. Direct radiation (marked with DIR in the figures) is measured by pyrheliometer Eppley NIP affixed on a sun tracker SCI-TEC, global radiation (GL in the figures) is measured by pyranometer Kipp-Zonen CM11 and diffuse radiation (DIF in the figures) that is the scattered component of solar irradiance reaching the Earth's surface is measured by also pyranometer Kipp-Zonen CM11 affixed on the same sun tracker using shading disks. The pyrheliometer is regularly calibrated to our absolute cavity pyrheliometer HF 19476 which is the regional standard for WMO Region VI and thus represents World Radiometric Reference (which means the reference radiometric scale) for the region. Previous comparison of HF 19476 to the World Standard Group was carried out in 2000 at the last International Pyrheliometer Comparison in Davos, Switzerland. All our instruments are in well-calibrated condition.

Using serial lines detectors are connected to a data acquisitor PC in Budapest or to automatic weather stations MILOS at the countryside observatories. Data base consists of both one minute and

ten minute averages that are calculated from the individual measurements (samplings) which are made by the detectors. Six individual measurements are carried out in each minute.

Concerning observed data the direct solar radiation that is measured by pyrheliometer is the irradiance from the solar disc that insolates a surface perpendicular to the direction of the Sun. Direct solar radiation that was needed for the investigation is the vertically incident component that is equal to difference of global and diffuse radiation. So it was calculated as difference of observed global and diffuse irradiance.

The study was carried out for the daily total for subsequent day and for the day after subsequent day. Predicted data used were the 24 hour and 48 hour cumulative surface fluxes from ALADIN. Daily totals for the day after subsequent day were calculated, evidently, as the differences of 48 and 24 hour cumulative fluxes. Forecasts released at 0 h were used in each case and characteristics of deviations of daily totals predicted by ALADIN from the observed daily totals were analysed. ALADIN predicts vertical component of direct radiation (that is incident on a horizontal surface) and diffuse radiation so forecasted global radiation values were calculated from them. Global radiation is simply the sum of vertically incident direct radiation and diffuse radiation. The study was carried out for

- Budapest-Lõrinc (φ : 47°25'45'', λ : 19°10'56'')

and for two countryside stations:

- Sármellék (φ : 46°41'15'', λ : 17° 09' 42'')
- Nagyiván (φ : 47°21'01'', λ : 20° 54' 33'')

In addition to Budapest this two countryside stations seemed to be most representative in respect of solar radiation, among the global radiation measuring sites of the Hungarian Meteorological Service. Direct and diffuse radiation measurements are in progress solely Budapest consequently only global radiation was studied for Nagyiván and Sármellék. So forecasted daily totals below were verified:

- direct radiation for the subsequent day (Budapest)
- diffuse radiation for the subsequent day (Budapest)
- global radiation for the subsequent day (Budapest, Sármellék, Nagyiván)
- direct radiation for the day after subsequent day (Budapest)
- diffuse radiation for the day after subsequent day (Budapest)
- global radiation for the day after subsequent day (Budapest, Sármellék, Nagyiván)

The investigation was made for the period of June-August 2001 that means 92 days.

Solar radiation outputs of ALADIN depend on the following parameters: solar zenith angle, N2, O2, total water vapour content, CO2, O3, water in both liquid and ice state (clouds), 3d cloudiness, aerosols. Concerning the considerably changing physical parameters, in reality solar radiation flux reaching the Earth's surface is affected mostly by cloudiness, total water vapour content and aerosols (obviously besides solar zenith angle that is determined by celestial mechanical parameters). Ozone, for example, has no effect on wide energy range radiation but on narrow spectral ranges only.

The factor that most considerably influences solar irradiance reaching the Earth's surface is undoubtedly the cloudiness. Among the radiation parameters direct radiation is which is affected by it most dramatically: cloudiness can make direct value equal to zero if each photon is absorbed in the clouds. It can occur frequently in case of thick clouds. Consequently the deviation of amount of forecasted cloudiness from that appearing in reality is of principal importance in respect of prediction. Also it is of crucial importance that whether forecasted cloudiness arrives when the real cloudiness does or on the contrary: whether cloudiness does not arrive at given place in the model when real cloudiness does.

Daily average cloudiness values were calculated as arithmetic mean of hourly cloudiness values without any weighting for Budapest. The resulted 'daily total cloudiness' is a draft parameter but in this first study it was considered sufficient. Satellite images were used for consideration of cloudiness

for both countryside stations since no human observer is employed in those sites so cloud coverage values were not available.

In cloudless cases solar radiation reaching the Earth's surface is affected by aerosol content and total water vapour content. Unfortunately, running of the model afterwards for parameters that have not been operationally output previously would have taken too much time so those parameters were not considered in this first study. It means that values of forecasted cloudiness and other influencing parameters were not available for the study but despite this fact useful conclusions for reasons of the differences are made based on the results. Study of 'goodness' of influencing parameters would be a next step of the investigation in the framework of which the parameters needed for the study would come to be computed during the operational model running.

3. Results for all cases

Predicted and observed data series are shown on *Fig. 1 - 5* for 24 hour forecasts for direct, diffuse and global radiation for Budapest, as well as for global in case of both countryside station. To save pages, the same parameters for 48 hour forecasts are shown for two countryside stations only (*Fig. 6 - 7*). It can be seen that variability of observed data series is considerably higher than that of predicted series. It is not unexpected actually since models usually smooth fluctuations. They are able to predict extrema with less reliability. Standard deviation of data series are shown in *Table 1*. It is conspicuous how lower the standard deviations of model data series are, as compared with those of observed series. In case of direct radiation, standard deviation of the predicted data series is 552.3, while it is 684.2 for the observed series. For diffuse radiation that is of considerably less variable parameter as a consequence of its nature, it is 184.2 and 286.1, respectively. Concerning global radiation, also it can be established based on the table values that differences of standard deviations and values of standard deviations themselves are very close to each other for all three stations. The differences are: 217.3, 201.8 and 248.2.

Fig. 1. **Observed and forecasted daily totals of direct radiation for 24 hour forecasts. Budapest, June - Aug 2001**

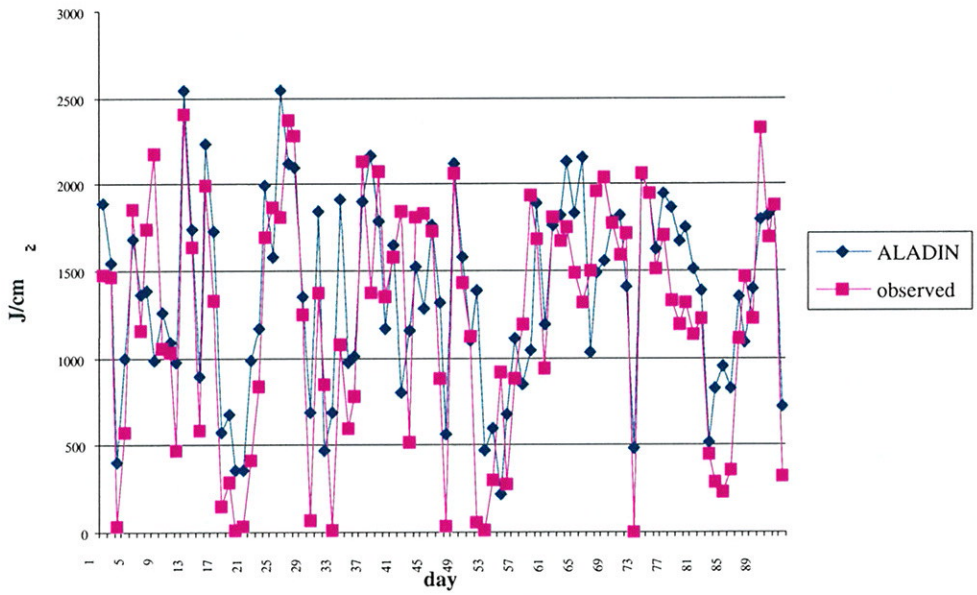

Fig. 2. **Observed and forecasted daily totals of diffuse radiation for 24 hour forecast. Budapest, June - Aug 2001**

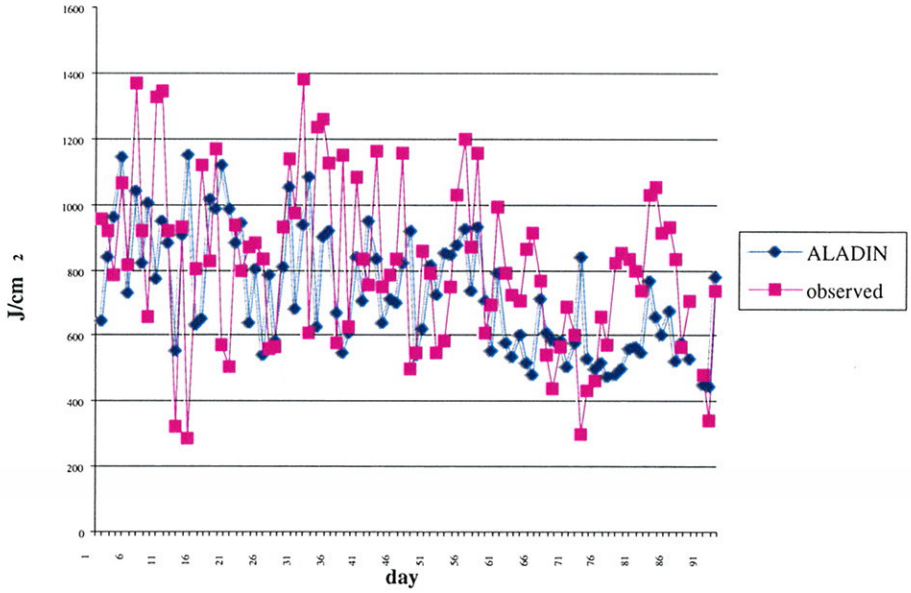

Fig. 3. **Observed and forecasted daily totals of global radiation for 24 hour forecasts. Budapest, June - Aug 2001**

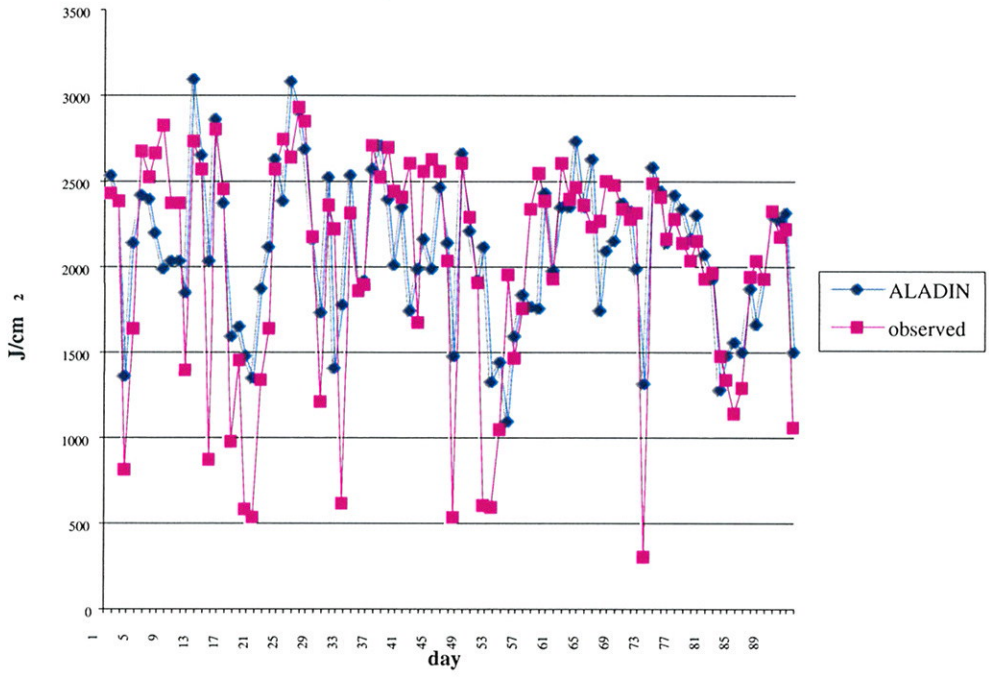

Fig. 4. **Observed and forecasted daily totals of global radiation for 42 hour forecasts. Nagyiván, June - Aug 2001**

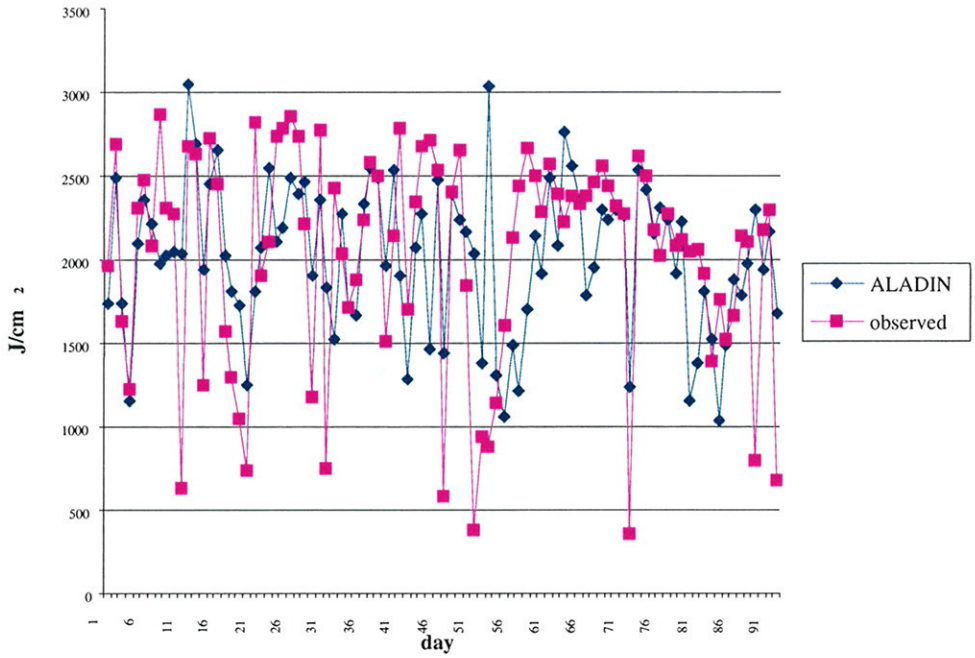

Fig. 5. **Observed and forecasted daily totals of global radiation for 24 hour forecasts. Sármellék, June - Aug 2001**

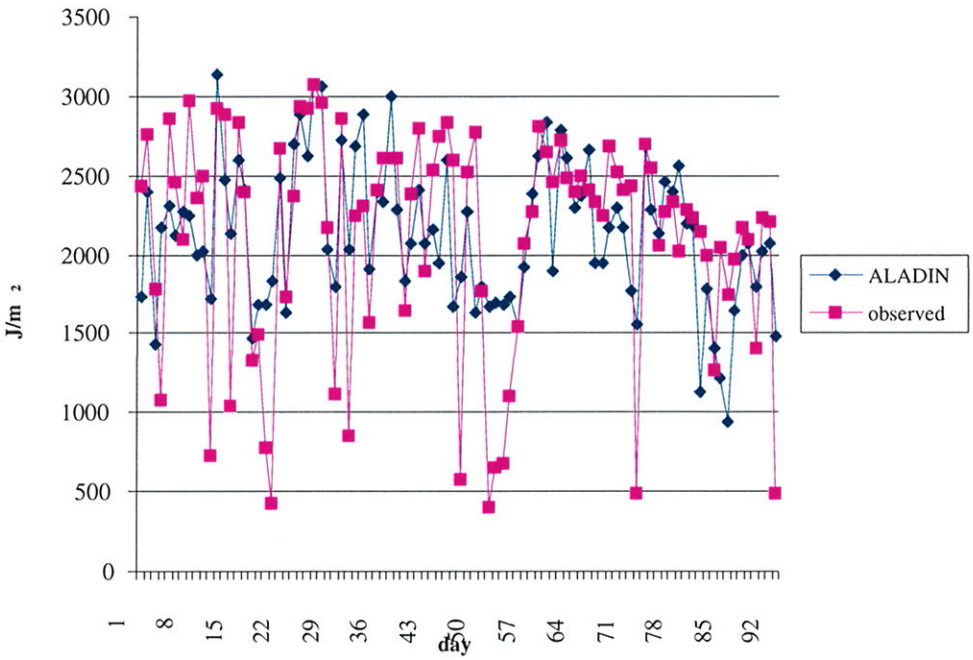

Fig. 6. **Observed and forecasted daily totals of global radiation for 48 hour forecasts. Nagyiván, June - Aug 2001**

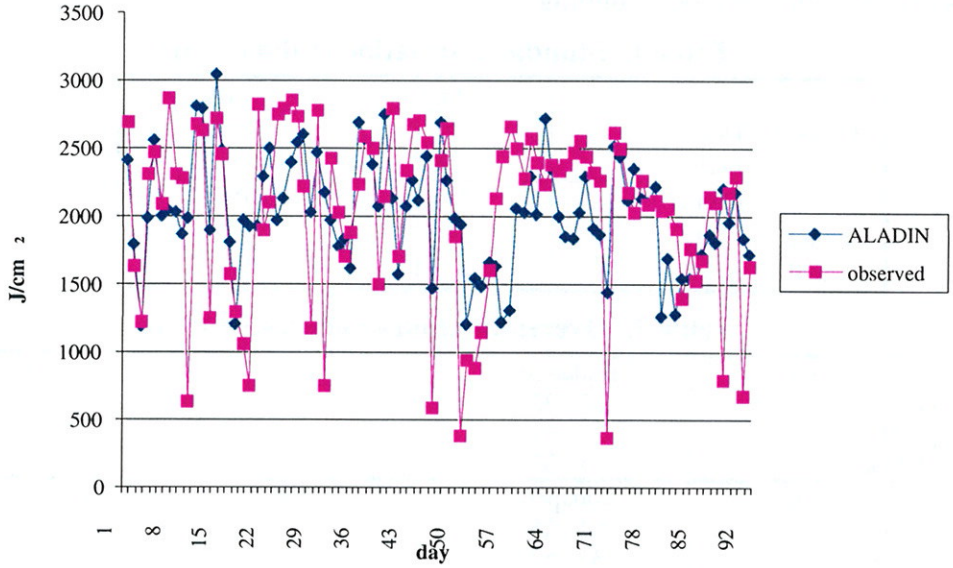

Fig. 7 **. Observed and forecasted daily totals of global radiation for 48 hour forecasts. Sármellék, June - Aug 2001**

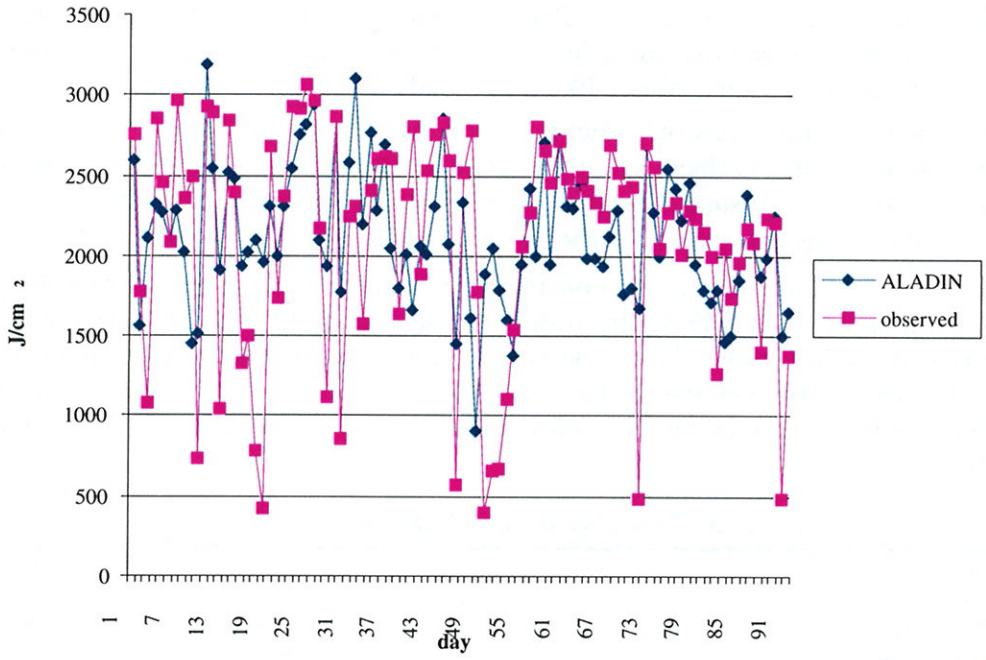

It is the most conspicuous from the figures that values of minima in observed data series are considerably low as compared with those occurring in model data series, mainly for direct and global radiation. On days when sky was covered by clouds almost throughout the day, daily totals of direct component hardly differed from zero as expected but in the same time such cases did not occur in the model. ALADIN considerably overestimated the irradiance reaching the surface for those days. Two cases are to be supposed: (1) ALADIN estimates cloud coverage erroneously on those days but it is not probable that it would have been mistaken for the most cloud-covered days right in each case. (2)

ALADIN clouds are not so effective radiation absorbers like the real clouds and they thus, when were present, could not cause radiation decrease of such magnitude like the real clouds did. It can be checked in case when, maybe in a possible next experiment, cloud coverage will be calculated with higher temporal resolution in model running.

Table 1. Standard deviation of data series

	ALA	OBS
Budapest – Direct	552.3	684.2
– Diffuse	184.2	286.1
– Global	435.9	653.2
Nagyiván – Global	444.2	644.0
Sármellék – Global	457.1	705.3

Table 2. Overestimation - underestimation

24 h	Budapest	Nagyiván	Sármellék
Direct	67 - 25	-	-
Diffuse	31 - 61	-	-
Global	55 - 37	37 - 55	40 - 52
48 h	Budapest	Nagyiván	Sármellék
Direct	64 - 28	-	-
Diffuse	35 - 57	-	-
Global	47 - 45	39 - 53	40 - 52

Number of overestimations and underestimations are shown in *Table 2*. It can be established undoubtedly that the model considerably overestimated direct radiation (67 – 25 for the 24 hour forecasts, 64 – 28 for the 48 hour forecasts), underestimated diffuse component (31 – 61 and 35 – 57, respectively), which was probably caused also by the non- sufficient radiation transfer effectiveness of ALADIN clouds. It can mean that in addition to that ALADIN clouds are not suitably effective, they did not scatter radiation in such a degree like true clouds do.

Also simulated monthly totals of global radiation were calculated for the three months used for the study from the forecasted values and they were compared with monthly totals calculated from observed values. Results are summarized in *Table 3* where percentage deviations that were calculated in the way as follows are also shown : $DEV\,(\%) = ((GALA - GOBS)/GOBS))*100$

One can establish that there is no considerable difference between simulated and true monthly totals. Deviation higher than 5 % occurred in one case only (8.14 % at 24 hour forecast for Budapest) among the nine deviation values. It is to be noted that on the one hand it was expected since errors for longer period considerably decrease effect of each other, on the other the users mainly do not need forecasts for monthly averages but for subsequent days so those relatively good agreements cannot considered too useful.

Table 3. Monthly totals of global radiation (J /cm2)

June	ALA	OBS	DEV (%)
Budapest	66 502	61 502	8.14
Nagyiván	63 793	62 980	1.29
Sármellék	66 798	64 942	2.86
July	ALA	OBS	DEV (%)
Budapest	62 002	62 311	-0.50
Nagyiván	60 382	61 768	-2.24
Sármellék	66 554	63 356	5.05
August	ALA	OBS	DEV (%)
Budapest	64 135	62 397	2.79
Nagyiván	61 748	61 501	0.40
Sármellék	62 219	62 844	-0.99

Also frequency distributions of differences between observed and predicted daily totals were studied. Differences for direct, diffuse and global radiation are marked with DIF_DIR, DIF_DIF and DIF_GL, respectively, in the figures. To save pages, differences for 24 hour forecasts are shown here for Budapest only. Intervals with a width of 200 J/cm2 were selected in the way that differences higher than 1000 J/cm2 were collected into one group. In *Fig. 8 – 13* percentage case numbers are shown. It can also be seen that overestimations dominate the figure for direct and global radiation and underestimations rather dominate it for diffuse radiation. Also it is clear from the figures that number of higher overestimations is larger in cases of 48 hour forecasts.

Using satellite images each day was explored to find out if higher differences occurred systematically. It was found what expected actually: higher differences occurred in cases when sky was almost completely covered by clouds above the given surface point and above its surroundings but in the same time smaller 'holes' or thinner cloud parts appeared in the cloudiness. The model obviously is able to predict those kind of phenomena in the least.

Fig. 8. **Frequency distribution of DIF_DIR (24 hour forecasts for Budapest)**

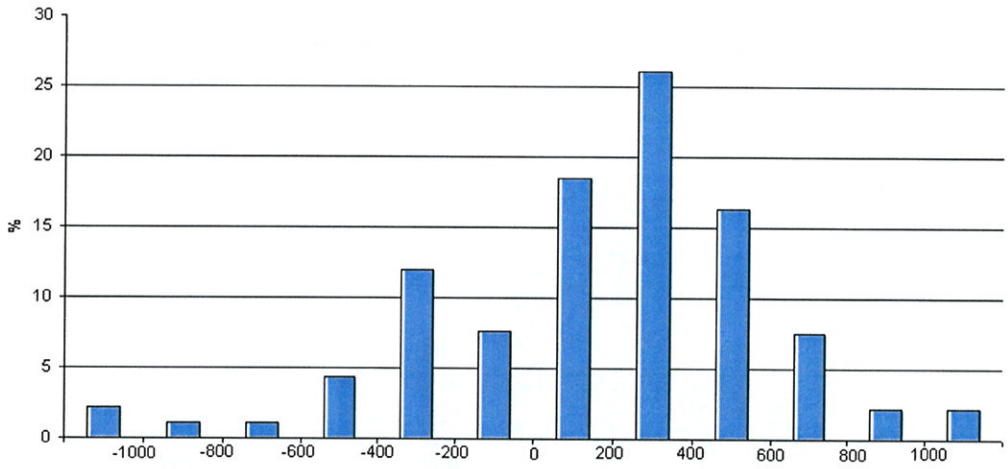

Fig. 9. **Frequency distribution of DIF_DIF (24 hour forecasts, Budapest)**

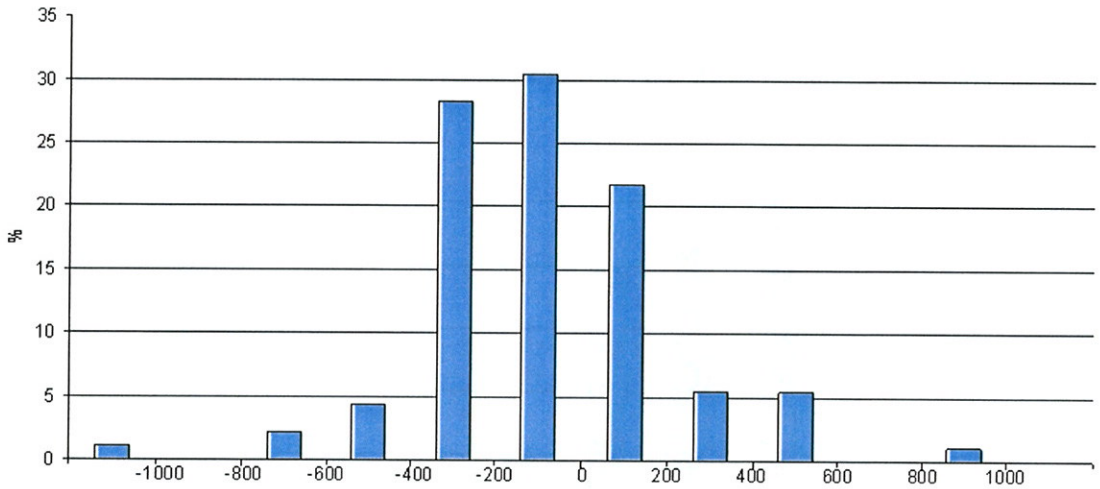

Fig. 10. **Frequency distribution of DIF_GL (24 hour forecasts for Budapest)**

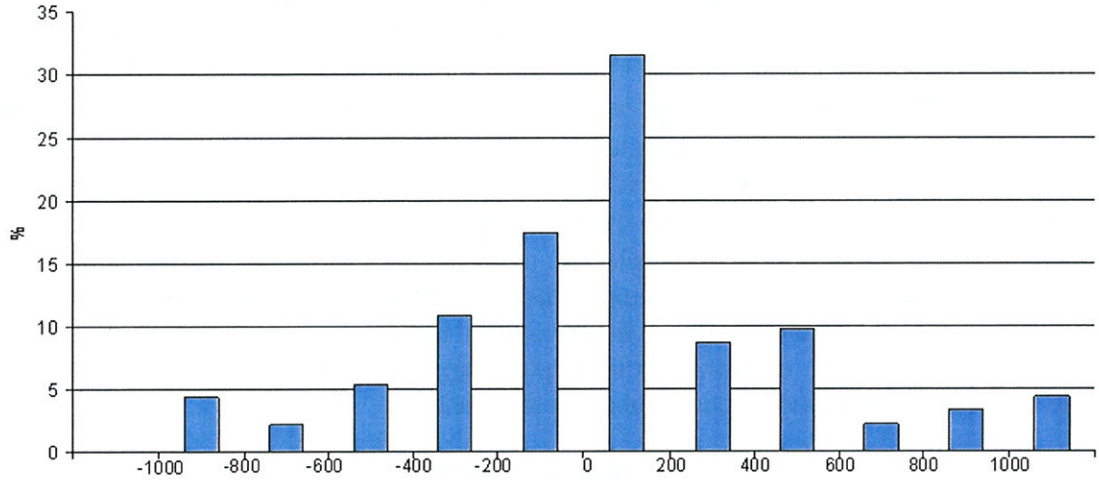

Fig. 11. **Frequency distribution of DIF_DIR (48 hour forecasts for Budapest)**

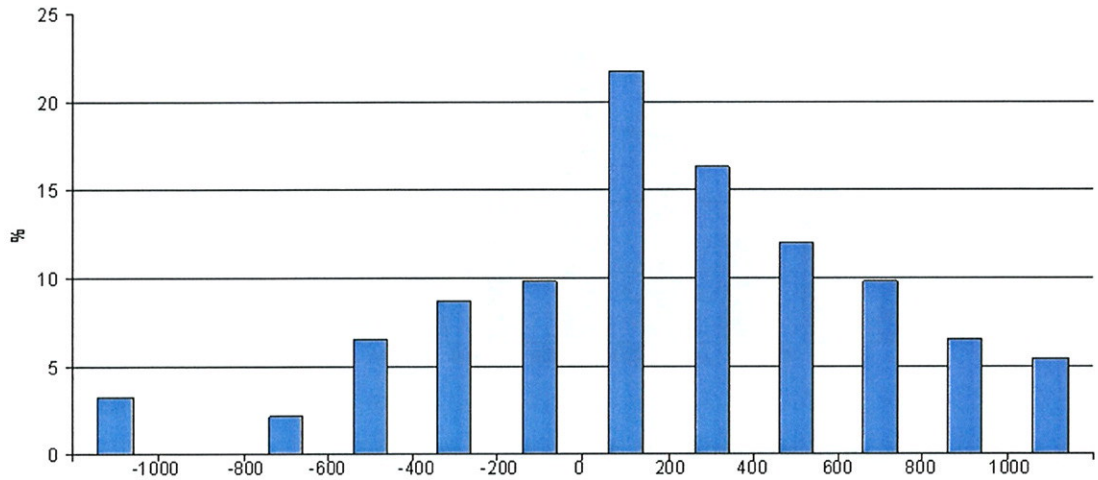

Fig. 12. **Frequency distribution of DIF_DIF (48 hour forecasts for Budapest)**

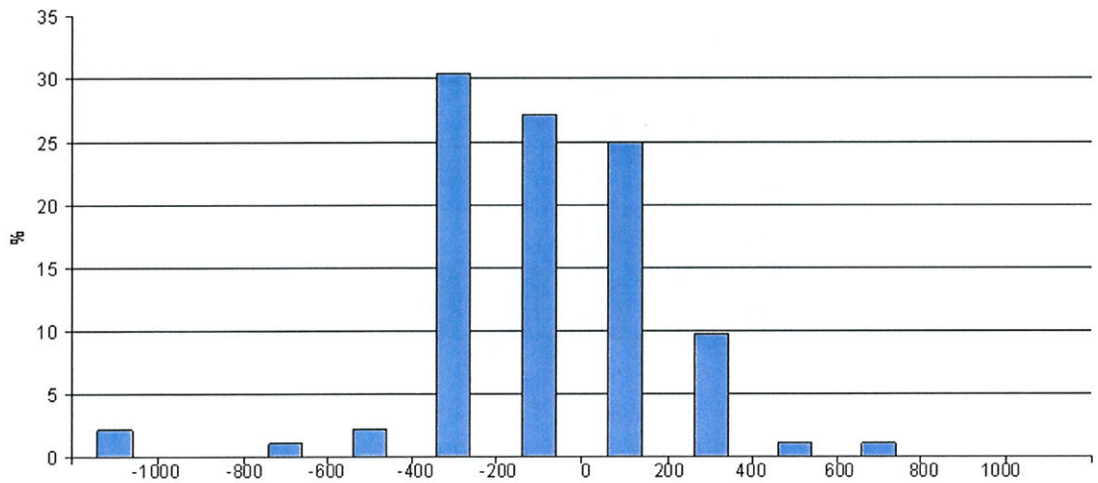

Fig. 13. **Frequency distribution of DIF_GL (48 hour forecasts for Budapest)**

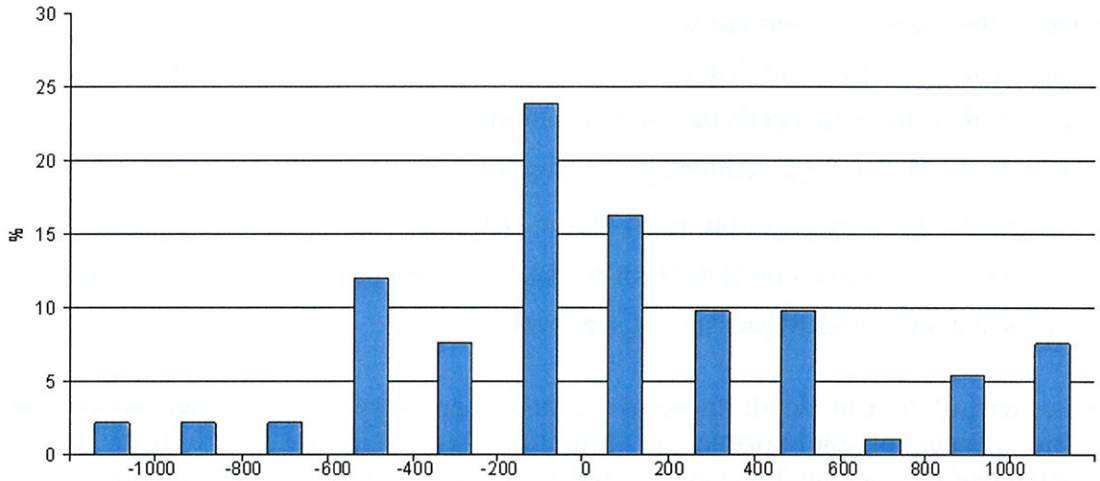

4. Results for cloudless cases

Two main factors affect solar radiation flux reaching the Earth's surface in case of wider energy range radiation: total water vapour content and total aerosol content of the air column. There was no possibility to compute them with the model afterwards since running the model again for 92 days would have taken up very much time. Despite it a study was still invented to find out how ALADIN would be able to estimate surface solar radiation fluxes in cloudless cases or in other words: how it would be able to estimate atmospheric radiation transmission. Days, among the 92 days, that were completely or 'almost' completely cloudless were selected. Term 'almost' means that values of a parameter called daily average cloud coverage were determined which, for lack of a better, was the arithmetical mean of hourly cloud coverage values. Those days were involved in the study when daily mean of cloud coverage values were not higher than 2 octa. Additional filtering was not reasonable to apply since, based on the hourly values of given days, it was clear that daily averages lower than 2 octa occurred on days solely when almost no any cloud appeared throughout the day. If sufficient number of days would have not remain or no effect would have been found, a filtering technique for selecting suitable cases would have been to apply: to examine whether the few octa cloudiness covered the solar disc or did not. But this filtering was not needed due to that 24 days were found that met the criteria given by us.

To represent radiation transmission condition of the atmosphere aerosol optical depth was selected. Aerosol optical depth values are available from our database of spectral solar radiation measurements carried out regularly with spectroradiometer LI-1800 that has a suitably designed tube to measure spectral intensity of direct radiation so it can be operated as spectrophotometer (in our practice it is used as spectrophotometer continuously).

The aim of the study was to obtain any information on reliability of ALADIN surface solar radiation forecasts concerning different atmospheric radiation transmission conditions. It is very important since considerable radiation extinction can in many cases occur even when sky is cloudless.

Aerosol optical depth values are available for Budapest-Lõrinc Observatory for each recorded solar spectra for the 10 standard wavelengths. Aerosol optical depth characterizes total columnal aerosol content of the atmosphere and can be calculated in the way as follows :

$$\tau_A(\lambda) = \frac{1}{M} \ln \frac{I_0(\lambda)}{I(\lambda) S} \left(\frac{P}{P_0} \tau_R(\lambda) + \tau_0(\lambda) \right)$$

where:

$\tau_A(\lambda)$: aerosol optical depth

$I_0(\lambda)$: extra-terrestrial irradiance at mean Sun-Earth distance

$I(\lambda)$: irradiance at the point of observation

S : correction factor for Sun-Earth distance

M : relative optical air mass (depends on solar elevation)

$\tau_R(\lambda)$: optical depth due to Rayleigh scattering of air molecules

$\tau_0(\lambda)$: optical depth due to ozone absorption: $\tau_0(\lambda)=a_0(\lambda)\,\eta$

where: $a_0(\lambda)$: absorption coefficient for ozone: η: total columnal ozone content

P, P_0 : current pressure and standard pressure at sea level

To determine aerosol optical depth those wavelengths are used where either no considerable gaseous absorption appears or solely ozone has absorption. At wavelengths where ozone absorbs, the ozone optical depth can be calculated and considered at the aerosol optical depth calculation based on our ozone measurements. Standard wavelengths are as follows (in nm): 368, 380, 412, 450, 500, 610, 675, 778, 862, 1024.

To use only one wavelength is practically sufficient to characterize quantitatively a given aerosol transmission condition of the atmosphere (several wavelengths are needed when, due to availability of both some aerosol model and aerosol size distribution, aerosol concentration would be intended to determine). In according to agreement the optical depth values calculated for 500 nm (τ500) are generally used so also they were used for our studies, namely their daily averages.

Relationship between daily average aerosol optical depth and difference of observed and predicted solar irradiances (DIF_DIR, DIF_DIF and DIF_GL in the figures) was studied for all three radiation parameters. Results are shown in *Fig 14 – 16*. Aerosol optical depth for 500 nm is represented on horizontal axis and differences between observed and forecasted irradiances (IALA - IOBS) are represented on vertical axis in each figure.

Results for direct irradiance is shown in *Fig 14*. Based on our five year long aerosol optical depth data series it is known that average value for Budapest-Lõrinc Observatory is approximately 0.3 for 500 nm. It is clear from *Fig. 14* that for the most part overestimations are found for values of τ500 lower than 0.3 and underestimations are found for τ500 values higher than 0.3. It means that the model underestimates direct irradiance reaching the surface in cases when atmospheric radiation transmission is high, namely when very small amount of pollutant is present and overestimates it in cases when atmosphere is considerably polluted. Based on it one can conclude that atmospheric radiation conditions predicted by the model are generally approach average conditions due to that the model draftly handles parameters influencing radiation transmission, namely its variability is lower than that of corresponding true parameters. The model predicts more polluted atmosphere compared with reality in very clear cases close to Rayleigh atmosphere. These findings are confirmed by results of the same study made for diffuse irradiance (*Fig. 15*). Pollutants and water vapour intensively scatters radiation consequently diffuse (scattered) irradiance observed at Earth's surface increases as larger amount of them is present in the atmosphere. It can be seen in Fig. 15 that in case of diffuse irradiance inverse effect was found as compared to that found for direct component: the model overestimates diffuse irradiance in cases of high transmission (τ500 < 0.3), namely it forecasts more polluted conditions than the true state of atmosphere and in the same time it underestimates in cases of lower transmission, namely it forecasts lower pollution than that appearing in true atmosphere. The same effect lies behind this phenomena like in case of direct fluxes so the explanation is the same: the model tends to produce such physical conditions of atmosphere that result in more average atmospheric transmission than those occurring in reality. Those mentioned above are valid for global radiation also (see Fig. 16) but

the effect is relatively less evident due to the fact that global irradiance is the sum of the previous two parameters so the effect in question decreases.

Fig. 14. **Values of DIF_DIR at different aerosol optical depths**

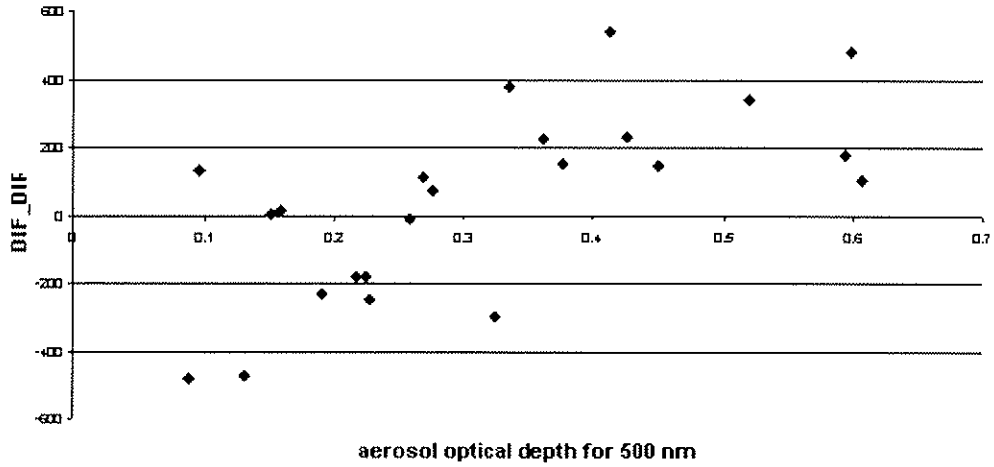

Fig. 15. **Values of DIF_DIF at different aerosol optical depths**

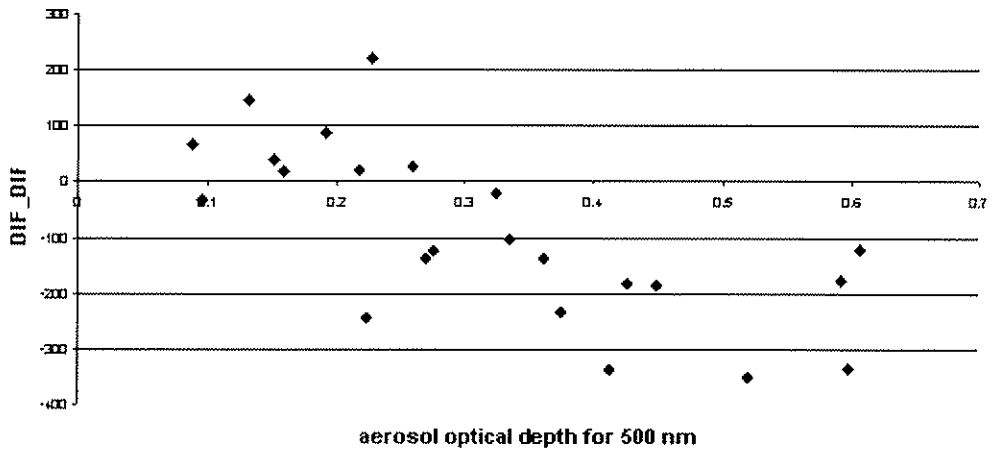

Fig. 16. **Values of DIF_GL at different aerosol optical depths**

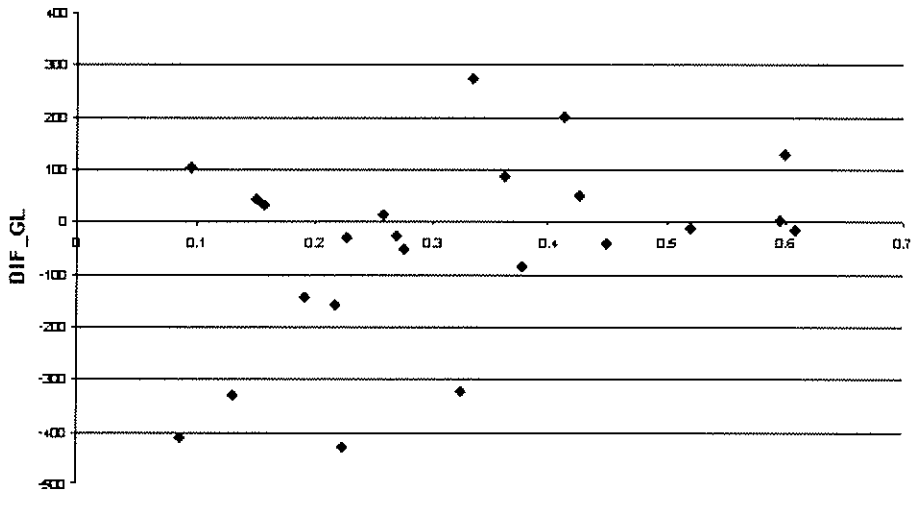

5. Conclusions

Based on results discussed above one can conclude those as follows:

(i) It is to be established, based on deviations of predicted values from observed irradiances, that ALADIN, essentially, estimates solar irradiances reaching the Earth's surface with good accuracy.

(ii) Analysing observed and forecasted data series it was found that ALADIN predicts far more less number of very low value of daily totals than the case number occurring in reality and those low values are considerably higher than the corresponding true values (which are in some cases very close to zero). Since the probability of that the model made a mistake in forecasting the cloudiness always just on days in question, as reason it is more probable that ALADIN clouds are less effective radiation absorbers than true clouds.

(iii) Forecasted data series are characterized by considerably lower standard deviations than observed series. It means that the model cannot suitably reproduce variability of daily totals of irradiances.

(iv) In cloudless or 'almost' cloudless cases (cloud coverage < 2 octa for daily averages) differences of observed and predicted daily totals for direct and global irradiances increases with increasing aerosol optical depth while inverse dependence was found for diffuse component. It means that in cases of extremely high transmissions (low turbidity) the model predicted lower transmission and when the transmission was extremely weak (high turbidity) it forecasted higher transmission. It means that parameterization of aerosols and total water vapour is not sufficiently fine in the model, namely the resulted radiation transmission scale of the model is not sufficiently wide.

Acknowledgements

Author would like to express his thanks for three of his colleagues: for Gábor Radnóti who produced ALADIN outputs for the study; for Ildikó Grób-Szenyán who produced satellite images needed and helped in analysing them; for László Nyitrai who calculated cloud coverage values.

Verification of ALADIN/LACE pseudo-TEMPs for Ljubljana

Mateja Irsic, *mateja.irsic@rzs-hm.si*
Neva Pristov, *neva.pristov@rzs-hm.si*
Environmental Agency of the Republic of Slovenia

1. INTRODUCTION

The verification of pseudo-TEMPs by ALADIN/LACE prognostic model for temperature and dew point temperature in comparison to radiosonde measurements was studied for Ljubljana. In the period between 1 January 2000 and 31 August 2001 radiosonde measurements and pseudo-TEMPs were archived for most of the days. Only in temperature analysis certain days were subsequently excluded due to uncompleted measurements. In Slovenia, radiosonde measurement is carried out only in Ljubljana at 6 UTC. The release of radiosonde takes place at approximately 5 UTC, the duration of measurement is approximately one hour. Since ALADIN forecasts by 00 UTC run valid at 6 UTC are available only a few hours before 6 UTC, we decided to verify the forecasts by 12 UTC run, valid at 6 UTC following day.

2. VERIFICATION OF TEMPERATURE PROFILE

The comparison between the forecasted temperature and the radiosonde measurement of temperature for one selected day is shown in Figure 1. The forecasted profile is defined by the values of temperature for 31 layers and the temperature at 2 m above model surface. Such profile is much smoother than measured temperature profile.

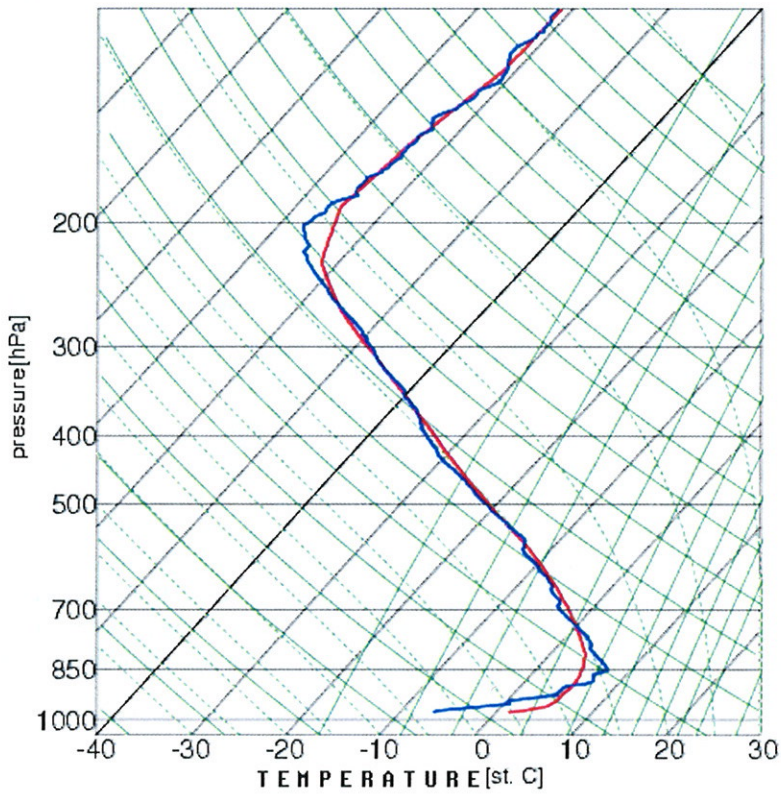

Figure 1: The emagram with ALADIN forecast (3 January 2000, 12 UTC +18 h) of temperature (red) and radiosonde measurements of temperature (blue) in Ljubljana, 4 January 2000 at 6 UTC.

The repetition time of radiosonde measurements is 10 s, which means that the measurements take place on more than 300 levels, which vary from one to the other measurement. The comparison of the forecasted and the measured temperatures was evaluated at the measured pressure levels. A linear interpolation was used to obtain forecasted temperatures at measured pressure levels (TAL12).

Figure 2 shows a scatter plot of the measured temperatures (T) and the forecasted temperatures (TAL12), for which linear interpolation to the levels of measurements was made. In the parts, where deviation from the odd quadrant line is sharper, the error is bigger. As evident in Figure 2, the deviation is the slightest in the middle interval for the temperature between 260 and 240 K.

The verification of temperature was made up to 100 hPa. Figure 3 demonstrates errors at standard pressure levels. The error is defined with median, lower quartile, upper quartile and extreme values of the T-TAL12 difference. The levels with narrower inter-quartile display better forecasts, which is between 850 hPa to 300 hPa. Differences were bigger around tropopause and also in lower layers, where the forecasted temperatures were usually overestimated.

Three mean vertical errors were calculated for every day: mean error (ME), mean absolute error (MAE), root mean square error (RMSE), which are shown in Figure 4. The poorest forecast of the temperature was at the beginning of February (Fig. 4 around day 350), which was a consequence of error more than 20 K in the part around 200 hPa.

Linear interpolation from the forecasted levels to measured levels was made, but to be sure that this interpolation was good enough, some additional interpolations were tested, i.e. spline interpolation with polynomial of third degree and Hermite splines; furthermore a very simple method, which does not involve interpolation but takes the nearest value, was employed. The method of interpolation did not have significant influence on mean errors.

Mean errors in temperature up to 100 hPa and up to 850 hPa, when method of linear interpolation was used, are shown in Table 1. Forecasts of temperature in lower atmosphere (up to 850 hPa) were poorer than forecasts of temperature up to 100 hPa. The mean error up to 100 hPa was negative, which means that forecasts were too warm on average. That was even more obvious when evaluating the lower part up to 850 hPa. On average, the errors were bigger in the lower part (up to 850 hPa) in comparison to errors in the part up to 100 hPa. That can be seen when comparing RMSE and RMSE 850 in Table 1.

days	number	ME	MAE	RMSE	ME850	MAE850	RMSE850
all	463	-0,19	1,10	1,46	-1,30	1,59	1,93
strong inversion	26	-0,22	1,17	1,64	-1,53	1,94	2,37

Table 1: Comparison of average errors in forecasted temperatures up to 100 hPa (ME, MAE, RMSE) and up to 850 hPa (ME 850, MAE, 850, RMSE 850) in Kelvin.

Daily errors (Figure 4) demonstrate that in certain periods the errors were more dispersed than in the others. Our forecasters stressed that the forecast of temperatures at the ground is usually wrong if temperature inversion is present. That is the reason why the cases with inversion were separated and errors calculated. All days, when the measured temperature increase between two measured levels exceeded 2 K, were separated. The criteria was limited to only up to 400 hPa, so that temperature inversion on tropopause was excluded. The number of days, which satisfied this demand, was 26. The forecasts with the specified temperature inversion were poorer than others. This is evident in Table 1 and it was true in the lower part of the atmosphere or when the temperatures up to 100 hPa were treated. It can be seen that average forecasts of temperature profiles in the cases of specified inversion were poorer than in all other cases.

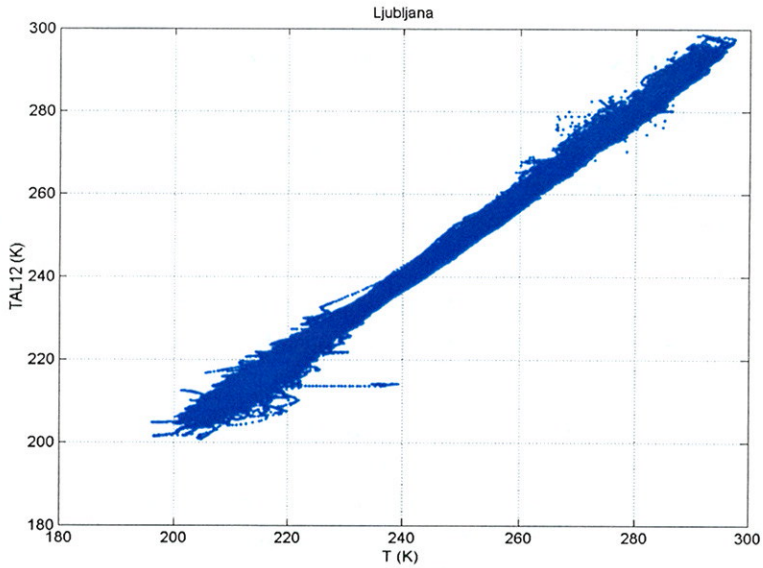

Figure 2: Scatter plot of the measured temperatures (T) and the forecasted temperatures (TAL12), for which linear interpolation was made to the levels of measurements between 1 January 2000 and 31 August 2001.

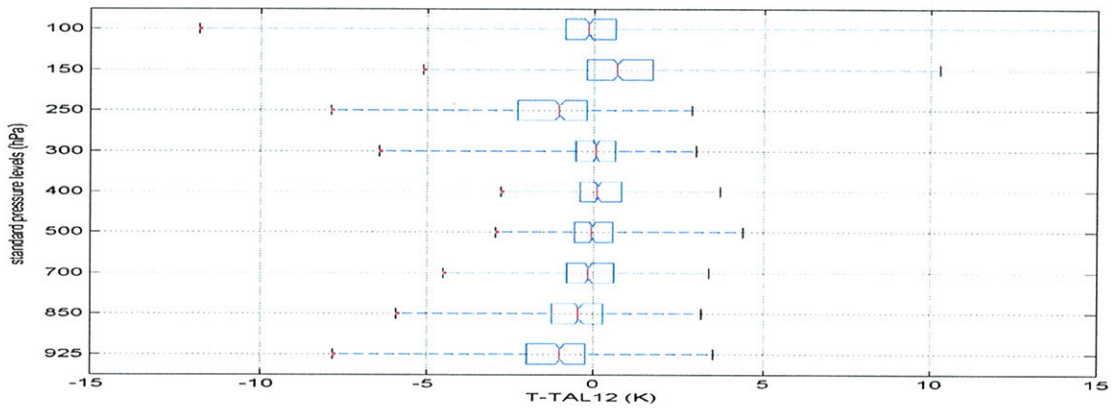

Figure 3: Distribution of temperature difference between measured (T) and forecasted (TAL12) at standard pressure levels. Red vertical lines mark median, blue vertical lines mark lower quartile (left) and upper quartile (right). Minimum and maximum errors are also indicated. Period as in Figure 2.

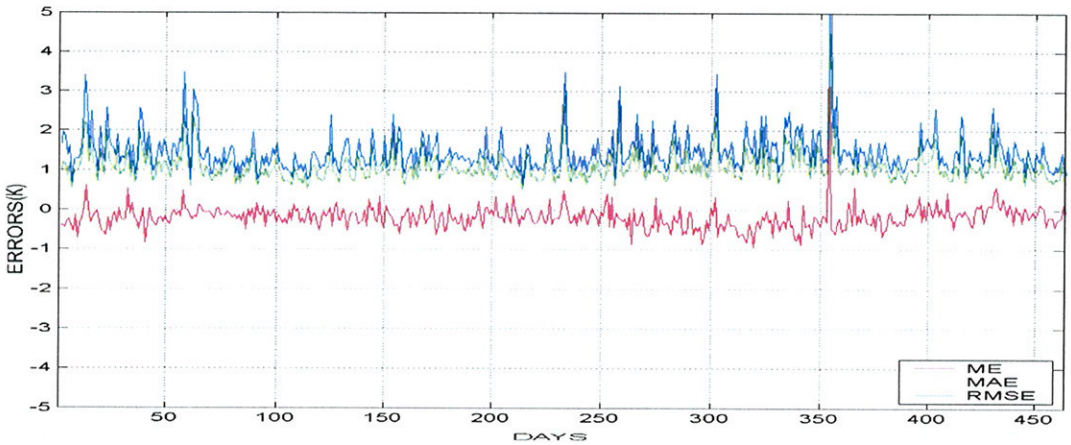

Figure 4: Errors in forecasted temperatures for 463 days between 1 January 2000 and 31 August 2001. ME in blue, MAE in green and RMSE in red.

3. VERIFICATION OF DEW POINT TEMPERATURE PROFILE

Comparisons for dew point temperature profiles were made using the same methods of evaluation. In the atmosphere, a thin dry or very moist layer of air can be present in comparison to the surroundings, which can be seen on the measured profiles, but cannot be predicted by the model limited by its resolution. So the forecasted dew point temperature profiles were expected to be poorer than the forecasted temperature profiles.

This evaluation took into account only the measurements and the forecasts for dew point up to 400 hPa. The reason for this is that the measurements, which are higher in the atmosphere, are not very reliable with sensor Vaisala RS 80.

Figure 5 demonstrates the scatter plot of measured (Td) and forecasted (Td AL12) dew point temperatures. The width of scatter is particularly large for lower temperatures. Figure 6 demonstrates errors at standard pressure levels. The distributions of errors at each standard pressure level are presented with median, lower quartile, upper quartile and extreme values. Forecasts at 925 hPa were generally better than forecasts at 500 hPa. Figure 7 demonstrates three errors for each day. The comparison between dew point temperature errors (Figure 7) and temperature errors (Figure 4) shows that dew point errors occur in larger intervals. Figure 8 presents mean errors for a chosen period up to two different pressure levels. MAE and RMSE for dew point temperature were much bigger for values up to 400 hPa than in the lower part (up to 850 hPa). ME was slighter when considering the atmosphere up to 400 hPa than when considering only the lower part up to 850 hPa. The reason for this was the fact that between 850 hPa and 400 hPa, ME was negative. There was a difference of more than 1 K between RMSE and MAE when considering the atmosphere up to 400 hPa (Figure 8), which means that some errors were very big. The same is evident in Figure 6 with some cases even exceeding -20 K at levels 700 and 500 hPa.

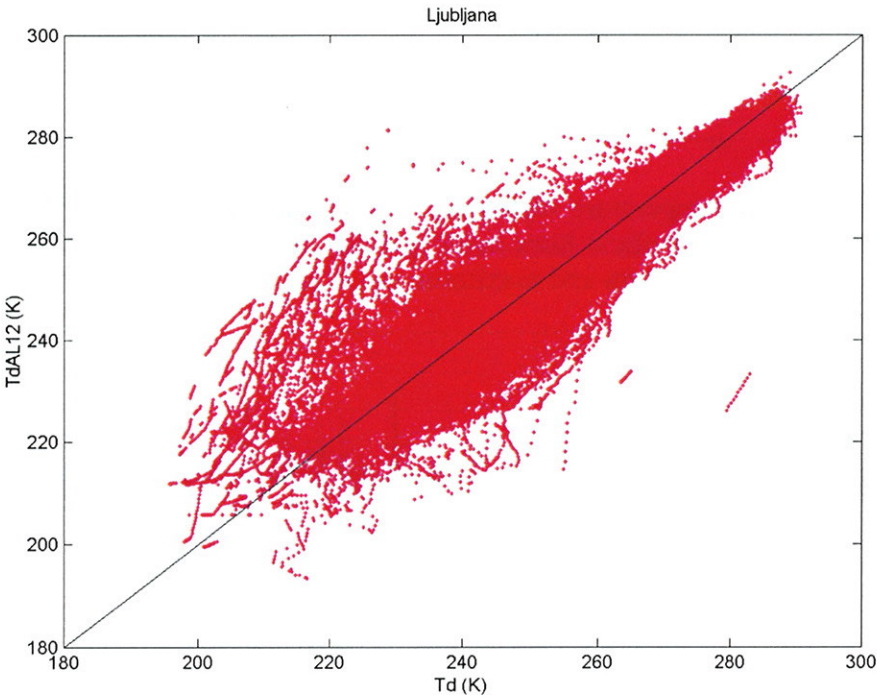

Figure 5: Scatter plot of measured dew point temperatures (Td) and forecasted temperatures (Td AL12), for which linear interpolation to the levels of measurements was made for days between 1 January 2000 and 31 August 2001.

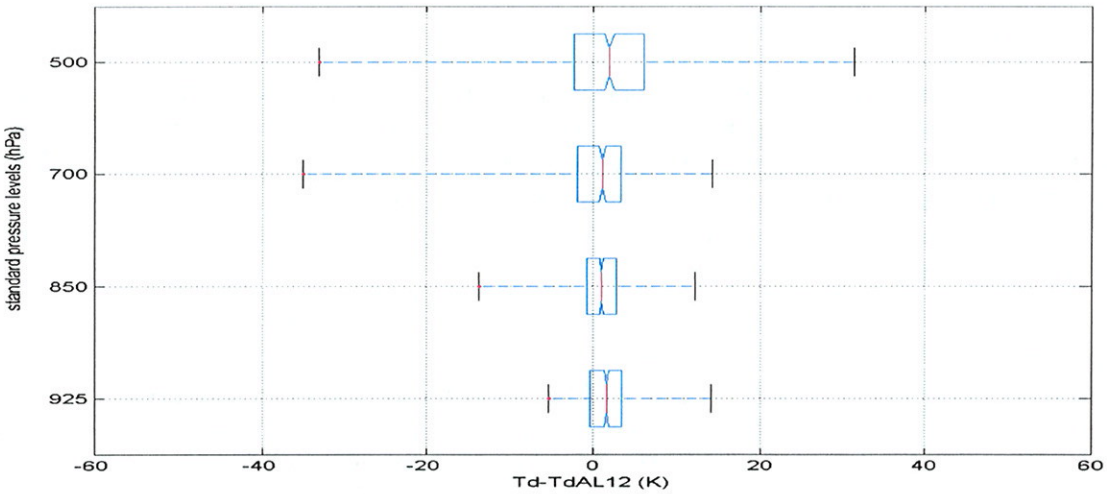

Figure 6: Distribution of dew point temperature error (Td- Td AL12) at standard pressure levels. Red vertical lines mark median, blue vertical lines mark lower quartile (left) and upper quartile (right). Minimum and maximum errors are also indicated.

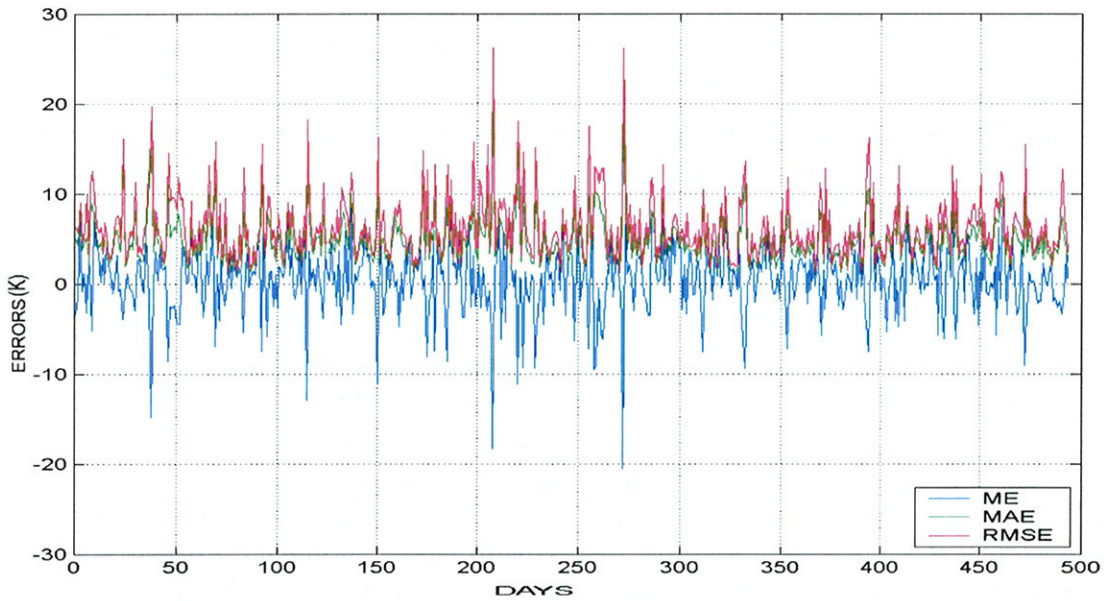

Figure 7: Errors in forecasted dew point temperatures for 493 days between 1 January 2000 and 31 August 2001 up to 400 hPa. ME in blue, MAE in green and RMSE in red.

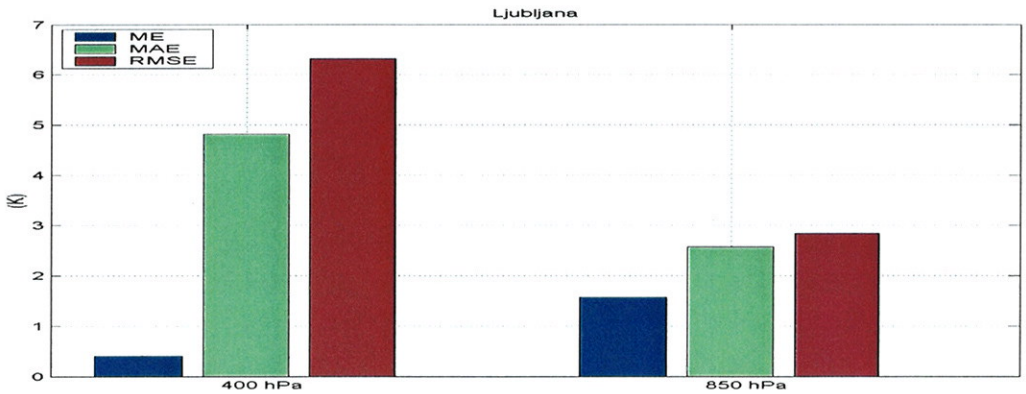

Figure 8: Errors in dew point temperatures up to 400 hPa and up to 850 hPa for the period as in Figure 7.

4. CONCLUSION

This article presents the objective verification of temperature and dew point temperature profiles by ALADIN/LACE forecasts for Ljubljana. Vertical profiles in the period between January 2000 and August 2001 at 6 UTC were compared with forecasts by run 12 UTC previous day, valid for 6 UTC next day. The forecasted temperatures from the ground up to 100 hPa and the forecasted dew point temperatures from the ground up to 400 hPa were linearly interpolated to measured pressure levels and compared with the radiosonde measurements.

The biggest errors in temperature forecasts occurred in the lower part up to 850 hPa and in the upper part above 300 hPa. The reason for this included a rapidly changing gradient in the lower atmosphere in comparison to that in the middle atmosphere (between 850 hPa and 300 hPa) and variation in tropopause height. The forecasted temperature profiles were slightly warmer on average, which was demonstrated by negative ME. The biggest part of errors was a consequence of poor forecasts in the cases of inversion in the lower part of the atmosphere.

The forecasted profiles of dew point temperature were on average colder, since ME was positive. Consequently, the atmosphere up to the 400 hPa would be, according to forecast, on average too dry for the chosen period. In the lower part of the atmosphere (up to 850 hPa), the forecasts of dew point temperatures were more accurately predicted (smaller MAE and RMSE) than in the part above it. This was due to expressive gradients of dew point temperature in the part higher than 850 hPa, which were changing from negative to positive and vice versa.

This study did not take into account that the duration of radiosonde measurements is approx. 1 hour, we treated it as if it were carried out at 6 UTC. Furthermore, it was taken into account that radiosonde measurements were advected by horizontal wind, and the horizontal shift can be bigger than model horizontal resolution. In that case, we should take into consideration the lower forecast of one model point and the forecast of the upper part of the model point beside it. Consequently, not only one column in the forecast model would have impact on verification results of the upper troposphere.

The forecasts of dew point temperatures were much poorer than the forecasts of temperatures, which was expected since moisture field is in general more variable as temperature field.

This study is important for our future work. The known correctness is particularly important when using forecasted profiles as a first guess in reconstructing measured vertical profiles of temperature and dew point temperature by polar - orbital satellites. In this study it was shown that the days when temperature inversion is present should be treated with more carefulness, especially in the lower part of the atmosphere and at the ground. On the other hand the forecasts of dew point temperature above 850 hPa are very insecure. When calculating the height of cloud tops based on satellite measurements, the conversion from temperatures to pressure levels is the most reliable for middle clouds.

Preliminary results of direct ALADIN 00 UTC output verification of surface weather parameters for six regions over Tunisia

(Evaluation period : September - December 2001)

Karim Bergaoui, Nihed Bouzouita, Abdelwahed Nmiri (*INM*)

INTRODUCTION

The work described here was motivated by the need to quantify the extent to which forecasts of ALADIN surface parameters are being reliable.

In order to best apprehend the operational performances of ALADIN_Tunisie model, we tried in this experimental phase to start an operational evaluation by installing a computational monitoring procedure, being inspired by experimentations of some European ALADINers countries applied to ALADIN/LACE model (Hungary, ...) in this field, with respect to the INM proper objectives in term of forecast quality.

This first synthesis relates to the period from 05 September to 31 December 2001.

METHOD OF EVALUATION

– **Intervals of forecast** : 06-18 UTC, 18-30 UTC et 30-42 UTC.

– **00UTC surface analysis** : Weather types :

- Anticyclone A
- Cyclone C
- Eastern part of the cyclone Ce
- Western part of the cyclone Cw
- Eastern part of the anticyclone Ae
- Western part of the anticyclone Aw
- Weak pressure gradient Wp
- Zonal flow Z

– **Locations :** we have divided the whole domain into six regions

Region I North-East	**Region II** North-West	**Region III** Center-East	**Region IV** Center-West	**Region V** South-East	**Region VI** South-West
Tunis	Jendouba	Kairouan	Thala	Gabes	Gafsa
Bizerte	Tabarka	Monastir	Kasserine	Jerba	Kebili
Zaghouan	Béja	Sfax	Sidi-Bouzid	Medenine	Tozeur
Kélibia	El-Kef			Tataouine	El-Borma
Nabeul	Siliana			Remada	

This cutting out makes apart the coast regions from the others (of relief). However, the region 1 (North-East) has been moved away (moved apart) from this synthesis because of the land-sea mask which did note have been considered here.

– **Controlled parameters** 10m wind, Cloudiness, 06h UTC temperature, 12h UTC temperature, precipitation quantity, surface humidity .

Evaluation method for the different parameters

• **Total cloudiness :**

OBS./FOR.	0	1-2	3-6	7-8
0	3	+2	+1	+1
1-2	+2	3	+2	+1
3-6	+1	+2	3	+2
7-8	+1	+1	+2	3

• **10m wind:**

3 : for difference in wind (between the forecast and observed value) = ±2m/s
2 : for difference in wind (between the forecast and observed value) = ± 3m/s
1 : for difference in wind (between the forecast and observed value) > 3m/s

• **2m temperature:**

3 : for difference in temperature (between forecast and observed value) = ± 2 K
2 : for difference in temperature (between forecast and observed value) = ± 2-4 K
1 : for difference in temperature (between forecast and observed value) > 4 K

• **precipitation quantity :**

OBS./FOR.	0 mm	<2 mm	2-10 mm	>10 mm
0 mm	3	+2	+1	+1
< 2 mm	+2	3	+2	+1
2-10 mm	+1	+2	3	+2
> 10 mm	+1	-1	+2	3

• **2m Humidity :**

3 : attributed to the difference obs./forecast = ± 10 %
2 : attributed to the difference obs./forecast = ± 10-20 %
1 : attributed to the difference obs./forecast > 20 %

The scores for the range 18h-30h are missed seeing that the observations of humidity are picked out of the BQR (Bulletin Quotidien de Renseignement) not including this range, but not of the SYNOP messages.

RESULTS OF THE EVALUATION

• Systematic Underestimation over the three ranges 06-18, 18-30 et 30-42 for the different controlled parameters excepted the case for the precipitation for which an overestimation has been seen over all the six regions.

• Degradation of the Global rate of successful forecast for the range 30-42 regarding the others , particularly for the case of the cloudiness.

• The error is more important (marked , pronounced) during the night for the temperature as well as the wind.

• The forecast is basically better for the wind over the entire domain than it is for the other parameters.

• The anticyclonic weather types (45 A cases) as well as the cyclonic types (33 C cases) predominate in the most cases but don't affect seriously the forecasts quality.

• The wind seems to be insensitive to the weather types.

Fig.1 - Rate of Global Successful Forecast of the different parameters per region (in %)
Calculated from the ratio of the forecasts number (with score 3) over the entire 25 principal stations. The observed data for humidity are not available for the range 18-30.

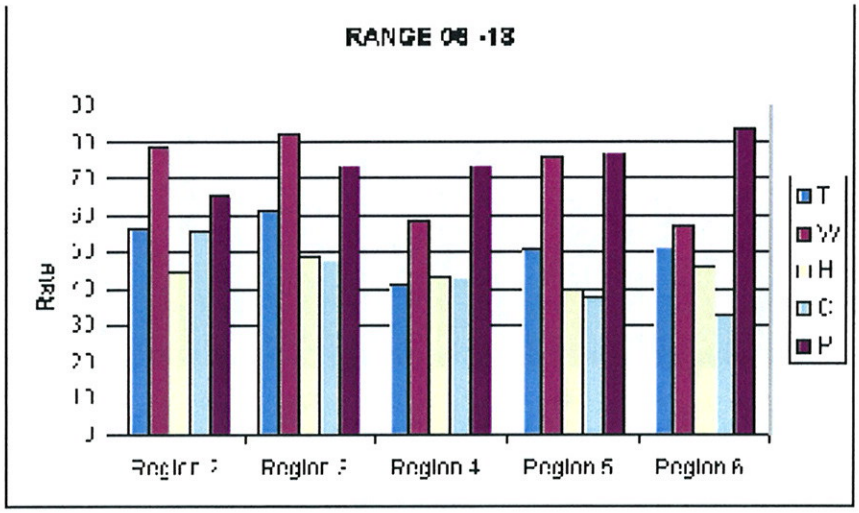

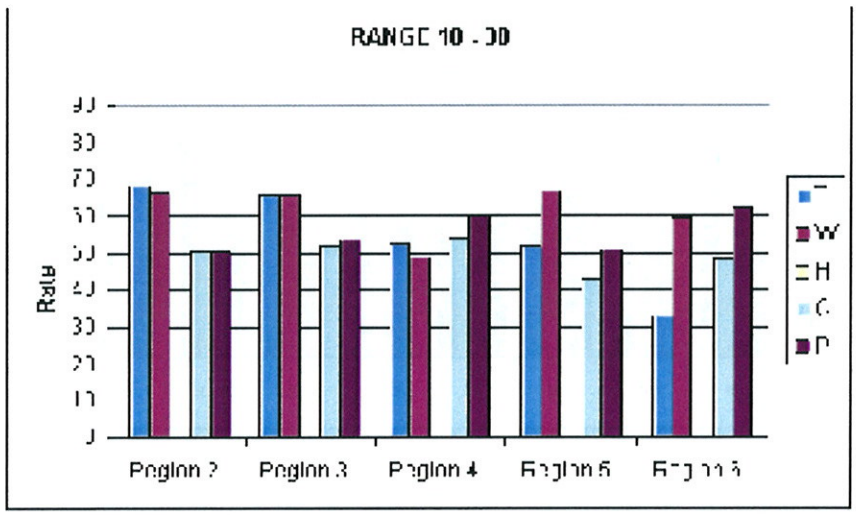

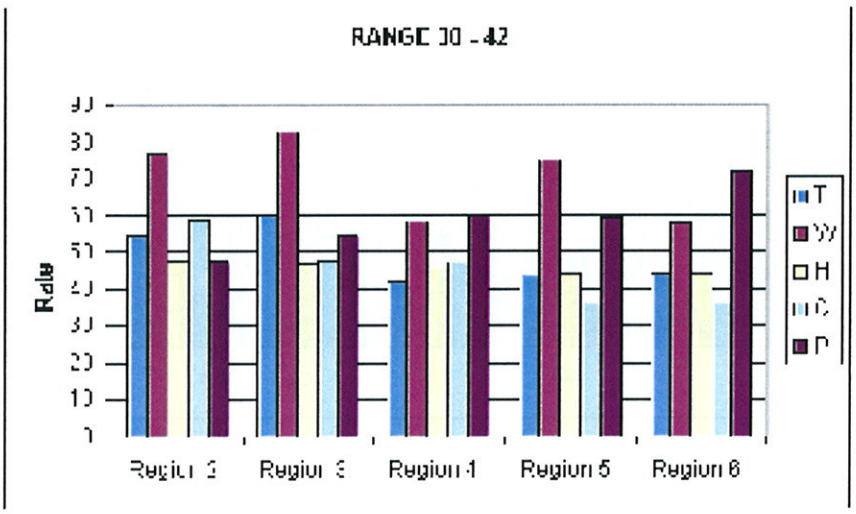

Fig.2 - Rate of Global Successful Forecast (in %), per weather type and parameter

Calculated from the ratio of the forecasts number (with score 3) over the entire 25 principal stations. The observed data for humidity are not available for the range 18-30.

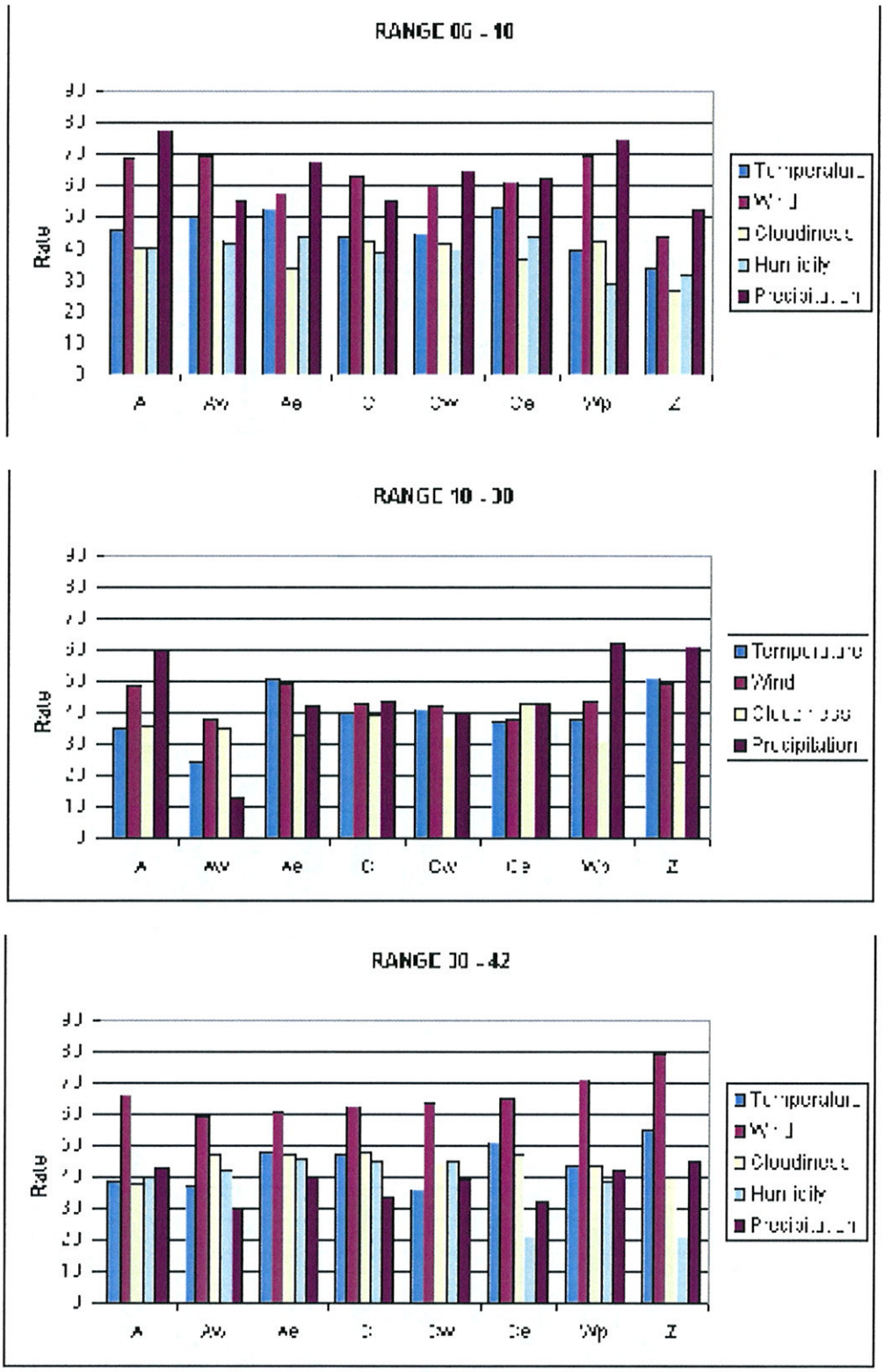

Impact of digital filtering initialisation DFI on CANARI analysis increments

Zahra Sahlaoui and Fatima Zahra Hiddou.
Direction de la Météorologie Nationale, Maroc

1. Introduction

The meteorological models are based on primitives equations. These equations have not only meteorological solutions but also other solutions without signification like acoustic waves and gravity waves.

The hydrostatic approximation filters vertical acoustic waves, but it doesn't affect the horizontal ones. There are other oscillations (gravity waves) that can noise the meteorological solution if they aren't filtered.

Several methods were developed to filter high frequency oscillations; such as normal mode initialisation (NMI) and digital filtering initialisation (DFI). Digital filtering provides an approach to initialisation that is conceptually simple and easier to implement than NMI. It involves generating a sequence of model fields and then applying a filter to the resulting time series for each model grid point and variable or for each model spectral coefficient. The filter is chosen to reduce the amplitudes of high frequency components of the time series to acceptable levels, but care should be taken to not destroy the increments. So what can be the impact of DFI on the analysis increments?

Concerning 3d-var analysis, Dziedzic (2000) demonstrates that DFI strongly dumps the analysis increments, but what about CANARI analysis. This study aim to quantify the influence of DFI on analysis increments produced by the model ALADIN/MOROCCO.

2. Description of the experiments

Two sets of experiments were run for 21/11/2001 at 0 h UTC. The first is performed without DFI (CANARI analysis). The second with DFI ; after CANARI analysis, the 0 h integration of the model follow to apply digital filtering.

In the beginning, the approach was to use an observation file containing just one observation extracted from a TEMP. The object was to avoid the superposition of increments resulting from different observations. The parameters chosen were :

- Geopotential (Z) at 500 hPa.
- Temperature (T) at 500 hPa.
- Humidity (HU) at 700h Pa.
- Zonal (U) and meridian (V) components of wind at 850 hPa.

Later, experiments using the full observation file were run with and without DFI.

3. Results

Maps of the analysis increments for each experiments were prepared to evaluate the impact of digital filtering. This results are presented below.

For each parameter, we drop analysis increments without DFI (left) and with DFI (right).

The summary of the comparison between the two sets of experiments (with and without DFI) demonstrates that digital filtering destroys the increments (values). Further, it strongly modifies the structure of the increments.

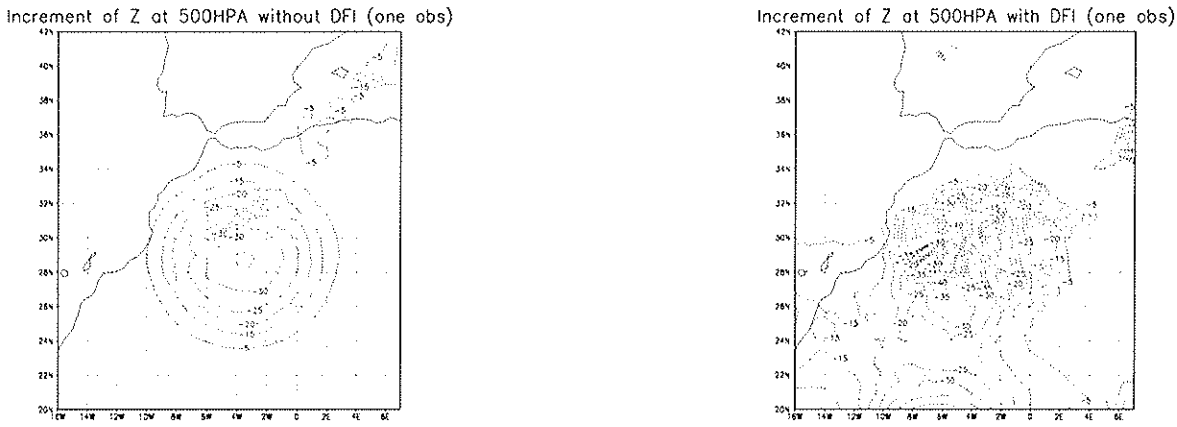

Figure 1. Increments of geopotential at 500 hPa without (left) and with (right) DFI.

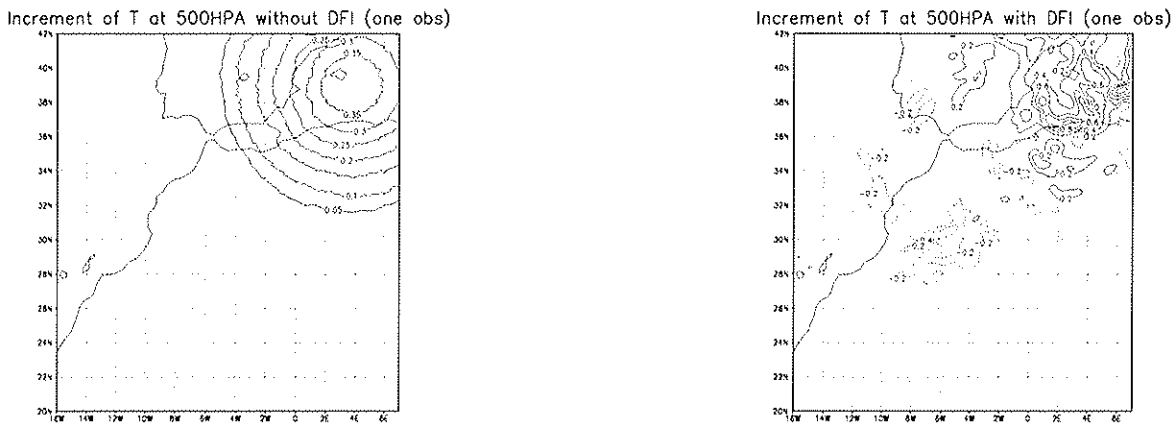

Figure 2. Increments of temperature at 500 hPa without (left) and with (right) DFI.

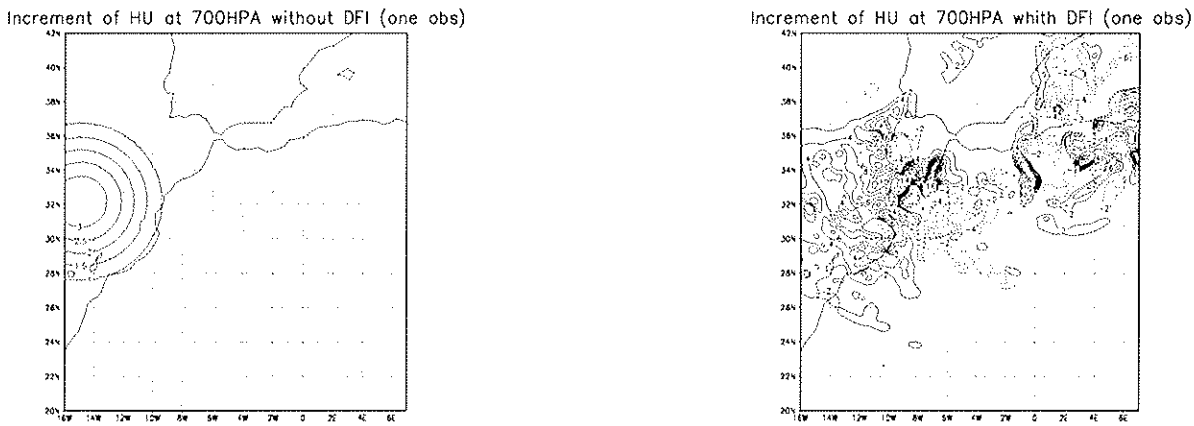

Figure 3. Increments of relative humidity at 700 hPa without (left) and with (right) DFI.

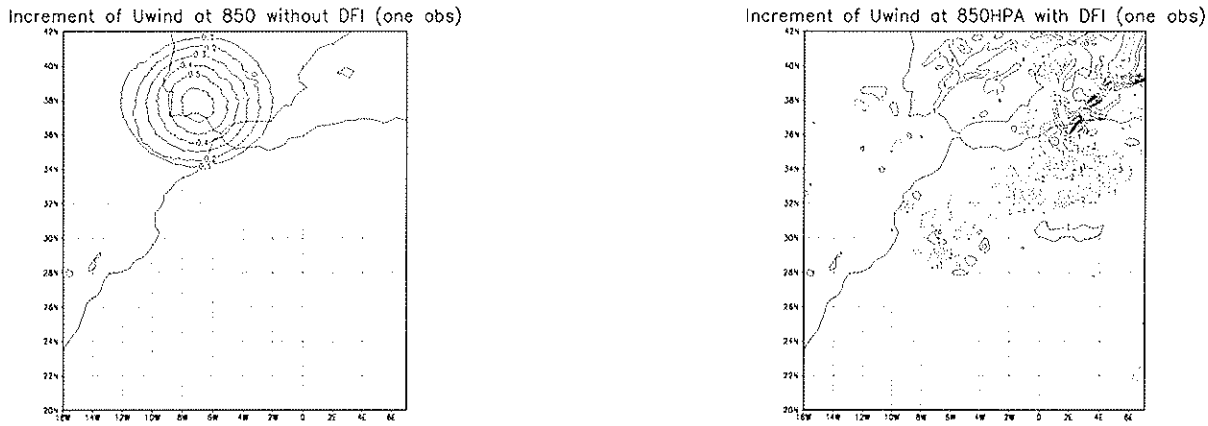

Figure 4. Increments of U wind at 850 hPa without (left) and with (right) DFI.

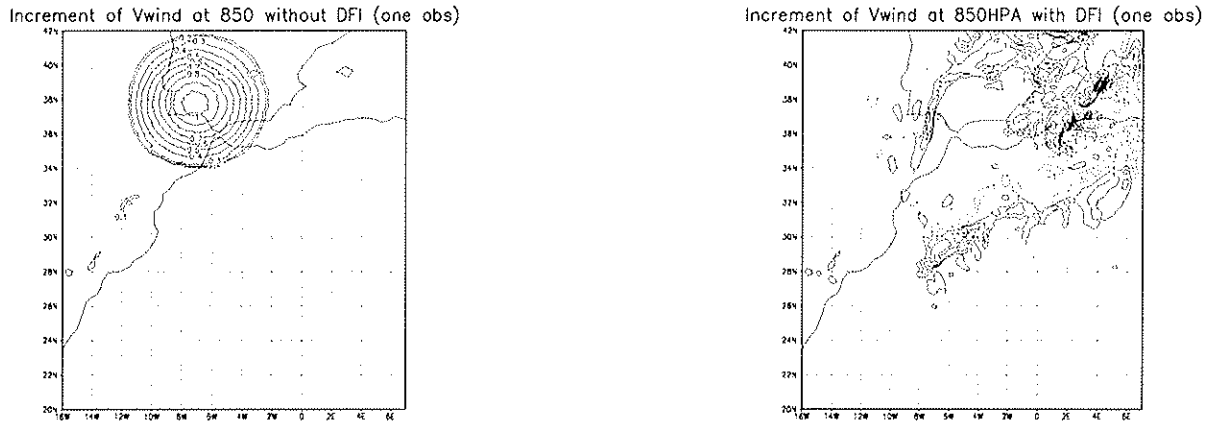

Figure 5. Increments of V wind at 850 hPa without (left) and with (right) DFI

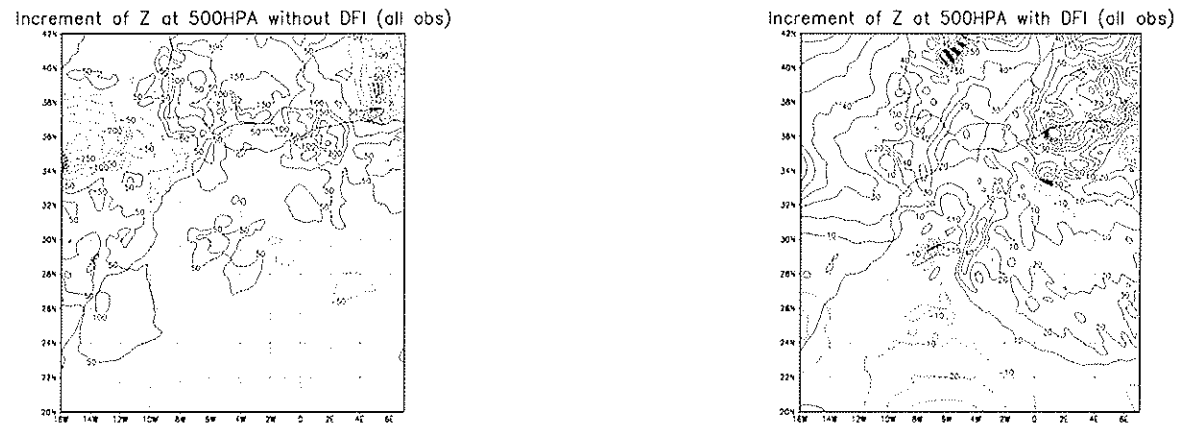

Figure 6. Increments of geopotential at 500 hPa without (left) and with (right) DFI; experiments with a full observation file.

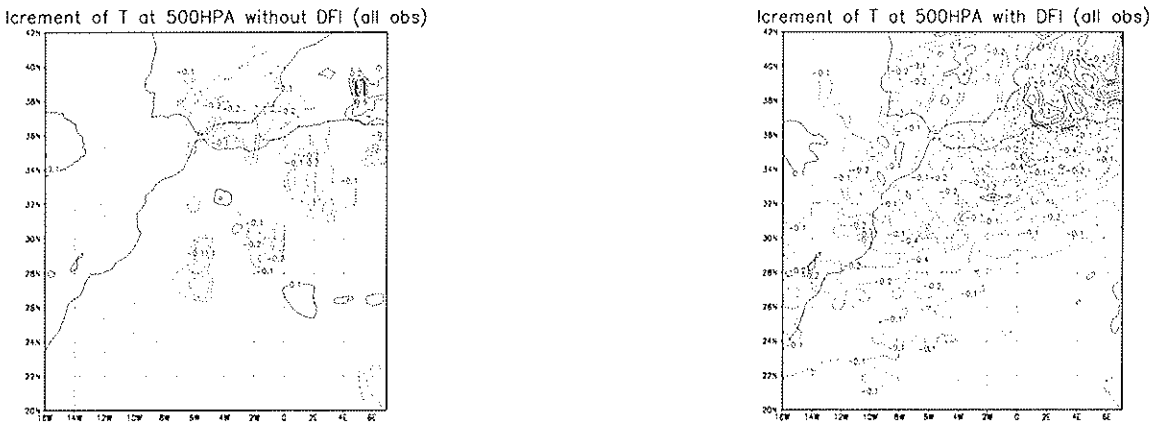

Figure 7. Increments of temperature at 500 hPa without (left) and with (right) DFI; experiments with a full observation file.

Computation of background error covariances over the Hungarian domain: sensitivity studies using the lagged-NMC method

Gergely Boloni (*boloni.g@met.hu*) - Andras Horanyi (*horanyi.a@met.hu*)

Computation of background error covariances is required in the context of data assimilation in order to estimate the solidity of first guess information obtained by an earlier model forecast. As in many NWP models, in ALADIN as well the NMC method was proposed to be used for the definition of background errors, that is based on two forecasts with different range (typically 36 and 12 hours) but valid for the same time. The background error statistics are computed then on the differences of the two forecasts accumulated for a few months (typically 3). After the first computations it turned out that the NMC method (originally used in global models) doesn't work efficiently on those smaller scales which are represented in ALADIN, rather on larger scales already treated by ARPEGE analysis. Accordingly, some efforts were made to modify the method in order to increase its efficiency on smaller scales. Finally the so called lagged-NMC method was found convenient to derive mesoscale background error statistics (Siroka at al., 2001). The lagged-NMC method is very similar to the original one (standard-NMC) described above with the modification that the lateral boundary conditions are exactly the same for the two forecasts taking part in the computation of departures. Consequently, providing the forecast differences, the large-scale information are diminished giving a relatively bigger weight to smaller scales. In 2000-2001 both standard and lagged background error statistics were computed in Budapest for the Hungarian domain of ALADIN (ALADIN/HU). Computation of standard statistics gave very similar results comparing to those obtained over other ALADIN domains. Using the lagged method a sensitivity study was also performed, that is exploring the sensitivity of background error statistics to the forecast range and to the difference of forecast ranges used in the NMC method. It means that not only 36h-12h, but all possible combination of forecast differences were created and accumulated as a base of the statistics. As the model is integrated until 48 hours the forecast range can vary between 6 and 48 hours and the difference between them from 6 to 42 hours. The main goal of this study was to choose the optimal statistics for the 3d-var scheme used in ALADIN and also to obtain some information about the predictability properties of the model. Several theoretical conclusions were made concerning the efficiency of the different statistics mainly based on the analysis of variance spectra (Horanyi and Boloni, 2001), however, running single observation experiments, it became clear that the lagged-NMC method is not as powerful in the case of ALADIN/HU as it was shown for ALADIN/LACE. We have the feeling that it is the consequence of the small difference between the resolutions of ALADIN/HU and its driving model ALADIN/LACE, which leads to a strong impact of the coupling information even on smaller scales, which means a too strong error variance reduction in the context of lagged-NMC forecast differences. In order to get a preliminary information about the impact of ALADIN/LACE on ALADIN/HU through coupling, the parallel verification of the two models was carried out that gave very similar scores (Boloni, 2001), thus confirming the results of the single observation experiments.

References

(1) Siroka, M., C. Fischer, V. Cassé and J.-F. Geleyn, 2001: The definition of mesoscale selective forecast error covariances for a limited area variational analysis. *Meteor. Atmos. Phys.* special issue of the SRNWP Workshop on high resolution modelling, Offenbach, 25-27/10/1999, Submitted.

(2) Horanyi, A. and G. Boloni, 2001: Lagged constant coupling background error statistics: preliminary results for the ALADIN/HU model. *Proceedings of the 10th ALADIN workshop "on scientific developments"*, 7-8 June 2001, pp. 113-119.

(3) Boloni, G., 2001: Further experiments with the combination of 3DVAR and blending by DFI: tests using incremental digital filter. *RC LACE internal report.* Available from the author.

Stabilization of NH dynamics - some underlying ideas

J. Masek (*SHMI*)

1. Introduction

Common goal of NWP models is to predict evolution of atmosphere given by set of nonlinear partial differential equations. However, it is not possible to work with continuous representation. Models have to be discretised both in space and time. Aim of this short article is to illustrate some basic ideas and assumptions which are used in effort to stabilize NH dynamics.

Three different temporal schemes will be described: leapfrog, semi-implicit (SI) and fully implicit, known also as predictor--corrector (PC). Current effort in ALADIN non-hydrostatic dynamics is to implement PC scheme. It was shown experimentally that SI correction, which works well in hydrostatic model, is not sufficient for NH dynamics. Instability of NH model was partially reduced by implicit treatment of complete 3D divergence, not only its linear part. This treatment requires iterations (`NSITER` scheme). Positive impact on stability indicates that implicit treatment of complete nonlinear model might stabilize NH dynamics. Recently it was recognized that change of prognostic variables can have strong impact on model stability. This opened a new way which can contribute to stabilization of NH dynamics.

Symbolical notation will be used. Spatially discretised state of atmosphere can be represented by column vector $\mathbf{x} \in \mathbf{R}^n$. In finite difference model vector $\mathbf{x}$ contains grid point values of all prognostic fields. In spectral model it contains spectral coefficients instead of gridpoint values. All admissible vectors $\mathbf{x}$ form the phase space. Temporal evolution is described by phase trajectory $\mathbf{x}(t)$. It is determined by equation:

$$\frac{d\mathbf{x}(t)}{dt} = M(\mathbf{x}(t)) \qquad (1)$$
$$\mathbf{x}(t_0) = \mathbf{x}_0$$

Vector $\mathbf{x}_0$ represents initial state. Operator $M : \mathbf{R}^n \rightarrow \mathbf{R}^n$ is nonlinear. For autonomous systems it does not depend on t. It can be interpreted as a vector field on phase space. Integral curves of this field are phase trajectories.

2. Temporal discretisation - from leapfrog to fully implicit

Equation (1) still have to be discretised in time. Standard notation will be used for this purpose:

$$\mathbf{x}^+ = \mathbf{x}(t+\Delta t) \qquad \mathbf{x}^0 = \mathbf{x}(t) \qquad \mathbf{x}^- = \mathbf{x}(t-\Delta t)$$

One common scheme used in NWP is leapfrog:

$$\frac{\mathbf{x}^+ - \mathbf{x}^-}{2\,\Delta t} = M(\mathbf{x}^0) \qquad (2)$$

It is an explicit 3-time-level scheme. The state $\mathbf{x}^+$ can be expressed as:

$$\mathbf{x}^+ = \mathbf{x}^- + 2\,\Delta t\; M(\mathbf{x}^0) \qquad (3)$$

Another scheme is fully implicit scheme. It can be obtained from equation (2) by time averaging the right hand side:

$$\frac{\mathbf{x}^+ - \mathbf{x}^-}{2\,\Delta t} = \frac{M(\mathbf{x}^+) + M(\mathbf{x}^-)}{2} \tag{4}$$

Fully implicit scheme is a 2-time-level scheme, because $\mathbf{x}^0$ disappeared from equation (4). It can be rearranged into the form:

$$(\mathbf{I} - \Delta t\, M)\, \mathbf{x}^+ = (\mathbf{I} + \Delta t\, M)\, \mathbf{x}^- \tag{5}$$

It can be seen from equation (5) that evaluation of $\mathbf{x}^+$ requires inversion of operator $(\mathbf{I} - \Delta t\, M)$. But since operator M is nonlinear, equation (5) must be solved iteratively. This can be done using predictor--corrector algorithm.

A step between leapfrog and fully implicit scheme is so-called semi-implicit scheme (SI). Basic idea is to linearize operator M at suitably chosen stationary state $\mathbf{x}^*$ and split right hand side of (2) into linear part and nonlinear residual. Linear part is treated implicitly, nonlinear residual explicitly:

$$\mathbf{L} = M'(\mathbf{x}^*) \qquad M(\mathbf{x}^*) = 0$$

$$\frac{\mathbf{x}^+ - \mathbf{x}^-}{2\,\Delta t} = \frac{\mathbf{L}\mathbf{x}^+ + \mathbf{L}\mathbf{x}^-}{2} + (M - \mathbf{L})\mathbf{x}^0 \tag{6}$$

Equation (6) can be manipulated into the form:

$$(\mathbf{I} - \Delta t\, \mathbf{L})\, \mathbf{x}^+ = (\mathbf{I} + \Delta t\, \mathbf{L})\, \mathbf{x}^- + 2\,\Delta t\, (M - \mathbf{L})\, \mathbf{x}^0 \tag{7}$$

Evaluation of $\mathbf{x}^+$ from equation (7) requires inversion of matrix $(\mathbf{I} - \Delta t\, \mathbf{L})$. If operator M was linear, it would be equal to its linearization $\mathbf{L}$ and equations (5), (7) would be identical. It means that in linear case SI scheme is equivalent to fully implicit scheme.

As was mentioned in introduction, results from numerical experiments indicate that fully implicit scheme is better than SI scheme which is better than leapfrog. All three schemes are of second order accuracy, so where does this difference comes from ? Answer is far from trivial, because considered system is nonlinear. At least some indication can be obtained by examination of linear system:

$$\frac{d\mathbf{x}(t)}{dt} = \mathbf{L}\mathbf{x}(t) \tag{8}$$

However, in this case there are only 2 different schemes to study because SI scheme is identical to fully implicit scheme. Analysis of linear system leads to following results:

- If system (8) has a neutral mode, corresponding modes of leapfrog scheme and fully implicit scheme are also neutral. (For leapfrog this is true only conditionally, Δt must be smaller than some critical value.) Both schemes introduce only phase error for such mode. Leapfrog scheme is accelerating, fully implicit scheme is decelerating (figure 1) .
- Since leapfrog is a 3-time-level scheme, computational mode exists. For practical usability time filter must be applied. It strongly damps computational mode, but introduces some damping also for physical mode. This violates desirable property from previous point.

  Fully implicit scheme is a 2-time-level scheme, so only physical mode exists. Time filter is not needed.
- If there exists a quadratic invariant for system (8), i.e. such non-zero symmetric matrix $\mathbf{G}$ that

$$\frac{d}{dt}\left[\mathbf{x}^{\mathrm{T}}(t)\, \mathbf{G}\, \mathbf{x}(t)\right] = 0,$$

  this invariant is conserved by fully implicit scheme.

It can be seen from given points that at least in linear case there are some advantages of fully implicit scheme over leapfrog scheme.

3. Choice of prognostic variables -- impact to stability

Evolution of atmosphere as a dynamical system has geometric nature. It does not depend on choice of prognostic variables. These variables plays a role of coordinates in phase space and can be chosen in infinitely many ways.

Situation changes when continuous system is discretised and approximate solution is constructed. Same numerical scheme applied in different coordinates can lead to different results. Choice of prognostic variables can affect qualitative behaviour of approximate solution. This can be illustrated on simple example. Consider following continuous system (phase space is $\mathbf{R}^2$):

$$\begin{aligned} \partial_t x &= -\omega y \\ \partial_t y &= \omega x \\ \omega &\neq 0 \end{aligned} \qquad (9)$$

It can be verified easily that distance from origin $r \equiv \sqrt{(x^2+y^2)}$ is conserved during system's evolution. Phase trajectories are circles centred at origin. Application of leapfrog scheme to equations (9) gives:

$$\begin{aligned} x^+ &= x^- - 2\omega\Delta t\, y^0 \\ y^+ &= y^- + 2\omega\Delta t\, x^0 \\ \Delta t &> 0 \end{aligned} \qquad (10)$$

System (10) can be analysed using standard techniques. There are 2 physical and 2 computational modes. Final form of physical solution is :

$$\mathbf{x}^+ = \mathbf{R}\mathbf{x}^0 \qquad \mathbf{x}^0 = \mathbf{R}\mathbf{x}^-$$

$$\mathbf{x} \equiv \begin{pmatrix} x \\ y \end{pmatrix} \qquad \mathbf{R} = \begin{pmatrix} \sqrt{1-(\omega\Delta t)^2} & -\omega\Delta t \\ \omega\Delta t & \sqrt{1-(\omega\Delta t)^2} \end{pmatrix} \qquad (11)$$

$$|\omega\Delta t| \leq 1$$

Matrix $\mathbf{R}$ is orthogonal ($\mathbf{R}^T\mathbf{R} = 0$), it corresponds to rotation by angle $\theta = \arcsin(\omega\Delta t)$. Distance from origin r is therefore conserved by system (10) :

$$r^2 = x^2+y^2 = \mathbf{x}^T\mathbf{x}$$

$$(\mathbf{x}^+)^T\mathbf{x}^+ = (\mathbf{R}\mathbf{x}^0)^T\mathbf{R}\mathbf{x}^0 = (\mathbf{x}^0)^T\mathbf{R}^T\mathbf{R}\mathbf{x}^0 = (\mathbf{x}^0)^T\mathbf{x}^0$$

$$r^+ = r^0 \qquad (12)$$

It is clear from equation (12) that leapfrog scheme applied in coordinates (x, y) is neutral, so it reproduces qualitative behaviour of continuous system (10). There is only phase error introduced, scheme is accelerating with factor $\arcsin(\omega\Delta t) / (\omega\Delta t)$ (figure 2).

New coordinates (ρ, θ) can be introduced now. They are defined on $\mathbf{R}^2$ without half-line "$y = 0, x \geq 0$" :

$$\begin{aligned} x &= \rho e^{\theta} \cos\theta \qquad \rho > 0 \\ y &= \rho e^{\theta} \sin\theta \qquad \theta \in [0, 2\pi] \\ r &= \sqrt{x^2+y^2} = \rho e^{\theta} \end{aligned}$$

System (9) rewritten into coordinates (ρ, θ) has the form:

$$\begin{aligned} \partial_t \rho &= -\omega\rho \\ \partial_t \theta &= \omega \end{aligned} \qquad (13)$$

Application of leapfrog scheme to equations (13) gives :

$$\rho^{+} = \rho^{-} - 2\omega\Delta t\, \rho^{0} \tag{14}$$

$$\theta^{+} = \theta^{-} + 2\omega\Delta t \tag{15}$$

Equations (14), (15) are uncoupled, so they can be analysed independently. Modes of equation (14) will be find first :

$$\rho^{+} = \lambda\rho^{0} \qquad \rho^{0} = \lambda\rho^{-}$$

$$\lambda^{2} + 2\omega\Delta t\, \lambda - 1 = 0$$

$$\lambda_{1,2} = \pm\sqrt{1 + (\omega\Delta t)^{2}} - \omega\Delta t \tag{16}$$

Root λ_1 represents physical mode ($\lambda_1 \to 1$ for $\Delta t \to 0$), root λ_2 represents computational mode ($\lambda_2 \to -1$ for $\Delta t \to 0$).

As for equation (15), solution on even time levels (t, $t+2\Delta t$, $t+4\Delta t$, ...) is completely separated from solution on odd time levels ($t+\Delta t$, $t+3\Delta t$, $t+5\Delta t$, ...). For physical mode separation between θ^{+} and θ^{0} is the same as between θ^{0} and θ^{-} :

$$\theta^{+} - \theta^{0} = \theta^{0} - \theta^{-}$$

$$\theta^{0} = \tfrac{1}{2}(\theta^{+} + \theta^{-})$$

In conjunction with (15) this gives :

$$\theta^{+} = \theta^{0} + \omega\Delta t \tag{17}$$

Combination of relations (16), (17) leads to following result for physical mode :

$$r^{+} = \rho^{+} e^{\theta^{+}} = \lambda_1\, \rho^{0} e^{\theta^{0} + \omega\Delta t} = \lambda_1\, \rho^{0} e^{\theta^{0}} e^{\omega\Delta t} = \lambda_1 e^{\omega\Delta t}\, r^{0}$$

$$r^{+} = \left(\sqrt{1 + (\omega\Delta t)^{2}} - \omega\Delta t\right) e^{\omega\Delta t}\, r^{0} \tag{18}$$

Amplification factor (18) is less than one for $\omega\Delta t < 0$ and greater than one for $\omega\Delta t > 0$ (figure 3). This means that application of leapfrog scheme in coordinates (ρ, θ) leads to damping for $\omega < 0$ and to unstable behaviour for $\omega > 0$.

It can be concluded from given example that choice of prognostic variables can influence qualitative behaviour of numerical scheme. However instability introduced by variables (ρ, θ) is very weak. Power expansion of amplification factor in equation (18) for small Δt gives :

$$r^{+} = \left(1 + \frac{(\omega\Delta t)^{3}}{6} + \ldots\right) r^{0} \tag{19}$$

It means that pathological behaviour for studied second order accurate scheme occurred at third order terms in Δt. This is not a problem for NWP, where correct behaviour up to second order terms is sufficient. However, studied system was too simple. In more complicated systems like Eulerian equations pathological behaviour can occur at second order terms. It might be caused by improperly chosen prognostic variables. Effort to find more stable NH prognostic variables is based on this fact. First experimental results indicate that there might be some better candidates than original pair.

5. Conclusions

Following facts have been illustrated:

- In linear case fully implicit scheme has some advantages over leapfrog scheme. It is believed that it could perform better also in nonlinear case, but it is not easy to give theoretical arguments for this.
- Nonlinear transformation of prognostic variables does not commute with temporal discretisation. Choice of variables can affect qualitative behaviour of discretised system. It was shown on elementary example that neutral behaviour can be changed to damping or unstable, but for second-order accurate scheme the amplification error is of third order, which is not interesting in NWP context. However, in more complicated systems instability due to choice of variables can occur at second order terms. So there is some chance that suitably chosen prognostic variables might stabilize (at least partially) NH dynamics.

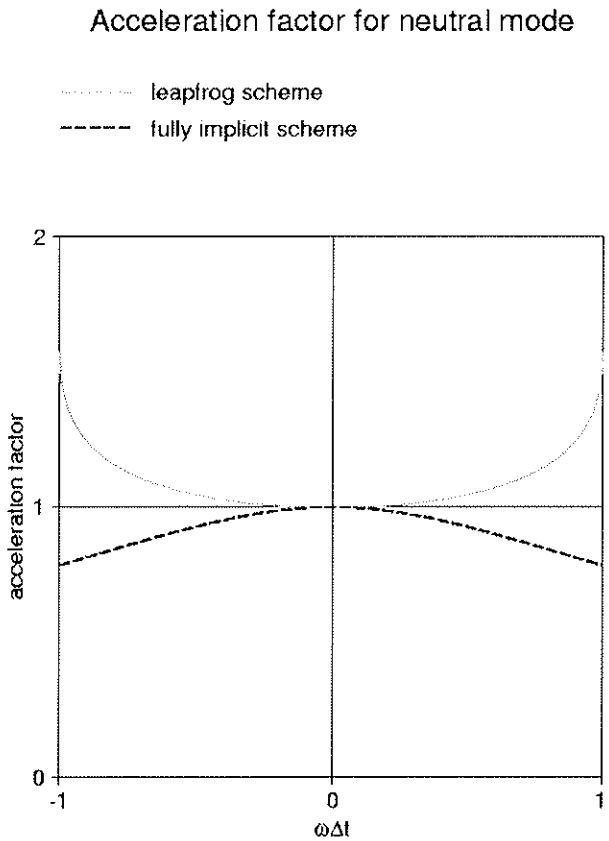

Figure 1.

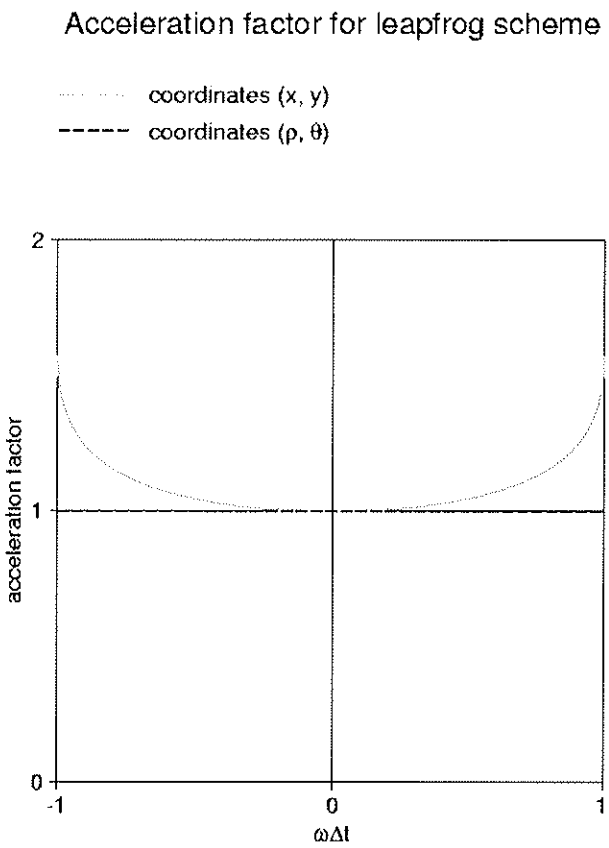
Acceleration factor for leapfrog scheme
coordinates (x, y)
coordinates (ρ, θ)
acceleration factor
2
1
0
-1
0
1
ωΔt

Figure 2

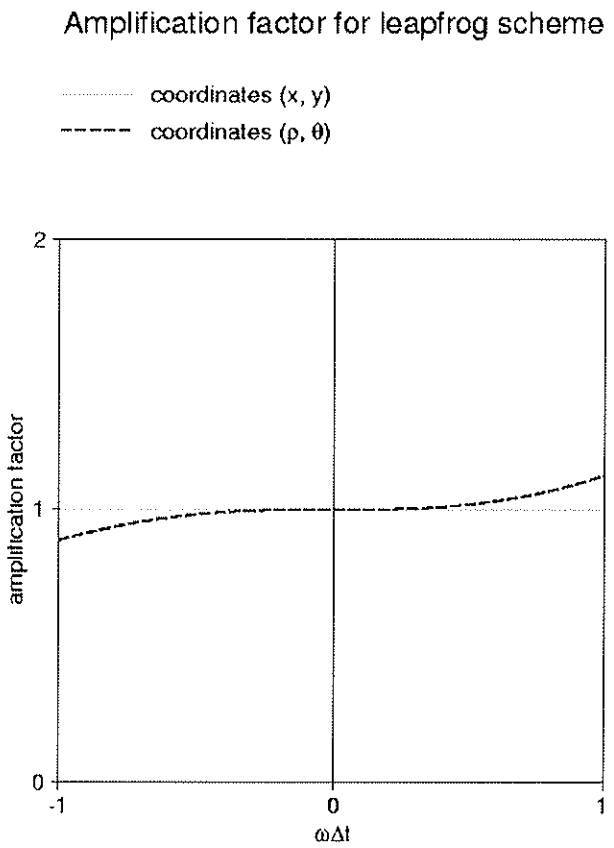
Amplification factor for leapfrog scheme
coordinates (x, y)
coordinates (ρ, θ)
amplification factor
2
1
0
-1
0
1
ωΔt

Effective roughness length in ALADIN

P. Nomérange
Royal Meteorological Institute of Belgium
Avenue Circulaire, 3
B-1180 BRUXELLES

December 18, 2001

1 Introduction

Due to the limited amount of computer power and storage space, horizontal spatial resolution of most NWP models has been limited to a few tens of kilometers or a few kilometers for the mesoscale limited area models as ALADIN.

This limitation is the source of some trouble in representing a correct view of the surface topography in the areas covered by NWP models since a lone value every 10 kilometers or so is far from sufficient to give a correct representation of the ground height profile in most areas.

While such a representation might be sufficient over flat terrain (plains, lakes, seas,...), mountainous areas are almost always a succession of high peaks and low valleys with very fast variations from one to the other, with a characteristic length of variation far smaller than the grid spacing of most NWP models. Most features of the topography are so lost when ground height is modelled by a lone value every 10 kilometer or so.

Resolved mountain ranges in most NWP models appear as solid barriers to the atmospheric flow, with maximum height being far smaller than the real maximum peak height found in the range and without any possibility for the wind to follow valleys or turn around the highest ridges.

While the problem of insufficient peak height can be easily solved by the so-called "envelope orography", which consists in adding the local standard deviation of ground height to the mean orography, the representation of "between peaks" currents must be adressed by other means, specifically parametrized subgrid-scale orography and processes.

2 The subgrid-scale orography in ALADIN

In order to add subgrid-scale orography information to the mean ground height data in each cell of an NWP model (and ALADIN in particular), additional parameters are computed from the high-resolution topography data sets that are available from radar satellites or other sources.

Those parameters are :

- the orography standard deviation, computed in each grid-cell of the model, gives an estimation of the variance between the highest and lowest ground in the cell, as well as their relative occurences.
- an orographic anisotropy factor, caracterising the kind of the subgrid-scale orography that can be found in every grid cell of the model : it tells us wether the subgrid-scale orography is mainly made of isolated peaks or ridge lines.
- the principal direction along which the subgrid-scale orographic features are oriented, that is mainly the orientation of the ridge lines present in each grid cell and that can not be resolved at the spatial resolution of the grid.

Those various parameters allows us to represent in each grid cell a pseudo-resolved local mountain whose height is given by the standard deviation of the orography, and which has an elliptical shape at the ground : it is oriented along the principal direction and its elongation is given by the anisotropy factor.

This new representation enables us to introduce a parametrization of some local effects that happen in the mountain ranges. Typically, this is the so-called "blocking effect", which is due to the fact that all of the air masses coming in contact with the mountains have not sufficient energy to climb the slopes and go over the highest ridges. Part of the air must then go around the peaks (through valleys for example) and is therefore slowed down much more than the air mass going above the ridge. The blocking effect is parametrized as an additionnal drag (called form drag) that is applied to the lower levels of the flow in mountainous areas.

The other effect that we can now introduce is the deviation of the wind due to the air mass going around the mountains. By analogy with aerodynamics, this effect is termed the lift effect and its parametrization has been the topic of a previous work.

3 The concepts of roughness length and effective roughness length

The influence of the ground on the momentum of the atmospheric flux is regulated through turbulent diffusion coefficients. Those coefficients are in turn computed from the so-called similarity theory, which assumes a logarithmic profile of wind speed near the ground. According to this theory, the variation of wind speed with altitude is given by :

$$\bar{U} = \frac{u_*}{\kappa} \ln \frac{z}{z_0}$$

where $\bar{U}$ is the average wind speed at altitude z, u_* is the square root of surface stress, also called friction velocity, κ is the Von Karman constant whose value is 0.4 and z_0 is the aerodynamic roughness length : the height at which wind speed becomes zero.

The existence of the roughness length is due to the fact that the surface of the Earth is not exactly flat but covered with *roughness elements* such as trees, buildings, hedges, ... As a consequence, the height at which the wind disappears is not ground level but is slightly higher. Depending on the nature of the ground covering, z_0 usually takes values fom 1 cm to 1 m.

Even if the logarithmic profile of wind is valid only in the planetary boundary layer, recent experiments and measurements suggest that such a profile also exists above steep orographic features and mountain ranges. This suggests that the subgrid-scale orographic features in NWP models can be treated as other very big roughness elements and the roughness length adapted consequently.

The enhanced roughness length has been called *effective roughness length* (z_0^{eff}) and could provide a way to represent the subgrid-scale orographic features without using the envelope orography. This hypothesis has been tested in the ALADIN model (which allows for the use of the envelope orography AND an effective roughness length at the same time) on a test case covering the Pyrénées.

4 The test case

The situation we have chosen to evaluate the effects of the effective roughness length on is the one on which the effects of the lift forces were tested in my previous work. The situation dates back to April 22^{nd}, 2000 at 12h UTC and the area of interest is the Pyrénées, between France and Spain.

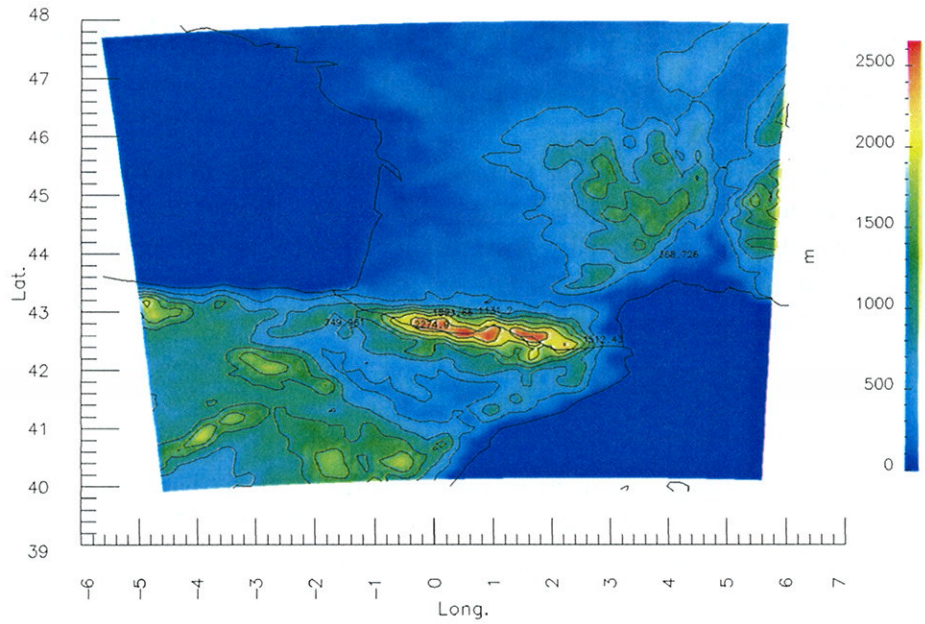

Figure 1: Original orography with envelope

The ALADIN model was used with the same 9.92 km horizontal resolution as the operationnal ALADIN-France configuration on a domain extending from 39.9^o to 47.9^o N latitude and from 4.6^o W to 6.0^o E longitude, thus covering France south of Britany and west of the Alps, the north-east part of Spain, the Bay of Biscay and part of the north-western Mediterranean Sea.

The orography (with envelope) and the original effective roughness length on the area are presented on figures 1 and 2. The orography has been extracted from Météo-France global data base at 2.5 km horizontal resolution. The effective roughness length was computed as a combination of the orographic variance at scales lower than 2.5 kilometers and of the variance at scales comprised between 2.5 kilometer and 9.92 kilometer resolutions according to the following formula :

$$z_0^{eff} = \alpha \left(\sqrt{\frac{n_1}{s_1}} v_1 + \sqrt{\frac{n_2}{s_2}} v_2 \right)$$

where the subscript 1 refers to the length scales smaller than 2.5 km and the subscript 2 refers to the length scales between 2.5 and 9.92 kilometers. n is the number of peaks in a grid cell of area s and v is the variance of orography in the grid-cell. The default value for the α parameter is set at 0.53.

The forecast on April 22nd, 2000 at 18h UTC was characterized by rather strong winds from the south all over the Pyrénées, thus creating an ideal

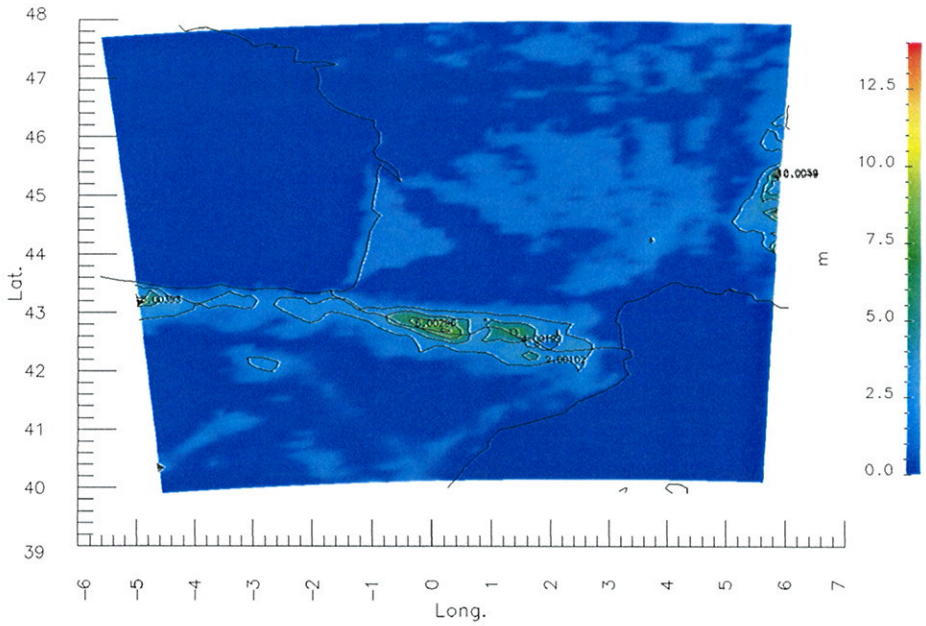

Figure 2: Original roughness length

situation for the study of orographic waves originating from these mountains. That situation is presented on figures 3, 4 and 5, respectively showing the low altitude winds and profiles of the potential temperature and the meridian wind at 0^o longitude.

The orographic gravity wave can clearly be seen on figure 4 between 3000 and 7000 m propagating downstream (north) from the mountains, as well as on figure 5 to the higher atmosphere. The wind pattern of figure 3 shows the dominant southern wind over the mountain range, followed by a northern wind just north of the Pyrénées. That is a typical sign of a recirculation loop, coupled with the existence of lee-side vortexes downstream of the ridges. The negative meridional winds can not be seen on the vertical profile since its vertical resolution is too coarse and the flow inversion layer is too shallow.

5 Experiments and results

In this section, I shall focus on the interactions between the use of an effective roughness length and the envelope orography. This was made possible by the fact that ALADIN is one of the only models to allow the simultaneous use of both an envelope orography and an effective roughness length. However, since a change in any of the two features means running a complete chain (that is : a 923 configuration to get the climatological files, an EE927 config-

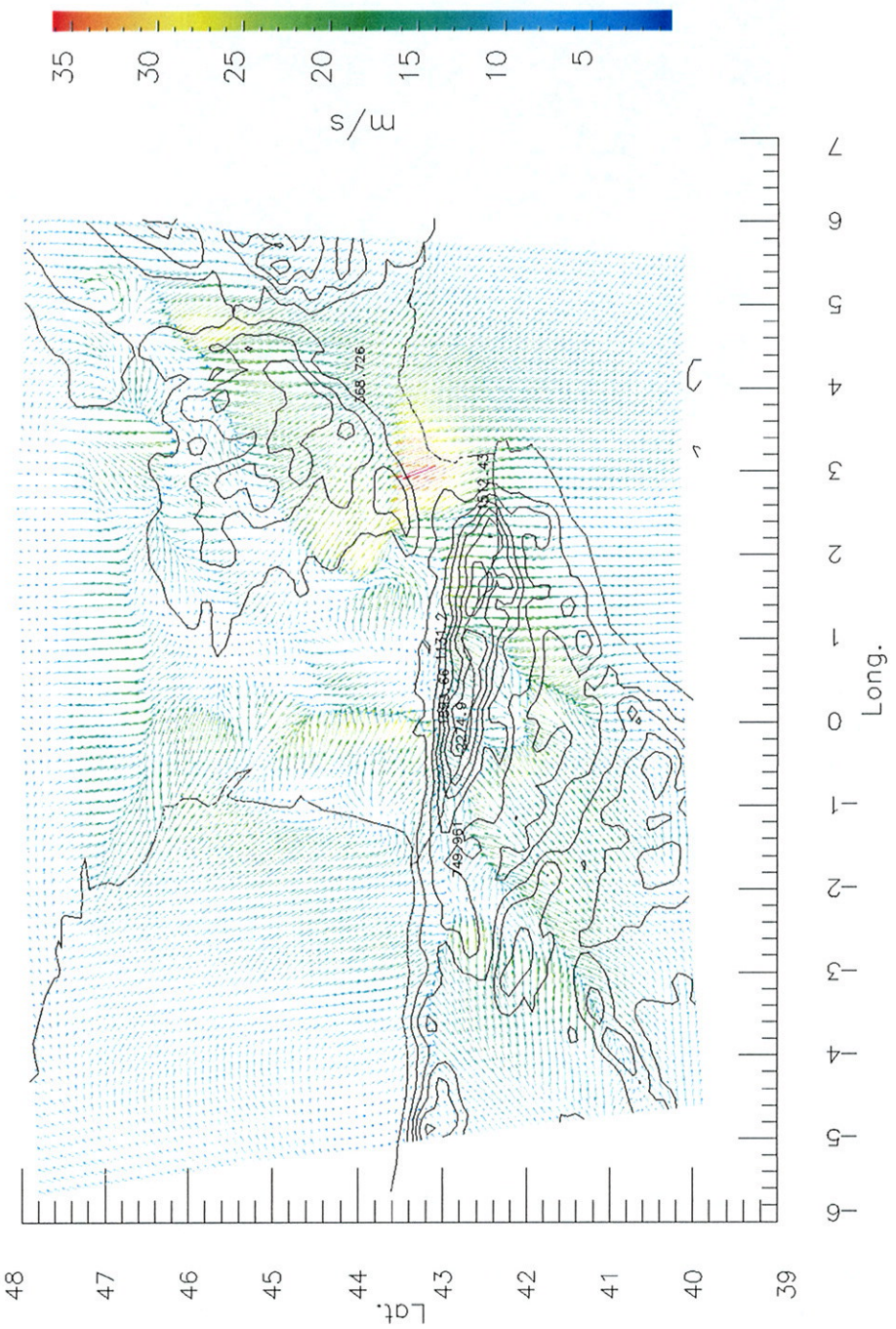

Figure 3: Low level wind field at 18 UTC, April 22^{nd}, 2000

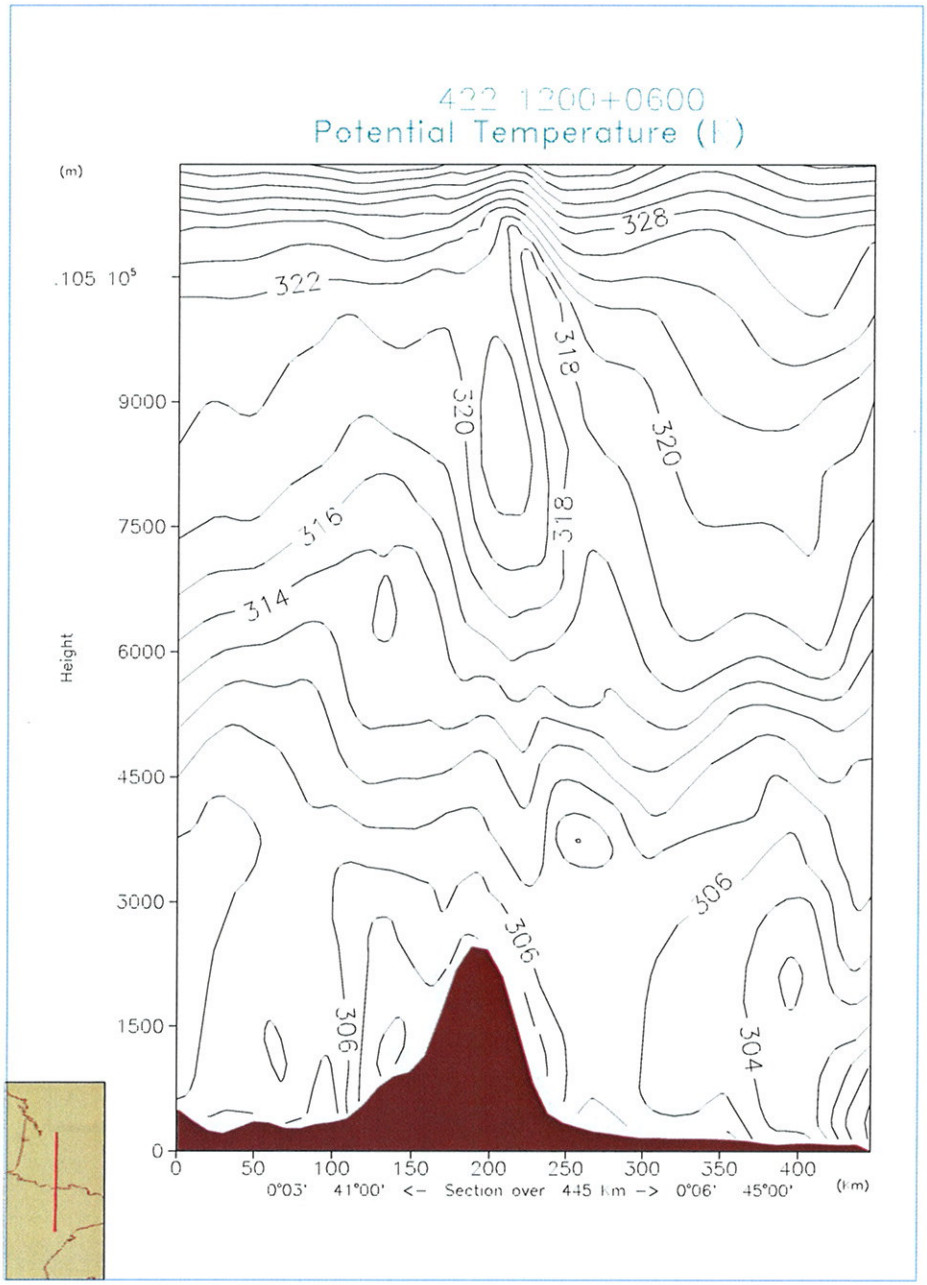

Figure 4: Potential temperature profile at 18 UTC, April 22^{nd}, 2000

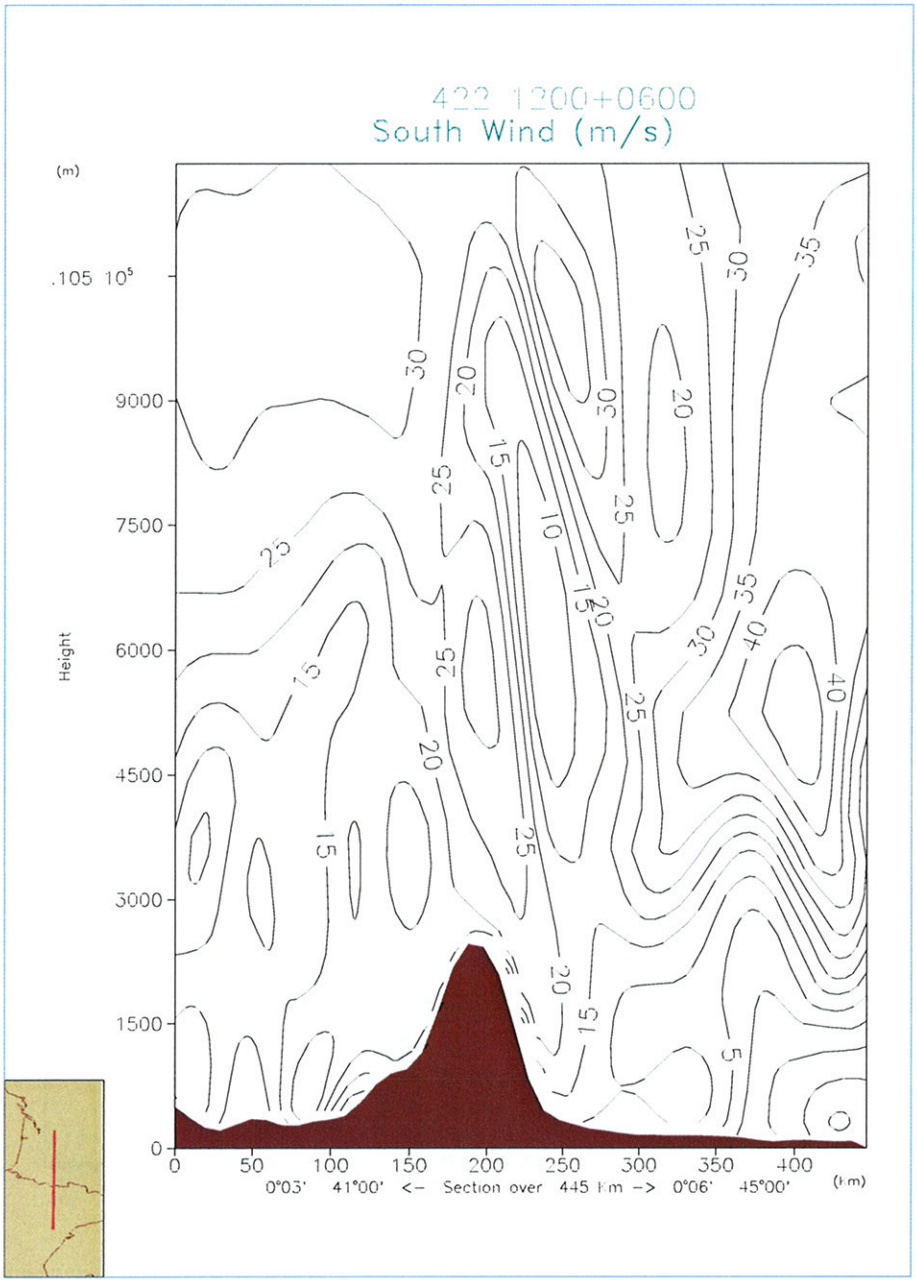

Figure 5: Meridional wind profile at 18 UTC, April 22^{nd}, 2000

uration to get the coupling files from the archived ALADIN-France runs, the forecast itself and the postprocessing), this is very expensive and unpractical and can not be done at will. I thus decided to investigate the cases of a doubled roughness length with envelope orography, the envelope orography alone without an effecetive roughness length and a standard roughness length (whose parameter α is fixed at 0.53) without envelope.

These situations have been compared from the points of view of the low-level wind, surface stresses and vertical profiles of potential temperature and across-mountain wind.

5.1 Potential temperature and across-ridge wind profiles

The following figures show the vertical cross-mountain potential temperature profiles we obtained with various combinations of effective roughness length and envelope orography. They are to be compared with figure 4.

- Figure 6 was obtained using the envelope orography but without effective roughness length. Its comparison with the default case (figure 4) clearly shows that the introduction of an effective roughness length smooths the amplitude of the orographic gravity wave triggered by the Pyrénées. This is the case at both high and low altitude and it can also be seen further downstream. Additionnally, the introduction of z_o^{eff} creates an area of quasi-neutral buoyancy on the lee side of the mountains some 70 kilometers downstream.

- If we increase the roughness length to double its standard value, as shown on figure 7, we see that, quite paradoxically, the gravity wave is reinforced at low levels when compared to the standard value. However, it is greatly weaker at higher altitudes and further downstream.

  In both cases, the upstream flow is almost not disturbed.

- If we now suppress the envelope orography but keep a standard value of the effective roughness length, we can see (on figure 8) that the addition of an envelope orography strengthen the gravity wave at each altitude and that it also has an effect on the flow upstream from the mountains. This is logical since the envelope orography is only an artificial rise of the model ground level, so making the ridges appear higher and steeper than they actually are.

The observations we have made here apply also to the comparisons of the cases without envelope and with no, standard or double roughness lengths.

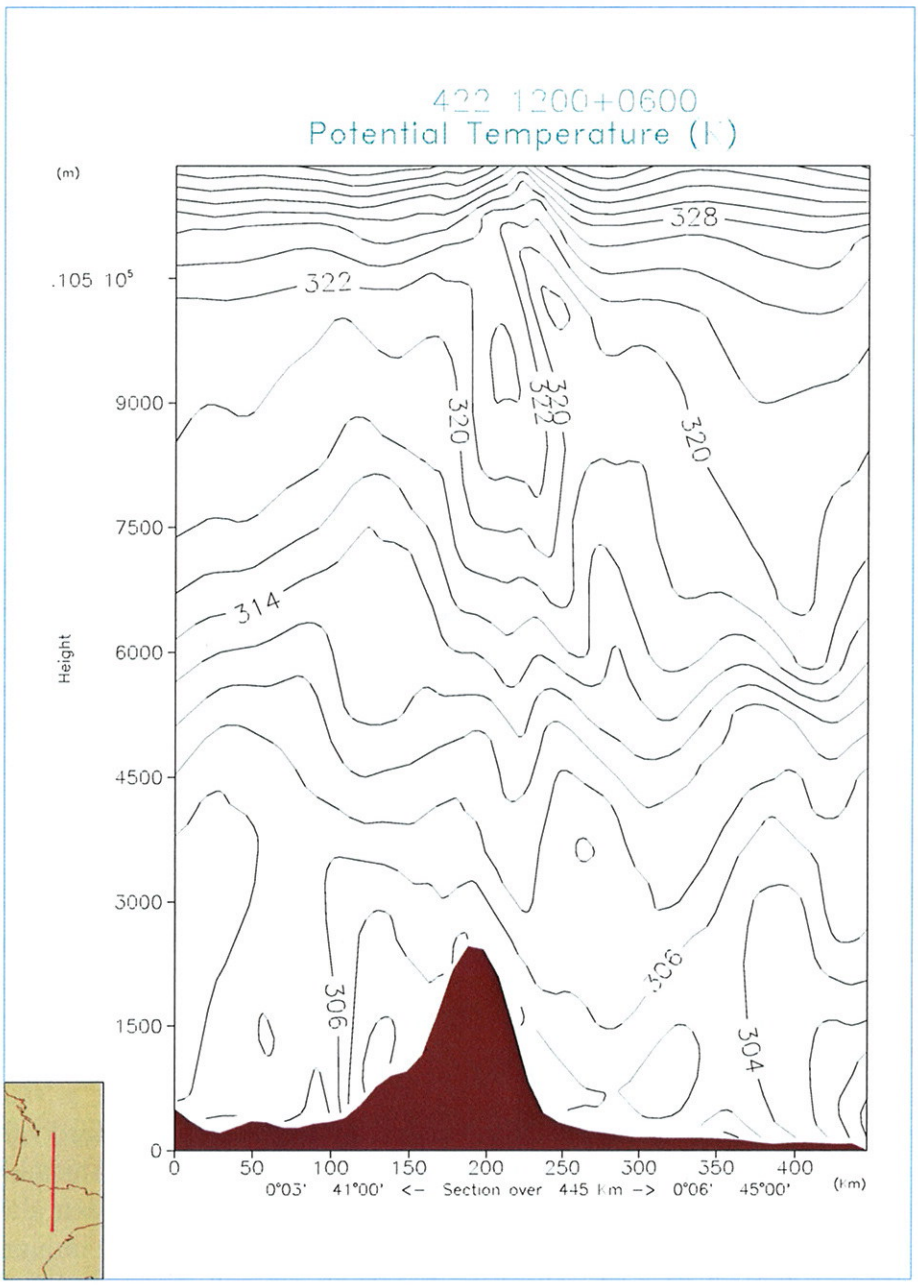

Figure 6: Potential temperature profile – No effective roughness length

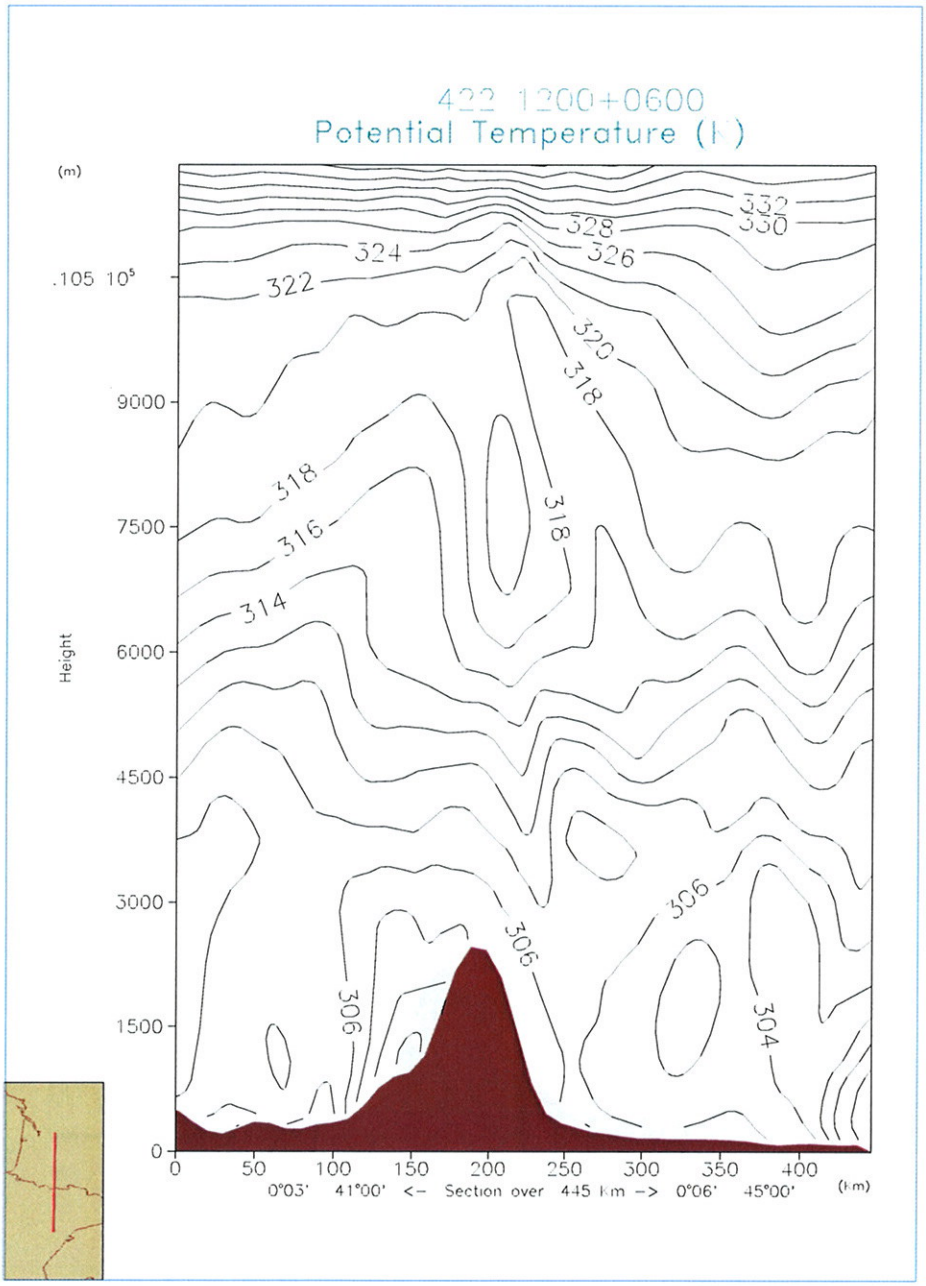

Figure 7: Potential temperature profile – Double roughness length

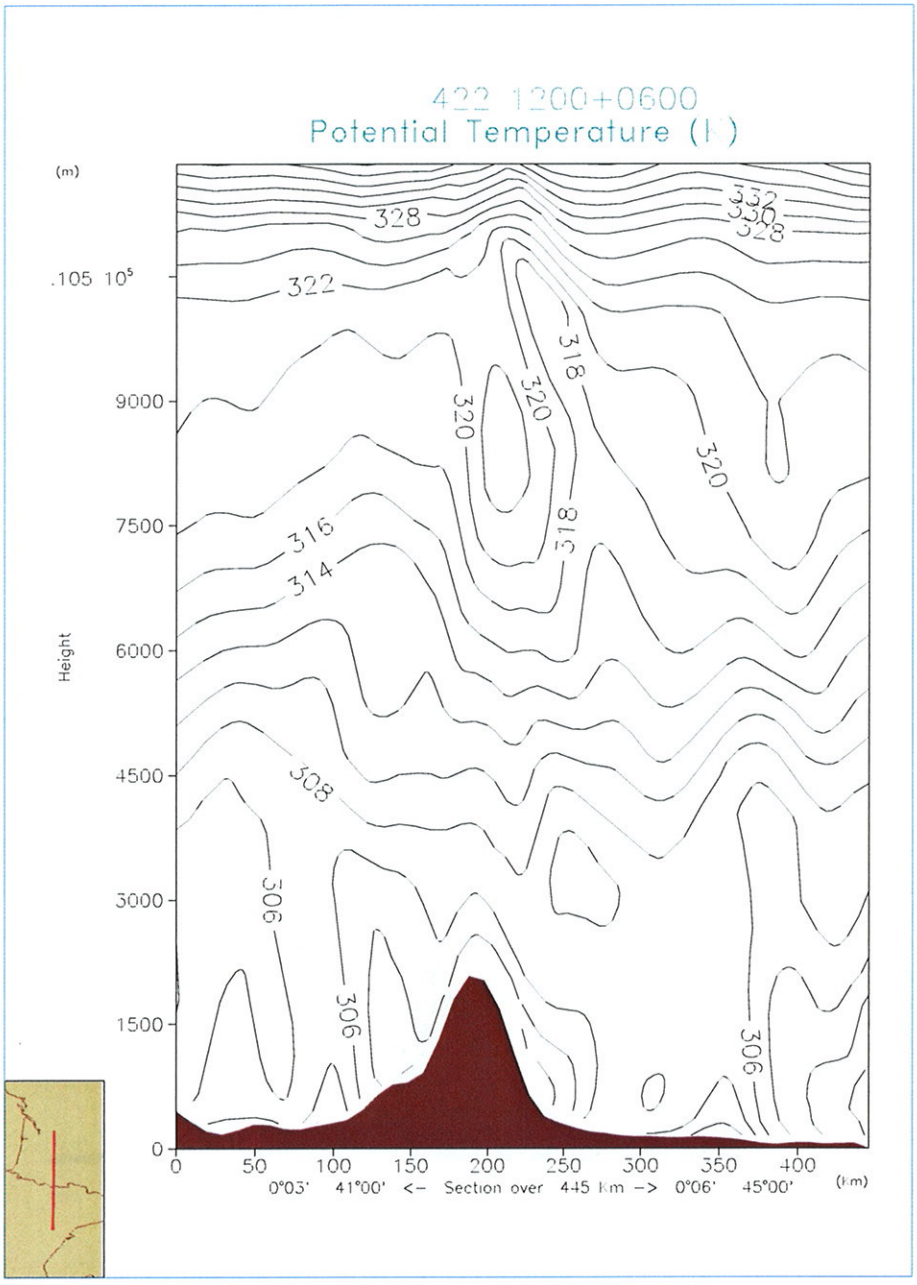

Figure 8: Potential temperature profile – No envelope

Looking now at the meridian wind profiles and comparing them with figure 5, we find that figures 9 to 11 illustrate that the envelope orography has still the effect of increasing the amplitude of the orographic wave, but now the influence of the variation of the roughness length is more regular. A continuous increase in the roughness length always has as a consequence the reduction of the amplitude of the gravity wave at all altitudes.

5.2 Low-level wind and surface stress

The differences in the low-level wind field due to the introduction of an effective roughness length are shown on figure 12. We can see that they are concentrated around the Pyrénées and in the areas of fast variation of wind speed or direction.

Close examination of the figure shows that, north of the Pyrénées, the roughness length's effect is to add a negative component to the windspeed, thus slowing down or reversing the wind on the lee side of the mountains. This, coupled with the neutral stability layer we already noted in the same area, points towards a boundary layer separation on the lee side of the mountain range.

If we double the roughness length, the same effects are reinforced near the Pyrénées but the differences in low-level wind are smaller than with the addition of a previously inexistent z_0^{eff}. Figure 13 illustrates this.

The variations of the surface stresses at the interface between the ground surface and the atmosphere that are due to the introduction of an effective roughness length are localised where this introduction is most important, above the mountainous areas. Indeed, figures 14 and 15, presenting the variations of surface stress due to the introduction and doubling of z_0^{eff}, show that those variations are not negligible only above the Pyrénées and some locations near the Spanish coasts.

6 Conclusions and perspectives

As had already been shown using other models and on other situations, the addition of an effective roughness length in NWP models in order to represent subgrid-scale orography as a collection of surface roughness elements has the effect of reducing the amplitude of the gravity wave triggered by the mountains. This smoothing is observable at all altitudes above the mountain range as well as downstream from it.

Additionnally, the introduction of an enhanced roughness seems to facilitate the separation of the boundary layer on the lee side of the Pyrénées and

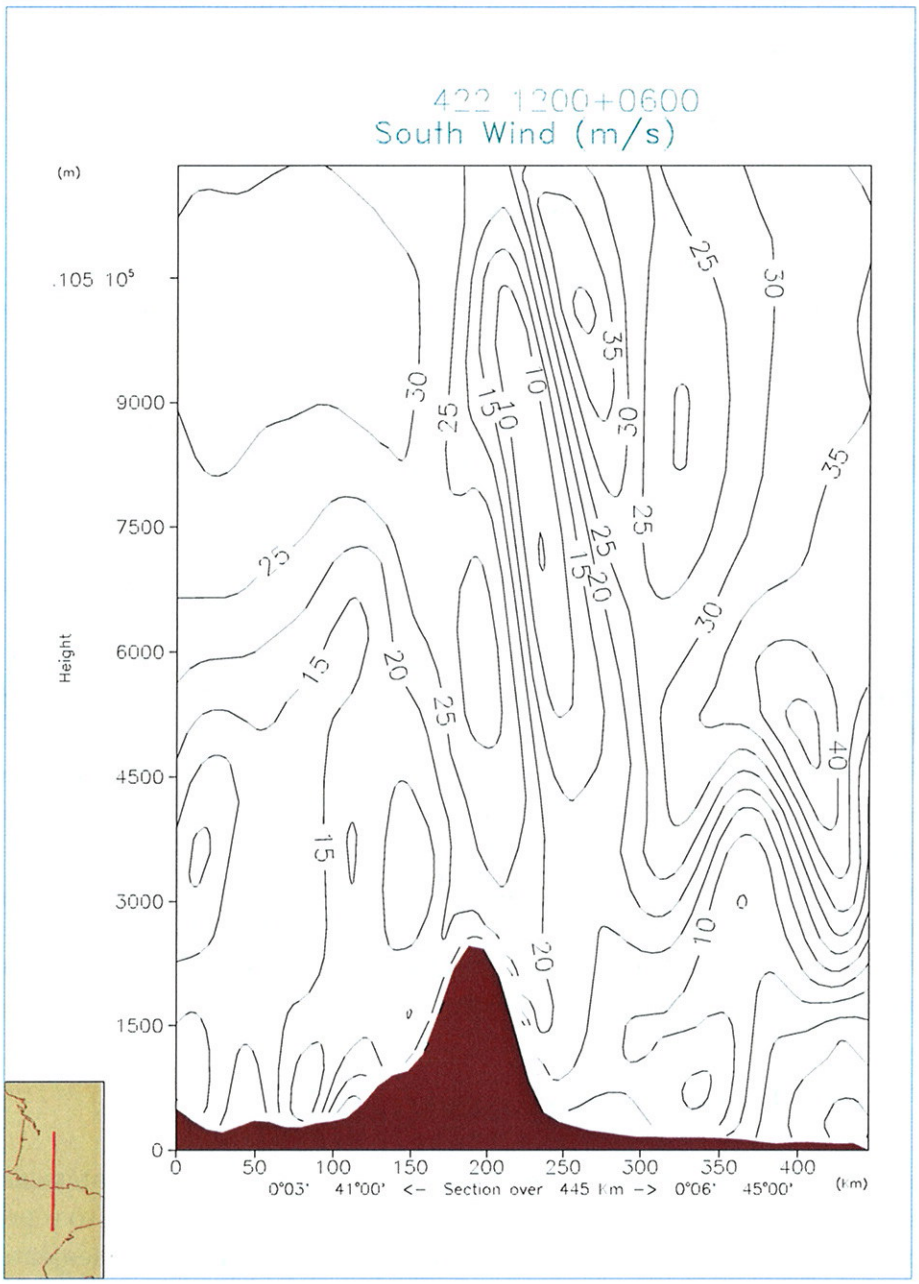

Figure 9: Meridional wind profile – No effective roughness length

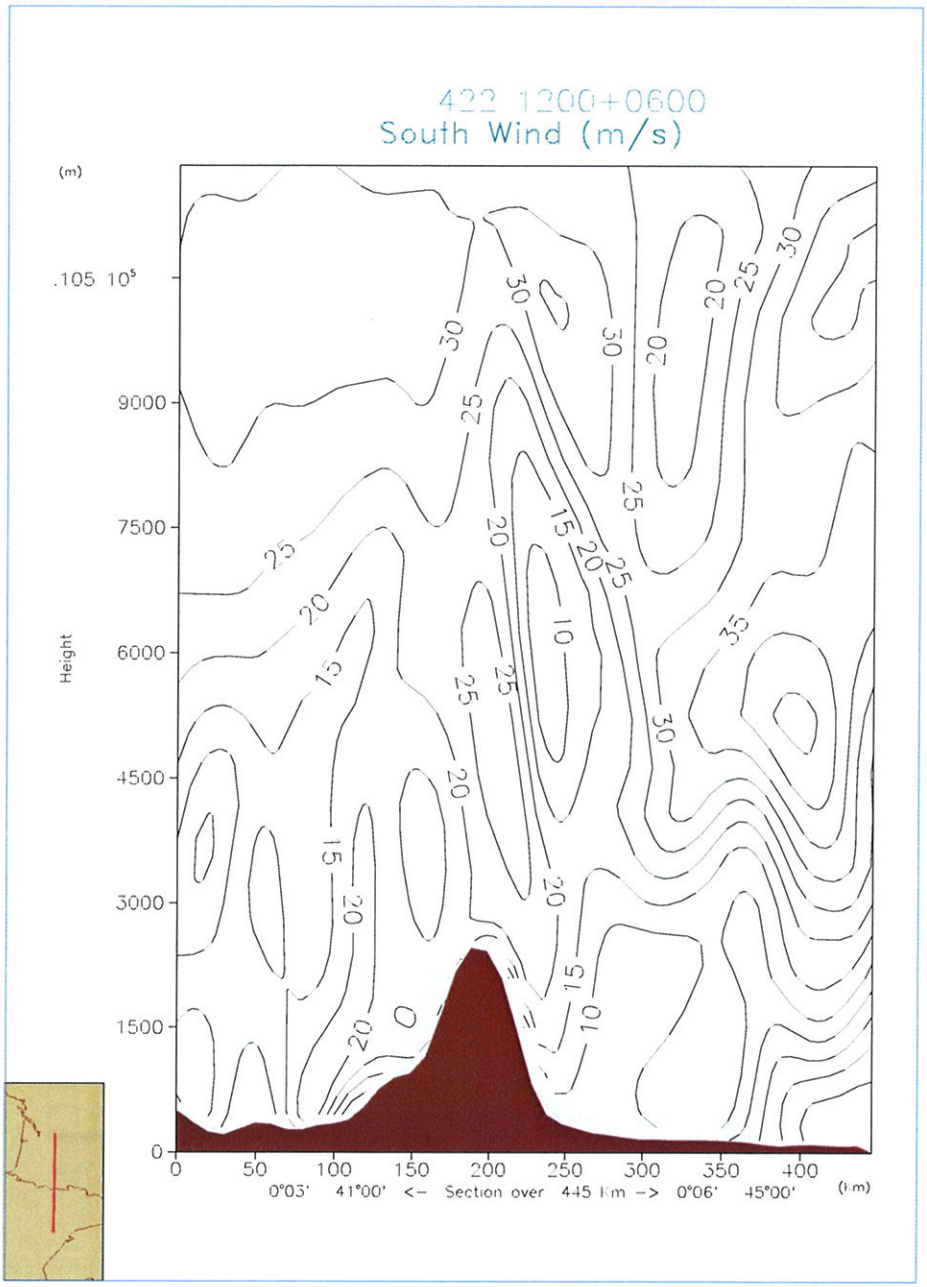

Figure 10: Meridional wind profile – Double effective roughness length

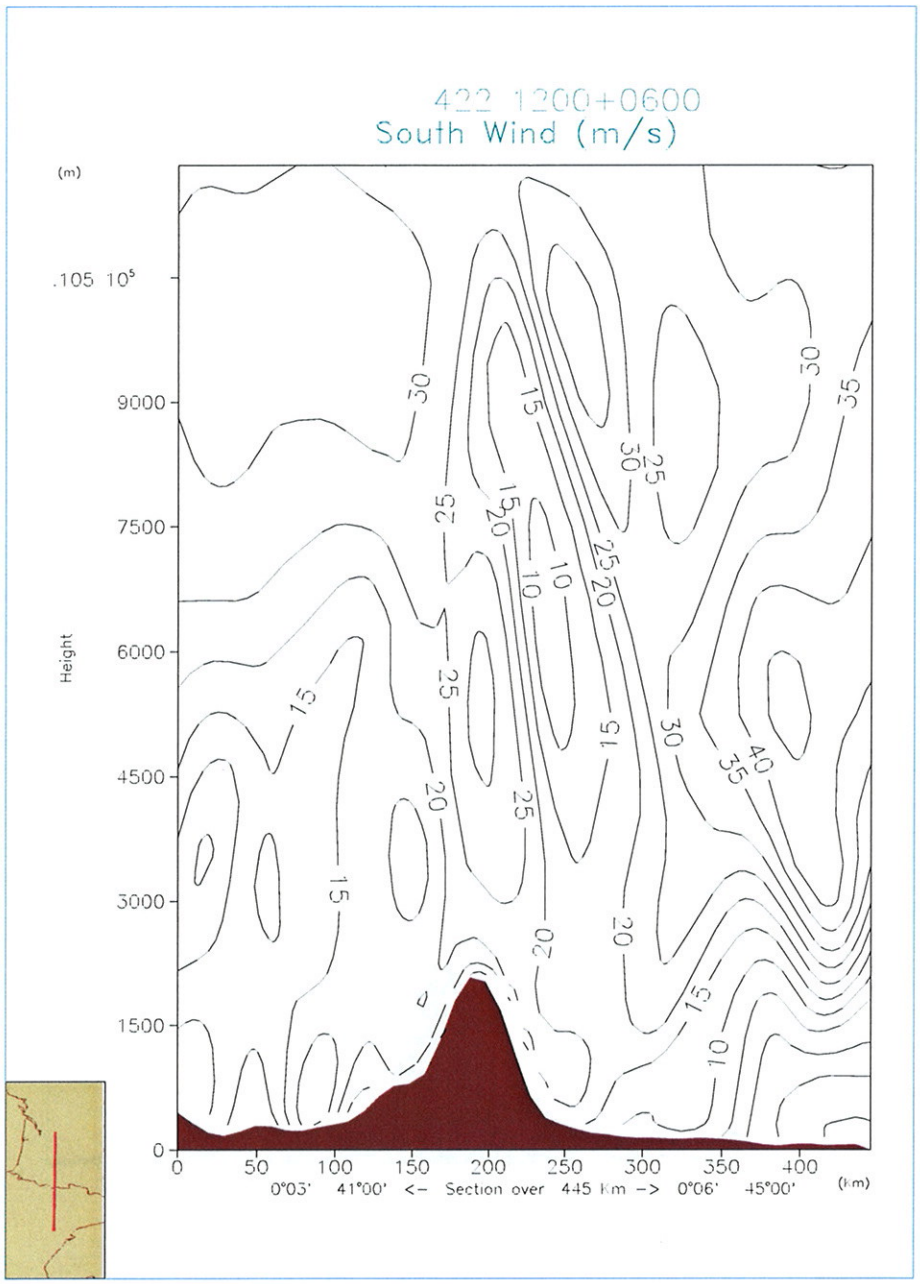

Figure 11: Meridional wind profile – No envelope

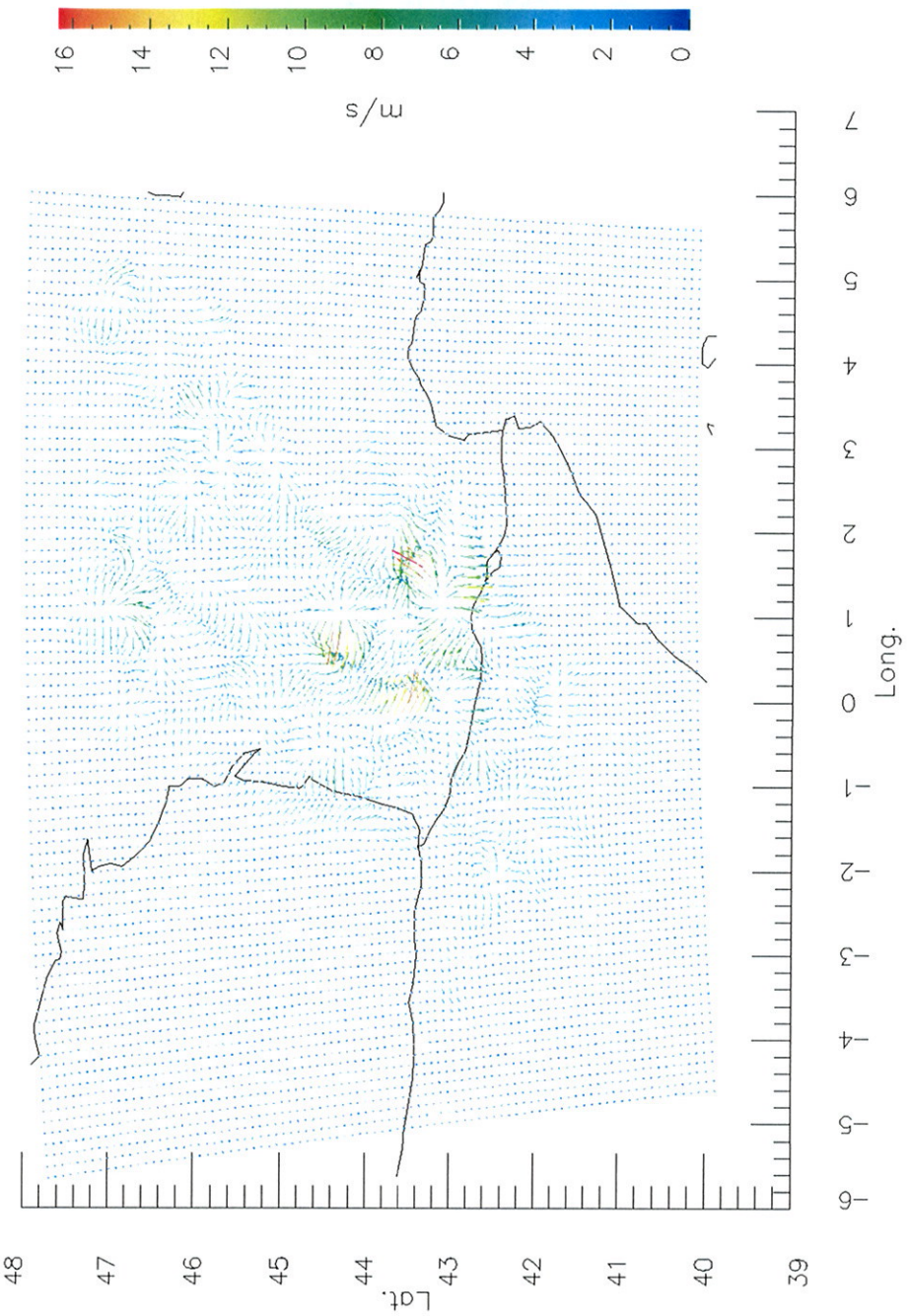

Figure 12: Differences in low-level wind due to the introduction of an effective roughness length

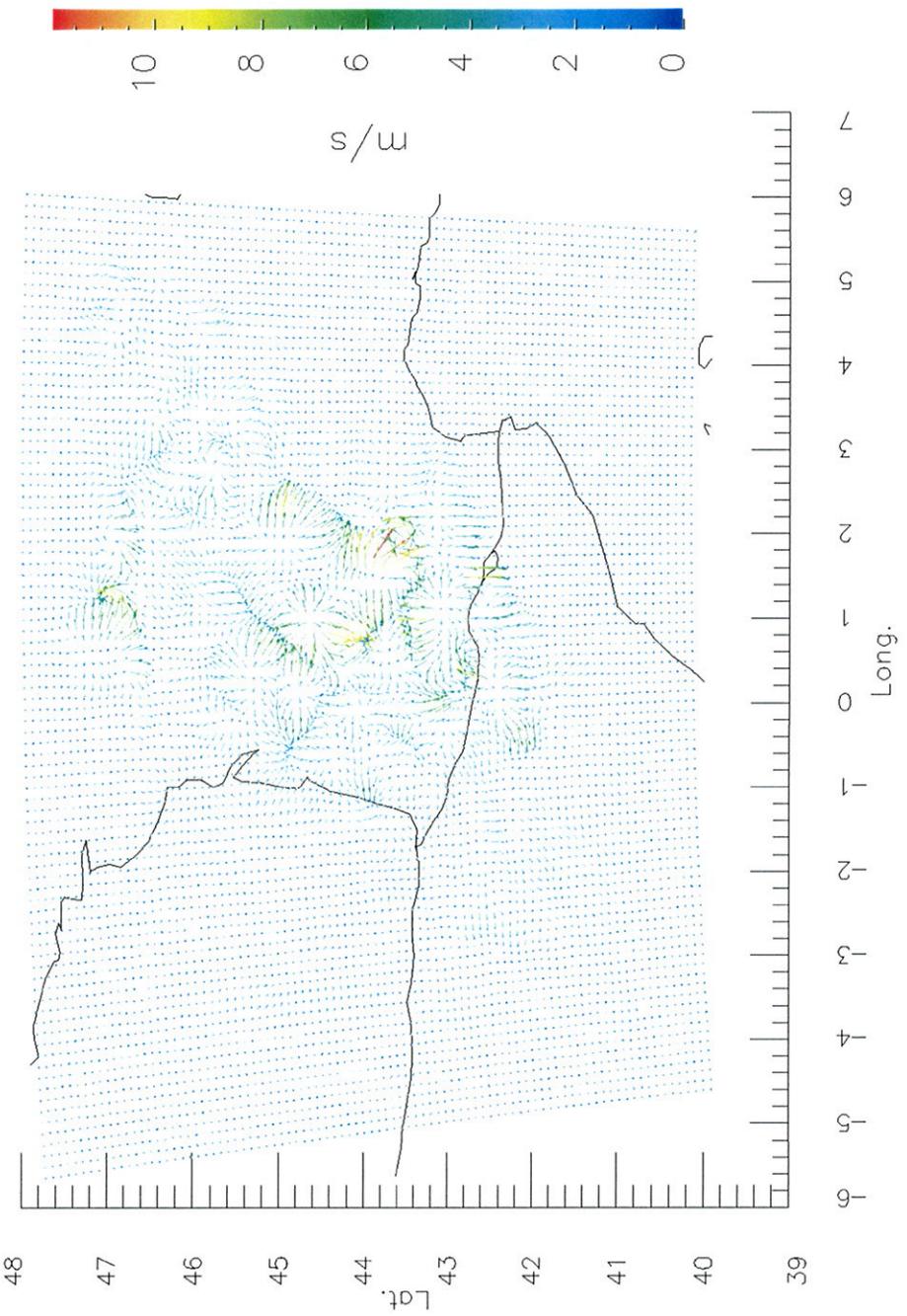

Figure 13: Effects on low-level wind of a doubling of the effective roughness length

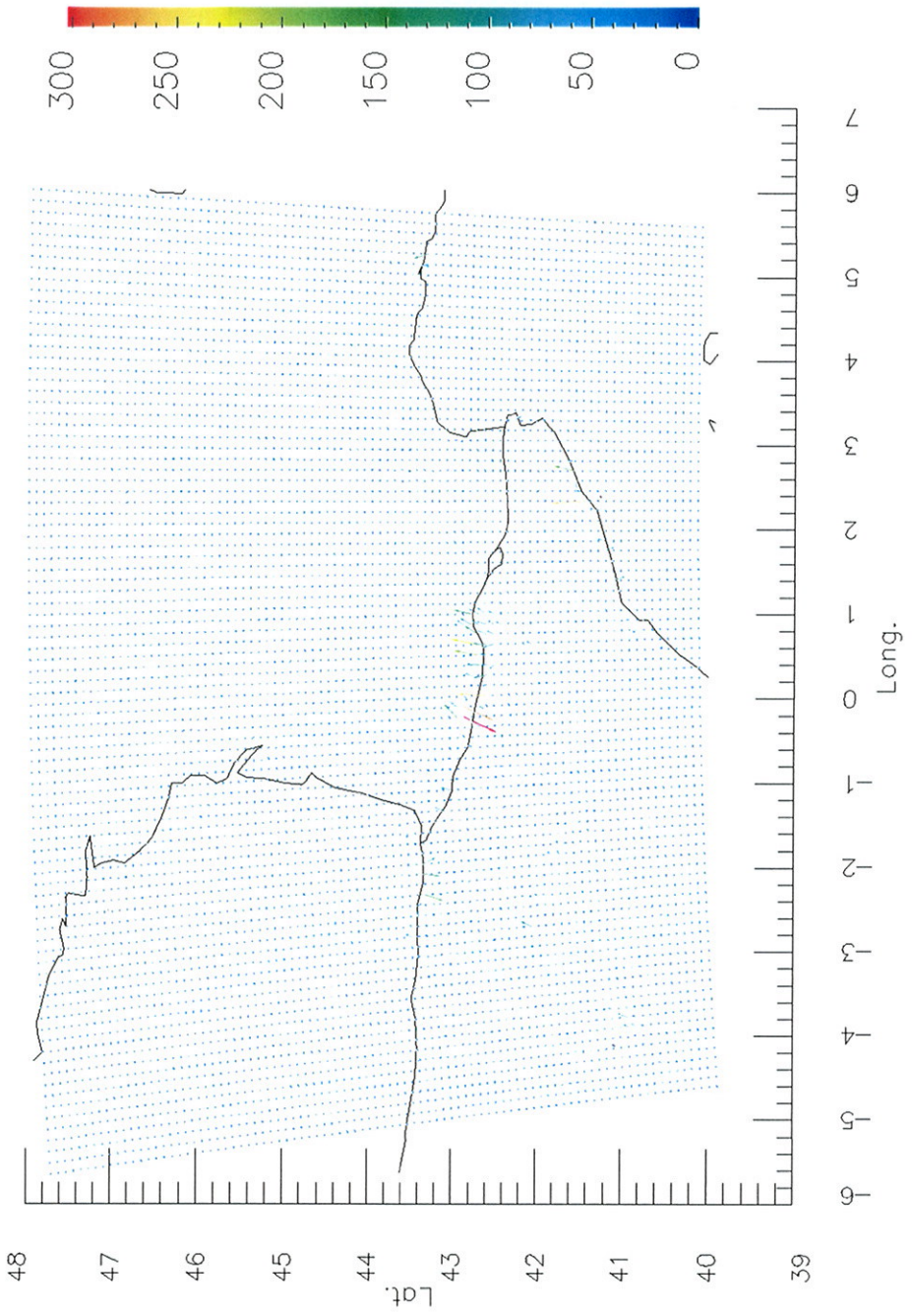

Figure 14: Effect of the introduction of z_0^{eff} on surface induced stress

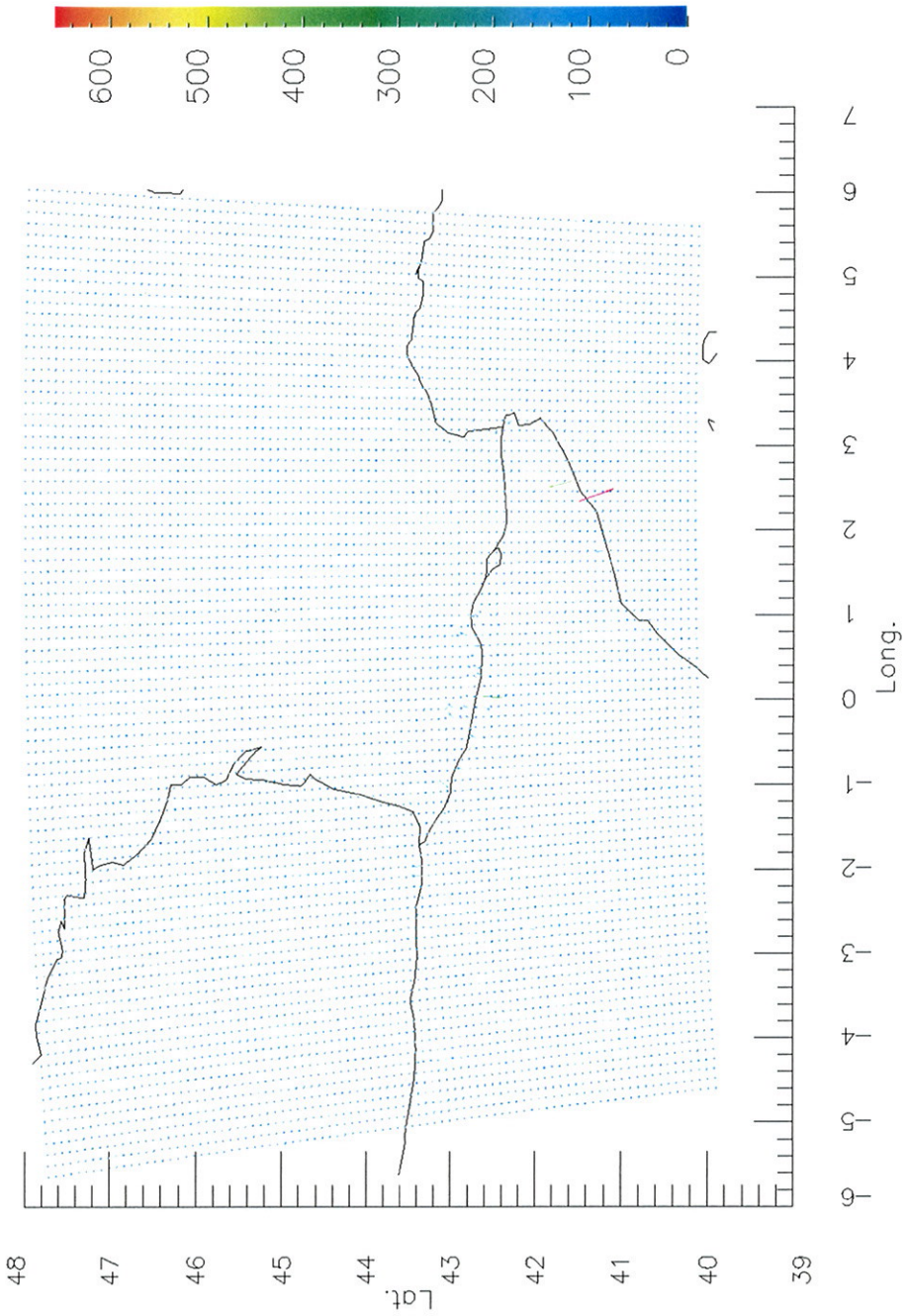

Figure 15: Effect of the doubling of z_0^{eff} on surface induced stress

the formation of lee vortexes. This should be confirmed by a study of the turbulent kinetic energy on the same area.

The effective roughness length has a tendency to affect mainly the high altitude because it acts on the turbulent vertical diffusion coefficients and vertical profiles of wind and temperature rather than on the low-level values of wind and ground stresses.

The theoretical basis for the use of an effective roughness length however remains thin, since the arguments supporting the existence of a logarithmic wind profile over ground are no more valid at the scales used by the NWP mesoscale models such as ALADIN. But field experiments and recent measurements (such as the PYREX experiment) tend to confirm the existence of a logarithmic layer above rugged terrain.

A problem that remains to be solved in ALADIN is the aspect ratio of the subgrid-scale orographic features : a ridge line seen from its side will not have the same roughness as the same line seen from the front. For this study, an isotropic roughness has still been considered, without consideration for the aspect ratio of the mountains.

The best solution for representing the effect of subgrid-scale orography might be a combination of an envelope orography (adaptable through the amplpitude of the height added to the average ground level) and a directional effective roughness length. Of course the combinations should be assessed from the high altitude fields quality, the bottom levels being more sensitive to the parameterization of form drag and lift effects.

Related basic literature

[Bai95] P.G. Baines. *Topographic effects in stratified flows.* Cambridge University Press, 1995.

[GBB+00] M. Georgelin, P. Bougeault, T. Black, N. Brzovic, A. Buzzi, J. Calvo, V. Cassé, M. Desgagné, R. El-Khatib, J.-F. Geleyn, T. Holt, S. Hong, T. Kato, J. Katzfey, K. Kurihara, B. Lacroix, F. Lalaurette, Y. Lemaitre, J. Mailhot, D. Majewski, P. Malguzzi, V. Masson, J. McGregor, E. Minguzzi, T. Paccagnella, and C. Wilson. The second COMPARE exercise : A model intercomparison using a case of a typical mesoscale orographic flow, the PYREX IOP3. *Q. J. R. Meteorol. Soc.*, 126:991–1029, 2000.

[GM90] A. Grant and P. Mason. Observations of boundary layer structure over complex terrain. *Q. J. R. Meteorol. Soc.*, 116:159–186, 1990.

[GRPD94] M. Georgelin, E. Richard, M. Petitdidier, and A. Druilhet. Impact of subgrid-scale orography parameterization on the simulation of orographic flows. *Monthly Weather Review*, 122:1509–1522, 1994.

[Mas88] P. Mason. The formation of areally-averaged roughness lengths. *Q. J. R. Meteorol. Soc.*, 114:399–420, 1988.

[Nom00] P. Nomérange. An evaluation of lift effect parametrization in ALADIN. Report on stay at CNRM/GMAP, October 2000.

[Stu88] R. B. Stull. *An introduction to Boundary Layer Meteorology*. Atmospheric Sciences Library. Kluwer Academic Publishers, 1988.

[WM83] N. Wood and P. Mason. The pressure force induced by neutral, turbulent flow over hills. *Q. J. R. Meteorol. Soc.*, 119:1233–1267, 1983.

Contents